Optimisation of small-cell deployment and backhaul network planning and dimensioning

Ishita Akhter

Submitted in partial fulfilment of the requirements of the degree of

Doctor of Philosophy

Department of

Electrical & Electronic Engineering

The University of Melbourne

August 2020

Abstract

In recent years, the evolution of mobile communication has projected a tremendous growth in the capacity demand of the cellular communication network. Hence, telecommunication service operators have been researching different methods to accommodate such enormous demand growth of data communications. One such approach was to deploy additional macrocells with advanced wireless technology to cater to the bandwidth demand. This approach was not a cost-optimal one due to limited signal spectrum, inter-site distances among cells, risk of higher electromagnetic radiation propagation. Hence, a heterogeneous network deployment is to encounter the increased capacity need would be a more robust solution. Such systems deploy small-cell Base Transceiver Station (BTS) with a smaller coverage radius, alongside the traditional macrocell BTSs, to counter the capacity need and related issues. The planning of such a Small-cell Network (SCN) requires extensive forms of studies, and the purpose would be to focus on specific aspects of network planning to influence the outcome of such tasks directly. These cellular wireless networks connect with a backhaul infrastructure to offer a cost-effective, high capacity, robust, energy-efficient and future-proof connectivity between these "small cells" and the core network.

This thesis presents relevant research studies performed to optimise the deployment of wireless small-cell networks. Firstly, using a novel network planning algorithm, a network of small-cells is planned for different 4G carrier frequencies. This framework also maintained the Maximum Allowable Path Loss (MAPL) level for the transmitted signal from SC. The framework incorporated geographical terrain factors of ground elevation and slope values, locations and fixed coverage area formation for the selected small-cells. An energy and cost-effective optimised backhaul architecture, based on the Gigabit Passive Optical Network (GPON) technology, leveraging an existing optical fibre network resources is separately planned and dimensioned to connect with the planned small-cell network approach mentioned above. Next, the two different SCN and GPON planning methods are combined under one optimisation framework to construct a simplified network planning method applied to any cellular technology or GPON type utilised. Finally, a network capacity analysis is done, concerning the data consumption by devices, based on the population density over the case study area and the assigned 5G Small-cell (SC) carrier frequency data rate. Based on that information and other known constraints and parameters, a corresponding optimisation

framework will be developed. This framework would utilise the concept of cellular frequency spectrum refarming to share the frequency spectrum of wireless signals. In turn, this allowed various types of cellular networks from different generations to function in the same wireless frequency spectrum.

In summary, the technical research contribution presented in this thesis describes multiple approaches to plan a wireless small-cell network. The research also dimensions an appropriate optical backhaul network, for different cellular and optical network characteristics, within the premises of a heterogeneous telecommunications network. Additionally, we discussed some future research directions evolving from our work, alongside concluding remarks.

This page is left intentionally blank

Declaration

This is to certify that

1. The thesis comprises only my original work towards the PhD,

2. Due acknowledgement has been made in the text to all other material used,

3. The thesis is less than 100,000 words in length, exclusive of tables, maps, bibliographies and appendices.

This page is left intentionally blank

Preface

This thesis comprises 100% of novel research works, which I performed under the supervision of Professor Elaine Wong, co-supervisors Professor Christina Lim, and Professor Thas (Ampalavanapillai) Nirmalathas for the degree of PhD (Engineering) at The University of Melbourne, and technical mentoring by Dr Chathurika Ranaweera of Deakin University. This thesis has not been submitted for any other qualification except for the degree mentioned above. All the work transcribed in the thesis was carried out after my enrolment in the PhD degree. No third party editorial assistance was obtained in the preparation of this thesis. Financial aid for this degree has been provided by the Australian Government and The University of Melbourne, under the Australian Postgraduate Award (APA) and the Australian Government Research Training Program (RTP) Scholarships. I have conducted the work penned in this thesis at the University of Melbourne. My research work included research question formulation, data analysis, implementation of the case studies, generation and discussion of corresponding research outcomes, and finally, the thesis writing, comprising about 80% of this research. The rest of the work consisted of essential discussions, some ideation elements, and my respected supervisors' feedback.

The publications mentioned in section 1.7 of this thesis comprise direct and original contribution from myself, as embodied within chapter 3 of this thesis. The conference paper, where I have been listed as the first author, incorporates my original works that form about 80% of the publication. It included problem formulation, case study implementation, outcome generation and paper writing under the listed co-authors' guidance.

For both the other two publications where I have been listed as a co-author, critical analysis from my research work in **Section 3.4.1** of **Chapter 3** was included. This **Chapter 3** work focused on a 4G LTE 1800 MHz frequency wireless small-cell network planning, incorporating geographic elevation, terrain slope and location information, alongside two directions of cellular signal propagation levels, as network planning parameters. *Section 3* of the conference paper titled **"Photonics for gigabit wireless networks"** incorporates this work and contributes to about 10%-15% of this paper. This paper contains my work in **Section 3.4.1** of **Chapter 3**, as one of the small-cell planning approaches to acting as the front-end of cellular network architecture. Within this paper, this network planning framework was proposed to

connect to an optical network backhaul, which would be the back-end part of this cellular architecture.

Next, in the conference paper **"Towards a Framework for Small-cell Network Planning"**, *Section I* and *Section II* explore this same 1800 MHz frequency cell planning in a more detailed manner. Within this paper, my work is about 30%-35% of the total work and serves as the first segment to form a small-cell network planning framework. Then this concept is extended towards an optimal power calculation study for this 1800 MHz small-cell architecture. Extending from both of these papers, we further enhanced this 1800 MHz small-cell planning by incorporating more progressive values of geographic factors as before, e.g., elevation, terrain slope and location. We incorporated a more comprehensive approach of three-direction cellular signal propagations for better signal coverage analysis and a different 900 MHz signal as the carrier frequency for the wireless cellular technology front. As a result, the resultant small-cell network planning for the 900 MHz frequency with more refined geographical parameters appeared different from the 1800 MHz frequency network planning, which was part of both the papers mentioned above and differed from the remaining research works that both papers produced.

My publication that is listed as in progress will comprise significant elements from chapter 6, with more than 80% of the contributions to come from myself. The rest of the contributions will be technical guidance, writing review, and so on, to be contributed by the proposed co-authors, Professors Elaine Wong, Christina Lim, Thas Nirmalathas and Dr Chathurika Ranaweera.

Additionally, alongside the MS-Word traditional spell-checking tool, the Grammarly third-party tool was used to perform spelling/grammar checks to ensure typographical and grammatical issues were identified and resolved.

I hereby confirm that all of the data collection, tools and resource manipulation carried out within this thesis have been done by myself, with strict supervision guidelines from my esteemed panel of supervisors, forming a novel research work for my PhD degree.

This page is left intentionally blank

Acknowledgement

Writing a note of acknowledgement is not an easy job as there is always a risk of losing focus and direction. However, I would try my best to offer this piece as subjective and thorough. Also, apologies in advance if I have missed mentioning anyone in this regard.

First and foremost, I would like to convey my gratitude to my panel of supervisors- my principal supervisor Professor Elaine Wong, co-supervisors, Professor Christina Lim, Professor Thas (Ampalavanapillai) Nirmalathas, and Dr Chathurika Ranaweera. Their unconditional support, thorough guidance, and the expectation of significant improvement in my work have certainly raised the bar and helped me complete my research work successfully. Moreover, thanks to the much esteemed University of Melbourne for allowing me this amazing opportunity of doing a PhD with proper financial support.

I am incredibly grateful to Elaine for supporting me throughout this PhD journey that also saw me going through unfortunate personal circumstances, especially my mother and grandmother's passing. Without her dedicated, sincere, and extremely professional approach as a supervisor, this journey would not have been made possible. I would also like to convey my gratitude towards my respectable co-supervisors for their ample encouragement and guidance to balance Elaine in supervising my PhD. I am utterly grateful to everyone for allowing me to take enough time to complete my PhD while dealing with other stressful issues in my personal life. Special thanks to my supervisors for letting me get hands-on valuable teaching experience as a sessional academic under their superlative guidance. Thas' wisdom, Christina's insights and Chathurika's motivation have been the driving forces into my work, alongside Elaine's incredible leadership in making this research work successful.

Moreover, I would like to express my gratitude to my current committee chair, Associate Professor Brian Krongold, for his valuable time in assessing my work while motivating and encouraging me. Additionally, I would like to thank Associate Professor Leigh Johnston for previously adorning my committee chair's role during my PhD's earlier stages.

An extraordinary mention should be given to Associate Professor Peter Dower of Melbourne University, then Dr Rajib Chakravorty of IBM Australia and Dr Sajeeb Saha of Deakin University. They have been great mentors for me throughout my PhD journey, and I am ever grateful for their valuable support.

This page is left intentionally blank

Dedicated to

The memory of my loving mother, Late Ms Shahana Akhter

This page is left intentionally blank

Table of Contents

This page is left intentionally blank

List of Figures

This page is left intentionally blank

List of Tables

This page is left intentionally blank

List of Abbreviations

ACM	Adaptive Coding and Modulation
ACMA	Australian Communications and Media Authority
ACS	Ant Colony System
BBU	Baseband Unit
BRAS	Broadband Remote Access Server
BTS	Base Transceiver Station
CAPEX	capital expenditures
CCI	co-channel interference
CCO	Coverage and Capacity Optimisation
CEC	Capacity Energy Cost
CFLNDP	Capacitated Facility Location/Network Design Problem
CIO	Cell Individual Offset
CO	central office
CoMP	coordinated multipoint transmission
dB	decibel
DoS	denial of service
DSL	Digital Subscriber Line
DTM	Digital Terrain Model
DU	Distributed Unit
EC	evolutionary computation
ECG	energy consumption gain
ECR	energy consumption ratio
eICIC	enhanced inter-cell interference coordination
eNodeB	E-UTRAN Node B
FA	functional architecture
FAP	Fibre Access Point
FEC	forward error correction
FSG	fractional separation green
FTTH	Fibre-to-the-Home

FTTN	Fibre-to-the-Node
FTTX	Fibre-to-the-X
GA	Greedy Algorithm
GAS	Greedy Adding with Substitution
GE	Grammatical Evolution
GNSS	Global Navigation Satellite System
GP	Genetic Programming
GPON	Gigabit Passive Optical Network
GPS	Global Positioning System
HeNB	Home E-UTRAN Node B
HetGen	heterogeneous
HetNets	Heterogeneous networks
HUE	Home User Equipment
ILP	Integer Linear Programming
INP	Impulse noise protection
IRC	Interference Rejection Combining
ISI	Inter Symbol Interference
kbps	kilobits per second
LB	Load Balancing
LoS	Line-of-Sight
LP	Linear Programming
LTE	Long-Term Evolution
MAPL	Maximum Allowable Path Loss
Mbps	Megabits per second
MCLP	Maximal Covering Location Problem
MCN	Multi-hop cellular network
MHz	Megahertz
MILP	Mixed Integer Linear Programming
MIMO	multiple-input and multiple-output
MS	Mobile Station
MSF	minimal satisfaction factor

NFV	Network Functions Virtualization
NLoS	Non-Line-of-Sight
OCS	Optimal Cell Size
ODN	Optical Distribution Network
OLT	Optical Line Terminal
ON	opportunistic network
ONU	Optical Network Unit
OPEX	operation expenditures
PA	Power Amplifier
PON	Passive Optical Network
PoP	Point of Presence
POS	Passive Optical Splitter
PtMP	Point to Multi-Point
PtP	Point to Point
QoS	Quality of Service
RAN	Radio Access Network
RBs	Resource Blocks
RF	Radio Frequency
RM	rural macro
RSRP	Reference Signal Received Power
RT	Remote Terminal
SA	Simulated Annealing
SC	Small-cell
SCA	Small-cell Arrangement
SCN	Small-cell Network
SDN	Software-Defined Networking
SFBC	Space Frequency Block Coding
SINR	Signal-to-Interference-and-Noise Ratio
SON	Self-Organising Network
SR	Spectrum Refarming
SUM	sub urban macro

TB	Terrain Block
TCAM	Transmitter Controlled Adaptive Modulation
TDD	time division duplexing
UE	user equipment
UM	urban macro
UMTS	Universal Mobile Telecommunications Service
W-CDMA	Wideband Code Division Multiple Access

This page is left intentionally blank

Chapter 1

Introduction

This research project aims at performing a discrete optimisation procedure for the optimal placement of wireless network small cells. Typically, wireless networks implement the "macrocell" coverage area infrastructure (base transceiver station areas with a coverage radius of 0.5 to 2 kilometre) [2]. These cell sizes can be made smaller to increase cell density and thus enhance network capacity. Moreover, spectrum refarming for the small-cell planning part is included to allow for more wireless signal spectrum utilisation for capacity enhancement. For wireless networks, backhaul infrastructure should provide cost-effective, high capacity, robust, energy-efficient and future-proof connectivity between these "small cells" and the core network [3]. Our research intends to employ presently rolled out National Broadband Network (NBN)'s Fibre-to-the-Home (FTTH) optical fibre network infrastructure as a proper backhaul solution for small cells deployment. This work is to be done by leveraging the existing network infrastructure-wireless (macrocell) and wired (core network). Therefore, using existing optical fibre node terminal locations and macrocell sites, small cells' positions would be optimised accordingly to increase network capacity and maximise coverage.

In recent years, the evolution of mobile communication has seen tremendous growth in bandwidth demand of the wireless network. Several driving factors are facilitating this enormous mobile traffic explosion. These can include-tariff reduction for mobile data service subscriptions, the introduction of powerful and smart mobile devices capable of handling data applications, and significant development within mobile data applications to manage more abundant multimedia contents [4]. The example of such enormous mobile communication growth over five years (2018 – 2023) in terms of mobile device usage is depicted below in **Figure 1**.
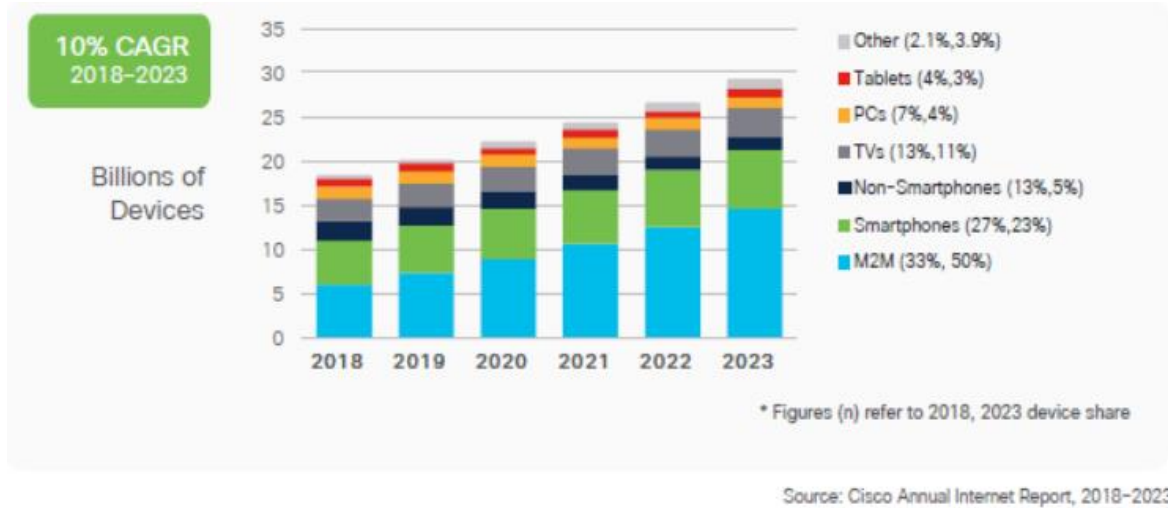
Figure 1: Mobile traffic growth statistics [5]

Hence, telecommunication service providers explore different approaches to accommodate this demand growth. One such strategy was additional macrocell deployment with advanced wireless technology. However, this proved relatively ineffective in meeting the additional bandwidth need [4] due to cost increment for deployment, limited available wireless spectrum; immitigable inter-site distances among wireless cells; risk of excess electromagnetic radiation. Therefore, Ranaweera *et al.* propose deploying a Heterogeneous network to encounter this demand for increased bandwidth. This type of network implements numerous small-radius microcells, i.e. "small-cells" or "femtocells", over the existing macro-cellular infrastructure [6]. According to a recent study, small-cell wireless networks have recently emerged as a viable solution to accommodate high data rate services requiring extra bandwidth provisioning [7]. This fact is consequently supported by Cisco, which establishes femtocells as a potential offloading medium for current and future mobile data traffic onto the fixed network [8]. In data communications, offloading is the mechanism where other corresponding network communication technologies are used to transport mobile data traffic, which was initially intended to be broadcasted over the mobile network itself [9]. Small-cells currently provide high throughput for indoor and outdoor hotspots where most data usage occurs [10]. As a result, many plug & play and cost-effective small-cell nodes are being developed, namely, lightRadio^{TM} cube [10] and Liquid Radio [11]. The deployment of small-cells is expected to grow in future. It is also expected that by 2017, 70 million small-cells would be deployed by mobile operators and also as picocells intended for high-capacity urban networks [12]. Small-cell and Wi-Fi offloading would also carry almost 50% of the total generated mobile traffic by

2013 [13]. Thus, it is evident that a heterogeneous network comprising both small and macrocells is justifiably an enhanced wireless network structure for current and upcoming cellular communications. This research question intends to develop an optimisation outline to plan a cost and energy-efficient optical fibre backhaul layout for the planned small-cell network, based on influencing parameters that affect the wireless signal propagation within such a network. A small-cell deployment is also heavily influenced by the type of network the small-cells will be deploying. For example, current small-cell scenarios are based on 4G or 5G cellular technology network types. Therefore, the network planning for both technology types would differentiate based on each technology's different parameters. For instance, as per the study in [14], 4G is still more widely deployed network type than its 5G counterpart, thus 5G deployment is still subjected to further research and experimentations. This study also highlighted that 5G would offer more connectivity than 4G with many different devices and would support more traffic handling capacity than what 4G offers.

Additionally, 5G network architecture incorporates a more centralised approach, with localised data centres at the "edge" of the network coverage area connecting with server farms. All these aspects would significantly affect the designing and deployment of a cellular network, resulting in different network designs for 4G and 5G technologies. It is essential for wireless network coverage areas or "cells" to have a proper backhaul infrastructure that is cost-effective, high capacity, robust, energy-efficient and future-proof. It should also provide connectivity between these cells and the core network [2]. Presently, optical fibre is deployed within fibre-to-the-home (FTTH) access networks to provide a better capacity for the end-users. The resources employed in FTTH installation can be re-used to provide this fibre backhaul without added equipment and aiding future upgrades to wireless networks [15]. Therefore, this research topic aims to design and optimise the fibre-based backhaul layout for wireless network small cell deployment.

1.1. Small-cells in a heterogeneous network

A heterogeneous network is a type of communication network that implements numerous small-radius microcells, i.e., "small-cells" or "femtocells", over the existing macro-cellular infrastructure [6]. According to Hoydis *et al*., the term "small-cell" refers to a radio network design concept, where the deployed BTS is much smaller in radius than that of the traditional macrocell [3]. A small-cell BTS can support a limited coverage area, which could

be about a 100 factor smaller than the traditional macrocell area. They are smaller, low-cost and low-power base stations, generally deployed within customer premises, connected to their wired backhaul connection and capable of offloading data traffic from the macrocell network existing alongside [16]. Small-cells can be deployed in a green, cost-effective, flexible and cooperative manner, within indoor and outdoor public or private premises, with either open or closed access. Examples of deployment sites may include small boxes atop existing street locations, metro hotspots, along with residential and enterprise environments.

A typical Heterogeneous network scenario can be seen in the following **Figure 2**.
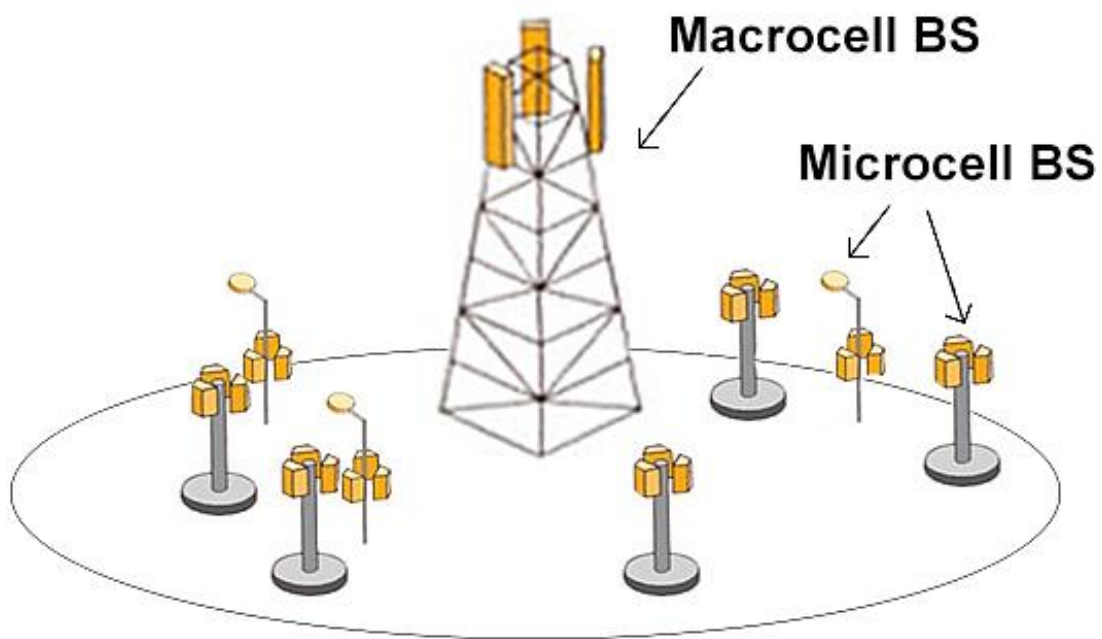
Figure 2: General heterogeneous network architecture

1.1.1. Small-cell network advantages

One research work also establishes that small-cells are advantageous in different ways, for instance-

Cost minimisation: Cost reduction by eliminating additional cell site rental; reducing backhaul provisioning and maintenance expenses by leveraging existing macrocell and backhaul infrastructure; self-organisation and optimisation of equipment with no additional network planning implementation [17].

High capacity provision: Dense small-cells can provide higher capacities up to Gbit/s/km2 and higher data-rates for an individual user with less bandwidth sharing [17].

Traffic offloading: Small-cells have traffic offloading capability from the macro cell, along with the ability to provide extended coverage at low cost [17]. The offloading from Wi-Fi is also an added enhancement to small-cell advantages [13].

Environmental sustainability: Ensuring environmental sustainability by decreasing cellular networks' ecological footprint using less transmit power, thus reducing electromagnetic exposure to the living and increasing cell terminal battery life [17].

1.1.2. Challenges in small-cell deployment

Despite the potential benefits that small-cells offer for wireless cellular communications, there have been significant restrictions that can prevail in terms of small-cell deployment within a heterogeneous network architecture, as follows.

Backhaul deployment and installation expenditure: The smaller coverage areas of small-cells result in their dense placement, increasing the total number of deployed cell sites. Consequently, this would result in an increased number of connections to small-cells from the backhaul architecture. Thereby, optimising backhauling cost should ensure ample connectivity from backhaul to small-cells and minimal connectivity resources [18].

Interference Management: Intercell interference is one of the most prominent challenges in a small-cell deployment scenario, as the cell sites are placed much closer than macrocell sites. Additionally, an increased number of interference sources and the prevalence of more cell edge areas than macrocell formation increases the chances of such interference occurrences. There have been proven interference mitigating techniques in macrocell networks such as MIMO-based coordinated multipoint transmission (CoMP) [18], which is also being adopted in the small-cell scenario for intra-cluster co-channel interference (CCI) [19]. However, there are still further research scopes to find effective inter-cell interference mitigating small-cells techniques [19].

Mobility Management: Mobility management is an evident issue in a small-cell scenario due to frequent handover among the cell towers. This frequent handover results in increased signal loading in mobility management, increasing the possibility of call drops [18]. Additionally, each cell can have the option of handovers from a more significant number of

neighbouring small-cells and communication among cells can face obstruction due to limited radio resources. It also becomes increasingly difficult for each small-cell to track all potential handover candidates for neighbouring small-cells [20].

Resource Scheduling: Scheduling and optimising the utilisation of the radio resources for small-cells can be quite challenging due to small-cell networks' very nature. Unlike macro cells, small-cell access points are not typically well structured and planned, causing difficulties in user distribution for each small-cell. The small radii of small-cells do not offer a larger area to divide the mobile users between the cell centre or cell edge locations. This phenomena also leads to less variation of signal strengths for different users. In the macrocell scenario, only a handful of adjacent cells can heavily influence the intercell interference aspects, while remote macrocell signal effects are considered negligible. The reason being that signal strengths from such distant cells usually attenuate over longer propagation path, thus not having enough strength to interfere with far away macro cell signals. However, in small-cells, such interference sources are more in number, as adjacent small-cells and remote cells can significantly influence interference aspects. Here, each small-cell signal can cross over and thus travel further than their designated cell coverage area due to smaller radii, causing interferences even in small-cells situated further away. Therefore, such constraints require higher complexities in scheduling and optimising radio resources such as power, frequency, time, and space to ensure ample coverage and less interference in small-cells [18].

Operational costs: Expenditures in small-cell operations and management can see a significant amount of expenses, as the number of equipment placed for such cell sites can be much higher than a typical macro cell scenario. This event increases the deployment cost and the maintenance costs alongside self-organising operations built into the small-cell itself. Additionally, obtaining proper frequency spectrum to be assigned with small-cells can be expensive [20], thus piling up on overall deployment costs [18].

Self-Organisation: Self-organisation of small-cells is critical to enhancing efficiencies within a heterogeneous environment [21]. Such self-organisation methods include processes such as self-healing, self-optimisation and self-configuration. The self-configuration process involves a cell's ability to configure itself typically for events, namely, the addition and removal of network features, alongside cells being rebooted and placed to a new location, especially for small-cells. Small-cells obtain prior information of the radio environment and then configure

related parameters, e.g., channel power and neighbouring cell lists, before the self-configuration operation is performed. For self-optimisation, corresponding network parameters such as handover control, physical resources, transmit power, access modes, admission control is continuously updated to ensure optimal small-cell performance at every stage of operation. The remaining self-organising feature would be self-healing, which attempts to resolve any technical issues at the times of small-cell operations. The method is to go back to a standard setting of small-cell operation in case of any technical problem [20].

Access Mode allocation: As small-cells support a specific limited number of users, it is essential that user access is organised and prioritised accordingly through appropriate access modes. Present user access modes include open access mode, closed access mode and hybrid access mode. Open access mode allows any user access provision to a small-cell, while closed access mode allows only a particular set of users to access the cell. Then hybrid access mode is an extension of sorts for the closed access mode where a limited number of random external cell users are allowed with small-cell access provisions. Since open access mode can increase expenses on behalf of the small-cell owning personnel, it should be allowed in specific situations, e.g., public places where small-cells operate under commercial cellular service providers. The closed access mode can also cause inefficiency in cellular performance by restricting external users from accessing cell services. This incident can occur if any nearby small-cells experience high signal levels from the cell, thus causing interference on the external users' behalf. The apparent solution could be introducing the hybrid access mode in this case, which, however, can also negatively affect small-cell performances. Additional external users to a small-cell can increasingly consume small-cell service and resources, thereby depriving the rightfully allowed internal users of their entitled small-cell services. Hence, the hybrid mode should also be applied carefully and optimally for a small-cell [20].

Security: Providing security to small-cells is an essential feature to ensure uninterrupted service to cell users. It is because small-cells are prone to security threats such as user information hacking [22], denial of service (DoS) attacks, unwanted user access [23]. There are existing security measures adopted within the small-cell scenario, such as implementing a secured gateway between the core network and access points in a small-cell backhaul connection [24]. There have been additional identified threats, namely man-in-the-middle attack and eavesdropping, compromising the cell user access list, which requires appropriate security measures for proper prevention. As small-cell deployment is increased

with time, extensive small-cell security measures should be researched and implemented accordingly [20].

Timing & Synchronisation: Appropriate timing and synchronisation mechanisms should be applied on small-cell networks to ensure interference-free cellular services. If there is an issue with the internal clock, Inter Symbol Interference (ISI) can be specifically evident for OFDM cellular systems as the transmission timing is affected [25]. Therefore it is essential to have the internal clock synchronisation in small-cells, with one such method described in the Precision Time Protocol (PTP) [26]. Another option for resolving the timing and synchronisation issue would be implementing a Global Positioning System (GPS) receiver with small-cells. However, the downside of using such a receiver would be to face GPS signal attenuation, thus eventually affecting synchronisation itself rather than enhancing it. Therefore, another alternative option can be to use TV transmission signals to perform timing and synchronisation of small-cell transmission, as such signals are available in a broader range of areas [13]. The timing and synchronisation issue for a small-cell can also be resolved using neighbouring small-cells for synchronisation method within the time division duplexing (TDD) systems for small-cells. This study uses signal transmission from adjacent small-cells [27] and a similar method [28] that employs small-cell preamble signal to arrange small-cell signal frames and synchronise the small-cell with the network. There are still provisions for further research on enhancing small-cell synchronisation and timing, specifically developing corresponding intelligent algorithms [20].

1.2. The small-cell network backhaul

Backhaul is the communication link in a cellular network that provides connectivity between the radio base stations and the corresponding radio controllers or switching nodes within the core network's cellular systems. This outcome is typically obtained through different means of transport media [29, 30]. The base stations deliver radio coverage towards individual mobile stations within a geographical area through a radio interface. Base stations maintain connectivity with the public switched telephone system/public data network (PSTN/PDN), other gateway and switching nodes and the core network via the mobile switching nodes through the backhaul [29]. Therefore, the necessity of a proper backhaul system is appropriately understood. The aim is to provide a backhauling architecture to small-cells in a

cost-effective manner than the macrocell scenario. This cost-effectiveness is achieved by properly dimensioning the backhaul deployment and lowering the Quality of Service (QoS) constraints in terms of coverage and capacity scenarios. An example of a backhaul network can be depicted in the following **Figure 3**.
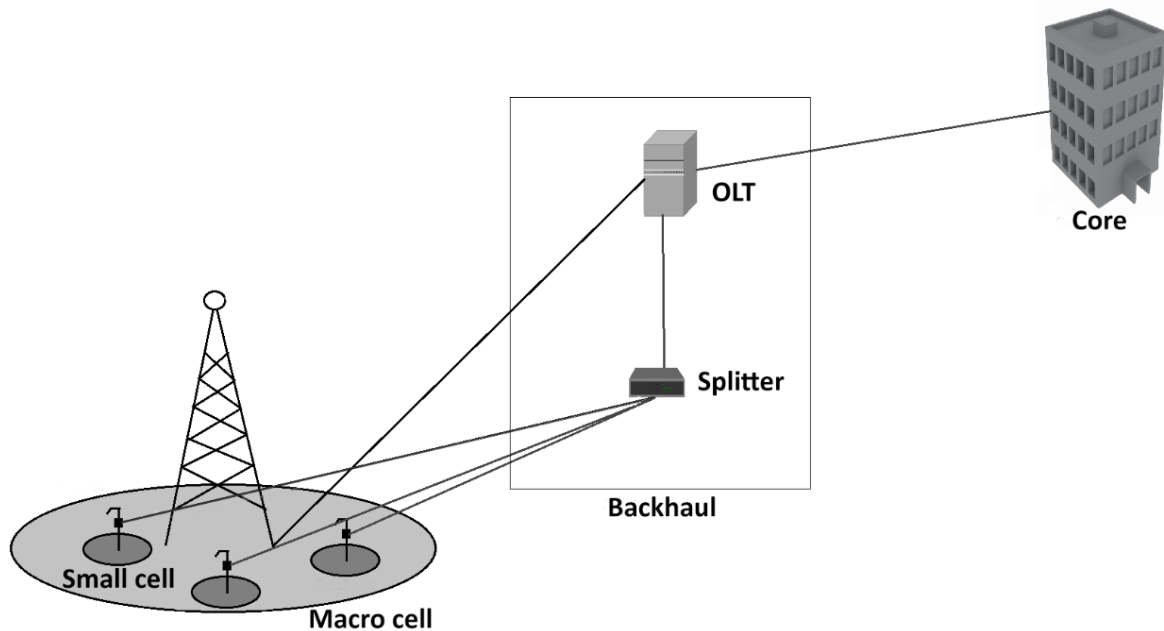
Figure 3: Small-cell backhaul architecture example with optical network

1.2.1. Small-cell network backhaul variants

An optimal approach should be achieved for planning and dimensioning an appropriate backhaul system for SCNs. The reason being different significant challenges faced in terms of selecting proper backhaul options for SCNs. According to the study done in [30], different forms of physical mediums such as copper, Ethernet, optical fibre, Wi-Fi, and WiMAX radio links have been deployed as backhaul solutions for wireless cellular networks. This study highlights both wireless and wired media as functioning backhaul options and emphasises their utilisations. Therefore, the usage of media-based backhaul implementations can be categorised as follows.

- Wired medium small-cell backhaul
- Wireless medium wireless backhaul

❖ Wired medium small-cell backhaul

Physical mediums with wired connectivity are among the most popular choices for being deployed as backhaul solutions for small-cells. The wired backhaul systems can provide higher availability and capacity than wireless mediums, making them a more viable solution to meet the busy tele-traffic hour demands of cellular networks. To meet up to the ever-increasing tele-traffic demands, wired backhaul deployments for some small cell deployment scenarios may not be cost-effective due to the associated expenditure of implementing possible new equipment. Moreover, in some instances, wired backhaul options may be the sole possible backhaul solution for the small-cell deployment premises. There are several choices for such backhaul options, namely Digital Subscriber Line (DSL) and Optical fibre, as reviewed in [31].

Digital Subscriber Line (DSL): Traditionally, DSL is used as a cellular backhaul technology. DSL extensively deployed telephone infrastructure utilising copper twisted pair with a typical capacity range from 256 kilobits per second (kbps) to 40 Megabits per second (Mbps) in the downlink [32]. The reliability of DSL as a backhaul solution is affected due to its asymmetric bandwidth and cross talk interference. The asymmetric bandwidth technology of DSL for uplink and downlink streams is rendered into capacity constraints, affecting small-cell capacity in a degrading manner. With its interference issue in DSL, termed as cross talk, where interference occurs between the copper lines in the same cable, ultimately it leads to data degradation within a DSL backhaul [30]. The DSL technology extension, called the Very High-Speed Digital Subscriber Line 2 (VDSL2), is introduced to encounter these issues. It provides enhanced capacities of around 40 and 30 Mbps at distances of 400 and 1000 m. The VDSL2 also incorporates vectoring and pair bonding techniques to mitigate the cross-talk interference issue. The vectoring method continuously cancels any rising interference and allows for copper lines to increase line capacity [33].

Additionally, the pair-bonding process within VDSL2 allows for bandwidth expansion by implementing inverse multiplexing, where multiple DSL lines are combined to provide an accumulated data rate. VDSL2 additionally deploys Impulse noise protection (INP) with forward error correction (FEC) to prevent data burst errors during transmission [33]. The third option within DSL is symmetric high-speed DSL (G.SHDSL) technology that uses both multipair bonding and can provide a symmetrical data stream of 22 Mbps over long distances in both downlink/uplink directions [33]. In terms of technological advancement, XG-Fast is

another variant of the DSL technology, offering a data rate of 10 Gbps through copper lines [34]. It is considered immune to cross talk issues due to single user technology and deploys signal coordination at both transmitter and receiver ends with enhanced equalisation techniques. XG-Fast also implements Transmitter Controlled Adaptive Modulation (TCAM), enabling higher DSL data rates [34]. XG-Fast offers a frequency range of 106 Megahertz (MHz), with 500 Mbps bandwidth over 100 m of distance. If a higher frequency range of 350 MHz is implemented, the data rate could reach a symmetric flow of 1 Gbps bandwidth over a 70 m distance. Besides, if multipair bonding is applied over a 30 m distance, within a frequency range of 500 MHz, the data rate of XG-Fast can reach up to 10 Gbps.

Optical fibre: Among these, the optical fibre-based network could be an optimal backhaul solution specifically for densely populated urban areas. Optical fibre links offer better reliability and predictability than a copper link with a significantly higher transmission distance of up to 100 km. It can also enhance the backhaul capacity of up to 400 Gbps of throughput, with a much lower latency [35, 36]. In optical fibre links, the fibre transceivers have their properties regulated by Ethernet standards. Also, it can offer an enhanced backhaul capacity by deploying several fibre pairs together. Such a higher capacity optical transport system can offer a bidirectional capacity of up to 8.8 Tbps. An optical fibre backhaul can be deployed using two infrastructures, FTTH and Fibre-to-the-Node (FTTN). FTTH has the advantage of a potential unlimited spectrum by deploying fibre connectivity to the end-user premises. In FTTN, VDSL2 technology offers connectivity in the last 1000 m with the cellular operator's copper connections, thus decreasing the cost of trenching new fibres to end-user premises while maintaining adequate user QoS [31]. Existing FTTN access networks for large telecommunication carriers can thereby be implemented as backhauls to provide better capacity and coverage to end-users through cost-effective leveraging of current FTTN installations [6, 15, 37-40]. FTTN is a variant within the Fibre-to-the-X (FTTX) architecture, where the x denotes different reaching positions for optical fibre, such as building/curb/home/node. All FTTx network variants, including FTTN, usually have two types of architectures-The passive optical network (PON) and the point to point (P2P) deployment [41].

In a PON, three components reside- Optical Line Terminal (OLT), positioned at the network provider's central office (CO) and acting as the interface between PON and the backbone network. Then Optical Network Unit (ONU) resides with the end-users, acting as a service interface to them and the Optical Distribution Network (ODN) that connects the OLT

and ONUs using optical fibres splitters. Thus, the ODN creates a tree structure where the OLT is the base and ONUs are leaves [42]. Hence, PON has a point-to-multipoint structure over a passive fibre plant, using fibres and splitters/combiners in the middle and active components at the ends [43]. The splitters/combiners stay between the central node and the end optical/electrical conversion (in the node/curb/home) equipment. On the other hand, Point to Point (PtP) employs aggregation nodes and access nodes as switches instead of splitters/combiners in the middle, i.e., between the central node and the end equipment. However, despite its advantages, the unavailability of fibre infrastructure nearby small-cell deployment area and corresponding installation/deployment expenses with such infrastructure could be much higher than a DSL backhaul.

❖ Wireless medium small-cell backhaul

Wireless transmission technology can also serve as an option for small-cell backhaul networks. It can provide more flexibility in reaching small-cell sites than that of wired backhaul options. Wireless technologies, including microwave Point to Multi-Point (PtMP), microwave PtP, millimetre wave PtP, sub-6 GHz PtMP, can be effective backhaul solutions. Their relevance for being a wireless backhaul medium can depend on capacity dimensioning, Line-of-Sight (LoS) transmission availability, network topology and carrier frequency. Also, the wireless backhaul deployment can be a combination of the different options mentioned above. They can eventually satisfy varying environmental conditions around the small-cell sites through appropriate trade-offs for signal directionality, carrier frequency, and network formats [31].

Signal directionality (LoS/NLoS transmissions): Non-Line-of-Sight (NLoS) wireless backhaul is an alternative solution to small-cell backhauling scenarios offering direct signalling between small-cell and core network is challenging to render. NLoS offers a broader coverage area than LoS in urban scenarios, making antenna alignment and deployment process more manageable. Usually, sub 6 GHz carrier frequency [44] based OFDM signals with a channel bandwidth of 10 to 20 MHz are chosen for such NLoS backhaul system. Such a system can suit propagation conditions and decrease the effects of multipath fading. Such NLoS systems typically deploy a PtMP formation from a hub module at the Point of Presence (PoP) to small-cells. PoP is a central access point where tele-traffic aggregation from connected small-cells is performed. The hub module antennas are placed at rooftops to be directed towards

the small-cells to provide less path loss and expand the range between PoP and small-cells. Hub modules typically deploy an array of antennas with enhanced directional beamforming to reduce interference and improve antenna gain. Interference is a compelling issue for NLoS backhaul in the unlicensed frequency spectrum due to the conflict of user equipment channel transmissions among operator and different technologies. Due to the low availability of spectrums at low-frequency bands, NLoS transmission cannot offer high capacity than LoS transmission [31].

Signal carrier frequency: Carrier frequency choices for wireless backhauls significantly influence coverage-capacity trade-off for small-cells due to their differences in signal losses. For example, the sub-6 GHz frequency is more suitable for NLoS links with omnidirectional antennas, offering adequate coverage if there are ample signal scattering and insignificant attenuation from the signal's penetration loss. The primary constraint is capacity due to spectrum-specific bandwidth restrictions. Also, appropriate interference regulation should be applied mainly in unlicensed spectrums as they can be shared by various other wireless technologies, hence affecting signal quality distinctively. Another choice of frequency is microwave, between 6-56 GHz, which has a shorter wavelength, and is profoundly affected by penetration and diffraction losses, making it more suitable for LoS backhaul links. It, however, can still operate for near LoS scenarios in low frequencies of the microwave spectrum. The shorter wavelength allows for smaller directional antennas with narrow beamwidth and high gain to be deployed, rendering antenna alignment feasible for optimal performances [35]. Microwave LoS backhauls are more suitable for long-range fixed links with fewer interference occurrences.

Additionally, microwave links above 10 GHz can suffer scattering and absorption losses in the rain, resulting in signal losses and affecting backhaul planning strategies. Microwave backhaul can be both PtP and PtMP, while PtMP formation offering more densification of network nodes. It decreases peak cell traffic within each small-cell, and total cellular traffic gets divided among adjacent cells, enhancing backhaul performance with multiplexing provisions applied [45]. Other wireless backhaul link types can be V-band (57–66 GHz) and E-band (70–80 GHz), which can only offer LoS transmission since they have much higher diffraction, penetration and absorption losses. The very short wavelength also requires highly compact antennas with very high gain and narrow beamwidth, with significantly precise antenna alignment for peak performance [35]. These bands can offer high

capacity short links of over 1 km as they have several GHz-wide bandwidth, along with much-mitigated interference due to high gain antennas and much higher penetration losses. V band signal gets affected by oxygen in the air, and E band is mostly by rain, thus restricting link distance to only a few kilometres in different areas. It is also assumed that V-band can provide better street to street and street to rooftop connections, and E band is more effective in the rooftop to rooftop scenario. Alongside LoS, NLoS solutions can also prevail for high-frequency bands using large gain antennas with appropriate alignments, accommodating narrower beamwidths [46].

1.2.2. Small-cell backhaul deployment challenges

Significant challenges can be observed while planning and dimensioning small-cell backhaul networks. Such challenges, therefore, can be defined as follows.

Physical design and architectural aspects: One of the primary challenges in designing a small-cell network backhaul is determining an appropriate physical architecture for a backhaul suitable for a specific small-cell network type. Three primary physical architectures can be deployed for small-cell backhaul [35]. These architectures are termed as full separation module, moderate separation module and full integration module. Depending on the type of SCN to be deployed, the backhaul network can be a separate architecture to that of the SCN, physically situated in a separate enclosure altogether. This structure is termed the full separation module. The moderate separation module provides a lesser degree of separation between SCN and backhaul by placing the SCN and backhaul sections within the same enclosure, yet they would perform as separate units. This formation is intended to protect the interconnections between the SCN and backhaul units from external elements, accidental damages, tampering, sabotage. The third option is the fully integrated module, where the backhaul and small-cell can be fully incorporated together. The small-cell Radio Access Network (RAN) can have the appropriate backhaul unit/card installed, or the backhaul unit can house the RAN itself. The fully integrated module provides highly efficient protection against outside forces, reduces size and cost to some extent and ultimately eases the deployment process. However, this integration format reduces flexibility in backhaul and RAN equipment selection [31, 35]. The availability of such different physical architecture of backhaul types creates more complexities in deployment and cost management. Therefore, SCN type, need of

coverage and capacity, and location plays a significant role in determining the type of backhaul type to be implemented.

Appropriate coverage provisions: Providing appropriate and ample coverage between the core network and the small-cell BTSs is quite challenging to achieve since different constraints are attached to different types of backhaul network options. For example, wired backhaul solutions are affected by their existing infrastructure and connectivity equipment and provisions. Simultaneously, wireless backhauls can be influenced by coverage of the transmission nodes, resulting in NLoS propagation due to their geographic location relative to the small-cell placement. As new connection deployment for wired backhaul is relatively expensive, the cost-effective solution is to utilise existing wired network infrastructure. However, it can likely result in sub-optimal backhaul planning and deployment for signal transmission to small-cells from the core network.

Conversely, LoS connectivity from wireless backhaul network gets severely restricted within shorter areas. It happens as long-distance LoS transmission in urban areas is complex and prone to signal losses due to lack of LoS link between backhaul and small-cell [31]. Also, specific wireless frequencies are prone to higher on-air attenuation due to gas molecule resonance in the air, causing further signal attenuations [38, 47]. Such atmospheric signal losses are also influenced by long-distance transmission paths, thus inducing the LoS backhaul option somewhat infeasible for more extensive coverage areas. Therefore, for long-distance area coverage provisions, the NLoS signal from the wireless backhaul network can be considered a viable option. Additionally, PtMP wireless backhaul is a good selection for better coverage compared to PtP connections. However, both PtMP and NLoS have a low capacity issue due to signal division in multiple transmission flows towards multiple small-cells for the former and restricted wireless signal spectrum availability for the latter [31].

Capacity attainment: One of the primary goals of small-cell deployment is to provide additional capacity to end-users in heavy hour traffic, future expansion and statistical variations of the network. Therefore, backhaul provisions must not create a bottleneck low capacity scenario from the core network to small-cells. For wired backhaul solutions, radio resource sharing, bandwidth availability and Signal-to-Interference-and-Noise Ratio (SINR) due to the modulation scheme applied in signal transmission affect the capacity of such backhaul options. However, wireless backhaul dimensioning to tackle worst-case transmission scenarios and

provide higher capacity can result in higher deployment expenses. Therefore, dimensioning backhaul networks should be based on quiet time peak cell throughput and the busy time mean cell throughput of the teletraffic signals [44]. The idea would be to design and optimise the backhaul option in terms of the busy time mean cell throughput. It is done so that each small-cell can experience an average signal quality, with less delivery cost associated with it, and then get a fixed signal resource amount to support attached end-users. However, this will ultimately reduce the capacity of backhaul towards small-cells and defeat the purpose of providing the necessary amount of capacity to end-users through small-cells [31].

Data synchronisation: A backhaul system should provide frequency and time synchronisations towards the small-cell transmission to ensure that signals are transmitted within their allocated communication channels. It would also ensure compliance with spectrum licence policies and system requirements. Time synchronisation is also critical for ensuring TDD systems' efficiency to mitigate interference between the downlink and uplink signal streams of small-cells physically adjacent to each other. Additionally, it would enable specific transmission-related features such as CoMP transmission/reception and enhanced inter-cell interference coordination (eICIC) [31]. One example of a timing and synchronisation tool would be the Global Navigation Satellite System (GNSS), which suffers from attenuation issue due to obstructions in transmission from the satellite in the sky [35]. Therefore, a backhaul solution to provide timing and synchronisation can be a more viable option due to its reliability. Newer technological solutions to timing and synchronisation methods such as over-the-air synchronisation techniques, local synchronisation server deployment or hybrid solutions combining such methods can ease the challenges of timing and synchronisation services to small-cells [48].

Cost optimisation: Since the backhaul part adds to a significant portion of small-cell deployment cost, it is essential to prioritise the cost-effective optimisation of backhaul deployment. The aim is to reduce the small-cell backhaul deployment cost to about 10% of a macro-cell backhaul. For small-cell backhaul total cost of ownership, the two primary components are capital expenditures (CAPEX) and operation expenditures (OPEX), further categorised into initial and ongoing (annual) costs. CAPEX initial costs include Ethernet switching, antennas and waveguides, and additional equipment costs, while annual expenditure can comprise backhaul upgrades and expansion costs. The OPEX initial expenses include costs of different components such as design, installation, commissioning of the network, spectrum

licensing, site development, site permissions, site analysis and upgrades. Such CAPEX and OPEX costs differentiate for wired or wireless backhaul solutions. The wireless backhaul costs would include expenditures for power connection cost per site, radio frequency (RF) works, site router deployment, annual maintenance and management costs per link. The wireless backhaul CAPEX costs are influenced by the backhaul network architecture, whether PtP or PtMP [49].

On the other hand, wired solutions see factors included such as fibre cost per metre, cable cost per site, DSL outdoor modem, and Ethernet leasing. The discussion above shows that it is crucial to minimise the cost of backhaul deployment to small-cells effectively. It can be achieved using backhaul design optimisation, reducing the antenna size, introducing advanced Adaptive Coding and Modulation (ACM) schemes and implementing mesh network architecture. However, these methods are subjected to research challenges in the future for appropriately finding solutions to efficient cost minimisation of backhaul deployment [31].

1.3. **Motivation of research**

We first measured and evaluated the 4G cellular network small-cell deployment and studied the fibre backhaul layout within our research work. Afterwards, both small-cell deployment and fibre layout were planned appropriately to optimise small-cells connectivity, coverage and capacity while ensuring appropriate cost and energy consumption efficiency. This optimisation approach was more generalised and envisioned regardless of the type of cellular network, either 4G or 5G, considering the influence of cellular signal propagation within our small-cell planning approach. Besides, we looked at the aspect of spectrum refarming by assigning appropriate frequencies to each selected small-cell location, based on the 5G cellular technology this time. It also addressed the user data consumption requirement by ensuring appropriate capacity is provided via each selected small-cell location within a particular cell coverage area that conforms to the frequency assigned to each such small-cell. These would incur the requirement of developing an optimisation framework amalgamating the previously mentioned optimisation elements to plan the small-cell architecture and fibre backhaul layout based on existing infrastructure. The intention would be to use mathematical algorithms to appropriately account for the related features and build an optimisation outline.

Therefore, such an optimisation context would be employed as a general benchmark, adequate for any small-cell-optical backhaul scenario.

Despite effective potentials in supporting data communications & networking growth capacity, small-cell deployment within heterogeneous networks can face significant practical implementation issues.

- Presence of obstructions between the transmitter and receiver resulting in direct LoS path loss [50]

- For an almost flat terrain ground maintaining LoS, terrain variation of as low as 15 cm causing signal loss of over 10 decibels (dB), after propagated ray reflected from terrain ground with phase change [50]

- Street orientation and building blocks weakening signal reception for cell areas with a smaller radius, as the signal is reflected off them. Larger building blocks with higher building density causes more attenuation in this case, as an antenna is placed under average building height [51]

- Expenses incurred in small-cell deployment due to factors such as infrastructure design, additional equipment installation, current technology enhancements and backhaul technologies & resources [35]

- Network capacity enhancement capability of small-cells, through co-channel deployment, can lead to increased interference since many of the small-cells may share the same RF spectrum [20]

- Approximation of nominal macrocell coverage area to account for the influence of macrocell performance impact over small-cell deployment, in terms of maximum coverage of user population [37]

- Reduction in component, link & network level energy consumptions for wireless networks can be rather challenging while maintaining and enhancing network capacity. This approach indeed has become quite a bottleneck for telecommunication networks [47, 52]

- Cell location zoning and site acquisition restrictions along with long delay and high costs in obtaining proper location [53]

- Limited information on the precise location of traffic hotspots [53]

- RF spectrum management in case of spectrum refarming for small-cells [54]

- Small-cell selection accuracy for mobile terminals [53]

Since the project also intends to investigate optical fibre network as a possible backhaul solution for small-cell deployment, we would also need to investigate the issues with such a deployment affecting telecommunication network performance, as depicted below.

- High installation cost is proportional to distance, e.g. the more area is covered by such a network, the higher the cost [30].

- Implementing appropriate and necessary access medium technologies based on corresponding factors, e.g. geography, user distribution, bandwidth needs, expenses [55].

- Optimally choosing between the PtP or PON, as PTP offers more data-bearing capacity [55] through dedicated optical fibre connections among nodes. Here, PON is more cost-effective as one transceiver at the local exchange OLT connects with multiple ONU devices.

Some existing optimisation-based methods [6], [37] - [39], [43] are already proposed to address the difficulties mentioned above. It involves separate optimisation procedures for both small-cell and optical fibre deployment, along with their combined presence in terms of functionalities, as the project scope suggested. The cellular network optimisation process typically intends to observe, validate and enhance network performance. Numerous parameters are involved within network coverage and capacity offerings in any cellular network, requiring continuous inspections and rectifications. Additionally, the number of subscribers and the amount of mobile traffic continues to grow with time. It necessitates for the continuous network optimisation process, to upsurge network efficiency and ensure ample revenue generation [53].

Wireless network coverage areas or "cells" should connect with a proper backhaul infrastructure that is cost-effective, high capacity, robust, energy-efficient and future-proof. This network provides connectivity between these wireless cells and the core network [2]. Previous research initiatives have proposed the FTTN optical access network as a prospective backhaul solution to provide better coverage, enhanced capacity, minimal expenses [5], [34] - [36]. However, several other factors associated with such optimisation scenario are yet to be observed and studied. Such factors may include the influence of macrocell coverage over small-cell deployment and its applicability to be used as a backup, in case of connectivity failure between small-cells, specifically for this scenario above. Alongside this, the issue of energy consumption in such a deployment scenario is also of critical importance. Also, the

dataset used by these research works tend to work based on fixed real-life network deployment constraints, thus not resulting in a general optimisation benchmark.

Therefore, all these issues mentioned above can act as the driving factors to motivate us for deciding on this research project, as titled above. Hence, we decided on forming our intended research question of developing a comprehensive, optimised SCN planning framework incorporating the provision for dimensioning a corresponding backhaul network architecture.

1.4. Objective of research

This research project aims to properly plan a small cell network as an enhanced wireless network structure and optimise a GPON layout as a backhaul solution. The small-cell network will be planned and employed alongside the existing wireless macrocell coverage areas, optimally projected cost for this approach would be determined, and proper energy efficiency will be ensured in the process. This approach also tends to decide on optimal RF technologies as a transport strategy for wireless data. Therefore, using the locations of fibre node terminals and existing macrocell sites, the location of small cells can be optimally selected to maximise capacity and coverage. Ultimately, the cost optimisation technique would ensure cost-effectiveness by working with present optical fibre and wireless macrocell infrastructure.

This project's primary stakeholder would involve major national telecommunication operators and their respective users to develop a wireless network. Additionally, the maximised cost and capacity of wireless infrastructure would allow opening up fresh & sustainable business opportunities in the telecommunications market. Additionally, cost, energy, environment and future expansion provisions by this research idea ensures robustness and sustainability in addressing the future consolidation of the National Broadband Network (NBN) and the densification of the mobile infrastructures.

Successful execution of this research would enhance the utilisation of sustainable cellular resources and address the energy consumption of communication technologies. If the proposed approach of backhauling for the wireless network becomes the optimal cost and energy-effective backhaul solution, it will provide a strong foundation and backhaul design tool for future generation wireless networks. Alongside this, chances of building a more

environmentally sustainable, simplified and high-performance wireless-optical amalgamated network would emerge significantly.

Risks for this approach involve testing the possible small location optimisation constraints and functions to check their credibility and effectiveness for a real-life wireless network application. Additionally, since we cannot foresee the possible performance outcomes for this backhauling approach in real life, it is still quite uncertain to establish this backhauling infrastructure as the optimum solution in wireless networks. However, the risks would be paid off once this backhauling approach establishes itself in real-life scenarios, as it would then ensure reduced expenses of network deployment, energy efficiency, robustness, possible future expansion.

This research topic's estimated cost would involve using proper simulation software and computers mainly since it is a theoretical research approach. Therefore, free and open-source simulators can be used to minimise this software cost.

The estimated completion time for this research area was set as the duration of the research study candidature. This time requirement would be essential to exercise the theoretical knowledge, build up simulation software skills, and adequately implement the developed research work.

1.5. Thesis Contribution

Based on the literature review done within the scope of the thesis, it is evident that in recent years, several optimisation research initiatives have been proposed/performed over both small-cell network and GPON, separately or jointly. From the literature, it can be concluded that research scopes can still prevail over optimisation for small-cell network planning and positioning. Interestingly, the reviewed studies did not consider geographical aspects of optimisation for small-cell network designing, planning and positioning. Therefore, we initiate the SCN planning method primarily based on geographical terrain effects over SCN signal propagations. Then we expand the planning process based on proper backhaul connectivity, ample capacity serving, and appropriate wireless frequency refarming to attain a cost minimised SCN planning and dimensioning method.

In **Chapter 3**, for our initial-stage SCN planning, we considered the terrain slope characteristics, land elevations, and optimal antenna height in an urban area to optimally select

locations for small-cell BTS placement for the 4G cellular technology. In our proposed framework, we first select potential locations for a small-cell deployment over said urban area, considering factors such as elevation prominence, terrain slope influences over signal strength level, and urban structure positioning. Secondly, a standard amount of area for all cell sites is chosen within the typical urban area small-cell radius range [56], where different sizes of cell areas were studied for developing the cell planning framework. Thirdly, we tested signal strength and coverage ability for each cell site for the selected cell area. We applied path loss formulas discussed in [56-58] and considering an antenna height just under average building height [59, 60]. Finally, we discarded redundant cell locations from the initial results to satisfy the maximum limit of 30 cell sites per km^2 urban area [61] for a selected cellular carrier frequency and technology type. The work mentioned here has resulted in three publications so far, as discussed in **Section 1.7.1**. As mentioned in this **Section 1.7.1**, the conference paper listing me as the first author incorporates my original works, forming about 80% of the publication. It included problem formulation, case study implementation, outcome generation, and paper writing guidance of the listed co-authors. The other two publications where I am co-author have been high-level journal and conference publications that incorporated critical analysis of my work in **Chapter 3**.

Next, in **Chapter 4**, we shift our focus towards developing a proper backhaul dimensioning and optimisation method, as an expansion to the SCN planning mentioned in **Chapter 3**. This optimised backhaul architecture provides connectivity between the core telecommunication network and the pre-selected urban area small-cell nodes, chosen through the initial automated SCN planning process. This optimised architecture is a Fibre-to-the-Home/Fibre-to-the-Premise 10Gigabit Passive Optical Network (FTTH/FTTP-10GPON) [62] planned over an existing Point-to-Point (PTP) optical fibre network that utilises existing fibre infrastructure and routes to interconnect different type of network nodes. The PTP network nodes are Central Office (CO), Fibre Access Point (FAP), and Remote Terminal (RT), while 10GPON nodes include OLTs, optical splitters, RTs similar to PTP and Optical Network Terminals (ONUs). To map the intended 10GPON over the existing PTP, we choose a subset of pre-existing CO locations for OLT installations, a subset of existing FAP locations for splitter installations.

Furthermore, in **Chapter 4**, a subset of PTP RT locations nearest to the pre-selected small-cells serves as a set of RTs for the 10GPON, and finally, ONUs are co-located alongside

the planned small-cell locations. The proposed optimisation framework utilises the Capacitated Facility Location/Network Design Problem (CFLNDP) to determine an optimal 10GPON network topology from existing PtP nodes and links, where selected nodes have required data serving capacities constraints. Hence, the subset of CO and FAP locations is chosen so that the sum of distances from each RT to its nearest FAP and each FAP to its nearest CO are minimised. The sum of all the node equipment installation (facility opening cost) would be reduced too, thus minimising overall network implementation cost.

In **Chapter 5**, after the SCN planning and backhaul dimensioning tasks are completed in **Chapters 3** and **4**, we aim for a unified optimisation process, engaging both the optical and the wireless part involved in the SCN planning. This process maps the optimised backhaul optical network and selects potential small-cell locations based on minimised distances among different levels of nodes within this whole convergent network. This optimisation framework can incorporate further optimisation attributes and constraints to provide a complete convergent and optimised small-cell and backhaul planning framework, more specifically to accommodate the 5G SCN planning process. This framework expands from the previously attained backhaul planning framework based on the previous CFLNDP optimisation problem, involving only the optical part of the total network architecture. The framework also includes minimising the sum of distances from each selected SC location to its nearby RT location and all SC node equipment installation costs. As this framework is primarily developed towards improving 5G SCN planning, we do not incorporate 4G SCN attributes within this framework.

Finally, in **Chapter 6**, we expand the planning into appropriate SCN dimensioning, based on population-based capacity attainment and appropriate frequency assignment for the wireless SCN portion. This work is in line with works done in **Chapters 3**, **4** and **5** as direct expansions to these chapters' research tasks. The idea was to construct a framework that would incorporate both SCN planning and a corresponding backhaul dimensioning within the same framework's premise. Hence, we started with a standalone 4G network SCN planning in **Chapter 3**, then connected this individual framework with a supporting backhaul planning in **Chapter 4**. Afterwards, we enhanced this **Chapter 4** framework, which was the consolidation of two individual planning frameworks, by combining an SCN and a backhaul planning within the scope of one single framework approach, as seen in **Chapter 5**. Ultimately, in Chapter 6, we further improved the Chapter 5 network planning framework by including the provisions of maximum population coverage and assignment of appropriate frequencies based on each

selected small-cell location's capacity managing ability. In addition to applying the theoretical ideology of the CFLNDP problem, we also included attributes from the maximal coverage problem [63] to ensure appropriate user population coverage is maintained within the SCN coverage radius restriction. Similar to previous work, the backhaul part is planned based on the CFLNDP problem. The SCN planning ensures that the maximum number of users within the SCN planning are covered optimally. This framework utilises 5G SCN planning, and therefore, 5G signal propagation characteristics are considered. Once user population coverage is finalised, appropriate frequency assignment is performed for each selected SCN node, based on its coverage area and user assignment capabilities. This frequency assignment process is termed frequency spectrum refarming, which assigns available wireless frequency spectrum bands primarily used in other communication technology such as satellite communication, military communication, and health services. This work's significant elements will be included within my publication listed as in progress in **Section 1.7.2**, where more than 80% of the contributions to come from myself. The rest of the contributions will be technical guidance and writing reviews provided by the respected co-authors mentioned.

1.6. Thesis outline

The following is an outline of the thesis for the above-titled project-

- Chapter-1 provides an introduction and scope of the project, highlighting and defining key background aspects within. It states the motivation and objective of the project and highlights a proposed thesis outline.
- Chapter-2 forms the literature review section to introduce small-cell network planning, backhaul dimensioning and optimisation. The chapter looks at both small-cell and PON optimisation procedures, individually and in a combined way. It investigates explicitly the related recent works done.
- Chapter-3 marks the start of describing the actual theoretical work done within the scope of this project. It emphasises the 4G wireless network small-cell planning framework based on path loss effects due to geographical terrain characteristics. It also includes results from corresponding case studies within each framework, highlighting successful implementations. The details of tasks performed for the accepted paper at the OECC/ACOFT 2014 conference has been described in chapter 3.

- Chapter-4 includes combining a small-cell planning framework in chapter 3 with the backhaul dimensioning and optimisation framework. It discusses the backhaul connectivity with the planned small-cell network, based on Gigabit Passive Optical Network utilising existing equipment and resources.

- Chapter-5 expands on the optimisation framework discussed in chapter-4, intended to design a Gigabit Passive Optical Network backhaul combined with a small-cell network. The idea would be to combine the two network parts into just a basic optimisation framework that plans both the small-cell network and backhaul network, based on minimising connectivity and installation costs primarily. It can then serve as a platform for an enhanced 5G SCN and backhaul planning.

- Chapter-6 is based on enhancements to the basic heterogeneous network planning framework of chapter-5. It focuses on implementing a 5G SCN planning framework based on capacity & coverage enhancement and cellular frequency spectrum refarming.

- Chapter-7 is the concluding chapter, discussing project prospects such as overall project summary, a future investigation that can be endured during practical formations, and an overall conclusion to the research work presented

1.7. List of publications

1.7.1. Work published

- Akhter, I., Ranaweera, C., Lim, C., Nirmalathas, A., & Wong, E. (2014, July). Small-cell network site planning: A framework based on terrain effects and urban geography characteristics. In *2014 OptoElectronics and Communication Conference and Australian Conference on Optical Fibre Technology* (pp. 422-424). IEEE.

- Nirmalathas, A., Ranaweera, C., Wang, K., Yang, Y., Akhter, I., Lim, C.,... & Skafidas, E. (2015, March). Photonics for gigabit wireless networks. In *2015 Optical Fiber Communications Conference and Exhibition (OFC)* (pp. 1-3). IEEE.

- Wong, E., Akhtar, I., Abeywickrama, S., Ranaweera, C., Lim, C., & Nirmalathas, A. (2014, August). Towards a Framework for Small-cell Network Planning. In *Proc. PIERS 2014, Session2A10 SC3: Advances in Optical Networking: Parts 2*(p. 544).

1.7.2. Work in progress

- Akhter, I., Ranaweera, C., Lim, C., Nirmalathas, A., & Wong, E. (2021). Small-Cell Network Planning and Backhaul Dimensioning by Cellular Spectrum Refarming Provisions.

This page is left intentionally blank

Chapter 2

Literature review

2.1. Introduction

The optimisation techniques over topics such as small-cell networks and corresponding backhaul option have been subjected to numerous research works so far. Before we proceed with our research project, it is essential to study and review prior research work on SCN and backhaul optimisation studies. A proper literature review can help us explore research works related to our proposed studies to understand the topic better. It would also help us identify gaps and future direction from previous studies to help us built our research question more appropriately as a novel idea. It would also help us establish the importance of choosing our research topic and justify our proposed research methodology. Overall, it will help us accomplish our research in an organised, methodical, and successful manner. Therefore, in this chapter, we discuss prior research studies closely related to the subject matter involved with our research. The aim is to determine research works already done on topics closely related to our research and justify researching our selected topic. Small-cell technology's very nature makes it necessary to optimise procedures performed for planning and deploying such networks. According to recent studies, it is evident that optimised small-cell deployment has become one of the most critical factors in ensuring proper cellular network performance. Several attributes have been significant influences affecting the planning and deployment of small-cell networks; hence they have been extensively reviewed throughout this chapter. The literature review process has been divided into the following segments.

- Small-cell network optimisation methods
- Small-cell backhaul optimisation scenarios
- Small-cell network planning approaches with backhaul dimensioning
- Small-cell spectrum refarming analyses

2.2. Small-cell network optimisation methods

Several facets of small-cell network optimisation scenarios have emerged in recent times, producing quality research literature in the process. For our proposed research work contents, we are reviewing some of such works, categorised as follows.

- Design Optimisation
- Capacity Optimisation
- Coverage Optimisation
- Energy Optimisation

As we are proposing our small-cell planning and optimisation approach, we review corresponding previous works to attain the above attributes in this chapter.

2.2.1. Design Optimisation

In wireless cellular networks, small-cells are deployed alongside existing macrocell infrastructure, forming a "Heterogeneous Network" for wireless communication technology [6]. It is of much importance that such deployment should be optimally planned so that it can support the necessary cellular network load. Recent focus has been directed towards small-cell network design optimisation aspect, and some of these attempts include-

- 3GPP heterogeneous deployment
- Adaptive architecture deployment
- 5G physical layer radio design deployment

❖ 3GPP heterogeneous deployment

A much notable and elaborate discussion on small-cell deployment optimisation has been presented in [64]. It states that a heterogeneous network comprises radio nodes with different radii and functions, namely the larger macro and the smaller micro and picocells, to optimise and enhance coverage, capacity, and overall network performance. Here, some small-cell nodes are positioned within single or multiple overlapped macro cell coverage areas to enhance capacity by lowering teletraffic activities. Some small-cells are located outside coverage areas to extend network coverage and accommodate more teletraffic to pass through the cells. Additionally, single or multiple SCNs are sparsely placed much farther from other

SCN groups/clusters to cover enough for the indoor/outdoor hotspots having the highest data usages in smaller areas. Concurrently many small-cell nodes are densely deployed with much fewer spaces to support higher data traffic over a comparatively larger region [64].

❖ Adaptive architecture deployment

Another unique network deployment approach was observed in [65] that proposes a new small-cell architecture that re-designs topologies and re-distributes frequency bands, adjusts with varying traffic demands, and aids in minimising interference. The proposed architecture includes distributed small-cell nodes and co-located Baseband Units (BBUs). These SCNs connect to the BBUs using a new wireless-switch for adaptively switching the connections between the SCNs and BBUs. In this deployment, SCNs using different frequency sub-bands can share individual BBUs, to associate the unconnected SCNs by sharing the sub-bands of the connected SCNs. It is achieved through a newly proposed switch algorithm, which accommodates increasing spectrum utilisation by 23.5%. It also improves the minimal satisfaction factor (MSF) for traffic demands by 144.2% and spectrum utilisation enhancement by 60.9% for small-cells with a radius of 0.5 km. This research also projects that the proposed architecture utilises a smaller number of BBUs, thus saving signal processing energy and mitigating the investment and energy consumption of the BBUs by up to 40%. Finally, small-cells deployment schemes allow for much-enhanced spectrum and energy utilisation compared with current small-cell network architectures.

❖ 5G physical layer radio design deployment

The design optimisation aspects were extended towards enhanced small-cell technology, e.g., 5G cellular communications. Such an example is evident in the works of Mogensen *et al.* [66], who developed a 5G design optimisation deployment framework based on eliminating compatibility constraints with past mobile technologies and forming the design primarily on the physical layer level. The design's primary aspect considers forming a new TDD-based 5G data transmission physical layer design with a proposed new data frame structure. The frame structure achieves low latency by constructing a data frame with a 0.25 ms transmission duration and optimised scheduling and HARQ design. This transmission duration leads to flexibility in UL/DL data direction as they can be changed every 0.25 ms to adapt to the fast-changing traffic demands, which is unforeseen in traditional LTE cellular

technologies. However, this rapid variation in transmission can lead to link/rank adaptation challenges causing unpredictable interference patterns, and the writers aimed to tackle this challenge in upcoming works. They also proposed the current mechanism based on handling such interference issues as possible solutions to this interference issue due to rapid traffic adaptation. An example of such a solution can be the frequency reuse mechanism for femtocells shown in [67]. The design also incorporated distributed synchronisations among distributed Access Points for coordinated operations such as interference reduction and frequency coordination. This work also discussed the influence of using Interference Rejection Combining (IRC) receivers for improving data transmission rates in high interference cases. Finally, for integration with IPV6 networks, an Ethernet-over-Radio link layer implementation is proposed over the TDD design in this research.

2.2.2. Capacity Optimisation

Several approaches have already been evaluated to optimise small-cell deployment in terms of capacity enhancement. In general cellular network terms, capacity in a cell is usually determined by several acknowledged calls or maximum sustainable data rate in a cell [68]. With the increasing demand for network capacity expansion to support projected enormous communication traffic growth [9], optimal solutions for capacity have also been emerging as an essential element within small-cell architectures. Recent capacity optimisation studies include-

- Cell sizing options
- Capacity relief provision
- Coverage-capacity joint enhancement
- Trade-off approach
- Capacity-energy joint approach
- Self-optimisation in capacity enhancement

❖ Cell sizing options

One example is the Optimal Cell Size (OCS) scheme for a 3rd generation time division duplexing Wideband Code Division Multiple Access Multi-hop cellular network (3G TDD W-CDMA MCN) multi-cell environment, as stated in [68]. With specific user distribution, demands and a particular cell capacity function, it determines the desired optimal cell sizes to

maximise the system throughput by balancing coverage and capacity. Their simulation model contained 3-Cells having 25 source nodes individually and multiple relaying nodes ranging from 0 to 160 in number, incrementing at a rate of 40 nodes. The source nodes and relaying nodes were consistently placed over a circular radius of 1.1 km with a BTS at its centre. The source node and relaying node are separated in communication to avoid unwanted mobile node relay signals during experimentation. The paper's simulation results focused on different cell sizes, e.g., 250 m, 390 m, 560 m, 780 m and 1100 m, to achieve capacity support for 1035 828 621 414 207, respectively. Additionally, the authors managed to show that this proposed OCS always calculates the optimal cell sizes for different nodal densities and traffic flows and assigns the source nodes (points) optimally among the three BTSs.

❖ Capacity relief provision

In a recent study [52], authors primarily discussed small-cell's ability in network capacity relief. They stated that using real traffic data from a few (1 to 3) small-cells within less than one-third of the busiest larger network sectors can increase the corresponding network capacity three times. Also, if small-cells are deployed within up to 30% of a cellular network's coverage area, the network's capacity could be tripled or at least be doubled without any spectrum or technological upgrades to existing infrastructure. It is usually achieved through precise deployment and planning of such cells by precise mapping of traffic hotspots intended to be covered with proposed small-cell deployment. Additionally, the study's data showed that more than 50% of cell sector data traffic gets generated within less than 25% of the cell sector area. It eventually emphasises deploying small-cells with much fewer coverage areas than a traditional macrocell.

❖ Coverage-capacity joint enhancement

The works presented in [69] shows a combined coverage-capacity optimisation in 5G Ultra-dense Heterogeneous networks (HetNets), as it represented a combined Coverage and Capacity Optimisation (CCO) and Load Balancing (LB) solution. Since CCO and LB are conflicting operations, a novel load aware user association methodology was designed through convex optimisation to ensure conflict-free operation of CCO and LB. The solution adopted genetic algorithms, sequential quadratic programming, and pattern search and accounts for coverage uncertainty from shadowing by applying stochastic approximation. By comparisons

with similar CCO-LB solutions, it was found that the proposed CCO-LB solution offered particular enhancements in terms of throughput, load distribution and spectral efficiency through a practical implementation framework. The study also emphasised the need for small-cell optimisation approaches combining SINR, signal strength and cell loads. The proposed optimised CCO-LB solution included Self-Organising Network (SON) functions such as antenna tilts, transmit powers, and Cell Individual Offset (CIO) as optimisation parameters. This solution provided better results than other similar studies, as it employs combined optimisation of all parameters that affect coverage and cell association hence shifting network load and achieving increased capacity. The solution in this work also enforced a smarter load aware cell association mechanism and better results since the optimisation process incorporated CCO by throughput maximisation. Additionally, LB in the objective function was applied by utilising a geometric mean.

❖ Trade-off approach

In [70], a trade-off approach is exhibited involving the cost, energy consumption and capacity within cellular networks. For this, a capacity estimating equation, along with theoretical expressions for cost and energy consumption, has been generated for both macro and smaller cells, which are later proven feasible with appropriate simulation results. The authors of the paper emphasised the trade-off model to prevent capacity saturation, leading to ambiguous optimisation outcomes [71]. This paper utilised the following formula for a one sector omni-directional pico (small) cell-

$$C_{cell,1} = BW \log_2 \left(1 + \frac{F_{(rcell)}^{-\alpha}}{2_{(rcell)}^{-\alpha}} \right)$$

$$= BW \log_2 \left(1 + 0.67 \frac{1}{2} \right)$$

$$= 0.4 BW$$

where,

BW = Bandwidth available in a cell-sector

r_{cell} = Radius of the cell

F = 0.67

Here, F is an adjustment factor for LTE [72] to avoid over-optimistic results and biased optimisation [71]. Then [70] also points out that network capacity can be enhanced explicitly by deploying ten pico cell sites per square km. The paper compared the small-cell deployment of a dense number of low-power 1-sector omni-directional picocells with a reference LTE homogeneous network. This deployment included 3-sector 2×2 Space Frequency Block Coding (SFBC) co-frequency microcells, generally with a 500 m radius, thus deploying two cell-sites per square km. The reference network's capacity was recorded at 50 Mbit/s/km^2 for a 20 m Hz frequency band. It was found out that as the small-cell deployment's cell-density increased from 1 to 16 per square km, network capacity density improved favourably. However, since that did not necessarily resort to cost and energy efficiency, the Capacity Energy Cost (CEC) trade-off was envisioned. This relationship effectively expresses that an optimal scenario can be reached for increasing network capacity within a minimal cost incurred (approximately 2.5 cell-sites per km^2 with 400 m radius), with higher energy consumption. Alternatively, the approach can reduce up to 31% operational energy by implementing a higher density of smaller and lower-powered cell-sites for an additional 14% cost for extra equipment. Thus, it clearly shows an evident trade-off between decreasing energy consumption and carbon emissions, with the operating costs [70]. Ultimately this led to a capacity enhancement with a minimised cost experienced.

❖ Capacity-energy joint approach

Another research initiative has been emerging through concentrating on small-cell network capacity increase with better energy efficiency. For example, work presented in a recent paper tends to derive a joint power and subchannel allocation scheme in dense femtocells environment to meet increasing communication capacity needs. Once the scheme was developed, appropriate simulation-based experiments were performed to check on capacity improvements for femtocells downlink. The obtained results then exhibit that this proposed scheme enhances system capacity by 5-15% compared to Improved-Iterative Water-Filling (I-IWF) scheme offering subchannel allocation for MSs. Also, a 20-70% capacity enhancement is observed compared to IWF only scheme that iteratively allocates power in a sub-optimal manner concerning interference from nearby transmitters [73].

Additionally, a recent research initiative for capacity optimisation was performed based on power and channel assignment within a femtocell (small-cell) [7] to enhance either the total

network capacity or the small-cell's minimum capacity. This publication was focused on an approximation algorithm for assigning channels and power to femtocells for total network capacity enhancement. Another algorithm was also introduced for individual capacity enhancement for each femtocell. Both these algorithms were then expanded for multiple consecutive channel assignments within current communication protocols. Finally, appropriate simulations were performed, and the results were shown to be near the upper bound on the optimal solution region [74].

❖ Self-optimisation in capacity enhancement

Self-optimisation of networks can significantly aid in capacity optimisation within the small-cell deployment. In a related research study, authors focus on a SON functional architecture (FA) to extend small-cell deployment capacity. The paper states that the opportunistic network (ON) scenarios can include self-organised capacity enhancement features through opportunistic modifications over small-cell deployment. The hypothesis intends to estimate the optimal user assignment to cells and Resource Blocks (RBs) to users, alongside proper power level distribution for cells, for enhancing network capacity. The authors also focus on traffic offloading via ONs involving small-cell deployment as a capacity optimisation method [75].

2.2.3. Coverage Optimisation

Coverage optimisation is also an essential element of a small-cell network that aids in significantly improving performance and efficiency. Different approaches have emerged in recent years within this aspect-

- Cell coupling-based coverage enhancement
- Genetic algorithm-based coverage optimisation
- Regression-based optimisation
- Self-organising coverage enhancement
- Location coverage optimisation
- Small-cell backhaul-based optimisation approach

❖ Cell coupling-based coverage enhancement

One algorithm-based research work advises for a decentralised algorithm providing femtocell coverage area optimisation. The algorithm updates the femtocell's pilot channel (The channel that associates a mobile station to the corresponding cellular network [76]) transmission power to maintain user load for the collocated femtocells evenly. It minimises coverage not-spots and eventually decreases this channel transmission power. This paper showed that this algorithm could offer a performance gain of 18% for supported user traffic compared to the constant transmission power. The algorithm was also able to significantly reduce transmission power by an impressive 80%, thus decreasing the possibility of pilot channel power leakage to adjacent cells [77].

❖ Genetic algorithm-based coverage optimisation

Similar algorithm-based approaches for small-cell coverage optimisation has also been investigated. It can include the use of Genetic programming (GP), an evolutionary computation (EC) technique for automated problem-solving without user input or advanced knowledge of solution structure. In a related study, this GP experimentation incorporates specific function & terminal sets, fitness function and specific evaluation scenario with running parameters. The experimentation results demonstrate that the proposed algorithm can optimise femtocell coverage to balance the load, eradicate coverage gaps and manage coverage overlap internationally through localised dimensions and statistics. The paper also suggested possible extensions to this GP-approach for producing algorithms with mathematical functions for better and precise outcomes. Such a GP approach can also aid in-network cost reductions and improved network adaptability [78]. In another initiative, a Genetic Programming (GP)-based approach for automatically deriving a distributed algorithm is proposed to dynamically optimise coverage of a group of small-cells [79].

❖ Regression-based optimisation

Expansion of the idea presented in the paper mentioned above by Ho *et al.* [79] is projected in both [80] and [81]. A regression-based optimisation approach for small-cell coverage is proposed, which derived an expression for individual small-cell's power settings in a network, with Grammatical Evolution (GE). This work focused on a grammar-based Genetic Programming (GP) setup that can modify solution structures and implement domain

knowledge within the findings. The authors here also describe that maximising small-cell coverage and minimising power consumption can be achieved by allowing the proposed algorithm to modify and control the femtocell's power settings. This work leads to automatic equation formation of coverage optimisation for cellular networks. Since the primary focus was on GE, a grammar-based GP [82], its behaviour in a dynamic real-world environment was also investigated. The GE was also modified, and a non-weighted fitness function was implemented to diversify the obtained optimisation solution. The authors also suggested implementing hybrid optimisation approaches for better results in the future [80]. Here, domain knowledge implies a combination of field-specific declarative, procedural and conditional knowledge [83]. The differences between [83] and [79] are that [83] faces a lesser amount of constraints and also uses different fitness functions.

Similarly, another work focuses on coverage optimisation using a genetic algorithm for a centralised self-optimising enterprise network with multiple femtocells. It is a heuristic approach where this genetic algorithm is based on a multi-objective function for dynamically updating pilot channel powers for the group of femtocells within the network. The work presented exhibited significant coverage optimisation in global traffic distribution and interference amounts between adjacent femtocells for any air interface. The paper shows that its centralised approach can achieve similar results compared to the de-centralised genetic programming-based optimisation done in [79], with the same objective function. This algorithm was then applied through simulations with appropriate network data and effectively mitigated coverage gaps through appropriate pilot channel power assignment. It also limits the coverage in case of coverage overlaps to minimise interference. The algorithm reaches an optimal or sub-optimal coverage solution within a few seconds, much applicable to a real-life enterprise network scenario [81].

❖ Self-organising coverage-capacity enhancement

The research work performed in [84] developed a self-organising capacity and coverage optimisation process for 5G cellular networks, which utilised the power adaptation method to enhance the coverage and capacity. This optimisation method comprises both self-configuration and the self-optimisation provisions for a 5G small-cell network. These two parts would modify the transmitted power of a small-cell or, as termed in 3GPP language, the Home eNodeB (HeNB), for coverage optimisation in different operational stages of the HeNB. Once

powered on, the small-cell or HeNB would detect the Reference Signal Received Power (RSRP) of a nearby macrocell. Next, it would record the presence of neighbouring HeNBs and then would use this information to determine a suitable transmit power for itself. As in this self-configuration process, the coverage area boundary information cannot be specifically obtained. Thereby, during the self-optimisation phase, the Home User Equipment (HUE) data can help determine the coverage area boundary information.

When a HUE enters a building, it faces a sudden path loss in its signal levels, indicating the coverage area's boundary. This information can also aid in regulating the transmit power for a small-cell. The optimisation study was performed over a suburban and dense urban area to simulate the optimisation model deployment effect. This optimisation study targets to improve the coverage ratio of macro eNB more than the required coverage ratio for a 5G network, then maximises the coverage ratio of the HeNB for a 5G network. Ultimately, this study's works showed that the optimised coverage ratio of a macro eNB is closer to the required coverage ratio of 90% of a 5G macro eNB.

Additionally, results show that a small-cell's optimised coverage ratio appears much larger than that of the most fixed transmitted power scenarios. The study obtains said ratio through the proposed power adaptation scheme within this study when a macro eNB can achieve its coverage goal. Moreover, the optimised coverage ratio was similar when the transmit power was at -20dBM. The reason for observing such a low transmit power is the dense placement of small-cells/HeNBs within the simulation premises. Here, the optimisation should keep the transmit power at a much lower level to tackle the high interference issues for a dense placement of small-cells/HeNBs. If HeNBs were placed further apart, the transmit power would have been higher than -20dBm for proper signal levels to reach the edges of the coverage area boundary for each HeNB.

❖ Location coverage optimisation

MCLP [63] is a location-based optimisation process that ascertains the smallest number and locations of facilities to confirm that all demand points are covered within a pre-set maximal service distance from a selected facility. Thereby, for a maximal service distance, the demand served, say population within that distance, are attended by a fixed number of facilities. Here, this population would be associated with a demand node, e.g., a location over the intended case study area. This scenario would serve as much demand, e.g., the population

within the service distance, using a fixed number of facility locations. Such a demand node will only remain uncovered if the closest facility from that node is located at a distance greater than the intended service distance. This maximal coverage problem [63] constraints ensures that one or more facilities are located within a demand point's intended service distance. In this case, the number of facilities selected to cover the service distance population should be fixed. Secondly, the solution to this problem should calculate the maximum amount of the population to be covered and the fixed number of facilities to achieve this maximal coverage. Such a maximal coverage problem [63] can be performed by either a heuristic approach or Linear Programming (LP). One such heuristic solution method is called the Greedy Algorithm (GA), which allows for a maximal cover for a fixed number of facilities within a given service distance.

For this algorithm, the optimisation process starts with an empty solution set and then one at a time, the most optimal facility locations are added to this set. Another heuristic approach would be the Greedy Adding with Substitution (GAS) Algorithm. The GAS algorithm selects new facility locations at each iteration as similar to the Greedy Adding Algorithm. However, it also improves the solution at each iteration by replacing each facility selected one at a time with a facility at another "unoccupied" site. If such a solution improvement is possible, it will imply that the newly selected facility location would provide a much better solution to the objective function. The issue with both these algorithms is the uncertainty of achieving globally optimal solutions. Hence, another solution option, the LP, can be applied that ensures global optimality of the solution. This outcome can be achieved by changing the two primary decision variables to non-negative integers instead of binaries, as initially suggested in the maximal coverage problem formulation [63]. It means that the first and second variables can have values other than 0 or 1. Here, the first variable indicates that a facility has not yet discovered a demand node within the service distance. The second variable signifies if a facility at a site is selected to perform population coverage within the service distance. If total coverage is not possible through LP, there might be all-integer or fractional solutions to the facility indicating variable. Ultimately, the MLCP has been established as a robust method to ensure proper population coverage [63].

❖ Small-cell backhaul-based optimisation approach

Small-cell network optimisation scenarios have been depicted in [6, 37-39] is also exhibited in [85]. This work also justifies using PON as a small-cell backhaul by considering that higher densification of small-cells requires more connections per site. Therefore, the PON backhaul architecture sharing fibre and central office equipment can offer more connections as backhaul option to these high-numbered small-cells compared to traditional PTP gigabit Ethernet link that works as macrocell backhaul. Moreover, the corresponding optimisation hypothesis is tested over the optimised design of a residential GPON-based backhaul network for multiple realistic splitting ratios and then compared the outcomes to a PTP architecture. Residential GPON deployments generally have a 1:32 split ratio and the highest network reach of 20 km, constrained by link expenses. As the total downlink limit of GPON is 2.5 Gb/s, the authors considered a decreased maximum splitting ratio of 1:16 to maintain each small-cell's maximum simultaneous data rate of 150 Mb/s, with smaller splitting ratios. The split ratio reduction to 1:16 splitters provides an additional power reach of 3 dB for this GPON network, making the ratio adequate to support larger network wire centres [85].

2.2.4. Energy Optimisation

Alongside deployment, capacity and cost optimisation, ensuring energy efficiency through an optimal approach is crucial for small-cell networks. Such research initiatives have been much in context for recent years-

- Design-wise enhancement
- Power control approach
- Throughput-oriented approach

❖ Design-wise enhancement

A much-renowned research publication envisions design changes within wireless cellular RAN to enhance its energy efficiency. A simulation setup measures energy efficiency parameters of a simplified cellular RAN, e.g., total energy consumption, energy consumption ratio (ECR), energy consumption gain (ECG) and capacity density of a RAN, for both a small-cell architecture. Then the same architecture with sleep mode turns the inactive cells off. The ECR indicates energy consumption by a network's equipment for full-duplex throughput.

Additionally, the term ECG is used, which is the ratio of the energy of a large cell, and energy of a small-cell, for the same user density in a given service area. The smaller the cell, the less energy it consumes, making the ECG ratio larger. According to the paper's findings, applying sleep mode and decreasing cell sizes increases ECG much further. Thereby, reducing the cell area of a RAN and implementing sleep mode offered much less energy consumption and ensured better energy efficiency than normal mode, along with larger macrocell based deployment. Additionally, to serve the same user density for a given service area, energy consumption is reduced about 100 times with the same QoS for sleep mode inducing if 100 times more cells are implemented [86].

Another prominent example of network design modification highlights implementing a modified network design called fractional separation green (FSG) network. The authors stated that this proposed novel infrastructure could project a significant 50% decrement of energy consumption jointly, with three main advantages over established heterogeneous deployments. Such advantages included-a) Shrinkage in transmission overhead, b) Re-arrangement of flexible topology, and c) Significant design-based optimisation. As signalling transmission consumes about 44% of the network's total spent energy, the FSG scheme decreases signalling overhead. It enhances the air-interface efficiency for data transmission from 56% to 71%, allowing for a 5% energy consumption cutback contribution for the global network. FSG architecture also offers the chance of flexibly configuring or switching off nodes without coverage infringement. It eventually results in data and signalling separation of functionality framework. When this was implemented on a 24-hour daily traffic profile from the EARTH traffic model, it reduces about 50% of small-cell activities while retaining the same data rate, resulting in 20% -30% of energy saving over global networks. Then FSG can allow for up to 3 dB gain of Power Amplifier (PA) efficiency and 40% improvement on corresponding average efficiency. It results in 100% energy efficiency upgrading for PA input power, 30% energy saving for macro base station alone, without improvement of other equipment.

Similarly, appropriate small-cell density selection within FSG also results in a 30% save of energy consumption. On top of these two approaches, this network scheme's hardware-specific enhancement can allow for further 200 W/km2 energy consumption reduction, which is about 15-20 in percentage. The traditional saturation region for small-cell heterogeneous networks can be updated from 40 Mbps/km^2 to 200 Mbps/km^2, allowing for less power consumption for a higher traffic saturation rate [87]. Additionally, a novel deployment

algorithm concerning issues arising from both the renewable power source base stations and the cell zooming technique is used in heterogonous deployment. The paper proposes that this algorithm successfully reduces power consumption, minimising carbon emission rates and operator costs significantly with evidence of retaining adequate spectral efficiency and coverage for a heterogeneous (HetGen) deployment. This work's experimental setup focused on three already established and investigated green cellular networks-heterogonous deployment problems, implementing renewable base stations and transmission power modifications. The task was to combine them to propose a unified solution through the said algorithm. However, the proposed algorithm experimented upon macrocell deployment, not a proper HetGen arrangement. It investigated possible effects, ignored inter-cell interferences between base stations and the possible trade-off between the capital expenditures and operational expenditures [88].

The research work done within the scopes of [89] explored a power optimisation approach in terms of a deployment point of view to ensure a proper transition from 4G to 5G technology. Since in 5G, the number of users would be much higher, utilising both transmit and receiver power becomes more necessary. Therefore, this study offers the implementation process for a power consumption optimisation scenario for 5G multiple-input and multiple-output (MIMO) and small cell. This study also determines the optimal number of small-cells and their appropriate locations for a range of deployment scenarios for two cases. The optimisation process determined optimal energy levels for the small-cells and maintained the QoS at the user end. The study showed that three Small-cell Arrangement (SCA) deployment arrangements would provide low-cost-optimal coverage and less power consumption for high user density. It would be accomplished with heterogeneous Urban Macro (UM) scenario for case 1 and UM presence scenario in case 2. Then in case 2, 8 and 4 SCA deployment arrangements for sub urban macro (SUM) and rural macro (RM) scenarios were provided with low cost and optimal power consumption in case 2.

❖ Power control approach

A group of researchers have extended the idea of [86] to enhance further the sleep mode technique for small-cells using appropriate algorithms. This approach allows the small-cell BTS hardware equipment to be perceptively inactive in idle conditions so that the cell energy consumption is regulated concerning varying cellular traffic load. The algorithms are based on

three different strategies-small-cell driven, core network-driven and user equipment driven approaches. When tested on a combined voice and data traffic model, the algorithms could project approximately 10–60 per cent of energy savings in the network than a no-sleep mode. However, the power consumption model implemented in the paper only involves energy ingestion of radio access elements within the network, not the user equipment (UE). Due to small-cell deployment, the transmitter-receiver is placed further closer, ensuing in decreased transmission power and extended battery life for UEs. For future research initiatives, the authors in the paper expressed their desire to concentrate on the aspects mentioned above. These included UE characteristics, backhaul energy consumption, the effect of energy consumption within random traffic flow in the network, alongside Sleep mode experimentations over real-life testbeds [90].

❖ Throughput-oriented approach

A research study for throughput-oriented energy optimisation focuses on the relationship between aggregated throughput and energy efficiency. This relationship was analysed over both a traditional outdoor macrocell-based network providing indoor and outdoor coverage and another network supporting some indoor coverage with small femtocells. Here, heterogeneous deployments involving both macro and femtocells can significantly improve and enhance system performance and energy efficiency compared to traditional macro and microcell deployments. They were also able to pinpoint the amount of energy reduction in mobile networks of macrocell deployments for low traffic conditions and high-density urban deployments. For this, they proposed different methods of energy saving. Firstly, the implementation of selective disconnection and power reduction of Evolved Universal Terrestrial Radio Access Network Node Bs (eNodeBs) [91] and HeNBs [91], which are SONs techniques for energy saving in dense urban zones with coverage overlapping. Secondly, selective disconnection over specific cells was used to turn off the radio section while keeping the connection for backhaul with the core network active, to assure faster powering up for the base stations on demand. The paper shows that this technique effectively allows for energy saving with a marginal effect on total throughput. For example, turning off 6, 15 or 24 cells can result in an energy reduction of 7%, 17% or 27%. A third option is to reduce transmission power for all base stations when indoor traffic is supported exclusively by femtocells. In this

scenario, say if transmitted powers are 46, 42, 38, 34 and 30 dBm, the energy savings can be 0%, 36%, 50.5%, 56% and 59% respectively [92].

2.3. PON optimisation scenarios

Akin to small-cell deployment, an optical fibre network as a backhaul solution is subject to different optimisation approaches. In these circumstances, FTTN is more of interest to our research, specifically PON FTTN, since it has already been proven as a desired option for a backhaul solution, as observed in [6, 15, 37-40]. Like the small-cell network planning discussed in the previous chapter, this deployment can face significant obstacles and restrictions that can drastically affect its performance. As a result, possible optimisation scenarios can be looked upon, as below.

- Design Optimisation

- Cost optimisation

The above optimisation scenarios are intended to be retained within our project's scopes, hence discussed accordingly.

2.3.1. Design Optimisation

SCN backhaul dimensioning by design optimisation is a crucial element that deals with appropriate designing/planning methods of such a network. It would ensure the proficiency of the backhaul network in delivering its services accordingly. Several such works are discussed as follows.

- Design algorithm approach
- Technology-oriented approach

❖ Design algorithm approach

A novel PON designing algorithm [43] has been proposed in this study to plan a PON with only the provided fibre route options, rather than considering other alternative routes. This algorithm could spontaneously produce the suboptimal point-to-multipoint network design that could connect every subscriber equipment. It means ONU to the OLT connectivity is possible through a power splitter for a combined optical fibre length close to a minimal value. This

incident can occur when the placements of the COs, users and set of appropriate optical fibre cable placement routes are known. Additionally, the splitting ratio of the splitters and the maximum acceptable length of the optical drop cable joining each optical splitter and corresponding subscriber(s) (ONUs) are also taken into account. The authors consider this PON designing a non-deterministic polynomial-time hard (NP-hard) problem, modelled as a graph G(N, E). In this graph G, locations of existing power poles (the possible optical power splitter locations) are represented by the set of nodes N and optical fibre paths are depicted by edges E. The numerical simulations in the study confirm the algorithm's feasibility in planning a suboptimal PON network design. This study also considered the total fibre length but ignored each subscriber's distance, and its nearest power pole was assumed to be negligible. In this case, the Delaunay triangulation graph randomly deployed 100 nodes and about 277 edges to simulate a suboptimal PON network, including power poles and possible optical fibre paths in urban area [43]. The idea employed within this paper was extended into multiple papers, namely [93-95].

An improved partitioning algorithm [93] for PON network design was established by analysing the PON architecture model. With specific input parameters, this algorithm can routinely compute the arrangement and number of OLT locations to optimise PON planning and enhance cost efficiency. In PON network designing, the location and configuration of OLT and Passive Optical Splitter (POS) location are the key parameters. The OLT is considered as root and POS as a branch to construct the network design. In this paper, first, a network cost model is proposed, then the partitioning algorithm is developed by optimising the network parameters. The authors in the paper stated that the PON architecture was divided into four planes. They then recognise the different equipment used in each plane, develop cost functions for each plane, and ultimately compute the PON architecture's total cost. Once done, they develop an optimisation algorithm termed the partitioning algorithm to prepare an optimal network design with minimised cost approach. The partitioning algorithm primarily focuses on setting initial OLT positions based on the partition number, choose the appropriate location for the Broadband Remote Access Server (BRAS). It allowed multiple OLTs to connect with the nearest BRAS in a star formation and adjust the number of PON nodes to minimise connection cost. Finally, the BRAS and OLT positions were re-set in case of modifications. With their approach, the paper's authors could minimise cost in optimal PON designing [93].

Another work applies a technology-independent Simulated Annealing (SA) metaheuristics method to construct optimal tree-based point-to-multipoint optical access network topologies. It delivered competitive solutions by 5-10% of the theoretical optimum level for multitudes of demand points in the network model. Here, Voronoi-diagrams were implemented for demand point clustering and assessment within their Simulated Annealing approach. This optimisation problem focuses on minimising network deployment costs involving cable plant (trenching & fibre), along with Distributed Unit (DU) equipment expenses, considering distance and capacity constraints. The proposed approach could minimise the difference between the theoretic lower bound by Mixed Integer Linear Programming (MILP) [96] under 10%. It was also capable of scaling up to ten or twenty thousand demand points, offering better scalability than similar approximation algorithms. The earlier fast technology-dependent heuristics could be better options for iterative computations, including PON deployment cost minimisation using adequate parameters or cost factors. However, the proposed SA method is efficient in the final stages of PON deployment planning when the desired network technology and related constraints are already selected, but a more proficient optimised network topology is required. Since time restriction is not imposed at this stage, the SA approach performs comparatively better than similar optimisation methods. Moreover, SA is independent of parameters and limitations of a particular access network technology, and therefore has better application prospects for both present and future PON technologies [94].

A similar approach to [93] has been proposed, incorporating a combination of ant colony algorithm and partitioning algorithm and a 0-1 nonlinear programming optimisation framework to form their partitioning optimisation method. As ant colony optimisation is more effective and more precise than contemporary PON optimisation algorithms, it is more appropriate for estimating the capacity of the bigger and complicated PON network. Alike [93], this new algorithm could automatically calculate the amount and organisation of OLT using node amount, the number of subscribers, service traffic and cost constraints, thus minimise network deployment costs. The authors developed both a cost function and an enhanced geographical location algorithm. Here, the location algorithm merges with the ant colony algorithm to solve the discrepancy between the local optimal solution and the overall optimal PON design solution. They particularly used the Ant Colony System (ACS), a better global search provision than other ant colony algorithms. ACS framework is based on ants'

movements within the colony as each releases pheromone scent to maintain directions for other trailing ants. The framework includes several basic ant colony optimisation steps, such as-selecting adjacent node locations, update pheromone trail information as ants move and only allow specific, i.e., global ants to release pheromones. These generate a directed graph with desired nodes, leading to a feasible solution. When ACS and partition algorithm is combined, the resulting hybrid approach performed the following-Initiate pheromone release by ants, i.e., set required algorithm parameters, developing solution set, local search through partition algorithm. Additionally, it will find the best ant for pheromone release, set a local rule to update the pheromone trail and set a global rule to update it [95].

❖ Technology-oriented approach

PON for wireless backhauling has been considered as a design-based, cost-minimised optimisation approach. Such a backhaul network can accommodate additional bandwidth, service portability, and user mobility demands. The study discussed converged network design to provision and then evaluated algorithms to use the PON architecture as a wireless backhaul option. Emphasis was also given on each access and backhaul segment's capacity requirements, physical layer constraints, and overall cost. Factors such as power budget, CAPEX elements including active ports, number of nodes, construction engineering requirements and OPEX elements including real estate requirements and power consumption were also observed. Both heuristic and stochastic optimisation techniques were applied for this optimisation framework. The findings depicted that the legacy methods for cost minimising may not lead to optimal backhaul designs without the inclusion of capacity/QoS requirements of enterprise-based subscribers and capacity migration effects. Hence, a stochastic optimisation method was developed using the simulated annealing algorithm to estimate near-optimal solutions, thus satisfying the overall requirements in established infrastructure and resource distribution to support user and service mobility [97].

2.3.2. Cost Optimisation

Cost optimisation is one of the significant concerns of optical network deployment. Optimising it can significantly reduce the overall cost of PON deployment. We aim to discuss an algorithm-based cost optimisation framework developed to design suboptimal economic estimations and architecture for PONs by modifying distribution network length. Here one

novel sub-algorithm focused on the minimum star topology, and two more sub algorithms approximated the minimum constructional length for the distribution network. The first sub-algorithm was angle-weighted, which located the minimum star topology network architecture's centre. The result was then compared to another similar approach, proving that this proposed sub-algorithm provided adequate accuracy with less complex computations.

Additionally, the other two sub algorithms were tested and evaluated for random end-points for determining the proper network infrastructure length. Finally, through the clusterisation method, all three sub-algorithms formed one cost-optimising composite algorithm for PON designing. This proposed algorithm was entirely based on theoretical assumptions without accounting for external conditions and real-life constraints. Thereby, future extensions incorporating real-life scenarios and applying existing optical infrastructure were provisioned within the paper [98].

2.4. SCN planning with backhaul dimensioning

In recent years, several research initiatives concerning wireless network optimisation have been undertaken through extensive investigations. One such attempt focuses on performing "Small-cell Optimisation" while employing an optical fibre network as a backhaul solution for such a network. There have been significant research studies published [37], [39], [85], which depicted optimisation procedures performed either jointly on both small-cell deployment and optical fibre backhaul or individually on each of them. In summary, several optimisation procedures that have been conducted in these sectors can be described as follows.

- Cost optimisation
- Design optimisation
- Coverage optimisation

2.4.1. Cost optimisation

One of the most influencing motivators for conducting a small-cell optimisation study in conjunction with incorporating a backhaul network in the process is to perform optimal cost minimisation. An example of such a study focuses on optimally placing small-cells within the same locality as existing optical network nodes and infrastructure. These nodes were preferably the RTs utilising existing infrastructure such as fibre connections and electrical powering up

options to minimise deployment cost. The traditional wireless networks deploy small-cells based on calculated user information and propagation patterns to ensure ample capacity and coverage both. However, such a deployment method requires expensive backhaul solutions that implement network powering up and equipment purchase, site acquisition. The study also noted that since signal propagation degrades with distance from the base station, it is better to place small-cells nearby existing macrocells, to enhance total network coverage and capacity provisions. Therefore, the study finds the subset of most suitable locations from a set of small-cell locations co-located with optical network RTs, to place small-cells. These cells are appropriate in adding to the macrocell areas' coverage and capacity and minimising cost by being situated near suitable macrocell and RTs. The study also includes recent studies on maximum covering problem and an Integer Linear Programming (ILP) based discrete optimisation of optical network design. These results establish that the existing macrocell network can also act as a basis for the further economic deployment of small-cell and associated backhaul network [37].

2.4.2. Design optimisation

Properly designing a combined SCN-GPON architecture can be challenging, rendering several high-quality research works in the past. Following our research works, as a basis, one such example is reviewed here. This study [39] aims to backhaul small-cells situated in RT sites of an existing PtP optical network. The study chose subsets of CO locations and a subset of Fibre Access Points (FAPs) through a cost minimising optimisation process. The selected CO locations were to be served as installation points for OLTs, while selected FAP locations should deploy optical splitters to connect with the RT sites housing the small-cell equipment. Within the study, an ILP formulation was applied to perform the cost-optimised design process. Several cost parameters were considered within this model, namely, fibre, equipment, and labour costs.

Although the fibre is already deployed, there is associated maintenance cost due to degradation over time. The equipment cost involves Ethernet switches, OLTs, splitters and ONUs as these will be new additions to the proposed network setup. The OLT costs involve several chassis, shared equipment and line cards. These were based on the number of PONs connected to the OLT, where an OLT chassis scan house several line cards with multiple PONs to be installed per card. The combined cost involving splitters is based on the number of splitter

enclosures plus splitters physically placed at selected FAPs. There are also splicing costs and labour costs associated with equipment installations. The framework includes appropriate constraints to maintain relationships among all variables and reach a cost minimised solution to represent the intended optimisation framework. The study results showed a significant 56% reduction in costs with an optimised PON deployment as backhaul compared to a PtP formation as a backhaul solution.

2.4.3. Coverage optimisation

An essential feature of incorporating SCN-GPON dimensioning and planning would be to ensure that proper coverage over a specific case study area is maintained o the maximum possible. It enhances the credibility of implementing such frameworks significantly, as evident from the following work reviewed. This study [85] aimed at backhaul optimisation based on the existing PtP optical network and explored the coverage maximising aspect of small-cell planning within the optimisation framework. This work performed three primary tasks-Selecting potential small-cell locations considering existing fibre infrastructure positioning, further refining the selection of these potential Small-cell locations. Here, a heuristic-based maximum-covering optimisation method was utilised, applying an ILP process to optimally plan and dimension a PON-based backhaul over existing dark fibres in a PtP optical network for these planned small-cell positions. The study showed that existing FTTN nodes and fibre links were utilised to deploy backhaul elements and power-up options towards small-cell sites to be planned as part of the said optimisation framework. The potential small cell locations were selected from geo-coded FTTN data on network nodes and links. It was based on an optimisation method that included radio coverage aspects, population density within the possible coverage area and small-cell location distances to existing macro-cell positions.

Some prior research suggested that small-cells should be co-located with RTs within an existing optical network. Moreover, this optical network would be leveraged to optimise a backhaul network for the corresponding SCN. The research showed that 90% of RT distances within proximity to each other are positioned within less than 600 m distance over the case study area. Therefore, it will be appropriate to position the small-cells with the RTs, since the coverage radii of such small-cells are within the 200-400 m range. Another aspect considered was not selecting such RTs placed near existing macrocells since users closest to macrocells would receive proper coverage. Therefore, the small-cell needed to be placed in RTs located

away to some extent and needed additional coverage provisions. Once the potential small-cell locations were chosen, a subset of those locations was selected to ensure that the maximum amount of region within the case study area was covered with that subset of small-cell locations. These small-cell locations were then used as inputs to design a backhaul network for the small-cell locations, based on a cost-optimised manner. As small-cells are more densely placed than macrocells, a PON backhaul that shares equipment and resources was more feasible in this study than conventional PtP Ethernet backhaul currently deployed for macrocells.

2.5. 5G Small-cell spectrum refarming analyses

The latest advances in wireless communication networks have introduced new trends, especially in the 5G sector. A critical advancement for wireless mobile communication can be spectrum refarming for the small-cell spectrum management allocation process. Spectrum Refarming (SR) is the process of sharing the frequency spectrum of wireless signals to allow various cellular networks from different generations to function in the same wireless frequency spectrum. Spectrum sharing in wireless networks is applied in two methods- Overlay spectrum sharing and underlay spectrum sharing. The overlay process allows the secondary users within the spectrum to access the idle spectrum of the legacy (primary) users as needed. Also, the underlay method allows the secondary and primary users to broadcast at the same band. There have been two primary SR models like this ideology, conveniently termed as overlay SR model and underlay SR model [54]. The two primary aspects of discussing spectrum refarming can be attributed to as follows.

- Benefits of spectrum refarming
- Challenges in spectrum refarming

2.5.1. Benefits of spectrum refarming

Several advantages can be observed in the process of spectrum refarming. For example- Refarming is cost-efficient as it can provide added capacity for upcoming and currently emerging wireless networks without the necessity to acquire additional frequency spectrum allocation. Refarming can also be adapted and upgraded to new generation networks, e.g., LTE and GSM, since increased network capacity. It is a process that can offer benefits to both indoor and outdoor urban coverage, in terms of reach, capacity and path loss, through both relatively

lower and higher frequency spectrums. For example, lower frequency refarming can provide enhanced coverage with more wireless reach, less penetration path loss than higher frequencies for better indoor urban coverage. Then with refarming involving higher frequencies, there is greater capacity than coverage for outdoor urban areas. An example of better coverage is that Universal Mobile Telecommunications Service900 (UMTS900) can allow 44% more areas to be served per Node-B than the same performed by Universal Mobile Telecommunications Service2100 (UMTS2100), allowing for more economical service providing initiative by operators.

Similarly, since 900 MHz offers lower path loss than the 2100 MHz spectrum, the 900 MHz networks would require fewer base stations, thus comparatively cutting costs around 50% to 70%. With spectrum refarming, QoS is heightened with fewer handovers on a smaller number of base stations. Also, as lower frequencies offer less penetrating losses for in-building mobile signal propagation, cost-minimisation is observed with refarming in terms of urban indoor mobile propagation [99]

2.5.2. Challenges in spectrum refarming

Spectrum refarming can exhibit different challenges and issues as well, despite being a desirable technological advancement. It allows for assigning an adequate amount of available adjoining spectrum where it would be required to allow for the synchronised operation of multiple mobile technologies within a frequency band. Then refarming can also face issues with the appropriate allocation of frequency bands for different mobile technologies. Application of frequency bands on both sides of the dividing point for the frequency spectrum should be allowed for the same mobile operator. Then careful use of guard bands should be implemented to avoid adjacent channel interference within the frequency spectrum. The problem of avoiding the possibility of service outage to existing users from GSM to LTE/5G systems, without compromising QoS, can also arise through recognising and managing mobile traffic formation.

Moreover, reconfiguring the spectrum when the frequency is interleaved between operators, then adhering to reformed coverage, traffic and interference after the reconfiguration process is done. Additionally, handling the issue of existing incompatible handset devices unable to function with the spectrum refarming can come forward, resulting in service

discontinuation and revenue stoppage. Another prominent issue can be rectifying the spectrum refarming of external interfering signal resulting in residues discarded by legacy signals [99].

2.6. Conclusion

This chapter mainly focused on studying previous research works related to our proposed research topic in a much broader prospect, for offering the background to our proposed work in this research project. Our literature review aimed to identify research works that have already been done within the broader context of our proposed research topic. This discussion primarily offered a summary and synthesis of appropriate research literature sources in line with our conceptual research framework. We also credited and recognised significant research advancements obtained by other eminent researchers through our literature review. Additionally, we aimed to provide a thorough analysis of existing research by maintaining quality, objectivity, accuracy, insights and clarity of the literature investigation. We attempted to identify inconsistencies in prior research, namely, open questions, research gaps, and study arguments. We looked at research studies in anticipation of seeing the relevance of their respective research outcomes concerning their topic context. We later justified the need for further research within our proposed area in a topic-by-topic manner in each of our result chapters. It offered additional literature review in a more constrained and relative manner to build a strong case to justify the need for research works to prevail.

Nonetheless, these constrained literature discussions focused on areas closely related to our proposed topic but conveying outcomes significantly different to what we are proposing within our project. Hence in this chapter, four segments have been discussed within **Sections 2.2** to **2.5**, focusing on different studies on SCN and backhaul planning. These segments concentrated on SCN planning characteristics such as optimisation methods, optimisation scenarios, corresponding backhaul planning and spectrum refarming applications.

In **Section 2.2**, four types of SCN optimisation approaches were discussed. These included design optimisation, capacity optimisation, coverage optimisation, and energy optimisation. In the design optimisation part of **sub-section 2.2.1**, literature was reviewed on SCN design methods based on the 3GPP heterogeneous deployment, adaptive architecture deployment and 5G physical layer radio design deployments. These works provide us with views on SCN formation alongside their macrocell counterparts to design a heterogeneous

cellular network architecture. In **sub-section 2.2.2**, we discussed capacity optimisation by cell sizing, capacity relief, combined coverage-capacity enhancement, trade-off, capacity-energy joint optimisation and self-optimisation in capacity enhancement. These studies emphasised a cellular network's capacity handling ability and corresponding enhancements through cellular network design augmentations. Next, the coverage optimisation part in **sub-section 2.2.3** reviewed topics such as cell coupling-based coverage enhancement, genetic algorithm-based coverage optimisation, regression-based optimisation, self-organising coverage enhancement, maximal covering location problem (MCLP), and small-cell backhaul optimisation. All of these approaches focused on enhancing cellular network coverage capabilities through network design modifications. The final sub-section for the SCN design optimisation discussed on the energy optimisation segment in **sub-section 2.2.4**. This section reviewed studies on energy optimisation for cellular network design reinforcements using design-wise enhancement, power control and throughput enhancement. Considering all these approaches of small-cell optimisation discussed in **Section 2.2**, it is evident that neither of these research works has specifically included geographical element influences as essential factors in terms of planning a small-cell network. Moreover, the influences of geographical factors over signal propagation and planning of a small-cell network were the main assumptions that we considered in our research work.

Section 2.3 comprises optimisation scenarios based on backhaul dimensioning through design and cost aspects. The design optimisation part in **sub-section 2.3.1** discusses prior research works based on cellular network design algorithm and backhaul technology-oriented approaches. In **sub-section 2.3.2**, a cost optimisation study was reviewed to design suboptimal economic estimations and architecture for PONs by modifying distribution network length through sub-algorithms. Ultimately, Section 2.3 reviewed research works on cellular network backhaul planning with design and cost optimisation methods. These studies were individual and separate works focused on optimising only standalone Passive Optical Networks, without exclusively considering them as an option for a backhaul network related to a small-cell network planning. On the other hand, in our proposed work, we considered optimal PON or, more specifically, GPON design as the only preferred option as a backhaul infrastructure to be connected with a small-cell network.

Next, **Section 2.4** discusses cost, design and coverage-based approaches of SCN backhaul planning. The cost optimisation segment in **sub-section 2.4.1** study optimally places

small-cells within the same vicinity as existing optical network nodes by leveraging existing infrastructure for cost minimisation. The design optimisation portion in **sub-section 2.4.2** then showed the justification of using an optimised optical PON design as an appropriate backhaul option compared to a PtP formation. In sub-section 2.4.3, a backhaul optimisation framework is proposed based on the existing PtP optical network and explored the coverage maximising aspect of small-cell planning within the optimisation framework. Altogether this **Section 2.4** focused on different SCN backhaul approaches focused on the PON-based backhaul architecture. These design approaches for cellular network backhaul dimensioning essentially assumed a brownfield (already implemented) small-cell network within their respective backhaul dimensioning approach. In retrospective, our research work always considered small-cell planning as an integral part of the scope of each of our proposed backhaul dimensioning methods.

Finally, **Section 2.5** emphasises spectrum refarming approaches for cellular networks. This section dealt with the benefits and challenges of applying spectrum refarming onto cellular networks. The benefits of spectrum refarming were highlighted in **Section 2.5.1,** while **Section 2.5.2** focused on the challenges that spectrum refarming can pose.

Therefore, considering the literature review presented in this chapter, we identified the recent relevant research before forming our envisioned research topic. From reviewing these research works, we can conclude that all of these research works individually discuss relevant optimisation techniques to perform small-cell network planning and backhaul dimensioning in their sophisticated methods. However, none of them conforms to the same research method that we have performed throughout our proposed research within this PhD project or solve the same set of problems together, which we have completed.

In summary, this chapter focused on establishing a proper literature review on our intended topic of small-cell and backhaul optimisation studies. The chapter showed the relevance of a literature review by discussing prior relevant research works to build a good knowledge of our intended novel research theme. It gave us a better perspective to identify research disparities to build our research idea on them. It also explained the necessity of our research work while justifying our intended research approaches.

This page is left intentionally blank

Chapter 3

Small-cell network planning by geographical terrain properties

3.1. Introduction

Small-cell networks have been an integral part of the recent revolutionary changes marking the wireless technology industry's progression. Such advancement in wireless technologies could be attributed to the move to cyber-physical systems that marked the 4th industrial revolution [100]. It eventually resulted in the enhancement of mobile connectivity for applications of multiple diverse digital systems. Hence, mobile operators would need to adapt to better design processes for ensuring enhanced network technologies. It would ultimately lead to a continued escalation of data traffic usages, alongside appropriate on-time connectivity provisions in many devices. Therefore, the need for upgraded mobile network architecture continues to push through. This approach would be leading to the deployment of small-cell topology to ensure ample coverage and capacity are provided with economic feasibility for both operators and end-users. As a result, viable enhancements in small-cell network architecture continue to be an anticipated and much-utilised research topic. Henceforth, the focus of this chapter is on the development of a small-cell network planning framework. This framework is based on an urban geographical case study area and incorporates geographical terrain influence over a specific urban area for small-cell network deployment. This framework utilises a simplified small-cell location selection method. Within the selection process, a set of potential locations are selected based on their cell coverage capabilities and signal level measurements, as influenced by the effects of surrounding terrain within the SCN planning area. Therefore, the effects of land terrain variation and urban geography over a case study area are studied for developing the intended small-cell planning framework.

Small-cells conduct wireless data propagation over the land through free space RF signalling, and such propagation must be planned carefully with appropriate cell-site positioning. Studies have already identified the possible effects of irregular land terrain and urban geography of built-up areas on cellular mobile RF signal propagations. The RF signal is

quite variable and randomly fluctuating over irregular terrain and in built-up areas. For irregular terrain land, varying geographical terrain can obstruct the direct LoS signal path between the transmitting cell BTS and receiving mobile station (MS). This phenomena initiates significant signal loss and causes NLoS propagation. It also leads to additional signal diffraction and reflections with possible further losses [101]. Even visibly flat terrain ground can incur signal losses of over 10 dB. It can occur even for a height variation of as low as 15 cm due to propagated rays being reflected off the ground as their signal phase changes [50].

Moreover, street orientation and building blocks in built-up urban areas reflect RF signal, significantly weakening it for the reception in cell areas with a smaller radius [50]. Additionally, urban area buildings acting as obstacles to propagated electromagnetic RF rays cause a diffraction phenomenon, which bends radio waves around the edge(s) of a significant obstruction, causing NLoS propagation signal [101]. Therefore, we need to consider corresponding signal propagation influencing aspects, namely urban area building positions and street formations, for RF signal propagation over built-up areas. Additionally, it is theorised that BTS antenna height over irregular terrain influences cell positioning by affecting coverage. A low height BTS antenna can reduce cell size and counter higher capacity demand. A higher-mounted antenna with additional gain can decrease path losses by terrain variation, especially around the average urban building height [59]. It is preferable for initial-stage cell planning to select an optimal base station antenna height for an appropriate location. Once an appropriate transmitting antenna height is selected, the target is to implement this cell-planning framework using an automated algorithm.

Previous research studies show that possible consequences of geographical terrain, urban street formations, and structural establishments on wireless RF signal propagations have been distinctively identified. Hence, the effects of geographic terrain on cellular signal propagation, optimal antenna height, building positions and street formations should be considered for appropriate small-cell location planning in an urban area.

3.2. Related works

The proposed framework primarily utilises the following theoretical information-

- SCN case study area selection
- SCN cell shape selection

- Cell coverage and signal level measurement

3.2.1. SCN case study area setup

was to determine the appropriate case study area for conducting our SCN case studies. Once we determined the case study area, we aimed at selecting the appropriate cell locations for our SCN network. This approach was based on geographical terrain variations, as inspired by a similar study done in [102] over Macrocell network planning. This study aimed to identify potential macro BTS locations with higher traffic demands by pinpointing them within a terrain grid area, considering the terrain variations over the case study area. An example of this terrain grid pattern can be found below in **Figure 4**. Here, the whole case study area is divided by a square grid pattern with each smaller square block representing the equal division of the total case study area., e.g., the enclosed area generated when the horizontal and vertical lines within the terrain grid intersect. The dots inside each small square indicates the position of each teletraffic demand amount. It is similar to the case study done in [102]. While this study aims to implement a terrain grid approach over our intended case area, the outcomes and purposes of this and our study are different. For our study, we aimed first to determine and justify a proper small-cell area shape and then pinpoint proper small-cell locations over the case study area. Both these tasks would rely on geographic terrain characteristics over our intended urban area for the SCN planning case studies we aimed to perform.

Further discussions on choosing a proper cell area shape and formulating the method to select small-cell locations optimally are provided in this chapter's following sections. The only common factor between our research and this work would be the terrain grid formation method. Henceforth, even though this work forms a part of the basis for our studies in this chapter, it still has differences with our envisioned approach. This research above deals with macrocell planning and optimisation, whereas our research approach focuses on planning the small-cell wireless network in an urban geographical area setting. Our work would also consider the specific nature of 4G wireless cellular technology and corresponding constraints to plan a small-cell network.
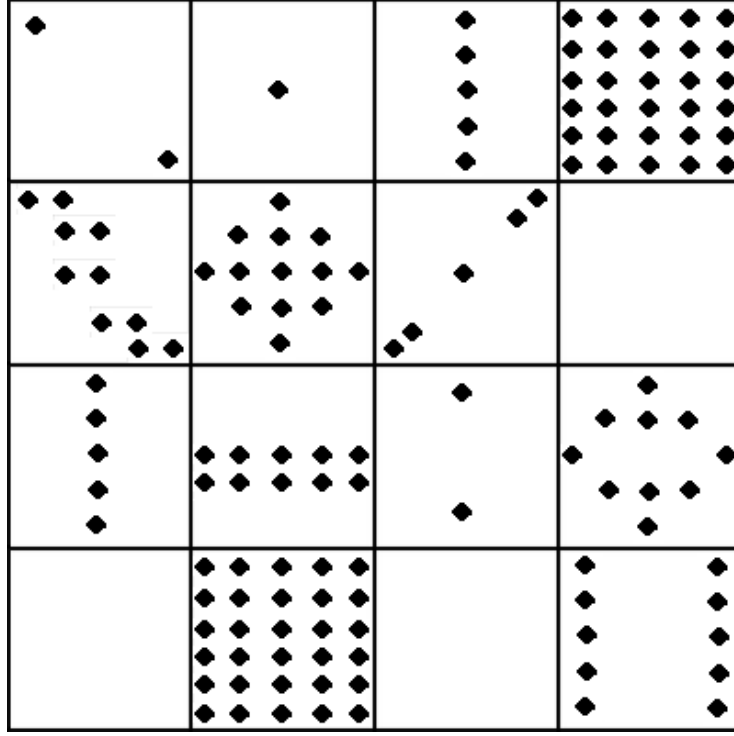
Figure 4: Terrain grid for BTS positioning by teletraffic demand [102]

3.2.2. SCN cell shape selection

The second basic theoretical concept to form the background to our urban area SCN planning framework was to determine a specific type of cell shape for the SCN. We aimed for an SCN planning that would provide the best signal coverage with the least amount of signal losses to encounter for our work. Therefore, we aimed at determining an appropriate cell shape type for each small-cell within the SCN. According to the study done in [58], a suitable urban area cell shape should be considered non-circular due to signal propagation being anisotropic, e.g. signal strength power level non-uniform in different propagation directions. For our case studies, the terrain grid for an SCN planning would divide the intended case study area into square blocks (See **Figure 4** above). As a result, a non-circular cell shape is chosen for an urban SCN planning framework as the most preferred cell shape. Therefore, to ensure the best signal coverage and conform with our aim to map our case study area into a terrain grid, we decided to consider a noncircular cell shape for our proposed SCN network. Again, this work differs from our intended research approach as it primarily develops a path loss model for small-cells. This work does not emphasise the actual small-cell/microcell planning studies, which is our primary focus of discussion in this chapter.

3.2.3. Cell coverage and signal level measurement

Once the case study area's nature was determined, we pinpointed our potential cell locations based on signal level measurements within each terrain grid square block. This cell location selection process was done based on mobile signal level measurements. The aim was to select a subset of potential SC locations, based on their path loss profile comparison, as projected from pre-selected sets of location points. Such pre-set locations were two sets of values over the case study area-sets of minimum and maximum elevation locations. We would then perform the signal level measurement for each maximum and minimum elevation points within every SC coverage block. Next, based on these path loss values observed from the maximum and minimum locations, we would compare them to find the most suitable SC location, which would show the least signal loss levels. This process is then repeated for all the SC coverage blocks, and the appropriate locations are selected-one for each block. The signal level measurements are based on two coverage approaches.

- LoS approach
- NLoS approach

Since we consider small-cells under rooftop level and nearby streets, it is vital to consider signal propagations in both LoS and NLoS directions, as obstacles can prevent LoS signal propagations. Thereby, in the following sections, we expand on these two path loss models.

❖ LoS approach

For determining LoS signal propagation without obstructions from each potential SC location, a path loss model by Nisirat *et al.* [57] is applied. It incorporates the Hata path loss model for small urban city microcells [103], with an added correction factor involving the geographic terrain slope effects. The original Hata path loss model is as below,

$$L_{LoS} = 69.55 + 26.16 \log f_c - 13.82 \log h_t - a h_r + (44.9 - 6.55 \log h_t) \log d \qquad (1)$$

where,

f_c = Carrier frequency

h_t = Transmitting BS antenna height

h_r = Receiving MS antenna height

And, the correction factor for a small-urban city would be,

$$ah_r = 0.8 + (1.1 \log_{10} f_c - 0.7) h_r - 1.56 \log f_c \qquad (2)$$

Since the Hata model is mostly applied in a macrocell environment, the slope correction factor's addition $\nabla_{DC}(S)$ to the model is proposed to fit the small-cell scenario aptly. This modified model used the average slope value S at the end of the measurement path to compute slope parameters A1, A2. The values of A1 and A2 depended on the nature of the slope value. This slope value can be positive, negative, or greater than 0% and less than 2%. Nisirat *et al.* [57] determined this through the elevation profile measurement data obtained from Google Earth software [104]. The regression parameters are as follows.

Table 1: Correction factor parameters

Regression parameters	1800 MHz	900 MHz
Low slope values	A1= 14.64 A2 = -2.21	A1 = 26.4 A2 = 3
Negative slope values	A1 = 34.4 A2 = 2.84	A1 = 24.5 A2 = 0.51
Positive slope values	A1 = 13.4 A2 = 0.35	A1 = 27 A2 = -1.8

Therefore, the total slope correction factor incorporating the above parameters-

$$\nabla_{DC}(S) = A1 + A2 \log(S) \qquad (3)$$

Adding this correction with the Hata path loss equation (3) provides the modified Hata path loss model below.

$$L_{LoS} = 69.55 + 26.16 \log f_c - 13.82 \log h_t - ah_r + (44.9 - 6.55 \log h_t) \log d + \nabla_{DC}(S) \qquad (4)$$

here,

S = Slope of terrain at measurement location $(\%)$

f_c = Carrier frequency 1800 MHz/900 MHz

h_t = Transmitting BS antenna height 9m

h_r = Receiving MS antenna height 1.5m

ah_r = Correction factor for small urban city

❖ NLoS approach

In the NLoS case, a diffraction building loss is considered and added with the LoS path loss results obtained using the method above in **Equation (4)**. Thus, the NLoS loss is obtained as below.

$$L_{NLoS} = L_{LoS} + L_{msd} \tag{5}$$

It is computed with the diffraction loss formula from the COST 231 Walfisch-Ikegami model [105] for antenna under rooftop level. The formula for this diffraction loss part is-

$$L_{msd} = L_{bsh} + k_a + k_d \log_{10} d + k_f \log_{10} f_c - 9 \log_{10} b \tag{6}$$

where,

$L_{bsh} = 0$

$$K_a = 54 - 0.8 \frac{d\left(h_t - h_{roof}\right)}{0.5}$$

$$K_d = 18 - 15 \frac{d\left(h_t - h_{roof}\right)}{0.5}$$

$$K_r = -4 + 1.5\left(\frac{f_c}{925} - 1\right)$$

h_{roof} = Rooftop height 10m

b = Building density 100m

3.3. 4G SCN planning overview

The 4G small-cell cell planning framework was intended for the two widely utilised 4G frequency bands-1800 and 900 MHz frequency bands [106]. The framework has been provisioned through two different stages-methodology and implementation. These two steps are described as follows.

3.3.1. 4G SCN planning methodology

The small-cell planning framework was implemented through the following steps-

- Terrain measurements
- Selection of potential candidate cell locations
- Path loss measurement approaches
- Determining slope angle
- Selection of carrier frequency
- Selection of cell coverage area value
- Selection of antenna height
- Setup of small-cell location and positioning
- Determining the structure and street positions

❖ Terrain measurements

Our intended SCN planning framework's case study area was based over a 900 m $\times$ 1800 m or 1.62 km^2 test area in the Melbourne CBD. The basis to locate appropriate potential cell sites was to use a similar approach to [102], involving planning a mobile network based on geographical terrain attributes. Hence, we first obtained geographic terrain elevation information over a specific case study area. For this, we divided the case study area into a two-dimensional (2D) rectangular terrain grid of multiple same-sized unit squares or blocks. Terrain measurements were obtained horizontally across the grid from left to right in each row to extract elevation value for each unit square area of 100 m $\times$ 100 m. Each 100 m square was divided into four smaller 50 m -sided squares. This illustrative enhancement aimed to find the centre of the 100 m blocks, the intersection point of the two 50 m lines inside each cell. We then measured the elevation value at the centre of each unit square area and stored this value in the corresponding cell of a terrain grid matrix having 9 rows and 18 columns. With this

arrangement, a total of 18 × 9 = 162 cells were included in the terrain grid layout, as shown in **Figure 5**. These values were then stored in the corresponding cell of a terrain grid matrix having 9 rows and 18 columns. This procedure was similar to the approach indicated by [107], and the obtained data format is termed as Digital Terrain Model (DTM). At this stage, the normalised variance of all of the terrain elevation values was calculated as 0.3928. This variance value implied that the obtained values have a little variation when inter-compared (since variance is less than 0.5), indicating the better accuracy of measurement for the obtained elevation values. This approach was adapted from [102], which states that a higher variance of terrain elevation values means the grid unit squares should be made smaller. A lower variance indicates that the selected grid square provides enough data points to maintain better accuracy.

This whole measurement process was initially performed using the Google Earth software [104] and the GPS Visualizer Elevation measurement tool [108]. The grids were created by drawing horizontal and vertical paths over the urban area's desired part, as displayed in Google earth photorealistic view. Once the elevation value in each 100 m ×100 m block within the terrain grid had been measured, the values were stored as elements in a terrain grid matrix. This whole process was done according to the order of their appearance in the terrain grid when the upper-left corner was considered as the first value. This grid formation process mentioned above can finally be seen in **Figure 5** below. Here, the magenta lines indicate the100 m × 100 m dimension grid division, and the cyan lines indicate the 50 m ×50 m grid lines. As shown in **Figure 5**, this can be further understood with a zoomed-in figure of one individual 100 m × 100 m block, showing the four 50 m × 50 m blocks in **Figure 6** below. Here, the 100 m × 100 m block centre is indicated with a red circle placemark. The next section then focuses on discussing the SC selection process itself.

Figure 5: The overall 1800 m × 900 m terrain grid divided into two block sizes
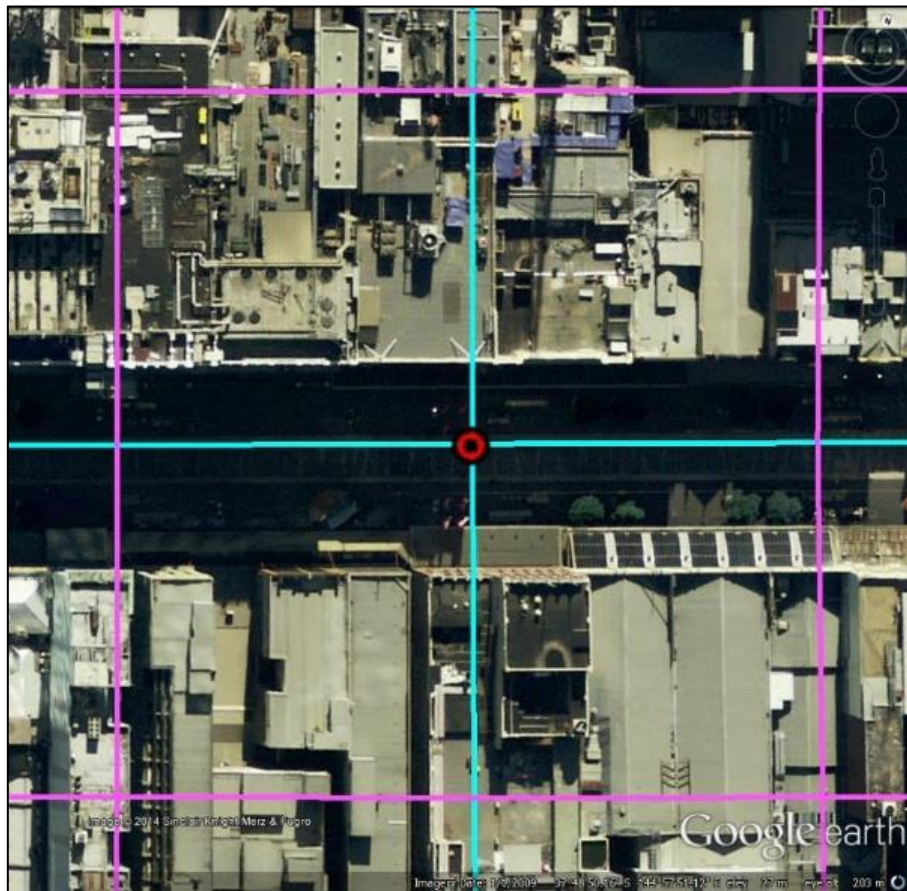
Figure 6: Magnified 100 m × 100 m block divided into 50 m × 50 m portions

❖ Selection of potential small-cell locations

Once the terrain grid was constructed, the terrain value matrix was generated, and the necessary slope information was obtained. We then selected specific types of areas from the terrain area to compare and select the potential candidate small-cell sites. There were primarily two area types selected for this comparative study. The first area type was with the highest/maximum elevation prominence among the four blocks of each coverage block and the second area contained the lowest/minimum elevation prominence from the four blocks of each coverage. The higher elevated areas were chosen based on the approach discussed in [102], which considered the most prominent elevations over a geographic terrain area as potential macrocell site locations. The least prominent elevated area was chosen primarily for comparison purposes with the higher areas as potential cell sites in terrain-induced path losses from the potential sites. The reason is that at relatively low heights of terrain in an urban area mostly surrounded by obstacles, they face more attenuation and cause more path loss theoretically [109]. The higher and lower elevated areas were computed based on our developed algorithm, which also calculated the specific locations of those positions within the terrain grid matrix. This novel algorithm is discussed in section 3.3.2 below. The next section focuses on path loss measurement approaches.

❖ Path loss measurement approaches

Adequate 4G LTE signal level projection was tested to evaluate this proposed framework's feasibility by implementing path loss measurement approaches. This projection was visualised towards each cell area's edge by each type of location through signal path loss measurements in both LoS and NLoS scenarios. These path losses were obtained by considering a BTS antenna at the height of 9m and an MS antenna height of 1.5 m. For both LoS and NLoS situations, we first measured the signal path in two directions-horizontally and vertically, as evident in case study 1. For case study 2, diagonal direction signal level measurement has been incorporated to examine further the accuracy of signal level measurement in each coverage block area.

The signal level measurement process for both case studies involved measuring edge-to-edge signal paths in three directions from each terrain block's maximum elevation points. We similarly estimated the corresponding path losses for the minimum elevation in each cell

coverage area and compared them with maximum elevations. All the measurements for both LoS and NLoS path losses for each potential small-cell location were then compared against two reference parameters. These were the LTE MAPL of 165.5 dB [61] and signal loss level calculated with COST 231 Walfisch-Ikegami formulae [105]-for both LoS and NLoS scenarios. This whole signal level measurement process involves utilising terrain slope correction factor, as introduced in work done by Nisirat [57]. In alignment with our work's purpose, the rooftop-to-rooftop diffraction losses were not considered within our calculation for NLoS path losses. The reason being the proposed antenna height to be 9 m for our planned case study area, which is below average rooftop height, for our intended case study area at Melbourne, Australia. We proceed to highlight the slope angle determination process adopted within the framework, as mentioned below.

❖ Determining slope angle

Path loss computation was applied for determining suitable small-cell positions, where slope angle is an essential part of this loss calculation process. For Case Study 1**,** direct slope angle data were extracted using Google Earth software. Afterwards, we changed case study 2 and based our slope measurement on the actual terrain slope calculation formula to simplify and rectify the slope measurement process. Both the methods are therefore discussed as follows.

➢ Measurement through Google Earth

One of the path loss models we are considering is [57] by Nisirat *et al.,* which is based on terrain slope characteristic between the transmitting BTS and receiving MS. Therefore, it is crucial to obtain information about the slopes for all potential candidate cells in three measurement directions: horizontal, vertical, and diagonal. The geographical terrain slope is the angle between the base terrain of the cell tower and the edge of the squared coverage area in the directions mentioned above. This slope information is essential in calculating the terrain-based path losses to predict accurate signal degradation level for each potential cell location in said directions. Usually, such a slope line is considered from edge to edge of a cell area. It means the slope should start from the edge nearest to a designated small cell location boundary and end at the farthest edge in the opposite direction. An illustrative example of such a slope path in all three directions is shown below in **Figure 7**. It shows a 2-dimensional (2D)

representation of slope paths in horizontal, vertical and diagonal locations, as indicated by the three blue lines. The transparent pink square represents the designated boundary area for that respective square block's potential cell location, denoted with yellow borders. In this example, the potential cell location is set at the centre within the boundary area (a white diamond) and can be placed anywhere within the boundary region. These slope lines can be exhibited in a much-enhanced manner, on a 3-dimensional (3D) representation of this above snapshot of **Figure 7**, in the following **Figure 8**. Figures 7 and 8 show that all slope lines start and end on the designated cell area edges marked with yellow borders. It is done to calculate the maximum path loss for the maximum slope length within a single cell area for its potential cell location. Also, slope lines are planned so that they pass through the intended cell location itself. Therefore, slope information along these lines are needed for improved path loss predictions. It should be mentioned that for case study-1; however, we only pertained to horizontal and vertical directions and corresponding slope information for coverage and path loss calculations.

Figure 7: 2-dimensional (2D) terrain slope in a 200 m × 200 m cell area
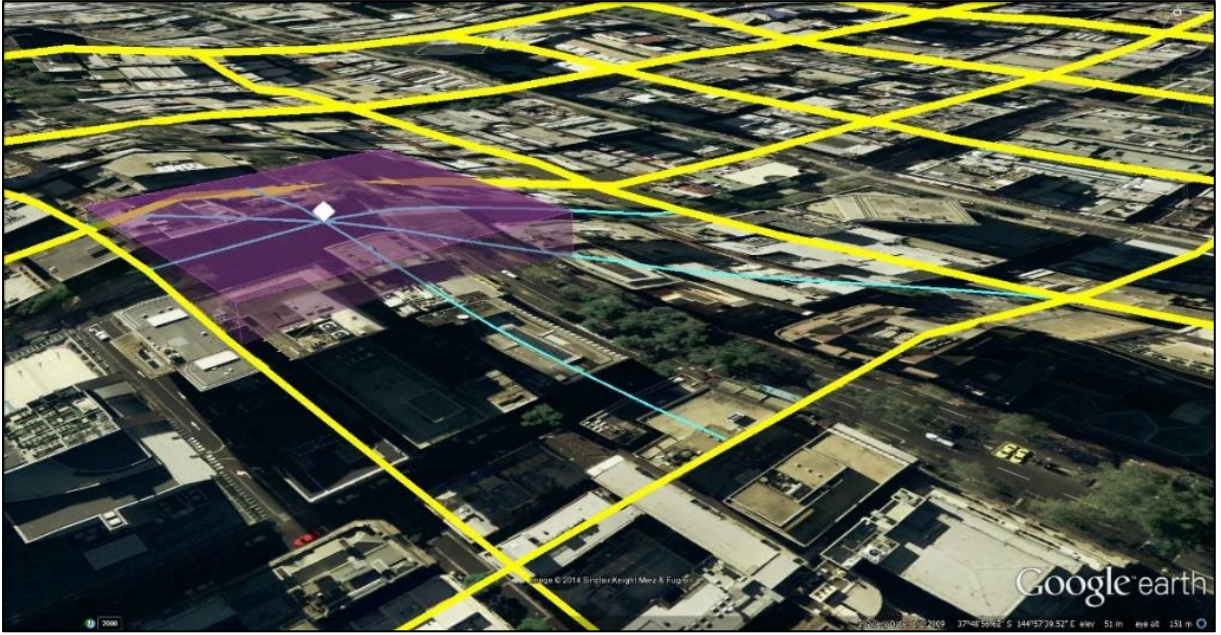
Figure 8: 3-dimensional (3D) terrain slope in a 200 m $\times$ 200 m cell area

➢ Slope measurement formulation

Another method to measure the slope accurately between two geographical points is their respective elevations and distance. Terrain slope between two points is the ratio between rise and run. In this case, the rise is the area difference in the vertical direction between two specific points, while the run is the difference between the same two points in the horizontal direction [57, 110, 111]. The following formula utilises the horizontal distance or run between two locations and the difference of elevations or rise for the same two locations. The formula is as follows.

$$\text{Slope between point A \& B} = \left(\frac{\text{Rise between point A \& B}}{\text{Run between point A \& B}} \right) \times 100\%$$

$$= \left(\frac{h_A \sim h_B}{d_{AB}} \right) \times 100\% \qquad (7)$$

Once the slope angle is determined for each potential SC location, we then discuss the carrier frequency selection process.

❖ Selection of carrier frequency

According to the study done in [106], the typical LTE frequencies range includes 900 and 1800 MHz. Since the designated and most common cellular frequency band in Australia is 1800 MHz [112], the first case study is based on this frequency. A second analysis was then performed using 900 MHz to assess the possibilities of employing 1800 and 900 MHz as LTE carrier frequencies. Next, we move on to justify the selection procedure of the cell coverage area value.

❖ Selection of cell coverage area value

For case study purposes, a Long-Term Evolution (LTE) network was chosen to test our framework. Here, a 200 m × 200 m area for each cell site was initially considered, corresponding to the typical small-cell area range of this selected network type of [85] [113]. To reflect this in our cell planning, we selected four 100 m × 100 m blocks, two horizontally and two vertically in a 2×2 manner and grouped them to form one intended coverage area. Such a formation over our intended case study area would create a terrain grid of 45 cells in total, thus invoking the need of planning a total of 45 cell locations, one for each cell coverage area. For each 200 m × 200 m cell area, this formation can provide with maximum 200 m signal propagation path length for both horizontally and vertically, and approximately 283m propagation path in the diagonal direction. This 200 m × 200 m block grid over Melbourne CBD's intended case study area is shown in **Figure 9** below.

Here in **Figure 9**, 200 m × 200 m blocks area for this geographic region was chosen as cell coverage area dimensions. This approach ensured that the final total number of cell sites over the proposed urban area would not exceed the maximum 30 cell sites per square-kilometre area limit for LTE 1800 MHz network [61]. Similar case studies were then performed over 900 MHz networks with the same 200 m × 200 m area for cell coverage approach. As the 200 m × 200 m area blocks were being chosen as cell coverage areas, an odd number of rows in a terrain grid can appear in some cases. It ultimately poses difficulty dividing the terrain grid into cells with four 100 m × 100 m blocks. It was resolved by considering two cells horizontally instead of four while forming one coverage area. In that case, the coverage block was rectangular instead of square, with 200 m width and 100 m height. This formation is evident in **Figure 9**, where the last row in the terrain grid is seen with such 200 m ×100 m rectangular

blocks. A more clarifying picture can be observed in the zoomed-in version of one single 200 m × 200 m block below. It shows the grouping formation of four 100 m × 100 m blocks inside, in **Figure 10** below.

Similar comparative analysis was performed over 300 m × 300 m cell coverage areas again for both 1800 and 900 MHz LTE networks. To construct such a 300 m × 300 m grid, nine 100 m × 100 m blocks were arranged in a 3 × 3 formation, three blocks horizontally and three blocks vertically. Such a setting would allow a maximum of 300 m signal propagation path length horizontally and vertically, and approximately 424 m propagation path diagonally in 300 m (300 m block). In this case, the whole grid would have 18 total cell areas, with each cell area having the dimensions of 300 m × 300 m in size., as depicted below in **Figure 11**. For further clarification, a zoomed-in snapshot of a single 300 m × 300 m block is also provided below in **Figure 12**. Afterwards, we emphasise the importance of selecting a proper antenna height to place the SC BTS.
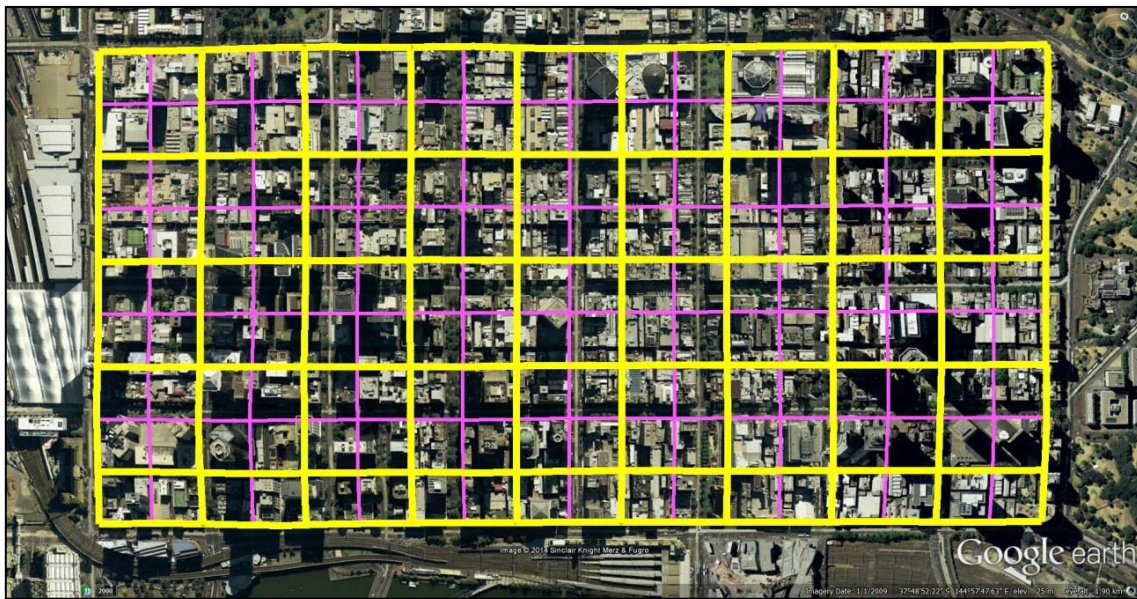
Figure 9: 200 m × 200 m block grid

Figure 10: 200 m $\times$ 200 m block zoomed into 100 m $\times$ 100 m divisions

Figure 11: 300 m $\times$ 300 m block grid

Figure 12: 300 m × 300 m block divided into 100 m × 100 m blocks

❖ Selection of antenna height

Our framework used a 9 m height for BTS antenna positioning, based on the findings [60]. This height is applied to keep the antennas above the tramlines of Melbourne CBD. This height also helped the antenna maintain a good antenna gain factor while still fitting the antenna height requirement of 5 to 20 m for urban small-cells. We used a fixed 9 m height above the ground for the transmitter antennas and performed the calculations for signal strength losses and cell coverage for our case studies. The next step was to finalise the small-cell location and positioning, as shown in the below section.

❖ Setup of small-cell location and positioning

Afterwards, we proceeded to remove redundant candidate site locations with the same maximum or minimum height in each coverage block. The cell site selection process was two-fold. We selected one cell site per $2 \times 2 = 4$ blocks in a 200 m $\times$ 200 m cell coverage area. Conversely, it could also be one cell site selected per $3 \times 3 = 9$ blocks in each 300 m $\times$ 300 m cell coverage area. The purpose here was to optimally reduce the additional number of final cell sites if the initially selected number of cells did not meet the cell limit requirement of a standard maximum of 30 cells/km2 [61]. In our approach, we selected all maximum and minimum prominent areas as initial potential cell sites. It led to multiple locations with the same maximum or minimum elevation within the same coverage area as potential cell sites at initial assumptions.

Once the path loss value for each location was calculated, redundant site locations with the same maximum/minimum elevation and higher path loss amount were removed immediately from the terrain grid. After the candidate maximum and minimum locations were determined, each position was studied for terrain induced LoS path losses and additional NLoS losses due to structures/buildings on top of the geographic land terrain. Based on the findings, the location with the least amount of path loss for both LoS and NLoS scenarios, among the three studied propagation directions, was finalised as the final cell positions. An example of the small-cell positioning for a maximum elevation point within a single cell coverage block is shown in **Figure 13**. Here, the pink square represents the whole area boundary within which the small-cell site can be installed, while the white diamond shape in the centre indicates the centre of the block. It is assumed that the whole boundary would have the same elevation level, and the small-cell can be placed anywhere within that boundary area. However, for uniformity, the boundary's centre point would be considered the default site for placing the small-cell equipment. A similar representation was also done for the minimum elevation location, where blue square indicated the small-cell site boundary and black diamond shape for the centre of the boundary, as shown in **Figure 14**. As the final step in our framework, we then determined the structure and street positions to place the small-cell BTS equipment, as discussed below.

Figure 13: Maximum elevation location position within a cell

Figure 14: Minimum elevation location position within a cell

❖ Determining the structure and street positions

After possible appropriate small-cell locations in an urban case study are determined, the final step is to consider the path loss and coverage profiles of the mobile signal in terms of encountering urban structures, e.g., low-rise buildings (under about ten-stories in height) and high-rise buildings (usually over ten-stories high). Low-rise buildings typically cause mobile signal diffractions, usually near or just under the rooftop of buildings, while high-rises can obstruct the signal and cause it to propagate in an NLoS manner [58]. Therefore, while placing the small-cells in a selected position, the most favourable locations would be the outside of a structure/building nearby to avoid the effects of signal diffraction/obstruction.

3.3.2. 4G SCN planning implementation

Once the project background is established, we implement the hypothesised ideas, obtain the results and present them in figures. First, we provide an overview of the small-cell network's overall implementation process in a particular geographic scenario. The implementation process is based on the following algorithm, which automatically selects the optimised locations to place small-cells based on the elevation and path loss parameters.

❖ 4G Small-Cell Network planning algorithm details

Following is the algorithm that acts as the structural backbone for our case study implementation. It involves incorporating data values generated from manual measurements, which then were further rectified using standard statistical parameters generated from such data values.

Step 1: INITIALISE

Terrain elevation values and corresponding slope values (data obtained from corresponding spreadsheet tabular files) in terrain matrix;

Step 2: DECLARE

Placeholder variables for location selection and path loss calculations;

Step 3: READ

Known path loss related parameters for calculations from **Equations**

$$\nabla_{DC}(S) = A1 + A2\log(S)$$ **(3)** and

$$L_{msd} = L_{bsh} + k_a + k_d \log_{10} d + k_f \log_{10} f_c - 9\log_{10} b$$

(6);

Step 4: CALCULATE

Common statistical parameters such as Standard deviation, Mean standard deviation, Variance, Mean of variance, Minimum variance value, Maximum variance value, Normalised variance (for terrain elevation matrix values).

Step 5: FIND

FOR

Cell area comprising of n number of area blocks of terrain matrix in both horizontal and vertical directions, where n is odd or even, depending on cell size

Find the maximum and minimum elevation value(s) within each cell area;

IF

Terrain matrix has n number of blocks in either or both horizontal and vertical directions unmatched to the required odd or even number of rows and columns to formulate the desired cell area

Find the highest/lowest elevation value(s) for k number of blocks horizontally/vertically for odd-numbered row/columns, respectively, when the required number of blocks needs to be even.

OR

Find the highest/lowest elevation value(s) for $n-2$ blocks horizontally/vertically for even-numbered row/columns, respectively, when the required number of blocks needs to be odd.

Step 6: READ

Slope values for corresponding maximum & minimum elevation locations (data obtained from corresponding spreadsheet tabular files);

Step 7: CALCULATE

Maximum & minimum location Horizontal, vertical & diagonal path losses for both Line of Sight & Non-Line of Sight scenarios respectively (Refer to **equations 3** and **5**, respectively)

Step 8: SAVE

Maximum & minimum elevation location position coordinates by row-column indicators within the terrain matrix;

Path loss information for maximum & minimum elevation locations;

Step 9: SELECT

Areas with same maximum & minimum elevation within individual cell area;

Step 10: DELETE

Records for maximum & minimum elevation locations with more path loss value(s), in case of multiple areas having the same maximum & minimum elevation within individual cell area;

Step 11: WRITE

Information on final maximum & minimum elevation locations, slope values, and path loss values, respectively;

Step 12: COMPARE

Maximum and minimum elevation location path loss values in horizontal, vertical and diagonal directions;

Step 13: FIND

Number of most occurrences of lower path loss values for both maximum & minimum elevations in horizontal, vertical and diagonal directions;

IF

Number of most occurrences of lower path loss values are seen for maximum elevation positions

THEN

Set all maximum elevation locations as potential small-cell locations;

ELSE

Set all minimum elevation locations as potential small-cell locations;

Step 14: END

❖ 4G Small-Cell Network planning formulation

This algorithm can be mathematically formulated in the following two approaches.

- Formulation of maximum elevation location selection
- Formulation of minimum elevation location selection

➢ Formulation of maximum elevation location selection

This following formulation method selects maximum elevation locations for 200 m × 200 m /100 m and 300 m × 300 m cell divisions-

Let,

X_{rci} : Maximum elevation in one terrain block

λ_{rci} : Path loss for each maximum elevation in a particular direction (horizontal, vertical, and diagonal)

Find → X_{rci}

Such that,

$$\lambda_{rci} < \lambda_{rcj,} \; i \; = \; 1, \; 2, \; \ldots\ldots, \; m; \; j \; = \; 1, \; 2, \; \ldots\ldots, \; m$$

r = row indicator for location coordinate,

c = column indicator for location coordinate,

$j \; \neq \; i$,

$m = 4$ for 200m × 200m cells,

$m = 2$ for 200m × 100m cells,

$m = 9$ for 300m × 300m cells

where m is a free variable

➢ Formulation of minimum elevation location selection

This following formulation method selects minimum elevation locations for 200 m × 200 m /100 m and 300 m × 300 m cell divisions, using a similar approach and the same indexing format as the maximum elevation location selection process.

Let,

Z_{rci} : Minimum elevation in one terrain block

μ_{rci} : Path loss for each minimum elevation in a particular direction (horizontal, vertical, and diagonal)

Find $\rightarrow Z_{rci}$

Such that,

$\mu_{rci} > \mu_{rcj},\ i\ =\ 1,\ 2,\ \ldots\ldots,\ m;\ j\ =\ 1,\ 2,\ \ldots\ldots,\ m$

❖ 4G Small-Cell Network planning algorithm steps

4G Small-Cell Network planning algorithm

Input	:	Terrain elevation matrix T, minimum & maximum elevation values X_{rci} and Z_{rci} respectively, corresponding slope values S, corresponding path loss values
Output	:	Potential small-cell locations
Step 1	:	INITIALISE T
Step 2	:	DECLARE X_{rci} Z_{rci} , λ_{rci} and μ_{rci}
Step 3	:	READ path loss related parameters
Step 4	:	CALCULATE Common statistical values from T
Step 5	:	FIND all X_{rci} AND, Z_{rci} in each terrain block
Step 6	:	READ S from Excel file FOR each X_{rci} and Z_{rci}
Step 7	:	CALCULATE λ_{rci} and μ_{rci} for all X_{rci} and Z_{rci} using S and path loss parameters for horizontal, vertical and diagonal directions from the X_{rci} and Z_{rci}
Step 8	:	SAVE (r,c) for selected X_{rci} or Z_{rci} , with corresponding λ_{rci} or μ_{rci}
Step 9	:	SELECT all the same-valued X_{rci} and Z_{rci} within one same terrain block
Step 10	:	DELETE additional X_{rci} or Z_{rci} for multiple same X_{rci} or Z_{rci} value within one terrain block

Step 11	**:**	WRITE final X_{rci} and Z_{rci}, with corresponding λ_{rci} and μ_{rci} values for each terrain block
Step 12	**:**	COMPARE each final X_{rci} and Z_{rci}, by corresponding λ_{rci} and μ_{rci} values
Step 13	**:**	FIND number of occurrences of lower λ_{rci} or μ_{rci} values in all directions FOR each final X_{rci} or Z_{rci} a terrain block; IF X_{rci} has more instances of lower λ_{rci} values among all three directions, its position is chosen as the small-cell location, OR Z_{rci} is chosen
Step 14	**:**	END

This above is a formal representation of the small-cell network planning algorithm that helped envision an urban 4G technology scenario small-cell cellular network. This algorithm took into account the significant influences of geographical characteristics that can affect small-cell locations' positioning to ensure proper signal coverage in an urban area case study region.

The following section highlights the algorithm's implementation to obtain relevant results for a 4G cellular technology-based small-cell network planning framework.

3.4. 4G SCN planning results

This section evaluates the outcomes obtained from implementing the 4G small-cell planning framework, utilising the 1800 MHz and 900 MHz frequency bands [106]. The results are direct outcomes achieved through SCN planning and methodology tactics, as mentioned in **Section 3.3**. We aim to establish that the proposed small-cell network planning framework can offer ample coverage within the selected cell coverage area. It should be achieved before the maximum degradable signal level is reached for the appropriate frequency bands utilised. The implementation process is divided into two case studies, which highlight the fact that the formation of the terrain significantly impacts cellular mobile signal propagation over urban geographic terrain itself, causing signal losses. By predicting the signal loss profiles in selected areas, appropriate small-cell sites can be chosen to establish a planned small-cell network. The two implementation approaches for this 4G SCN framework are as discussed below.

- 4G small-cell planning for 1800 MHz

- 4G small-cell planning for 900 MHz

3.4.1. Small-cell planning for 1800 MHz

This SCN framework implementation approach aimed to form a simple small-cell network planning framework for an LTE 1800 MHz cellular network over the Melbourne CBD area. In the initial study, only signal level measurement profiles in horizontal and vertical directions were included with one type of small-cell coverage area size of 200 m × 200 m /100 m. In this case study, we performed the small-cell location selection based on only the maximum elevation locations as the potential locations. This approach saw the elevation selection process performed using the Google Earth software [104]. Within this process, approximated elevation values were considered by the software, resulting in the same value elevations on multiple occasions within one 200 m × 200 m coverage block. Therefore, we further rectified the selection method by removing the unwanted geographic location points by mobile signal loss measurements studied from each location. Here, the geographical position showing the least path loss was selected in the case of multiple maximum elevation locations in each coverage block. Finally, we introduced the concept of justifying maximum elevation locations as potential small-cell locations by comparing them with minimum elevation locations in terms of signal loss profiles. We adopted only one variation of the cell coverage area to implement the 1800 MHz carrier frequency small-cell planning, which was the 200 m × 200 m /100 m cell area, as discussed below.

❖ 200 m × 200 m /100 m area small-cell planning

This section discusses the selection of appropriate small-cell locations from a list of potential geographic points. One aspect of this section is that it utilises 200 m × 100 m for studying and planning the SCN framework in a few instances. It was a slight deviation from the anticipated 200 m × 200 m coverage block size. The case study area is 900 m × 1800 m, and after the framework divided most of this area into 200 m × 200 m. This section henceforth discusses the following sub-points-

- Initial maximum elevation locations
- Signal loss profiles for 1800 MHz
- Final small-cell planning for 1800 MHz with fixed antenna height

➢ Initial maximum elevation locations

In this section, the initial cell planning is depicted, where first, all maximum elevations within each coverage block are selected as potential SC sites. Then the fact that maximum elevation locations can be potential small-cell sites is established. This selection process chose 52 initial locations for small-cell site establishment over 45 coverage areas, as shown in **Figure 15**. Here, the pink blocks and white placemarks within each block denote maximum elevation location boundary and corresponding cell position. In this case, the number of total potential small-cell locations, however, exceeds the limit of 30 cells per square-km as indicated by the limit imposed in [61]. Thereby, we used a further selection refining method based on the signal loss profile to remove the redundant locations in each terrain block of 200 m × 200 m. The finalised and optimised small-cell planning is projected, which reduces the number of cell sites from 52 to 45. We next discuss the signal level measurement processes for both LoS and NLoS approaches.

Figure 15: Initially proposed 52 maximum elevation locations

➢ Signal loss profiles for 1800 MHz

This section discusses the signal level measurements for our pre-selected maximum elevation locations. The objective was to rectify and select an appropriate number of small-cell locations to maintain the 30 cells per square-km restriction [61]. It was performed by comparing signal loss profiles for maximum and minimum elevation locations selected within

each 200 m $\times$ 200 m coverage area block. The signal loss profiles are measured in dB, and obtained results are plotted by putting the index of values, i.e., rank in positioning order on the x-axis against their corresponding path loss value in the y-axis. For example, cell location-1 has a path loss of 124 dB, so the number 1 is on the x-axis while 124 would be put on the y-axis. This section has the following two parts-

- LoS signal loss profiles
- NLoS signal loss profiles

LoS signal loss profiles: Here, **Figure 16** contains the horizontal LoS path loss profile. It depicts calculated LoS propagation losses for maximum and minimum elevation terrain locations in horizontal directions towards the coverage block edge. Then similarly, **Figure 17** depicts the comparison processes of the vertical direction LoS path loss levels. There is, however, a significant drop in signal levels noticed in **Figure 17**. This phenomenon occurs as 9 of the 45 coverage areas for the case study region have 200 m horizontal and 100 m vertical dimensions instead of the intended 200 m $\times$ 200 m areas, thus weakening signal strength levels. It effectively makes the vertical signal propagation paths shorter, generating smaller path losses. Both plots in **Figure 16** and **Figure 17** are generated by plotting LoS signal measurements from each maximum and minimum elevation location. These signal levels are compared with the LTE MAPL value [61] and the Walfisch-Ikegami [105] LoS signal levels to determine the locations that exhibited lesser path loss levels select them as potential SC locations. Here, for both these cases, most maximum elevation losses are relatively lower than minimum elevation losses. Both calculated losses also appear lower than the LTE MAPL value but higher than the LoS path loss calculated in [105], with COST 231 Walfisch-Ikegami model for 200 m -sided small-cell blocks. Unlike the Nisirat model [57], the COST 231 Walfisch-Ikegami model does not account for any correction factor on the terrain slope effect in the case of urban area LoS propagation loss. This factor eventually adds to our calculated LoS and NLoS path losses and ultimately aid in our aimed SCN planning.
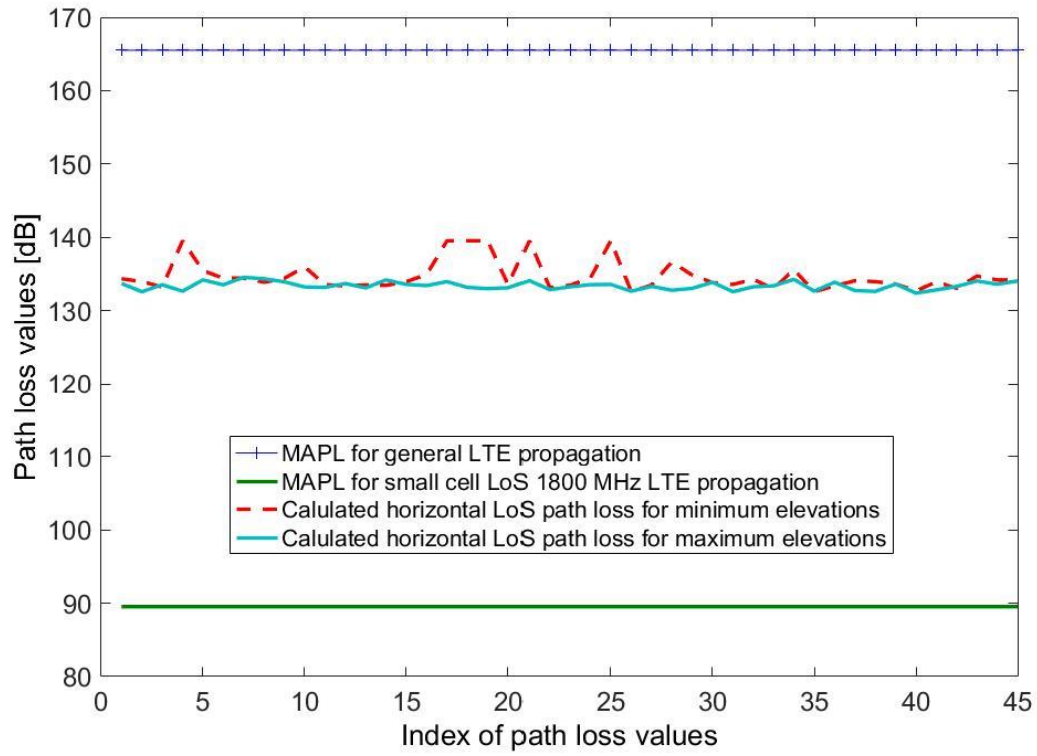
Figure 16: Horizontal LoS path loss profile for 200 m $\times$ 200 m cell area
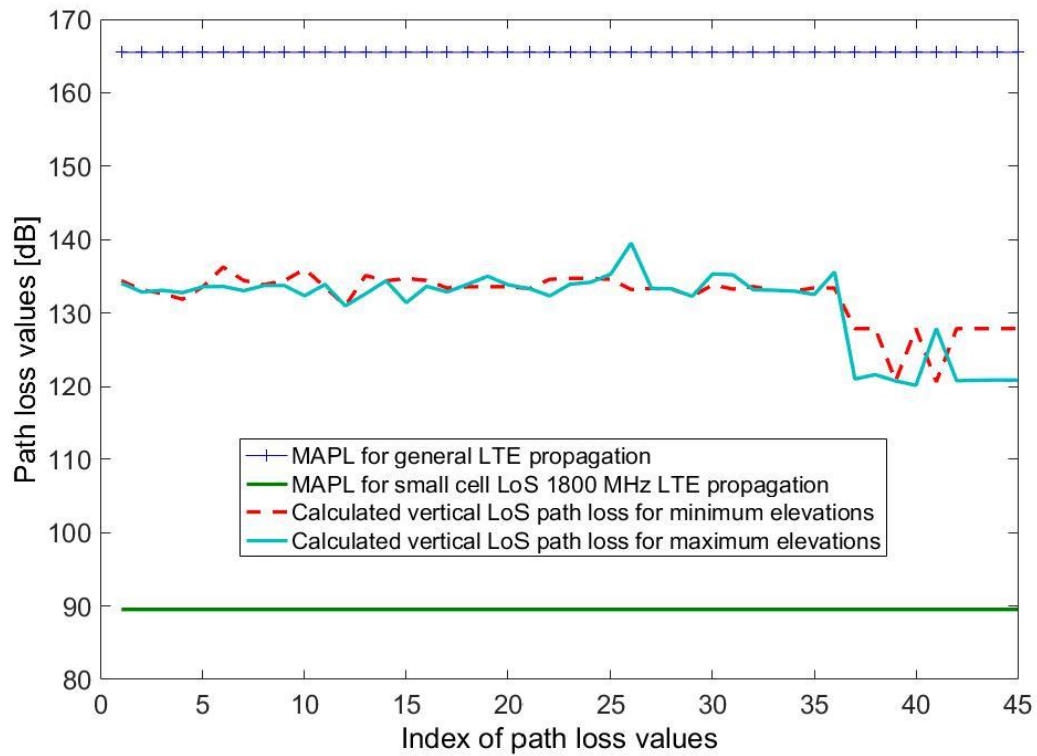
Figure 17: Vertical LoS path loss profile for 200 m $\times$ 200 m cell area

NLoS signal loss profiles: **Figure 18** plots the NLoS signal loss levels in horizontal directions from each maximum and minimum elevation location within our case study. It is similar to the LoS loss profile shown in **Figure 16**. Then resembling the loss profile of **Figure 17**, **Figure 19** displays the plotting and comparison of vertically projected signal loss levels. This figure shows a drop in signal loss levels similar to **Figure 17**, again due to some cell areas having 200 m × 100 m dimensions. Again, both horizontal and vertical NLoS signal loss levels were compared against reference values-in this instance, the previously included LTE MAPL value [61] and the Walfisch-Ikegami [105] path loss calculation value for NLoS scenario only. Similar to the previous LoS signal loss comparisons, the 1800 MHz NLoS losses also remain below the LTE MAPL value but relatively higher than the Walfisch-Ikegami model NLoS path loss. Akin to the LoS scenario, even in this NLoS signal loss case, the Walfisch-Ikegami model does not account for any terrain induced path loss effects. However, this Walfisch-Ikegami NLoS calculation does consider building diffraction loss.
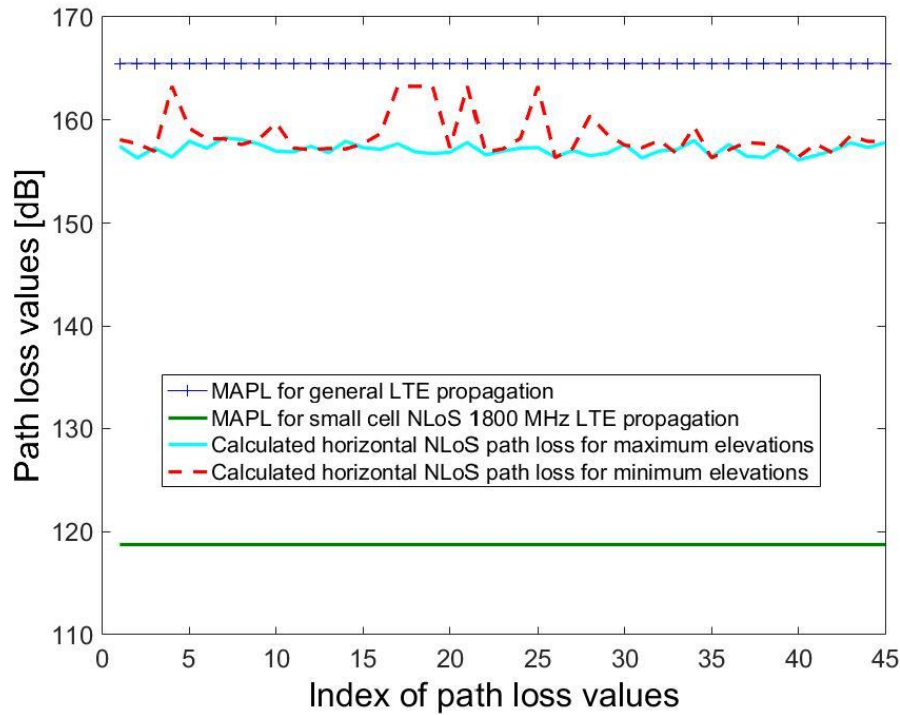
Figure 18: Horizontal NLoS path loss profile for 200 m × 200 m cell area
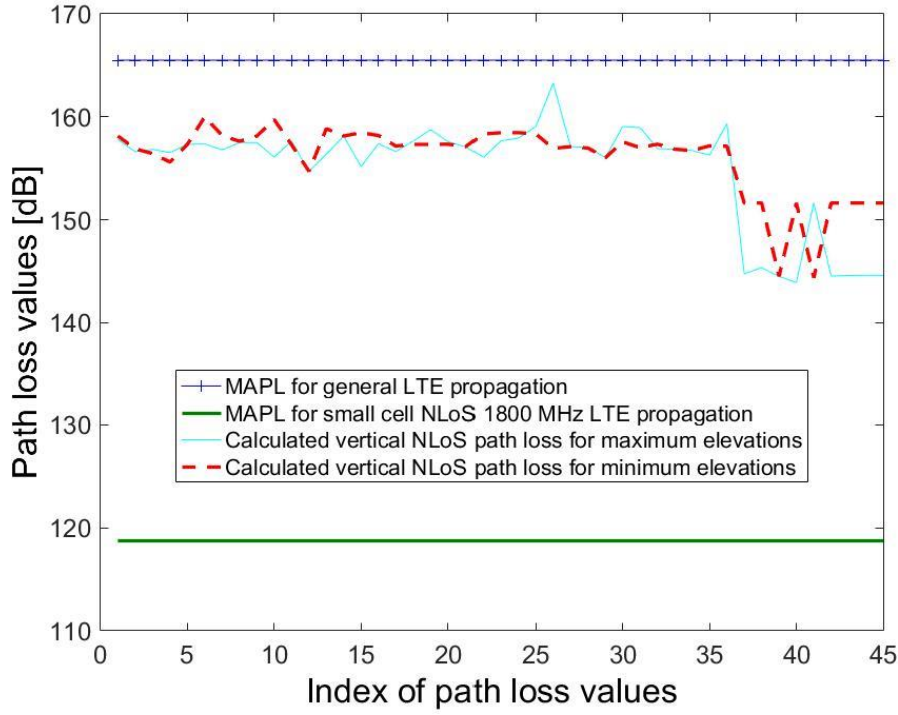
Figure 19: Vertical NLoS path loss profile for 200 m × 200 m cell area

➤ Final small-cell planning for 1800 MHz

Finally, **Figure 20** shows the final version of our 1800 MHz LTE cell planning framework. It consists of 45 cell sites for all 45 cell coverage regions, each having a fixed area of 200 m ×200 m. For this step, we discarded site locations with the same maximum height from each coverage block to finalise potential sites for our cell planning. Here we retained only the highest elevation point with the least path loss within each coverage block since, in most instances, the maximum elevation locations exhibited lesser path loss levels for both LoS and NLoS scenarios. Therefore, each cell had one designated cell location assigned in each 200 m × 200 m coverage area, making it a total of 45 final small-cell site locations. It was achieved for the said case study area of 900 m × 1800 m within the Melbourne CBD region. It also satisfies the maximum cell capacity of 30 cell sites/km² area, since with our proposed cell planning framework, per km² area would have approximately 27.78, e.g. 28 cells only [1]. The final 45 cells are then shown in **Figure 20** below.

Figure 20: Final small-cell planning for 1800 MHz LTE network

3.4.2. Small-cell planning for 900 MHz

The cell planning for the 900 MHz frequency small-cells expanded the SCN planning method described in case study 1. Here, more accurate and fractionalised elevation values were used for the selected potential locations by utilising the GPS visualizer online tool [108]. This process obtained more accurate and fractionalised elevation values based on the exact geographic coordinates of pre-positioned placemarks. This approach reduced the possibility of having multiple locations with the same maximum/minimum elevation value. We also expanded the signal level measurements by introducing measurements in the diagonal direction from each potential location. Alongside, we improved the whole signal level calculation process by introducing a more refined slope measurement approach through mathematical formula [57, 110, 111]. Furthermore, this case study was extended to include cell-planning aspects for two different coverage area types-200 m × 200 m and 300 m × 300 m terrain square block areas. Unlike case study-1, we complete the SCN planning framework by considering locations offering the least signal loss levels, regardless of their maximum or minimum elevation values. Here, only locations exhibiting lesser path losses are selected as SCN locations. As before, we plan the 900 MHz SCN over the same Melbourne CBD stretch of 900 m × 1800 m or 1.62 km2 of land, over which we conducted our case study 1. This case study has the following sections-

- 200 m × 200 m cell area
- 300 m × 300 m cell area

❖ 200 m × 200 m area small-cell planning

This section is the first part of our expanded SCN planning, based on the 900 MHz 4G SCN planning, for the 200 m × 200 m cell area. This section highlights the SCN planning framework deployment by incorporating maximum and minimum elevation locations as potential SC locations. In total, the following steps are included-

- Maximum elevation locations
- Initial minimum elevation locations
- Final minimum elevation locations
- Signal loss profiles for 900 MHz and 200 m × 200 m cell area
- Final SCN planning for 900 MHz and 200 m × 200 m cell area

➤ Maximum elevation locations

All maximum elevation locations selected in each 200 m × 200 m block SC placement boundary indicated with pink rectangles, and the desired SC placement position was shown as a white diamond-shape in the centre. Here, 45 total maximum elevation locations are selected for 45 cell coverage areas. The purpose again is to establish if the maximum elevation locations can be set as potential small-cell sites. Additionally, each coverage block's minimum elevation locations were needed to compare with the maximum elevation location to find the most appropriate cell location sites. Therefore, the next section depicts the specific minimum elevation locations with a figure.

Figure 21: 45 maximum elevation locations

➤ **Initial minimum elevation locations**

The possibility of having the same elevation values within the same coverage area can still prevail, despite using the more accurate GPS visualizer online tool [108]. Hence, 46 minimum cell locations were obtained for 45 coverage areas, as seen in **Figure 22** below. Here, the blue blocks and black placemarks within each blue block denoted minimum elevation location boundary and preferred cell position. Therefore, the task was to eliminate the additional small-cell site based on lower path loss, and the result is in the next section below.
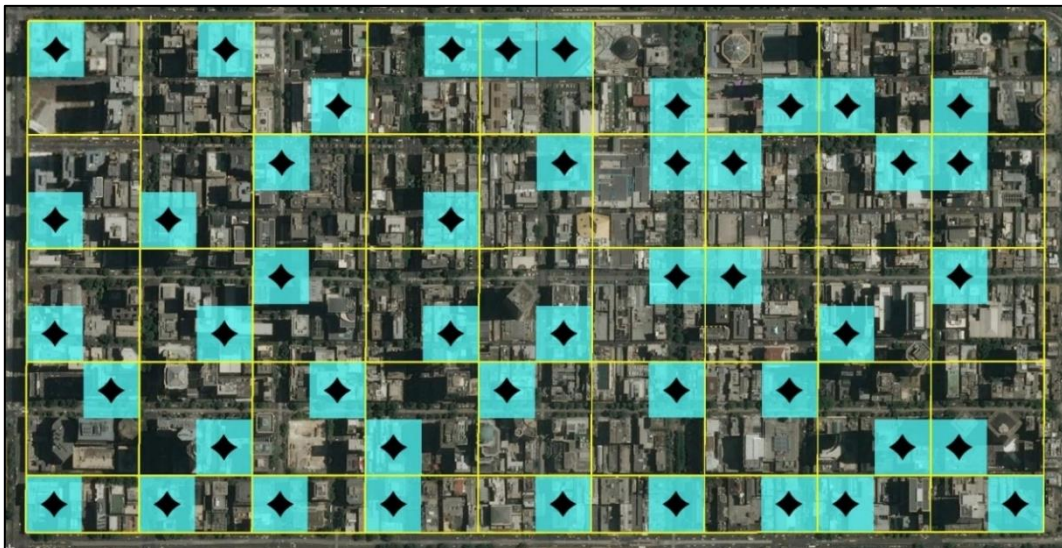
Figure 22: Initial 46 minimum elevation locations

➢ Final minimum elevation locations

For our case study, the minimum elevation locations were also chosen from 200 m × 200 m coverage blocks. It was done to compare the path losses between two external outlier values-the maximum and minimum elevation locations from each 200 m × 200 m coverage block. For this, we needed to consider only one minimum elevation location in each coverage area. Hence, we eliminated the additional minimum elevation location(s) by selecting the location(s) exhibiting lower LoS and NLoS signal loss within the same coverage area. The finally selected minimum elevation locations are shown in **Figure 23,** with the SC placement boundary indicated with blue rectangles, and desired SC placement position was shown as a black diamond-shape in the centre. Next, we proceed to exhibit and discuss LoS and NLoS signal loss profiles for each minimum and maximum elevation locations. It determines the most appropriate small-cell locations based on the lowest exhibited signal loss level by each maximum and minimum location.

Figure 23: Final 45 minimum elevation locations

➢ Signal loss profiles for 900 MHz and 200 m × 200 m cell area

This section discusses the signal loss profiles for the 900 MHz frequency on two approaches-

- LoS signal loss profiles
- NLoS signal loss profiles

LoS signal loss profiles: **Figure 24** exhibits the horizontal LoS signal loss profile, based on signal loss levels experienced around cell area edges from each maximum and minimum location. Figure 25 shows that the vertical direction LoS path loss levels are plotted and compared with reference values similar to previous signal level plots in **Figure 24**. **Figure 26** adds to further rectification of the signal loss comparison process, as it depicts the LoS path losses in a diagonal direction from each maximum and minimum location. Here, the LoS signal measurements were plotted and compared alongside the LTE MAPL value [61] and the Walfisch-Ikegami [105] LoS signal level. In most locations, the maximum elevation losses are relatively lower than minimum elevation losses. Again, all calculated losses appear lower than the LTE MAPL value of 165.5 dB [61]. When compared, our projected LoS path loss values calculated with the Nisirat model [57] remain significantly lower than the Walfisch-Ikegami [105] values in both horizontal and vertical directions. However, the calculated path losses are either equal or lower to the Walfisch-Ikegami values in almost all location points in the diagonal direction. After this, we focus on the generation process of the NLoS signal loss profile.
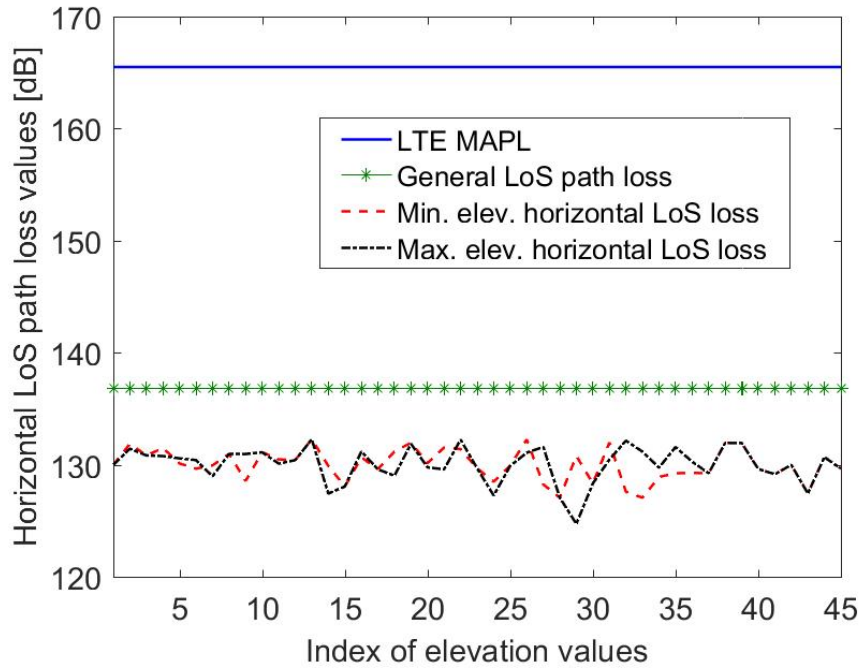
Figure 24: Horizontal LoS path loss profile
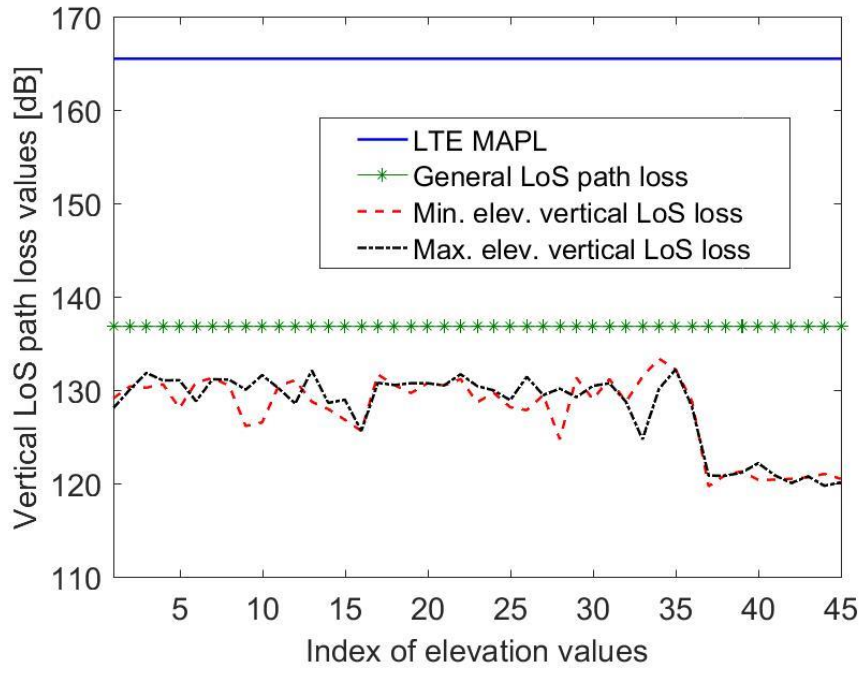
Figure 25: Vertical LoS path loss profile
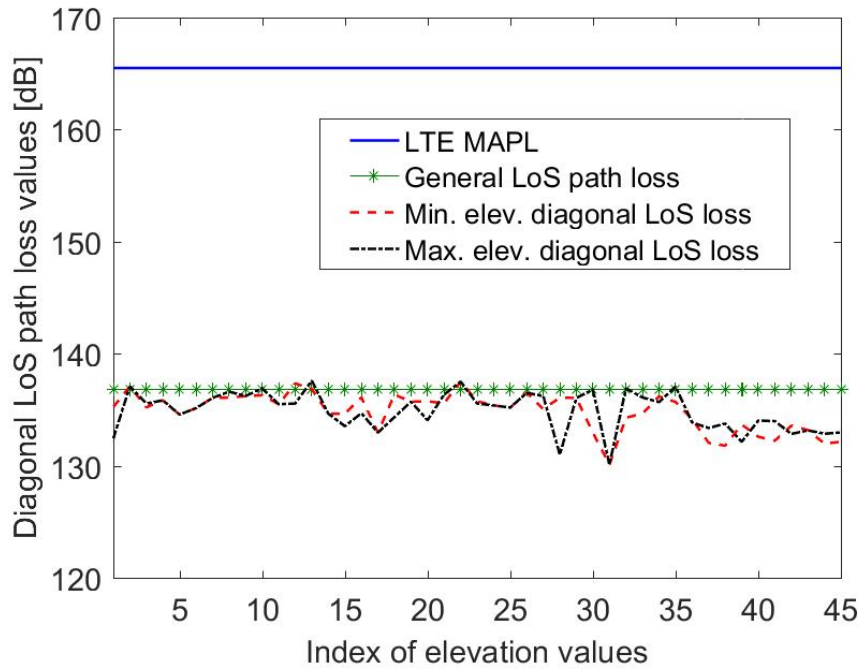
Figure 26: Diagonal LoS path loss profile

NLoS signal loss profiles: **Figure 27** exhibits the horizontal direction path loss values compared to fixed reference values, similar to the LoS signal loss plot of **Figure 24**. **Figure 28** displays the plotting and comparison profiles of vertically propagated cellular signal loss levels alongside the reference signal loss values, similar to those of **Figure 25**. Finally, **Figure 29** shows the NLoS signal level plotting for diagonal directions, similar to the plotting and comparison process of previous signal loss profiles, e.g., **Figure 24**. All horizontal, vertical and diagonal NLoS signal loss levels were evaluated against LTE MAPL value [61] and the Walfisch-Ikegami [105] path loss calculation value. As per previous observations in case study-1, the NLoS signal loss levels for 900 MHz frequency also appear to remain below the LTE MAPL value of 165.5 dB [61]. For such an NLoS propagation scenario, the relevant Walfisch-Ikegami signal loss values in both horizontal and vertical directions stayed below the MAPL. However, in the diagonal direction, the calculated path losses are either equal or lower to the Walfisch-Ikegami signal loss values in most location points. Once all the signal loss profiles were generated, we finalised the small-cell locations to complete our SCN planning, as indicated in the following section.

Figure 27: Horizontal NLoS path loss profile
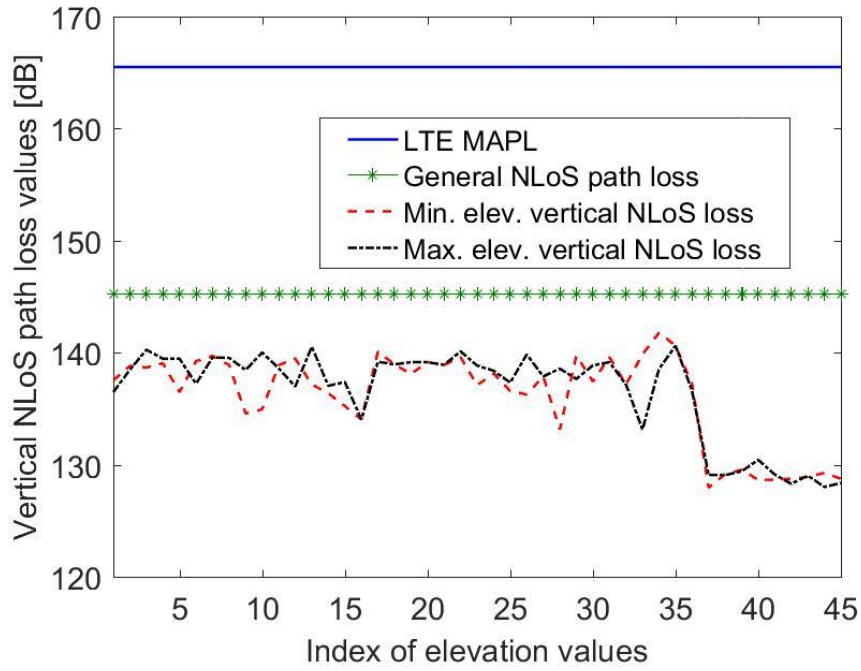
Figure 28: Vertical NLoS path loss profile
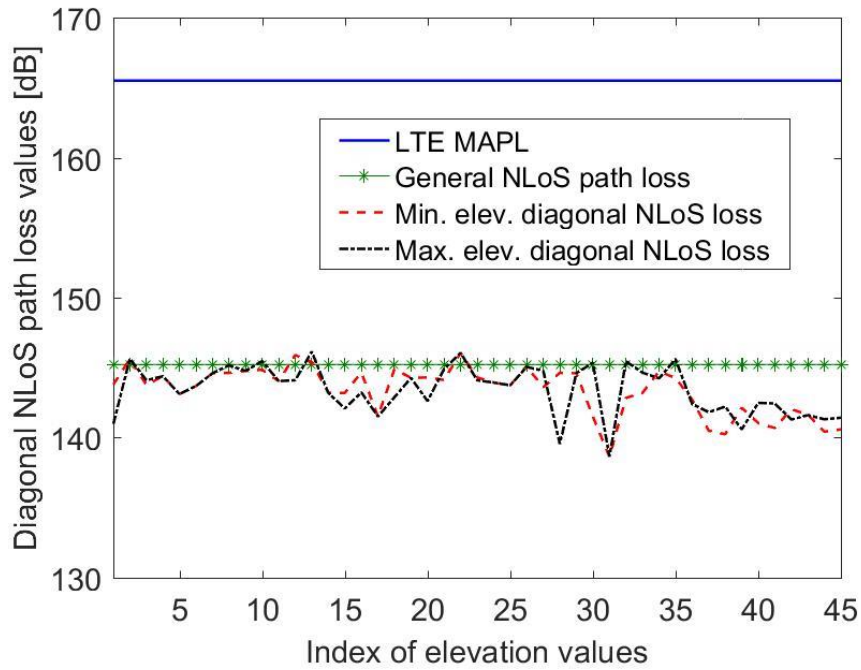
Figure 29: Diagonal NLoS path loss profile

➢ **Final SCN planning for 900 MHz and 200 m × 200 m cell area**

Figure 30 depicts the final version of the 900 MHz LTE cell planning framework. Here, each of the 45 cell coverage areas has one potential cell site, 200 m ×200 m for each. Expanding from the SCN planning process of **Case study 1**, we select only the locations exhibiting fewer path losses, regardless of their elevation values. In most instances, the maximum elevation locations exhibited lesser path loss levels for both LoS and NLoS scenarios, with the rest of the locations showed lesser path losses for minimum elevation locations. Eventually, each 200 m × 200 m coverage area was assigned one SC location each, totalling 45 final small-cell site locations for the said case study area. There are 30 maximum elevation locations, while the rest 15 are minimum elevation locations. The specific maximum and minimum elevation SC location position and corresponding cell boundaries are depicted in **Figure 30** below. This arrangement also satisfies the LTE maximum cell capacity of 30 cell sites/km2 area [1]. Our framework selected 45 cell locations over a total of 1.62 km^2 area, implying that in per km2 area, there would be approximately 28 cells only. The next part of the chapter then describes the small-cell planning method for the 300 m × 300 m cell coverage area.

Figure 30: Final small-cell planning for 200 m × 200 m 900 MHz LTE network

❖ 300 m × 300 m area small-cell planning

This section is the first part of our expanded SCN planning, based on the 900 MHz 4G SCN planning, for the 200 m × 200 m cell area. This section also follows the same approach as the 200 m × 200 m area cell planning, with the additional step is to highlight minimum elevation locations explicitly. Therefore, the following steps are discussed-

- Initial Maximum elevation locations
- Final maximum elevation locations
- Minimum elevation locations
- Signal loss profiles for 900 MHz and 300 m × 300 m cell area
- Final SCN planning for 900 MHz and 300 m × 300 m cell area

➤ Initial Maximum elevation locations

Similar to case study-1, **Figure 31** below depicts the 19 initial maximum locations for all 18 coverage areas. There is one coverage area that has two maximum elevation locations in this scenario. As a result, we aim to discard one of these two locations by selecting the location with relatively lower path loss towards the coverage area boundary. The result of discarding the additional location is shown in the next section.
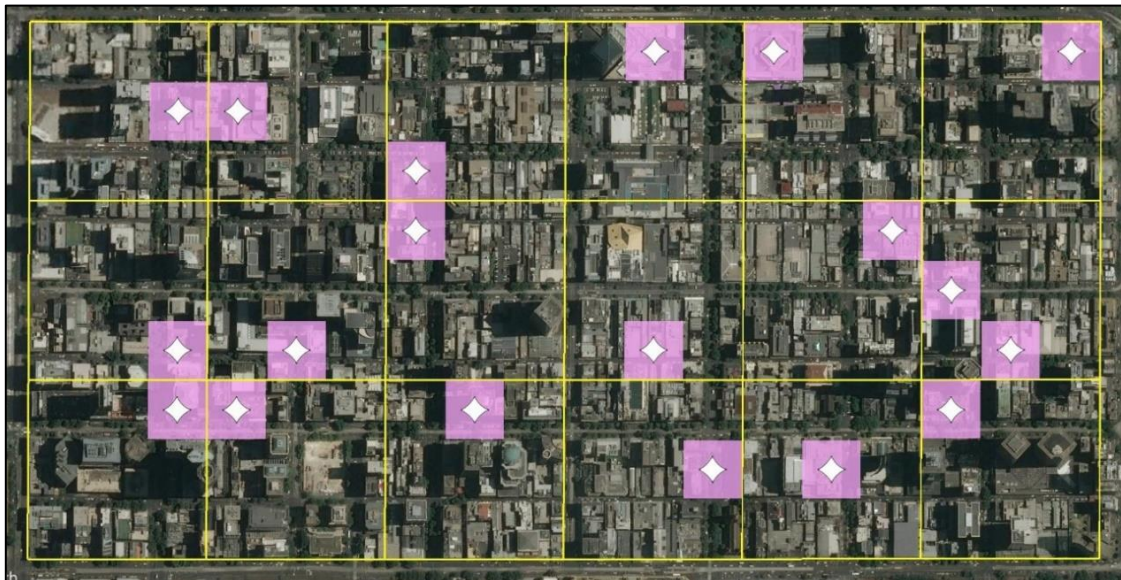
Figure 31: Initial 19 maximum elevation locations

➢ Final Maximum elevation locations

In this section, discarding additional maximum elevation location to reduce the maximum elevation locations to one for each coverage area is shown in **Figure 32**. The basis of removing the additional maximum elevation location was to compare the two location's signal loss profiles and select the location with less path loss levels in most instances. This arrangement, therefore, allows for each coverage area to have one maximum elevation location. The next section then highlights the minimum elevation selection process.
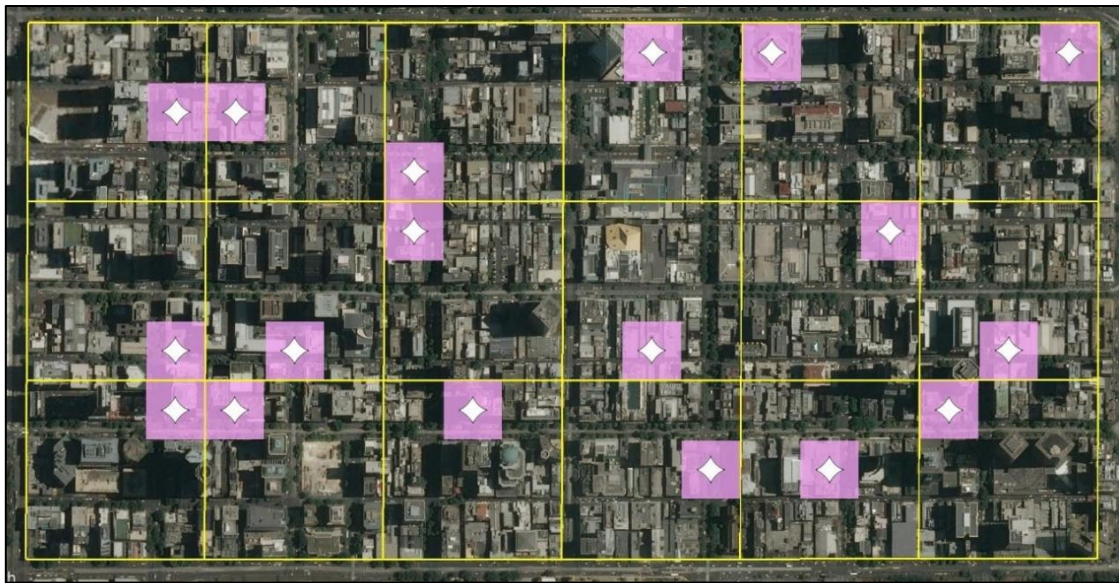
Figure 32: Final 18 maximum elevation locations

➢ Minimum elevation locations

Using the same method in **Case study-1,** the minimum elevation locations for the 300 m × 300 m were selected and shown below in **Figure 33.** The selection method picked one minimum elevation location for each coverage area based on the location having the minimum elevation within each coverage area. It results in the selection of a total of 18 locations for 18 coverage areas. Here, none of the coverage areas had multiple minimum locations with the same elevation within the same cell coverage area of 300 m × 300 m. Therefore, the process of discarding additional cell locations was not needed here. Hence we proceeded towards the following step: to elaborate the signal loss profile generation for the 900 MHz frequency signal.

Figure 33: Final 18 minimum elevation locations

➢ Signal loss profiles for 900 MHz and 300 m × 300 m cell area

There were two categories of signal loss profiles studied for the 900 MHz frequency-

- LoS signal loss profiles
- NLoS signal loss profiles

LoS signal loss profiles: **Figure 34** below depicts the LoS signal loss profile. These losses were calculated with the Nisirat model [57] for signal propagations in the horizontal direction towards the coverage area edges, from each maximum and minimum location. Then in **Figure 35**, the LoS path loss profile in the vertical direction is plotted. Finally**,** the LoS path losses in the diagonal direction from each maximum and minimum location are displayed in **Figure 36**. All three LoS signal profiles were plotted and compared alongside LTE MAPL level [61] and the Walfisch-Ikegami [105] LoS signal value. The maximum elevation losses appear relatively lower than minimum elevation losses in more instances from the obtained plots. It is seen that all calculated LoS signal losses are lower than the LTE MAPL value of 165.5 dB [61]. The LoS path loss value was obtained by COST 231 Walfisch-Ikegami formula [105] in both horizontal and vertical directions. However, in the diagonal direction, the calculated path losses are either equal or somewhat higher to the Walfisch-Ikegami values in almost all locations. Here, the Nisirat model [57] was used to analyse the terrain slope effect on urban area LoS propagation loss. As a result, additional signal loss levels get added to the calculated LoS and

NLoS path losses within our studies. We also worked on the generation method for the NLoS signal loss profile, as shown in the figures below.
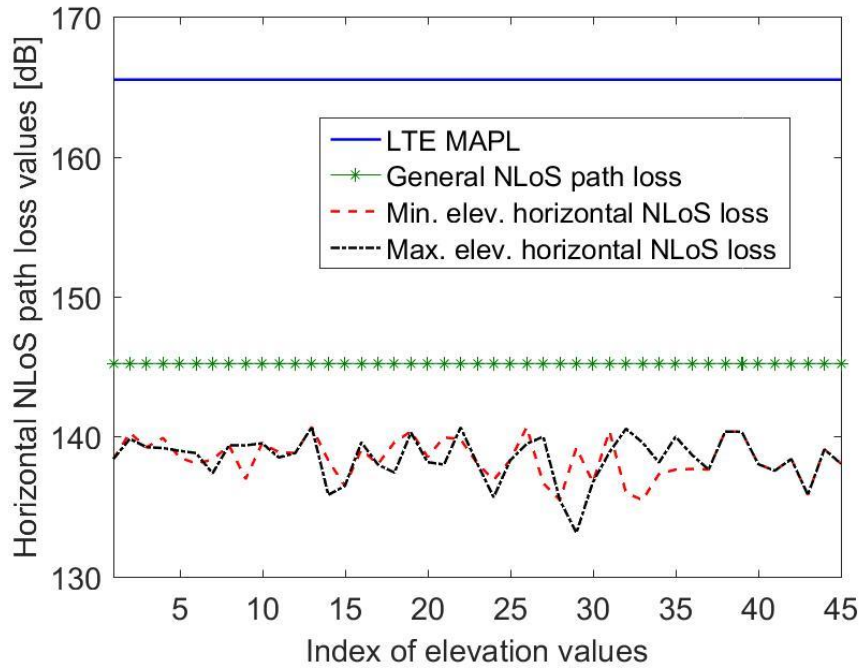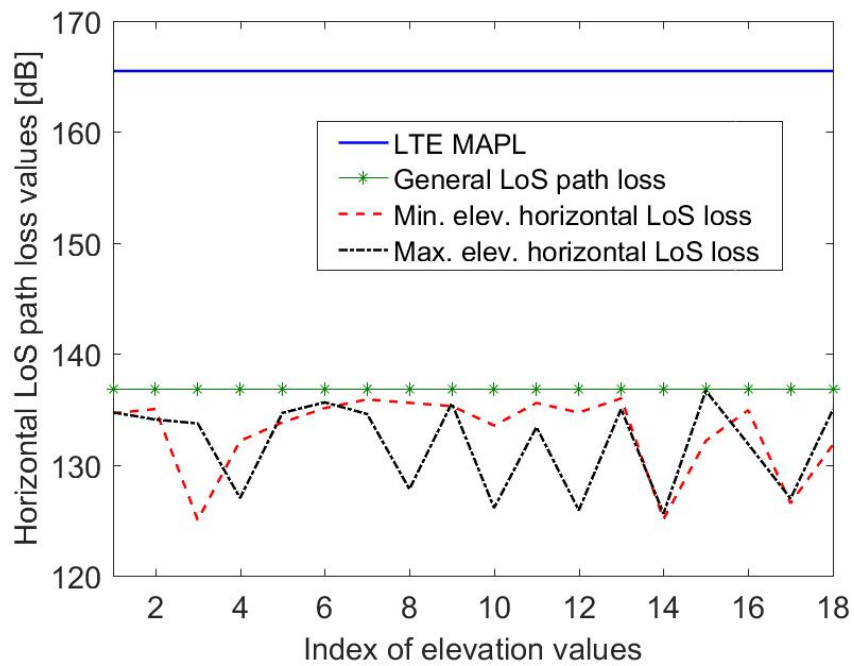

Figure 34: Horizontal LoS path loss profile
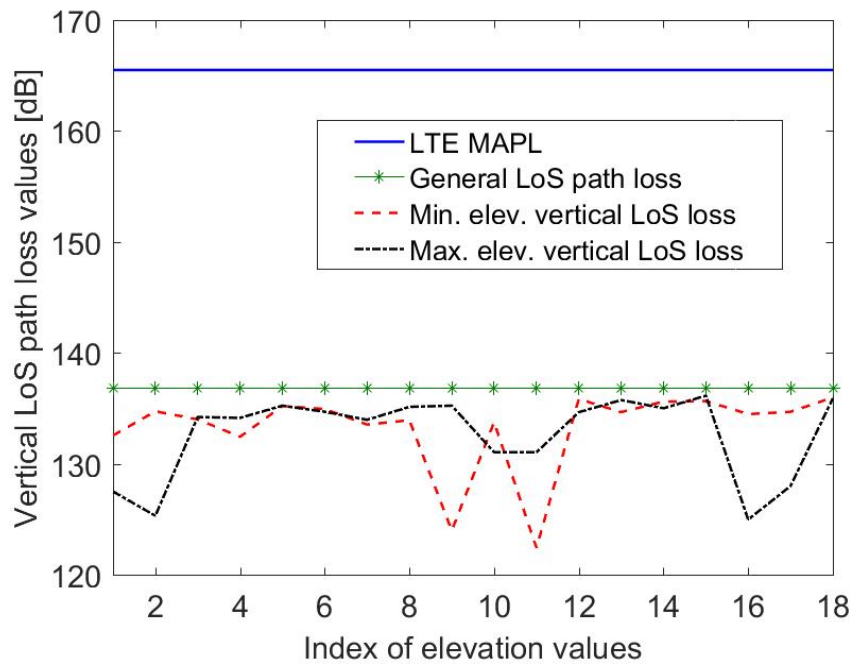
Figure 35: Vertical LoS path loss profile
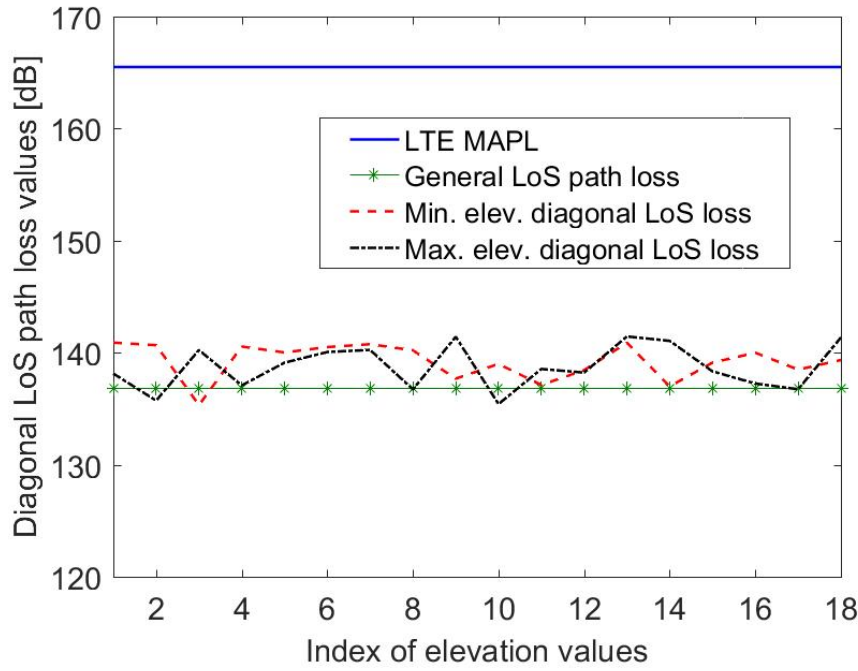
Figure 36: Diagonal LoS path loss profile

NLoS path loss profiles: **Figure 37** presents the horizontal direction NLoS path loss profiles for maximum and minimum locations. Next, in **Figure 38,** the vertical direction NLoS signal losses are plotted. Figure 39 shows the NLoS signal level profile for diagonal direction from all maximum and minimum locations. All the horizontal, vertical and diagonal NLoS signal loss levels were eventually compared against the LTE MAPL value [61] and the Walfisch-Ikegami [105] path loss calculation value for NLoS setting. Again the NLoS signal loss levels for all three directions, as mentioned below, also remain lower than the LTE MAPL value of 165.5 dB [61]. Compared with Walfisch-Ikegami values, the signal loss levels appeared relatively less in both horizontal and vertical direction signal loss profiles. However, for diagonal direction signal losses, our calculated path losses obtained by the Nisirat path loss calculation model [57] are either equal or lower to the Walfisch-Ikegami signal loss values in most instances. Due to the added path losses, accounting for the terrain slope correction factor within the Nisirat model [57]. Eventually, as the last step of this cell planning procedure, we finalised the 300 m × 300 m coverage area small-cell location selection described in the coming section.
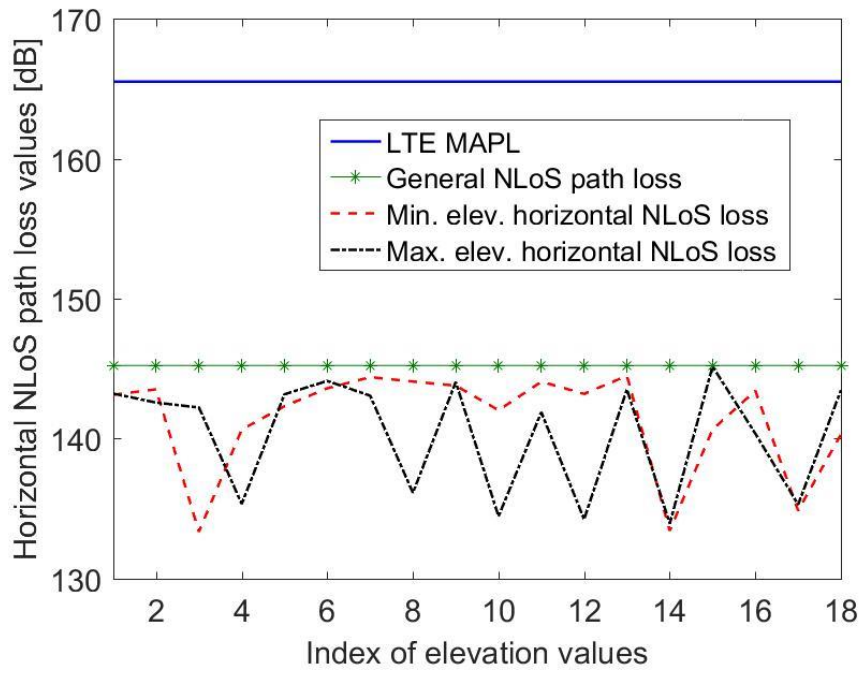
Figure 37: Horizontal NLoS path loss profile
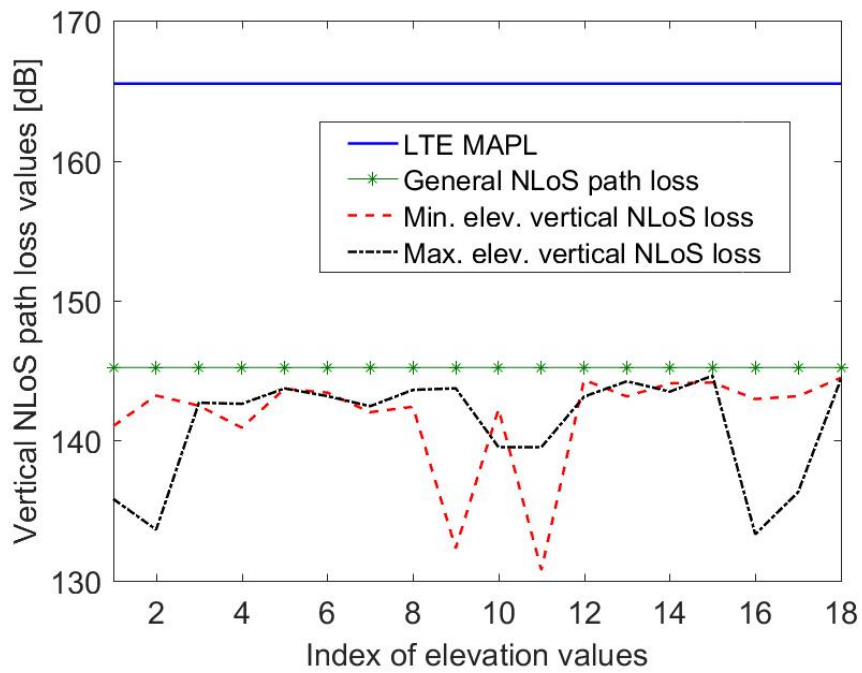
Figure 38: Vertical NLoS path loss profile
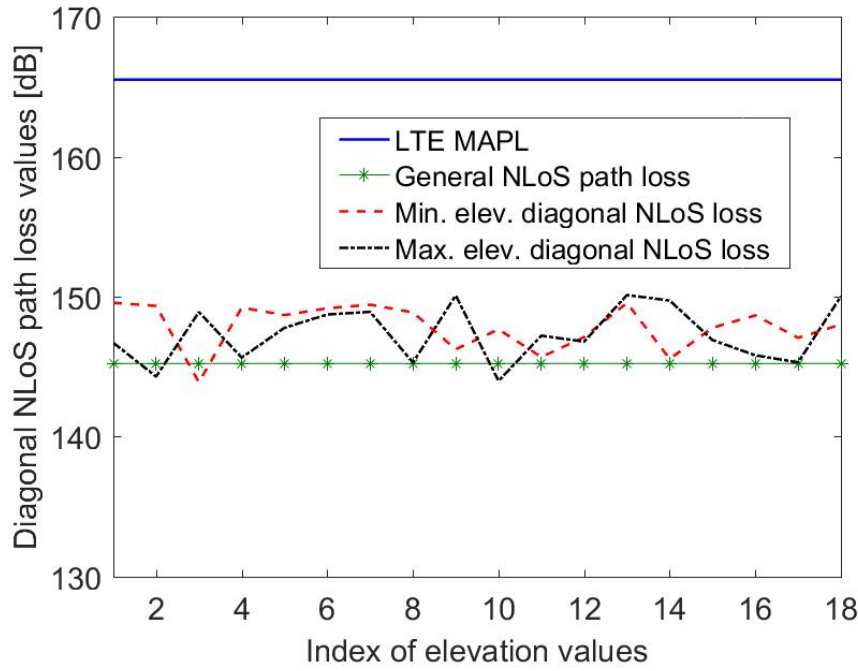
Figure 39: Diagonal NLoS path loss profile

➢ Final SCN planning for 900 MHz and 300 m × 300 m cell area

Figure 40 shows the 900 MHz LTE cell planning framework's final version for 300 m ×300 m cell coverage areas. Here, each of the 18 coverage areas has one cell site selected, totalling 18 small-cell locations. The aim was to select only the location exhibiting less path loss in each coverage area, irrespective of its maximum or minimum elevation value. It is evident in the figure below, where a combination of both maximum and minimum elevation locations is seen in the final SCN formation. Here in more instances, the maximum elevation locations exhibited lesser path loss levels for both LoS and NLoS scenarios than those for minimum elevation locations. In the rest of the instances, the minimum elevation locations showed fewer path losses than their maximum elevation counterparts. There are 10 maximum elevation locations and 8 minimum elevation locations among the selected 18 locations. Again, this also satisfies the LTE maximum cell capacity of 30 cell sites/km^2 area, as 18 cell locations were selected over a total of 1.62 km^2 area with this proposed cell planning framework. With this proposed formation, per km^2 area would have approximately 11 cells small-cells, much less than the 30 cell sites/km^2 limit.

Figure 40: Final small-cell planning for 300 m × 300 m 900 MHz LTE network

3.5. Conclusion

The purpose of the two study approaches within this chapter was to establish a generalised simple SCN planning framework that considers the influences of surrounding area geography, specifically the urban area geographical terrain influences. The works within the chapter have been aimed to address a crucial element in terms of SCN-planning. This aspect was the impact and influence of geographic area aspects such as geographical elevation and terrain slope factor over the propagation of mobile signals. It certainly eliminated previous research gaps, where only higher elevations were considered suitable SC locations, without considering the effect of terrain slope influences in combination with the geographic elevation values [109]. The chapter focused on two study approaches, using two different frequency bands as operating parameters to implement an SCN planning framework under the 4G network technology. In this instance, the SCN case study area was a rectangular portion of geographic land, mapped into square-shaped coverage blocks of equal dimensions. Each block was then considered a cell coverage area, where one suitable location per block was selected. From the outcomes obtained with both of these planning studies, it has been evident that a novel SCN planning framework was established based on terrain influence, cell coverage area, antenna height, and appropriate signal coverage. Additionally, the SCN planning framework integrity was maintained by adhering to specific mobile communication parameters. These include

frequencies of 1800 & 900 MHz; individual coverage block with 100 m, 200 m and 300 m sides, adequate antenna height of 9m and signal losses under MAPL value of 165.5 dB.

The studies reflected a scenario where both geographic land elevation and terrain slope factors together significantly influenced mobile signal propagations from each selected SC location towards each cell coverage area's edge. It was evident that once terrain influences were accounted for, path losses can be less regardless of mobile network transmitter and receiver's elevation position. It can be attributed to several factors. For example, a cell position can be such that the distance between it and the edge of the designated cell area is less than the intended typical propagation distances. In such a case, even minimum height can exhibit less path loss when terrain slope-based calculations are applied.

Additionally, the amount of slope value and nature of slope played crucial roles in determining path losses. Usually, the lower the slope, the less signal loss a receiving antenna position will encounter. Moreover, a less negative slope will incur more signal loss, along with a positive slope. It is merely attributed to the fact that a higher slope will block/diffract/reflect a signal more and significantly reduce its received power to cause more signal loss. Ultimately, utilising these factors, the most suitable location within each coverage block was chosen as the preferred SC location, from which the least signal propagation loss would be exhibited towards the cell edge.

In summary, the overall case study approaches implemented within the chapter ultimately led to developing an appropriate and feasible 4G small-cell network planning framework. It was a planning approach considering the effects of urban geographic characteristics over mobile signal propagations within the SCN area. This case study's findings have already been published as a novel research work within our conference article [1].

This page is left intentionally blank

Backhaul optimisation for pre-planned 4G small-cell network

4.1. Introduction

This chapter discusses the development and implementation process of a 4G small-cell network backhaul framework. The process adopted in this chapter is based on a combination of two different frameworks for the selection of locations/placement of small-cells in a mobile communication network. The first framework selects small-cell locations in an urban geographic setting, following the same terrain grid-based framework discussed in **Chapter 3**, a methodology published in the study [1]. For the first framework, cellular coverage over a particular stretch of a geographic area is mapped by dividing this area into several square-shaped smaller terrain block areas to form a grid. Afterwards, this framework is used to select one SC location per terrain block.

The second framework performs a cost minimising optimisation process to plan out the backhaul network between the pre-selected fronthaul SC network and the core network connectivity for cellular locations. It was done by incorporating information around existing fibre network connectivity. This proposed backhaul optimisation process is primarily based on the CFLNDP method [114], comprising some shared elements from existing theoretical discussions of network optimisation scenarios. This CFLNDP optimisation method is well known to be NP-hard [114]. The research discussed in this chapter takes an approach to perform the optimisation in stages by initially determining the PtP optical fibre deployment and followed by an optimisation stage for determining the GPON design. We adhere to the optimisation method because the primary setting is in alignment with our envisioned optimisation approach. This method aims to identify suitable locations of facilities to meet the demand of goods flow passing through the most optimal roots. For our research work, the optimisation study premises is entirely different, as we want to locate the most optimal small-cell locations connecting to the existing optical network nodes to be served as backhaul to the front-end of these small-cell locations. We considered a different hierarchical network

approach with data demand-serving nodes at each hierarchy level in our optimisation setting. Therefore, the cost modelling equation developed in our optimisation scenario contained multiple summed up components in each cost component calculated, as it considered connecting multiple hierarchy nodes in terms of calculating each type of link cost component. We only considered the location and link costs in our optimisation setting, not a transportation type of cost, as done in the original CFLNDP problem formulation.

The differences in the cost equation formulation led to incorporating more multiple types of constraints within our optimisation study than that seen in the original CFLNDP problem. Our optimisation problem was also considered for a hierarchical setting, where all types of optimisation costs were considered for each stage of a multi-level hierarchical network structure. Thereby, there were significant differences between the CFLNDP method and our optimisation method in terms of cost modelling equation and form constraints. Hence, our optimisation work has its novel significant contributions within the thesis.

We base our SCN backhaul framework over a typical existing PtP fibre network infrastructure to optimise the design of an FTTH GPON access network. The network design problem determines a graph representing the network topology from a given list of potential locations for nodes and links. Each node and edge of the graph was assigned suitable cost parameters for associated equipment and fibre link, respectively, depending on the node and edge capacity and utilisation. For an existing PtP fibre network, each fibre-fed RT is connected to the CO through intermediate nodes called FAPs by a pair of fibres. The FAP can be a manhole or a splicing box with access to the existing fibre. It allows placing splices between high fibre count feeder cables originating from the CO and low fibre count distribution cables terminating at the RTs.

As mentioned, this GPON based backhaul network would offer connectivity between the front-end small-cells with the core cellular network. Hence, we needed to envision a network planning scheme that was easily deployable and suffice to the extensive need for proper capacity attainment. Also, backhaul planning should be generalised enough to be connected to the front-end small-cells. Our literature review has already established that PON technology is more viable as a small-cell backhaul option. Therefore, we chose a PON-based backhaul, particularly GPON, over other similar PON architecture, e.g., the EPON, due to the advantages it provides. For example, as per the study done in [115], GPON provides better

performance in terms of improved line rate, packet-based data transfer, better ethernet support capability, adequate bandwidth, and ensures proper QoS when compared with EPON. GPON can offer better legacy, current and future services than EPON, with better scalability and improved security. Besides, GPON can offer better video services through IPTV and CATV technologies and enhanced convergence between packet or circuit-based data services through its adaptation layer within its network structure, which EPON does not adhere to in general. Thereby, although EPON offers more cost-saving in comparison with GPON, the significant advantages offered by GPON comprehensively renders it a more preferred backhaul option within our network planning framework.

The proposed GPON based backhaul network would need new equipment to be installed. It would include OLTs in selected COs, splitters in selected pre-existing FAPs, and optical network units (ONUs) in selected RT locations, providing the network connectivity to the specific small cells. We require the SCs to be positioned in locations favourable for cellular signal propagations to counter the effects of geographic terrain surrounding the SCs. As a result, the SC and RT locations may or may not be co-located. Hence it is convenient to place the ONUs in the RT locations and then connect it through wires with the SC. For a typical FTTH-GPON, splitters could be used at multiple locations to form a multi-stage split network topology, and due to the loss of splitters, most practical designs could use up to two stages. In such a network, fibre cables could be classified into about three different types. This categorisation depends on where such cables are located in the multi-split network. These would be- between CO and first stage splitter or the first stage and the second stage splitters or the second stage splitter and the remote terminal. A standard GPON can typically have a split ratio of up to 1:64 to backhaul to a total of 64 terminal nodes [6]. For our case study in this chapter, we only adopted 1:2, 1:4, 1:8, 1:16 and 1:32 as the splitter restrictions to maintain decent capacity provisions to be offered by each small-cell selected. Hence, the largest 1:64 split is not considered as it would reduce each small-cell's capacity, stemming from per connection of a splitter. In this case of 1:64 split, each connection stemming out from a splitter will have a significantly smaller portion of the total data (10GPON / 64 connections = 0.15625 GBps) when compared with the smaller ratio of 1:32 (10GPON / 32 connections = 0.3125 GBps). Here, small cells' capacity is also instrumental in choosing the best split ratio for our proposed network design. It would be done in terms of cost comparisons among all split type GPON designs obtained through the GPON optimisation process.

We opted to use the link and facility components to match our optimisation framework's existing optimisation resources. It was done instead of applying the three generalised categories of our standard optimisation model-link, facility and transport components. We omitted the transportation cost component since we were not establishing any new fibre routes, rather re-using existing fibre ducts to set up links between different GPON node levels, as mentioned above. Additionally, RT and SC nodes were not considered within the optimisation process, as the aim was to plan a simple backhaul connectivity network to pre-selected 4G SCs. Also, for simplification, each selected RT location was chosen based on visual proximity from each SC location. In summary, the work done in this chapter proposed a backhaul dimensioning process through appropriate optimisation methods to provide connectivity between the core mobile network and pre-planned small-cell locations over an urban geographic area.

4.2. Related Works

The most relevant literature to the research described in the chapter is presented under the following three key topics to set the context of the research-

- GPON optimisation problem formulation
- GPON optimisation problem implementation

4.2.1. GPON optimisation problem formulation

We propose a GPON backhaul optimisation framework based on the CFLNDP optimisation method [114], where facilities have constraining capacities on the amount of demand they can serve. We simply consider this as a starting point to our problem formulation process.

The objective function for the optimisation framework for this CFLNDP model is-

$$\sum_{(i,j)\in L} t_{ij}Y_{ij} + \sum_{i\in N} f_i Z_i + \sum_{(i,j)\in L} c_{ij}X_{ij} \tag{8}$$

Where,

$\sum_{(i,j)\in L} t_{ij}Y_{ij}$ = Total cost for transporting the flow/demand on a link (i,j) from the node i to

node j (labour and travel cost)

$$\sum_{i \in N} f_i Z_i = \text{Total cost for constructing a facility located at node } i \text{ (Equipment cost equivalent)}$$

$$\sum_{(i,j) \in L} c_{ij} X_{ij} = \text{Total cost for constructing link } (i, j) \text{ (Fibre cost equivalent, variable costs)}$$

Unique identifiers i and j indicate indexes of two different nodes within the network between which connections can exist for optimisation purposes.

There are distinctive parameters and decision variables to support optimisation constraints for planning and dimensioning any optimised network. These are discussed in the following sections.

➢ Standard optimisation model parameters

As per the discussion in [114], there are default general parameters and cost-related parameters involved in forming the CFLNDP problem.

⚪ General parameters

General parameters are a set of potential points to be selected as parts of the intended optimised network. For example, in the case of a network-

N = Set of potential locations where selected network nodes can be placed to minimise cost

L = Set of (undirected) links in the network to connect between selected nodes

K_i = Capacity (e.g., data bandwidth restriction) of ith node facility

D_i = Demand (e.g., data bandwidth demand) at i^{th} node

➢ Cost parameters

The cost parameters for the CFLNDP optimisation problem are divided into three categories-

- Link costs
- Transportation costs
- Facility costs.

Here, facility and link costs are fixed while transportation cost is variable.

Transportation cost parameters: Transportation cost is a parameter that indicates the cost associated with preparing a link for transportation of flow, say data flow from small-cells to the core network. For example, in a greenfield (no deployment placed) scenario communication network, where no deployment has been placed, transportation cost can be trenching and ducting to lay new fibres, along with the cost of labour. For instance-

t_{ij} = Cost of transmitting per unit flow over the link (i, j)

Facility cost parameters: While optimising and planning a network using CFLNDP, the selected nodes are required to establish facilities to cater to the demand required at demand nodes. It involves the installation of equipment and constructing of actual facilities on desired network nodes. Example is-

f_i = Cost of establishing a facility at node i

Link cost parameters: Link cost refers to the cost of connecting between a pair of selected nodes at different stages of an optimised network. The link costs depend on the type and length of links used in the optimisation framework. Depending on the network's requirement, single or multiple direct links can be implemented between each two network stage nodes. Link cost components comprise the distance between each node stage of the proposed GPON backhaul and per-unit cost for covering these distances with optical fibres. Such parameter may include-

c_{ij} = Cost of constructing a link (i, j) between network nodes i, j

➢ Standard optimisation model variables

The model variables are referred to as decision variables since they influence the outcome of the actual framework. Like the cost format, these variables can also be categorised as transportation, facility and link variables.

Transportation variable: This variable determines the number of transmitted flow, e.g., the amount of data that flows through each connecting link of two different stages of network nodes. Usually, this is a non-binary/integer variable and can be denoted as follows.

Y_{ij} = Total flow over the link (i, j)

Facility variable: This indicates the possibility of a facility being placed at a selected node of the desired network. The format of the variable is binary since it will indicate true if a facility exists at a particular node and false if it does not-

$$Z_i = \begin{cases} 1, & \text{if a facility exists at node } i \\ 0, & \text{otherwise} \end{cases}$$

Link variable: This variable is associated with the selected links to connect two nodes of different stages within a network. Similar to the facility variable, this again is binary as it indicates either a link exists between two particular nodes or not. -

$$X_{ij} = \begin{cases} 1, & \text{if a link } (i, j) \text{ exists} \\ 0, & \text{otherwise} \end{cases}$$

D_c = Demand at c^{th} CO, indicated by the required number of fibres to serve the FAP subscribers from each cth CO client. If one CO supports multiple FAPs, then demand at CO will be the sum of the total number of fibres branching out from each CO, e.g., four fibres going towards the next stage (FAP splitter) for, say, a direct PTP connection

D_f = Demand at f^{th} FAP, indicated by the number of splitters required to serve the RT nodes from each fth FAP client. The intention is to support multiple RTs are by one FAP with the use of splitters. Thereby, the demand at each FAP will be the sum of the total number of fibres branching out from each FAP splitter. For example, four fibres are going towards the next stage of RT nodes for, say, a 1:4 split ratio connection from each FAP splitter

D_r = Demand at r^{th} RT, indicated by the number of fibres required to serve the small-cell subscribers at each sth node. In this case, it by default equals 1 for every RT as 1 RT connects to 1 small-cell only. Additionally, the RT and small-cells here have fixed pre-selected locations; hence this parameter is disregarded for this case study.

$\sum_{c \in C} D_c$ = Total demand at all CO(s), for example, connecting to 4 FAPs at the next stage to support a total of 35 small-cells at the end

$\sum_{f \in F} D_f$ = Total demand at all FAP(s), for example, connecting to 16 RTs at the next stage to

support a total of 35 small-cells at the end

$$\sum_{r \in R} D_r = \text{Total demand at all RT(s), disregarded in this study as RT to small-cell}$$

demand is fixed for each RT

$$\sum_{c \in C} D_c + \sum_{f \in F} D_f + \sum_{r \in R} D_r = \text{Total network demand}$$

For example, connecting to 4 FAPs + 16 RTs + 35 small-cell/ONUs = 55 connections in total, from CO to small-cell. In this case, a total of 64-55=9 fibres remaining unused from all RTs, considering a default 1:64 connection restriction for a GPON.

4.2.2. GPON optimisation problem implementation

We applied the MILP [96] as the preferred execution method for our GPON-based backhaul optimisation framework. Such a method is applicable when some of the problem variables hold actual real values: integer or float points, alongside binary variables. Linear programming involves multiple components [96] such as-

- Variables
- Objective function
- Constraints
- Variable bounds

Variables: The unknown component of the optimisation problem we want to find out through the optimisation scenario. Variables are primarily adjustable, and their values influence the best outcome or value for the objective function to achieve our goal of planning and designing a specific real-life scenario.

Objective function: The objective function is the primary mathematical expression that includes the variables to produce an expected outcome to satisfy our requirement for a planning scenario, e.g., profit management, communication network design, factory production.

Constraints: Another form of mathematical expression that proposes limitations in optimisation scenarios to emulate real-life restrictions on resources that affect an optimisation process's possible outcome. For example, the actual amount of available equipment needed within a planned network optimisation process.

Variable bounds: This condition pertains to the limitations imposed over the range of values that a variable can obtain. It ensures that a variable's value should remain within real-life restrictions to produce a realistic outcome of a planned optimisation scenario. Examples can include the rate of products to be delivered from a factory daily.

4.3. GPON backhaul planning overview

The GPON optimisation framework for small-cell backhaul dimensioning aims to connect a pre-planned 900 MHz frequency band SCN [106]. The work's novelty selects an SCN that is pre-planned with another novel framework, as shown in **Chapter 3**. It then expands that into connecting with a newly planned GPON backhaul based on facility location problem to maintain supply and demand of data bandwidth.

The methodology of the framework and its implementation is described below.

- Individual SCN-GPON planning methodology
- Mathematical model of the GPON optimisation framework

4.3.1. GPON backhaul planning methodology

The following steps consist of the SCN-GPON optimisation framework construction-

- Selection of the SCN deployment area
- Existing PtP optical network area selection
- Mapping of existing PtP network elements
- SCN planning process for the selected area
- RT location selection within the planned SCN area
- Selection of the GPON split ratio
- Selection of the number of PON ports
- Cost modelling of the planned GPON

❖ Selection of the SCN deployment area

We have chosen The University of Melbourne Parkville campus as our target deployment area for this case study. The Parkville campus characteristics can be assumed as urban for the propagation of cellular radio waves. In this scenario, there is a presence of buildings within proximity of each other and a varying amount of expected population density

per coverage block area throughout the day. We begin the SCN planning by considering the campus as a grid of equal areas of square-shaped coverage blocks. It was done in dimensions of 100 - 300 m (depending on specified small cell coverage range) on each side of these square areas. Here, one SC would be placed in each coverage area while the coverage blocks serve as the potential area to be covered by each SC placed within them. Here, each of these smaller coverage blocks was divided into four cells. Then, a unique elevation value was attached to each of these "cells". We simplify the data representation by assuming that the terrain elevation all over each said "cell" area is the same. This process then generates a grid of the selected target deployment area, mapped onto a corresponding matrix of specific grid information for our SCN planning. Here, the number of rows and columns in the actual geographic terrain grid will be the same in the grid matrix. In this case, each terrain grid cell's elevation values can be the value for each corresponding grid matrix cell. This approach follows the same method of terrain grid utilisation, as seen in [107]. However, there is a significant difference from **Chapter 3** in the terrain grid formulation.

Previously in **Chapter 3,** all the blocks within the rectangular case study terrain were considered coverage area blocks for SCs. In this chapter, however, only the coverage blocks co-located with the Melbourne University campus building locations were chosen to be included in the case study. Here, these building locations provided the best candidate positions for the placement of small cell infrastructure. The SCN planning then selects appropriate SC locations based on path loss profiles, as done in **Chapter 3**. In this chapter, we aimed to perform case studies on three coverage block sizes, for example-100 m $\times$ 100 m, 200 m $\times$ 200 m and 300 m $\times$ 300 m. These coverage blocks divide the whole case study area into a terrain grid of different block sizes. Examples of these terrain grid divisions for 100 m, 200 m and 300 m dimensions of square coverage blocks are shown in figures 41-43. Such dimensions are chosen to align with the usual small-cell radii range, as stated in the works of [85] and [113]. Then we discuss the optical network area selection method to determine the backhaul network layout to provide connectivity to the selected small-cells.
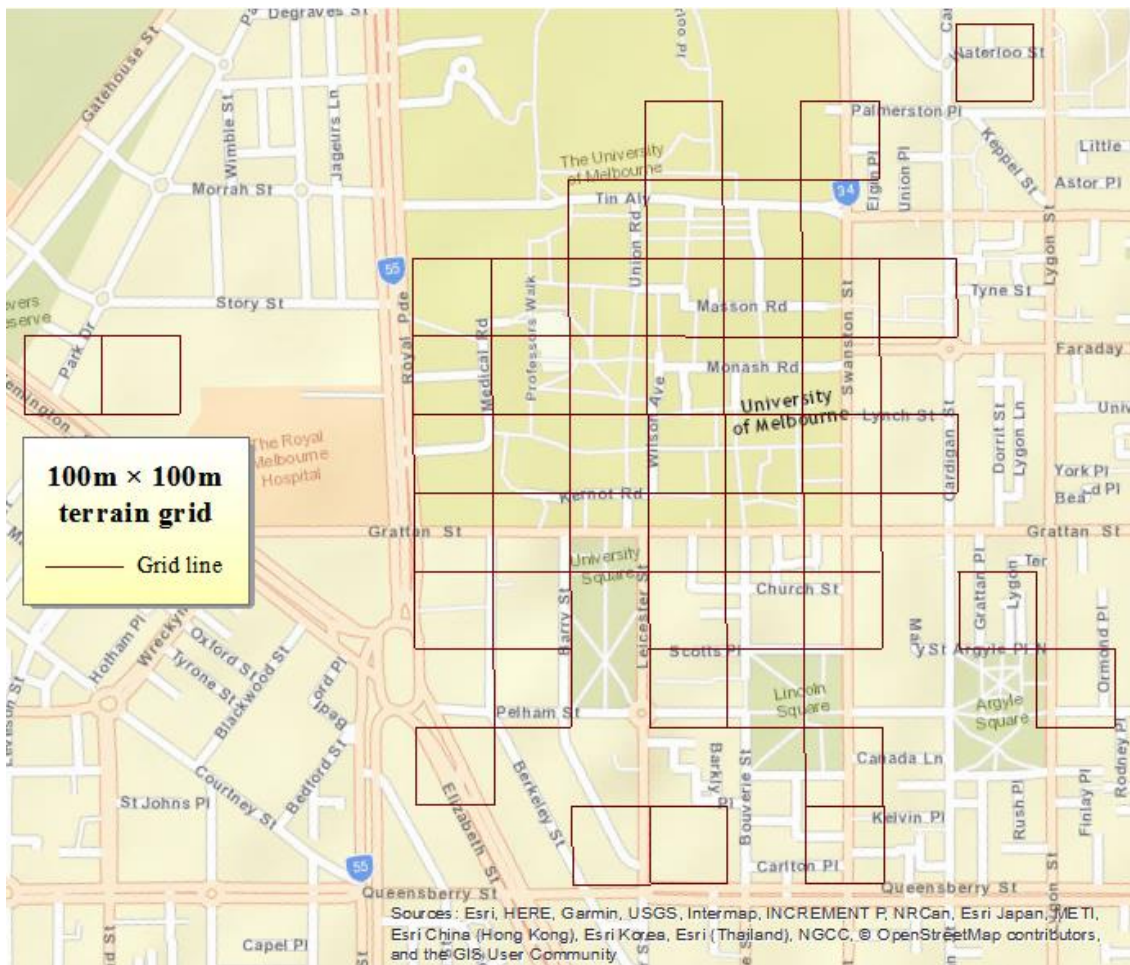
Figure 41: 100 m × 100 m terrain grid over University of Melbourne campus

Figure 42: 200 m × 200 m terrain grid over University of Melbourne campus
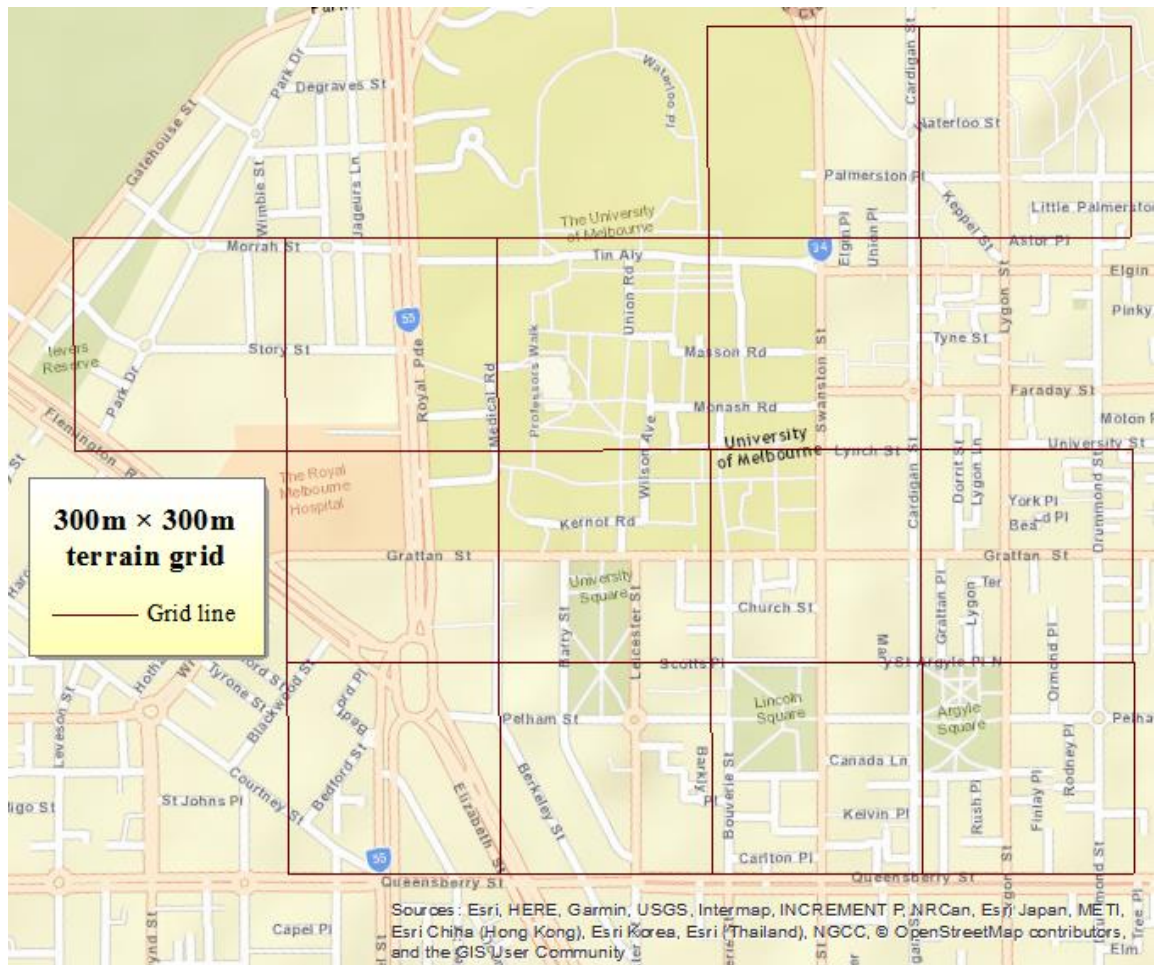
Figure 43: 300 m × 300 m terrain grid over University of Melbourne campus

❖ Existing PtP optical network area selection

The University of Melbourne campus has its optical fibre network utilised to plan the backhaul network for an already proposed SCN within our case study. The existing optical network over the campus is a Ring Optical network, with different geographical locations used for implementing a PtP optical fibre network. It thereby would provide the necessary data connectivity for The University of Melbourne Parkville campus. The following diagram in **Figure 44 i**ndicates the university campus landmarks' names and positions corresponding to the existing PtP optical network. In this formation, specific buildings were used as COs, splicing boxes within building premises were used as FAPs and some other buildings themselves as RTs. These nodes are already connected with established fibre ducts, so at least for the GPON part of our framework, no additional link establishment works are needed to be

done. We then located the existing PtP optical network node locations' positions and highlighted the findings in the following section.
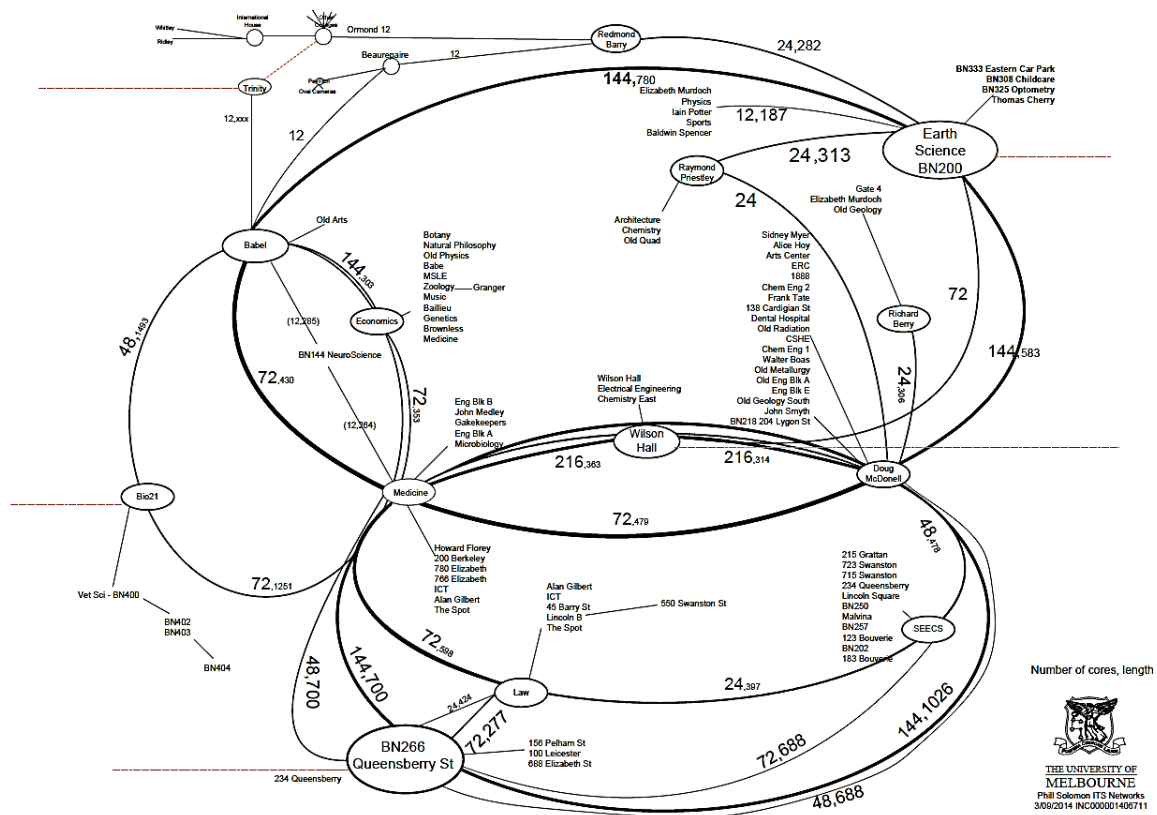
Figure 44: University of Melbourne Optical network diagram [116]

❖ **Mapping of existing PtP network elements**

The actual optimisation framework for dimensioning the GPON framework as backhaul to the pre-planned SCN involves optimally selecting the existing PtP node locations. Such nodes include RT, FAP and CO positions over the existing PtP optical network. The RT locations are chosen to place ONUs to connect with a nearby SC, while CO and FAP locations are selected to place the GPON components OLT and optical splitters, respectively. There are 82 RT locations, 11 FAP locations and 2 CO locations within the University of Melbourne Parkville campus. The following figure represents the PtP optical network, mapped on to the geographic location map. The following section then describes the SCN planning process.
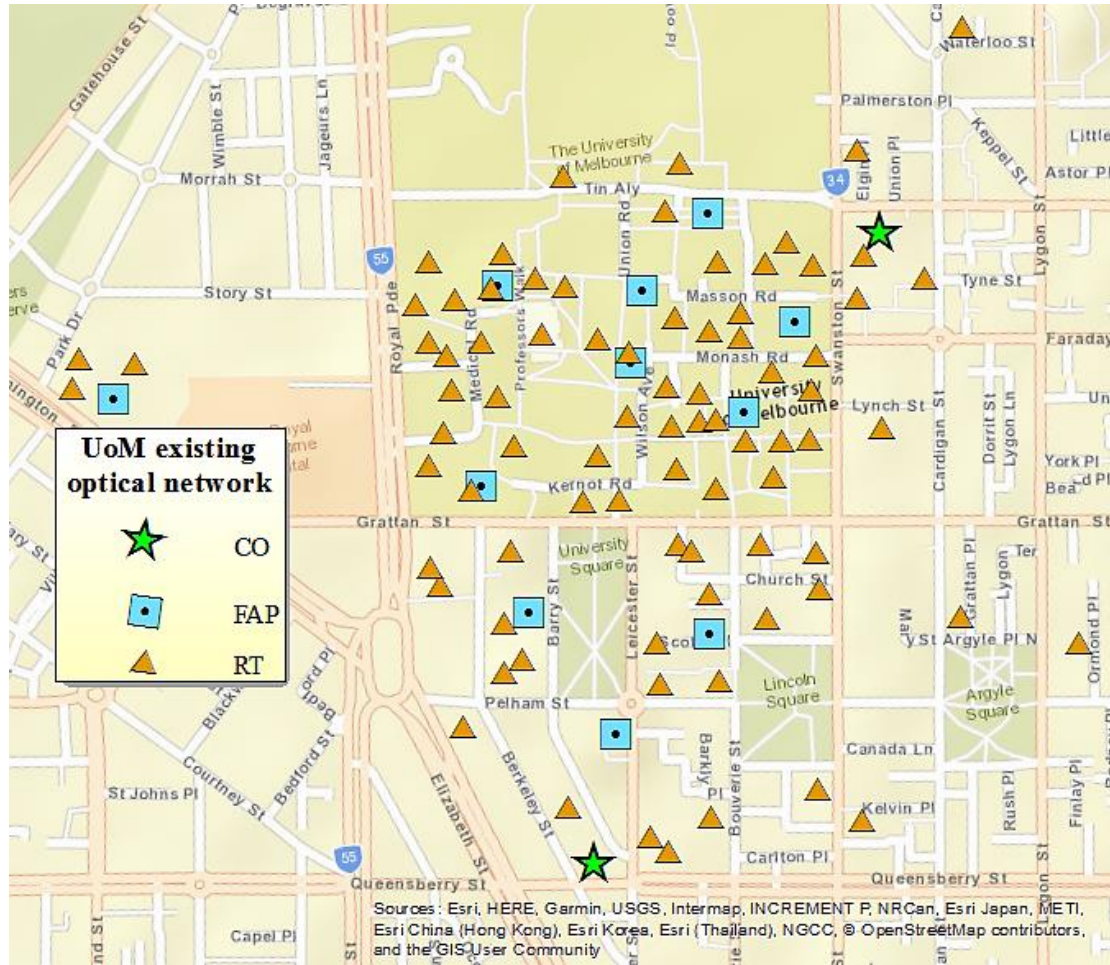
Figure 45: University of Melbourne existing PTP nodes geographic map

❖ **SCN planning process for the selected area**

The first step of this SCN-GPON framework is to select the SC locations, and the backhaul dimensioning would be performed afterwards. The SC location selection process here is obtained through the same method discussed in **Chapter 3**. Thereby, after selecting one maximum and one minimum elevation location for each coverage block, we finalised the appropriate SC location for all our three separate block-sized terrain grids. Again, this selection process is based on best signal coverage scenarios, from each maximum and minimum elevation point, within per coverage block. The maximum and minimum elevation points were chosen for their projected path loss levels from each location. Here, the idea was to select a potential SC location by comparing two opposite extremes of path loss values. Therefore, each location projecting the lowest path loss, regardless of having a maximum or minimum

elevation, was chosen as a proposed location for an SC site establishment for the 900 MHz 4G LTE SCN.

❖ RT location selection within the planned SCN area

The RT selection process is based on visual examination of the coverage area maps to select one RT location from each coverage block in case multiple existing RT locations resided there. As a result, the RT selection process was not included within the GPON optimisation framework since it did not involve any optimisation method. The process involves mapping all the terrain grids having different block sizes over the case study area, then aligning with the existing RT locations to identify the blocks where multiple RT locations would exist. Once done, the next step would be to choose one RT location per coverage block and finalise all RT locations in the process. The idea is to choose an RT location that visually appears closest to the SC in a coverage block from the multiple RT locations existing within that same block. The number of RT locations selected in this process would be different as the coverage blocks' size is different for different terrain grids. The next section then describes the selection process of particular split ratio types for the optical splitters to be placed on selected FAP locations. However, this process can easily be automated in situations where a geographic information system can provide the necessary features for this process, for example, location selection through the p-median method [117].

❖ Selection of the GPON split ratio

In this framework, we typically achieved multiple FAP location selections to install the desired number of splitters. Here, the split ratio for each splitter type is fixed at the same level to restrict the number of outgoing fibres from a FAP towards multiple RT locations [6]. For example, if the split ratio is fixed at 1:2, then from each FAP, a maximum of 2 outgoing fibres can reach the RT locations. For comparison purposes, an alternative way is suggested where no fixed split ratio is used for the splitter type. For this, a splitter type is placed on selected FAPs based on the number of actual outgoing fibres from each FAP towards RT locations. Such an arrangement can be seen in situations where one FAP can allow two outgoing fibres. It invokes the need of placing a 1:2 splitter there while another FAP might have eight outgoing fibre connections, prompting the placement of a 1:8 splitter at that particular FAP. For our case studies in this chapter, we aimed for five split ratio types-1:2, 1:4, 1:8, 1:16 and 1:32. We then

determined the type of line card to be placed in the OLT on the CO location, based on the number of GPON ports they can allocate.

❖ Selection of the number of PON ports

In addition to the split ratio choice, there is another aspect of planning a GPON: the number of PON ports situated inside a line card [6]. It indicates the number of PONs that each line card can support. This number is dependent on the type of PON technology to be used. For example, GPON can support up to 16 PONs, whereas XG-PON and TWDM-PON each support 4, and WDM-PON support 1 PON connection [118]. For our case study, we considered two types of PON ports-4 and 8, as typically used in current PON deployments [119]. It limits the outgoing fibre connections from the OLT placed in CO location(s) towards the FAP locations housing the optical splitters [6]. We then determined the SCN-GPON cost component hierarchy.

❖ Cost modelling of the planned GPON

The network optimisation model here is based on a three-level connectivity architecture. Here, the OLT to FAP splitter connection was by level 1 fibre, FAP splitter and ONU in RT was connected by level 2 fibre, and RT to SC connection was by level 3 wires. Multiple splitters can be installed in the same node of an optical network, except at the OLT. It is because, in an OLT location, neither a user nor a splitter exists. This GPON architecture's cost involves operational costs for current equipment, alongside purchasing and installation costs for adding new equipment. These cost parameters can directly influence the amount of equipment used. For example, the sum of splitter and fibre costs are linear functions of the fibre lengths and number of equipment placed, depending on the level they are both installed together. Here, the optimisation problem determines the splitters' position and the fibres to minimise the overall cost while satisfying the demands and respecting capacity constraints. The next step was to determine the proper RT locations that would house the ONU component in each.

4.3.2. GPON backhaul planning implementation

Several case studies can execute the optimisation framework implementation process based on GPON technology. The approach here would be to acquire the corresponding

modelling results and present them in figures/charts after the framework's theoretical background is established through proper analysis. Here, the optimisation process requires SCN planning to be implemented first, which was performed using the same method described in **Chapter 3**. Since this SCN implementation has already been discussed in detail in **Chapter 3**, therefore, in this chapter, we would only focus on describing the GPON optimisation framework implementation process that comprises the following sections.

- GPON backhaul planning parameters
- GPON backhaul planning variables
- GPON backhaul planning objective function
- GPON backhaul planning constraints

❖ GPON backhaul planning parameters

The backhaul planning optimisation framework depended on two types of cost elements-Link and facility cost components. As earlier mentioned, our optimisation framework left out the transportation cost part altogether since transportation activities involving new fibre routes would not be established within the case study premises. Therefore, the link cost component in our framework was based on the operational costs of the links. As we planned to include new GPON components such as OLT, splitter and ONUs as part of our GPON establishment, the facility cost had been retained in the optimisation framework. The locations of FAPs, COs, RTs and SCs directly determined the cost of connecting a small cell with the OLT via ONU and splitters. With a fixed operating cost per unit length of the fibre, the "fibre-length" for each RT–FAP pair and FAP–CO pair was pre-measured and put into the framework as parameters. The fibre length of such a pair was usually the real distance along with the existing fibre infrastructure. Each of the COs, FAPs, and RTs within a GPON could have a unique identifier associated with them. The optimisation parameters are denoted as follows.

CO = The set of CO locations where $|CO| = N_c$

FAP = The set of FAPs where $|FAP| = N_f$

RT = The set of RT/ONU locations where $|RT| = N_r$

N_c = Number of total CO locations (Capacity at CO stage)

N_f = Number of total FAP locations (Capacity at FAP stage)

N_r = Number of RT/ONU locations (Capacity at RT stage)

N_p = Number of PONs per line card

M = Big M integer for conditional operations

e_r = Cost of OLT rack

e_{sh} = Cost of OLT shelf

e_{cc} = Cost of OLT control card

e_{lc} = Cost of OLT line card

e_{fsp} = Cost of an optical splitter

e_{spl} = Cost of fibre splicing

fi_{cf} = Feeder fibre per meter installation OPEX

fi_{fr} = Distribution fibre per meter installation OPEX

R_f = Split ratio

d_{max} = Maximum transmission distance

d_{cf} = Distance of each feeder fibre

d_{fr} = Distance of each distribution fibre

q_{cf} = Feeder fibre per meter OPEX

q_{fr} = Distribution fibre per meter OPEX

❖ GPON backhaul planning variables

Similar to the GPON optimisation parameters, the GPON backhaul optimisation framework's variables were considered for link and facility cost components. In each instance, the variables consisted of integer and binary categories since our optimisation implementation process was a MILP optimisation problem, incorporating both integer and binary decision variables. Our proposed GPON backhaul deployment could be mainly categorised into three stages of geographic locations that correspond to the three PtP network node types- the COs, the FAPs and the RTs. These were the facility equipment installation locations in the network planning process. CO locations housed equipment such as OLTs, Ethernet switches, and in-house fibre connecting equipment. Ethernet switches connected to OLT, while OLT included the network and PON line cards, followed by fibre distribution panels. The total cost of OLT depended on the required number of OLT chassis, shared equipment, and line cards, which were affected by the number of PONs connected to that OLT. Typically, an OLT chassis supports several line cards, and each line card supports multiple PONs. Ethernet switches connected the access network to the metro network, so they were typically the first elements of a CO. Then fibre distribution panels after OLT connected the outside plant fibre (feeder) to fibre jumpers entered the CO and terminated on the OLT shelf. In such an arrangement, multiple direct links were established using feeder fibre from selected CO location(s) to select the FAP location(s). In **Figure 46** below, a visual representation of this planned SCN-GPON architecture is given.

The subsequent stage of GPON deployment was the FAP location selection. For this, a selected subset of the set of all FAP locations was chosen for placing optical splitters so that connections to multiple RTs can be implemented from each selected FAP location. The cost of a splitter is proportional to the split ratio and the type of installation enclosure. The total splitter equipment-related installation cost for a FAP depends on the number of enclosures and splitters installed at that FAP. Those multiple links from each FAP location towards RT locations were planned using distribution fibre. In the end, from RT to all SC locations, a single link from each RT was set up using drop fibre. In this work, the locations of RTs and SCs were pre-selected and not optimised within this SCN-GPON framework. As a result, the drop fibre costs and SC and RT equipment cost components were not considered within the framework. Here, both link and facility cost components had two types of variables-Integer and binary, as denoted below.

I_{cf} = Number of CO-FAP connections (Demand served by CO stage)

I_f = Number of FAP splitters (Demand served by FAP stage)

N_{lc} = Number of line cards at OLT stage at CO location (Demand served by FAP stage)

$$O_c = \begin{cases} 1; \text{ if the } c^{th} \text{ CO is selected to place OLT equipment} \\ 0; \text{ otherwise} \end{cases}$$

$$S_f = \begin{cases} 1; \text{ if the } f^{th} \text{ FAP is selected to place splitter equipment} \\ 0; \text{ otherwise} \end{cases}$$

$$X_{cf} = \begin{cases} 1; \text{ if the } c^{th} \text{ CO is connected to } f^{th} \text{ FAP splitter} \\ 0; \text{ otherwise} \end{cases}$$

$$X_{fr} = \begin{cases} 1; \text{ if } f^{th} \text{ FAP splitter is connected to any } r^{th} \text{ RT ONU} \\ 0; \text{ otherwise} \end{cases}$$

Figure 46: SCN-GPON architecture

❖ GPON backhaul planning objective function

The GPON backhaul planning optimisation framework's objective was to minimise the different costs involved within, e.g., link and facility costs, to select appropriate link and notes to construct our GPON backhaul part of a small-cell network. So, the objective function elements included the decision variables for the link and facility cost components, and the function aims to calculate the total cost of GPON implementation. It was done by determining the most cost-optimal values to the decision variables and placing them onto the function to calculate the total cost. Hence the following objective function served as our cost modelling equation for the backhaul optimisation process.

$$
\text{minimise} \left[\begin{array}{l} \left(e_r + e_{sh} + e_{cc}\right) \sum_{c \in CO} O_c + e_{lc} \sum_{c \in CO} N_{lc} O_c \\[2mm] + \left(e_{fsp} + e_{spl}\right) \sum_{f \in FAP} S_f + \left(e_{fsp} + e_{spl}\right) \sum_{f \in FAP} \left(I_f - S_f\right) \\[2mm] + \left(fi_{cf} + q_{cf}\right) \sum_{c \in CO} \sum_{f \in FAP} d_{cf} I_{cf} + \left(fi_{fr} + q_{fr}\right) \sum_{f \in FAP} \sum_{r \in RT} d_{fr} X_{fr} \end{array} \right] \tag{9}
$$

Within the objective function, the two primary cost components-Link and facility, were divided into several subcomponents. They can be described as follows.

$\left(e_r + e_{sh} + e_{cc}\right) \sum_{c \in CO} O_c = $ Total cost to install an OLT at the selected CO location

$e_{lc} \sum_{c \in CO} N_{lc} O_c = $ Cost for line card installation at all selected CO locations

$\left(e_{fsp} + e_{spl}\right) \sum_{f \in FAP} S_f = $ Cost for the first splitter installation at selected FAP locations

$\left(e_{fsp} + e_{spl}\right) \sum_{f \in FAP} \left(I_f - S_f\right) = $ Cost for other splitter installations at selected FAP locations

$\left(fi_{cf} + q_{cf}\right) \sum_{c \in CO} \sum_{f \in FAP} d_{cf} I_{cf} = $ Cost of using distribution fibre between OLT and splitter

$\left(fi_{fr} + q_{fr}\right) \sum_{f \in FAP} \sum_{r \in RT} d_{fr} X_{fr} = $ Cost of utilising feeder fibre between splitter and ONU

❖ GPON backhaul planning constraints

Since the backhaul planning optimisation framework would not consider the transportation cost component, the framework's constraints would primarily include the link and facility components within the CFLNDP method. These constraints can be categorised as follows.

- Feeder fibre capacity conservation
- Feeder fibre conditional connectivity
- Distribution fibre capacity conservation
- Split ratio restriction
- PON reach limitation
- Optical splitter-ONU conditional connectivity
- OLT equipment restriction
- Splitter equipment restriction
- Line card connectivity restrictions
- Integer variables
- Binary variables

➤ Feeder fibre capacity conservation

$$I_f = \sum_{c \in CO} I_{cf}, \qquad \forall f \in FAP \tag{10}$$

This constraint ensured that each splitter at the FAPs, connected with only one OLT in the CO. It indicated that the number of feeder fibre connections from OLT was equal to the number of splitters at the FAP level since the OLT in CO only connected with FAPs that have splitters.

$$\sum_{c \in CO} X_{cf} = S_f, \qquad \forall f \in FAP \tag{11}$$

Each FAP location selected for housing a splitter should connect with only one connection of the OLT line card port, where the OLT was placed on a selected CO location, thus maintaining connectivity conservation.

$$X_{cf} \leq O_c, \qquad \forall c \in CO, \ \forall f \in FAP \tag{12}$$

Each CO location to which an optical splitter was connected should house at least one OLT.

➤ Feeder fibre conditional connectivity

$$X_{cf} \leq I_{cf}, \qquad \forall\, c \in CO,\ \forall\, f \in FAP \tag{13}$$

$$I_{cf} \leq X_{cf} M, \qquad \forall\, c \in CO,\ \forall\, f \in FAP \tag{14}$$

These inequalities expressed the conditional relation for the number of connections between c^{th} CO and f^{th} FAP and a connection possibility between the cth CO and f^{th} FAP. The first inequality indicated that if there were no connection from the cth CO towards the fth FAP, the CO would have no OLT placed in it. It indicates that as I_{cf} was zero, then X_{cf} was set to zero too. The second inequality implied that if there were at least one connection from the cth CO towards the fth FAP, the CO would have an OLT placed in it. Again, it means that when I_{cf} is non-zero, then X_{cf} was also set to 1. The above constraints are non-linear and can also be expressed as, $X_{cf} = \min\left(1, I_{cf}\right)$.

➤ Distribution fibre capacity conservation

$$\sum_{f \in FAP} X_{fr} = 1, \qquad \forall\, r \in R \tag{15}$$

Each ONU placed at the RTs should connect with at most one FAP to maintain distribution fibre connectivity conservation.

$$X_{fr} \leq S_f, \qquad \forall\, f \in FAP,\ \forall\, r \in RT \tag{16}$$

Each FAP location to which an ONU was connected should house at least one optical splitter.

➤ Split ratio restriction

$$\sum_{r \in RT} X_{fr} \leq R_f I_f, \qquad \forall\, f \in FAP \tag{17}$$

This inequality applied additional connection conservation limitation for the distribution fibre link, based on the split ratio for each optical splitter in use. Here, at each fth

FAP with a splitter, the total number of outgoing connections towards r^{th} RT was equal or less to the product of the total number of splitters at the fth FAP and the split ratio. It maintained the connection limit set by the fixed split ratio at each splitter. For example, a FAP with a 1:4 split ratio will have 4 splitters at that FAP to connect to RTs, and that FAP could have a maximum of 4×4=16 outgoing connections towards the RTs.

➢ PON reach limit

$$X_{cf}d_{cf} + X_{fr}d_{fr} \leq d_{max}, \qquad \forall\ c \in CO, f \in FAP,\ \forall\ r \in RT \qquad (18)$$

The combined length of feeder and distribution fibres between the ONU and OLT should never exceed the maximum allowed transmission distance of a PON itself. For example, a 1:64 split individual 10GPON reach can be extended up to 50 km of transmission distance, as per the study done in [120]. Therefore, the combined length of feeder and distribution fibre links should remain under 50 km for this scenario.

➢ Optical splitter-ONU conditional connectivity

$$S_f \leq I_f, \quad f \in FAP \qquad (19)$$

$$I_f \leq S_f M, \quad f \in FAP \qquad (20)$$

The two inequalities here denoted the conditional relation for the number of splitters at the fth FAP and the possibility of a splitter being housed at that FAP location. With the first inequality, it was implied that if there is no splitter placed at the fth FAP location, then that FAP location was not selected for housing any optical splitter, i.e., if I_f was zero, then S_f was also set to zero.

The second inequality indicated that if there was at least one splitter placed at the fth FAP, then it meant the fth FAP would be a selected location for placing a splitter., i.e. if I_f was non-zero, then S_f would be 1. Since it was a condition-based constraint, it was a non-linear relationship by nature for the possibility of a splitter at f^{th} FAP location and the total

number of splitters placed at that FAP. This relationship could be expressed as, $S_f = \min\left(1, I_f\right).$

➤ OLT equipment restriction

$$\sum_{c \in CO} O_c \leq N_c \tag{21}$$

The total number of selected CO locations to place OLT equipment should not exceed the total CO locations within the existing PtP optical network premises.

➤ Splitter equipment restriction

$$\sum_{f \in FAP} S_f \leq N_f \tag{22}$$

The total number of selected FAP locations to place splitter equipment should not exceed the total number of FAP locations within the existing PtP optical network case study area.

➤ Line card connectivity restrictions

$$N_{lc} \geq \sum_{c \in CO} \sum_{f \in FAP} \left(\frac{I_{cf}}{N_p}\right) \tag{23}$$

$$N_{lc} \leq \left\{\sum_{c \in CO} \sum_{f \in FAP} \left(\frac{I_{cf}}{N_p}\right)\right\} + 1 \tag{24}$$

A single line card installed within the OLT could only support up to a fixed number of, say N_p PONs. Therefore, every N_p number of PONs would need one new line card to be placed at the OLT.

The first constraint described that the required number of line cards for the cth CO location could be at least the number of CO-FAP fibre connections divided by the number of PONs connected to the cth CO. The second constraint indicated that the maximum number of line cards at the OLT could be one more than the number of CO-FAP fibre connections, divided by the number of PONs connected to the cth CO.

➤ Integer variable constraints

$$I_{cf} \geq 0, \qquad \forall \, c \in CO, f \in FAP, \tag{25}$$

$$I_f \geq 0, \qquad \forall \, f \in FAP \tag{26}$$

$$N_{lc} \geq 0, \qquad \forall \, c \in CO \tag{27}$$

The integer variable constraints put restrictions on integer variables to complement the development of the cost optimisation framework. Therefore, the above numerical inequalities indicated that the integer variables could be either zero or any non-zero value.

➤ Binary variable constraints

$$O_c \in \{0,1\}, \qquad \forall \, c \in CO \tag{28}$$

$$S_f \in \{0,1\}, \qquad \forall \, f \in FAP \tag{29}$$

$$X_{cf} \in \{0,1\}, \qquad \forall \, c \in CO, f \in FAP \tag{30}$$

$$X_{fr} \in \{0,1\}, \qquad \forall \, f \in FAP, \, r \in RT \tag{31}$$

All binary variables above indicated that all of them could have a value of only 0 or 1, thus putting restrictions on the values they could take.

After identifying the proper variables, parameters and constraints relevant to the cost-modelling objective function, the following section lays out the results for implementing this cost function to generate our anticipated optimised GPON backhaul architectures.

4.4. GPON backhaul planning results

This section reflects three case study results obtained from implementing the SCN-GPON planning approach in three scenarios. These results are acquired through relevant case studies after adapting to the network planning methodology and implementation approaches mentioned in **Section 4.3**. The case studies would expand the previously planned SCN to link to the core network via a planned and well-dimensioned backhaul architecture. The technology selection for the SCN planning has been set at 900 MHz 4G LTE for this case study. The primary purpose was to plan the backhaul network in a cost-optimised manner. More specifically, we select the GPON backhaul node locations through an optimisation method to

ensure proper connectivity among all the SCN and GPON node, with appropriate link connections in between. There were potential small-cell locations pre-selected over the University of Melbourne area based on their terrain-influenced signal propagation properties. This proposed small-cell network planning framework would offer adequate signal coverage over the case study area. The case study area was divided into three different coverage block area grids of 100 m × 100 m, 200 m × 200 m and 300 m × 300 m, as the authors in this paper, Iannone *et al.* [37], deduced that maximum cell radii should not be more than 700% The idea was to plan and place one SC unit over each coverage block area. It would be done in a way that the maximum degradable signal level for 4G LTE cellular signal [61] is attained until the edge of each such coverage block.

As discussed in the previous **Chapter 3**, the SCN planning reflected that the surrounding geographic terrain significantly impacted cellular mobile signal propagation over the urban area of signal propagation. Once the small-cells were selected through our proposed SCN planning framework, we then selected appropriate nodes and link positions from the existing PtP active optical network. It was done over the case study area to ensure all equipment costs were optimally minimised. This complete framework was a composition of two different selection frameworks, where the first framework selected the SC nodes, while the second one dimensioned the backhaul part to the SC nodes. As discussed previously in this chapter, the proposed backhaul network included essential GPON components, namely OLT, splitter and ONU components. We extensively used the ArcMap module of the ArcGIS software suite [121] in this case study to visually pinpoint our provisional set of PtP network nodes, e.g. CO, FAP and RT nodes, into specific ArcGIS maps. We then selected the most suitable subsets of locations to position our proposed GPON network nodes from those set of locations. We started from the end of the network, the SC nodes, and went up towards the hierarchy's top layer. Here, the network's top layer comprised the CO locations layer, selecting optimised positions in each network node layer. After we selected the desired SC locations over the case study area of the University of Melbourne with three different block sizes, we mapped them out using the Google Earth software [104]. Then we selected one RT location within the same coverage area block as each selected SC, based on visual observations over the map. These RT locations were picked based on visual proximity to the SC position in each coverage block to position the ONU component of the proposed GPON backhaul in those RT locations. Using these RT locations as inputs, we performed our optimisation process over the FAP and CO locations to

select the OLT and splitter equipment's optimal locations, respectively. All the corresponding maps showing the case study area and associated network nodes were obtained using the ArcMap module of the ArcGIS software suite [121].

For the GPON backhaul planning, the approach was to use the CFLNDP optimisation method. Here, CO locations were the equivalent of a set of network nodes, and the fibre connections going out from the CO locations could be considered links of the network [114]. The idea was to minimise deployment cost by planning a network structure that incorporated selected nodes and links. Additionally, this was done so that the total cost of network deployment was minimised through the optimal selection of node and link usages. We aimed for five split ratio types for optical splitters and two types for the number of PON connections within the line card. We added two scenarios into our case studies for comparison purposes, the no fixed split scenario and the PTP backhaul scenario. We obtained total costs associated with each of these scenarios and separated them into link and facility cost components. We then arranged the results into clustered column charts, as seen below. The charts represented the total cost and different cost components within the total cost values for different optical network types, as mentioned above. The values were obtained by running the optimisation framework simulation for these different scenarios above. This framework planning process was conducted for three following case study scenarios-

- 100 m × 100 m SCN-GPON framework
- 200 m × 200 m SCN-GPON framework
- 300 m × 300 m SCN-GPON framework

4.4.1. 100 m × 100 m SCN-GPON framework

This section is the first scenario in our SCN-GPON optimisation case study. It is based on a 900 MHz 4G SCN planning [1] for the 100 m × 100 m cell area, followed by designing an optimised backhaul based on facility location optimised method [114]. This section comprises the following sub-sections-

- 100 m × 100 m cell area SC location selection
- 100 m × 100 m cell area RT location selection
- 100 m × 100 m framework cost comparisons
- Final 100 m × 100 m network map examples

❖ 100 m × 100 m cell area SC location selection

The resulting SCN planning can be shown in the following **Figure 47.** The pink squares indicated each potential location block within which an SC can be placed. The diamond shape inside the pink square designated the cell's centre where actual SC equipment would typically be placed. For this scenario, all maximum elevation locations were found to be the suitable SC positions, with the lowest path losses within each coverage block, following the methods described in **Chapter 3**, again shown in **Figure 47**. The next section then discusses the RT selection process for the SC/ONU connectivity.
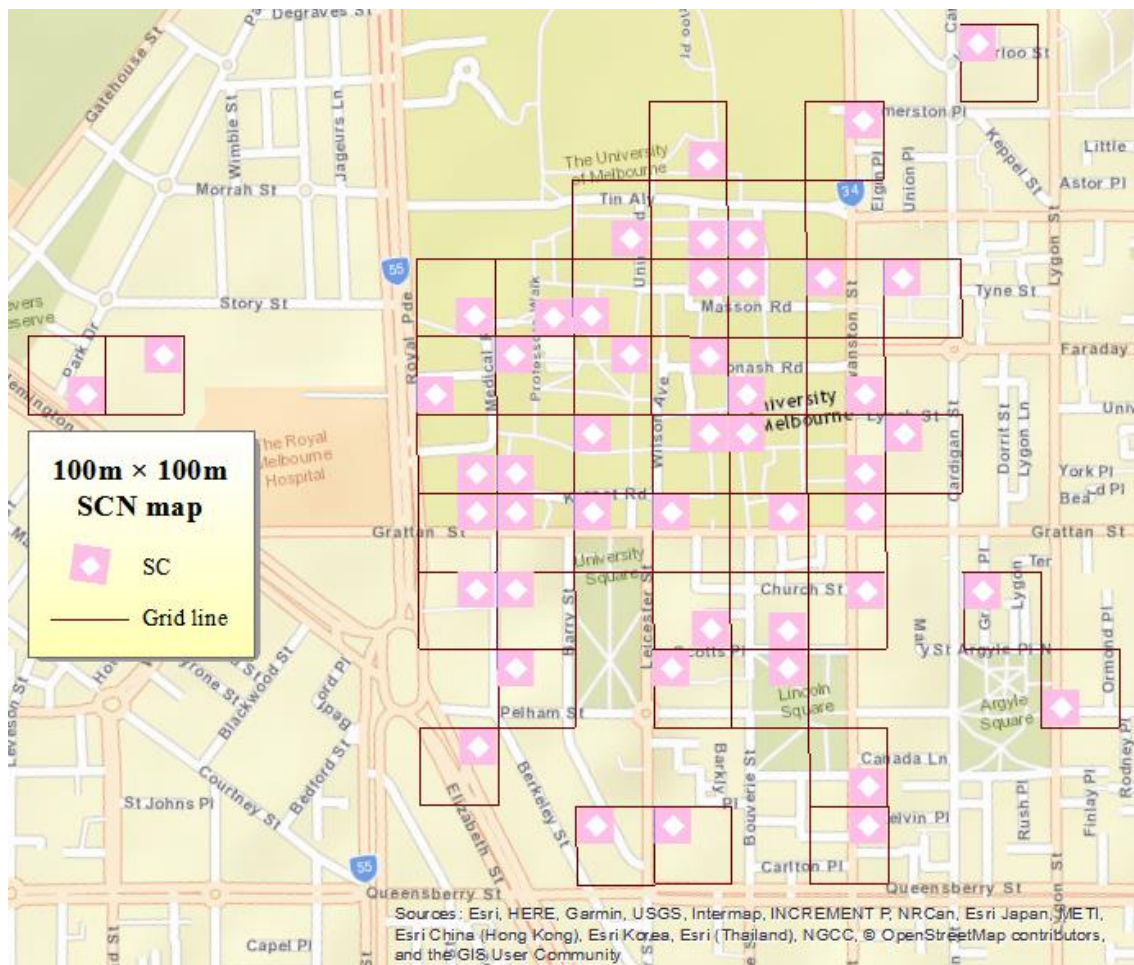
Figure 47: 100 m × 100 m SCN planning over University of Melbourne

❖ 100 m × 100 m cell area RT location selection

Once the SC planning and positioning are done, we select RT locations to house the ONUs. This process was done to connect the SC with the optical GPON backhaul using the ONU. This RT selection process was divided into two parts-

▪ Initial RT mapping with 100 m × 100 m SCN
▪ Final RT selection for 100 m × 100 m SCN

➢ Initial RT mapping with 100 m × 100 m SCN

First, we imposed the 100 m × 100 m terrain grid SCN map over the case study area through the ArcMap tool [121], then plotted it with the existing RT locations. The following diagram depicted the scenario where multiple RT locations existed within several 100 m × 100 m coverage blocks. The next section then depicts the finalised RT mapping process.
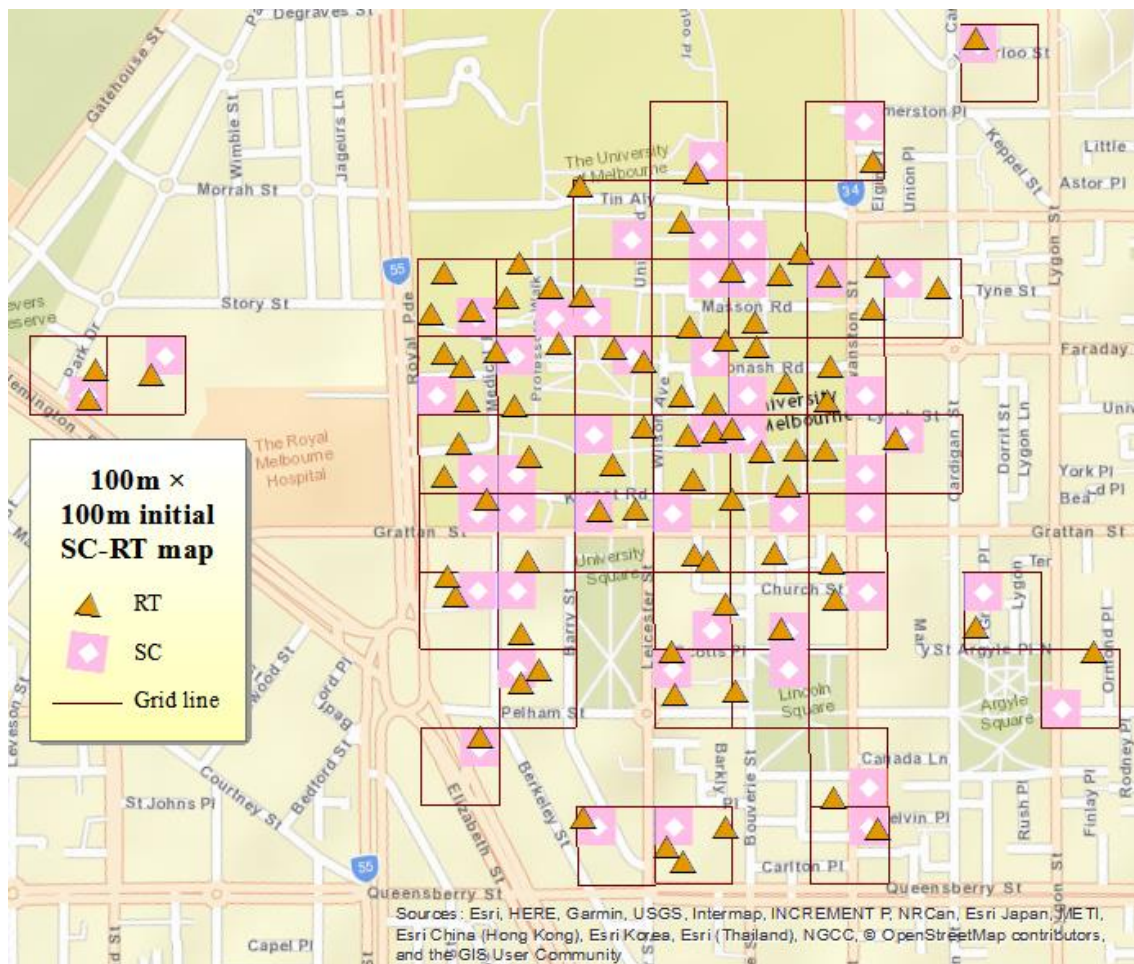
Figure 48: Initial RT locations for 100 m × 100 m SCN map

➢ Final RT selection for 100 m × 100 m SCN

After incorporating the visual approach of measurement over the case study area, we then selected one RT that appeared visually nearest to each selected SC location within each 100 m × 100 m coverage block. All RT positions over the case study area were selected, as shown in the resultant diagram below. These selected RTs would house an ONU to connect with the nearby SC equipment, thus providing the SCN-GPON interfacing. Once the SC and RT location information was sorted out, these were applied as inputs to the GPON optimisation framework, which was the second part of all our optimisation studies for this chapter. The resultant RT map is, therefore, as follows. The next session discusses the framework cost comparison scenarios.
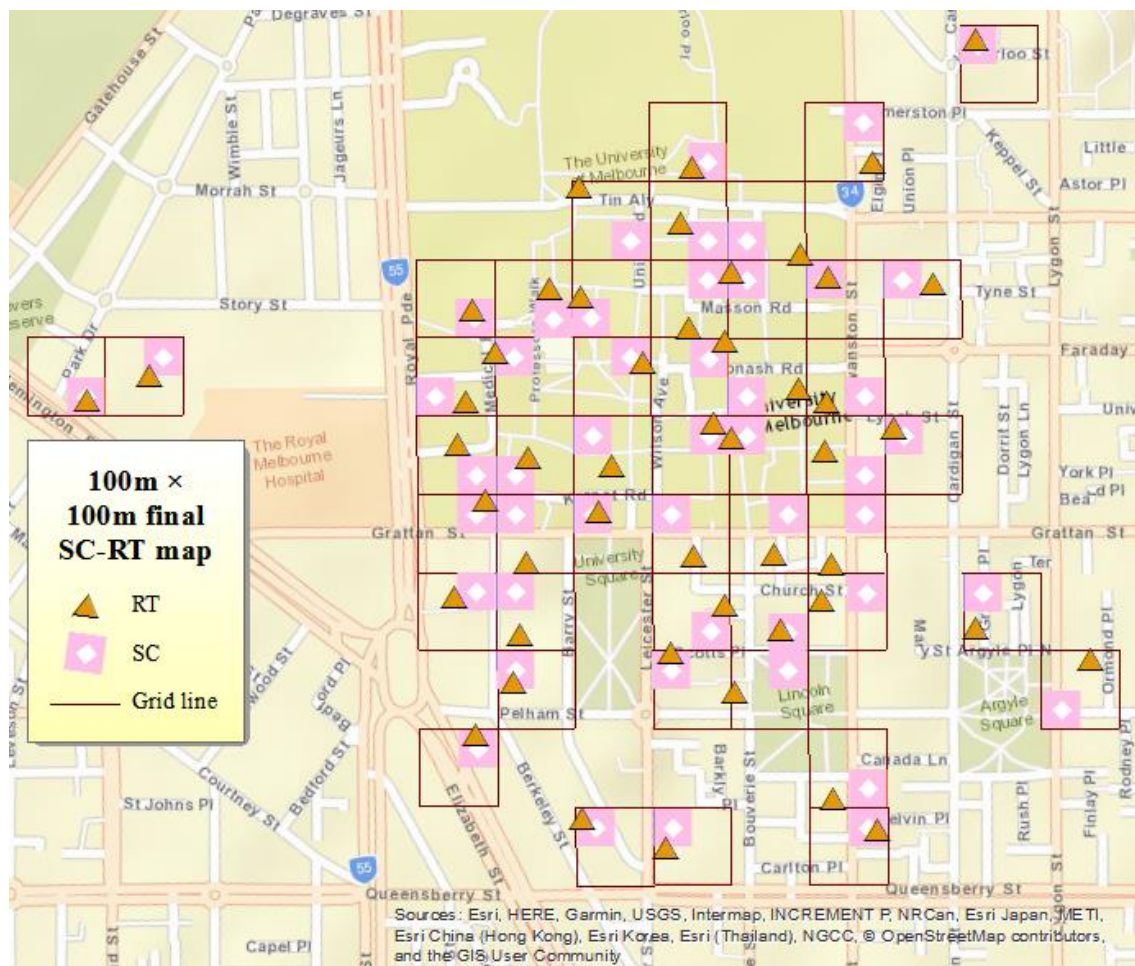
Figure 49: Final RT locations for 100 m × 100 m SCN map

❖ 100 m × 100 m framework cost comparisons

The GPON backhaul cost optimisation scenario for a pre-planned 100 m × 100 m SCN comprised multiple sections, depending on the different allocations for a fixed number of PON ports in the OLT line card. For typical GPONs, there are always options for choosing line cards based on their number of port connections, which would affect the total cost values for the different type of GPON planning scenarios. Therefore, we performed the following relevant case studies-

- Number of OLT PON ports 8
- Number of OLT PON ports 4

➤ Number of OLT PON ports = 8

This section of the case study was done for an OLT line card equipment with eight ports for PON connections. The results are plotted in **Figure 50**. There were minimal differences observed among some fixed and non-fixed split ratio cost values, while cost differences for these scenarios compared to the PtP scenario were significant. When the individual different cost components were observed, it was evident that for the fixed split scenarios (1:2, 1:4, 1:8, 1:16 and 1:32 splits, respectively), the OLT equipment costs stayed the same. At the same time, the line card and splitter equipment costs decreased as the split ratio increased. The reason being that with the increase in the split ratio, the number of outgoing connections from each splitter increased, allowing for less number splitter equipment usages per location. Also, an increase in split ratio meant that number of PONs connecting to the OLT also decreased. It happened while backhaul connectivity was provided to a particular number of SCs, thus effectively lowering the OLT equipment cost.

Interestingly, the fibre usage costs kept decreasing except for the 1:32 spilt scenario, where a slight increase in optical fibre cost was noted. Since the 1:32 split scenario, it happened to provide total connectivity through utilising less FAP locations for optical splitter placements (two locations in this case). Additionally, the CO location chosen by the framework was different from the other split scenarios. Also, the fibre routes from this CO location were different from all the FAP locations. Thereby, the number of utilised fibres for CO-FAP distribution fibre varied than the other fixed split scenarios, thus increasing the fibre cost. Compared with the no fixed split scenario, the idea was to study the effects on cost consumption

for a GPON, whether a fixed or no fixed split scenario would be more feasible. Eventually, it was found that a fixed split scenario would be the better choice in GPON optimisation for our case study, rather than the no fixed split case. Finally, this case study's different outcomes showed that a PtP backhaul network formation would incur far more costs than any GPON scenario simulated. The simulated results show that a 1:16 split ratio GPON planning is the most cost-optimal backhaul design for this case study. This backhaul planning was done for a 100 m × 100 m SCN, along with 8 PON ports at the OLT line card for the GPON portion. The cost comparison chart is displayed below. Then in the next section, 4 PON port scenario cost comparison is discussed.
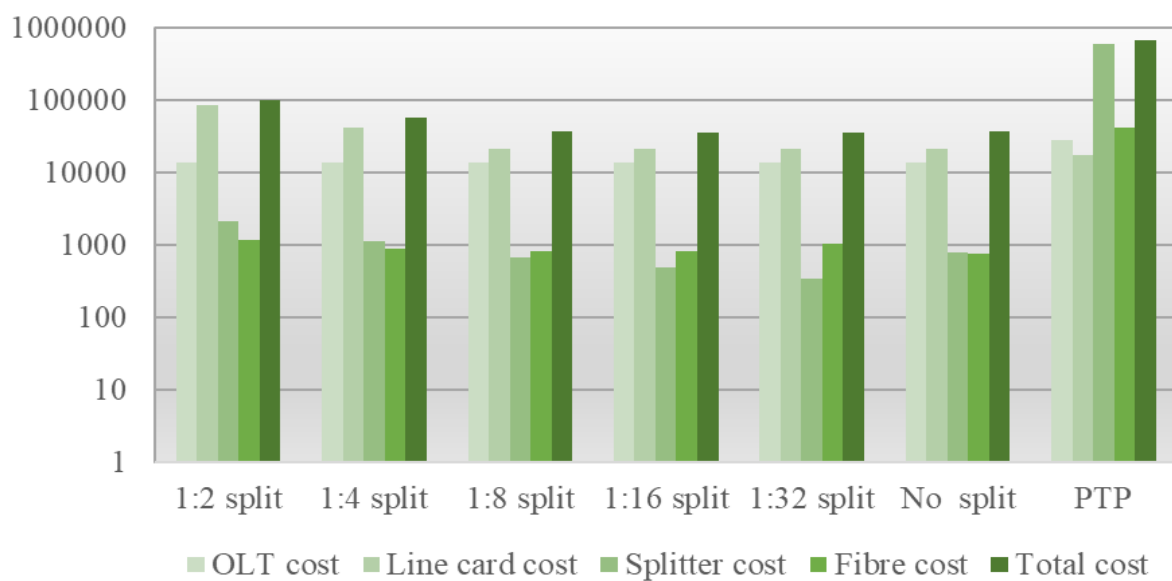
Figure 50: Cost comparisons for 100 m × 100 m, 8-PON SCN- GPON planning

➢ **Number of OLT PON ports = 4**

A second optimisation scenario in the GPON backhaul planning for the 100 m × 100 m case was performed for a maximum of 4 PON ports in each OLT line card. The results are shown in **Figure 51**. The results were displayed similar to the format shown in **Figure 50** in terms of total cost and different cost components. These new results depicted in **Figure 51** displayed both similarity and difference in trends, shown in **Figure 50**. For example, some split scenarios had more total cost values than the 8 PON connection scenario results. It occurred due to the decrease in the number of PON ports within each OLT line card to connect with all-optical splitters placed in selected FAP locations. The smaller number of PON ports per card enforced more line card deployment in the OLT placed in a selected CO location. Like the 8

PON case, most of the fixed split scenarios exhibited fewer cost values than those of no fixed split and PtP scenarios. As previous, the OLT equipment value stayed constant, while the line card and splitter costs decreased with an increase in split ratios.

Moreover, fibre usage cost kept decreasing with higher split ratios, except for the 1:32 scenario. It happened as again the selected CO location was different from other split scenarios, and the corresponding fibre routes extending from that selected CO towards the FAP stage were also different. Finally, among all scenarios, 1:16 split ratio GPON was the most cost-optimal solution, chosen for the implementation purposes, as the same in the 8 PON port scenario. The cost comparisons also revealed that the no fixed split scenario and the PtP scenario showed higher cost values than all other split scenario cost values. The corresponding cost comparison chart is provided below.
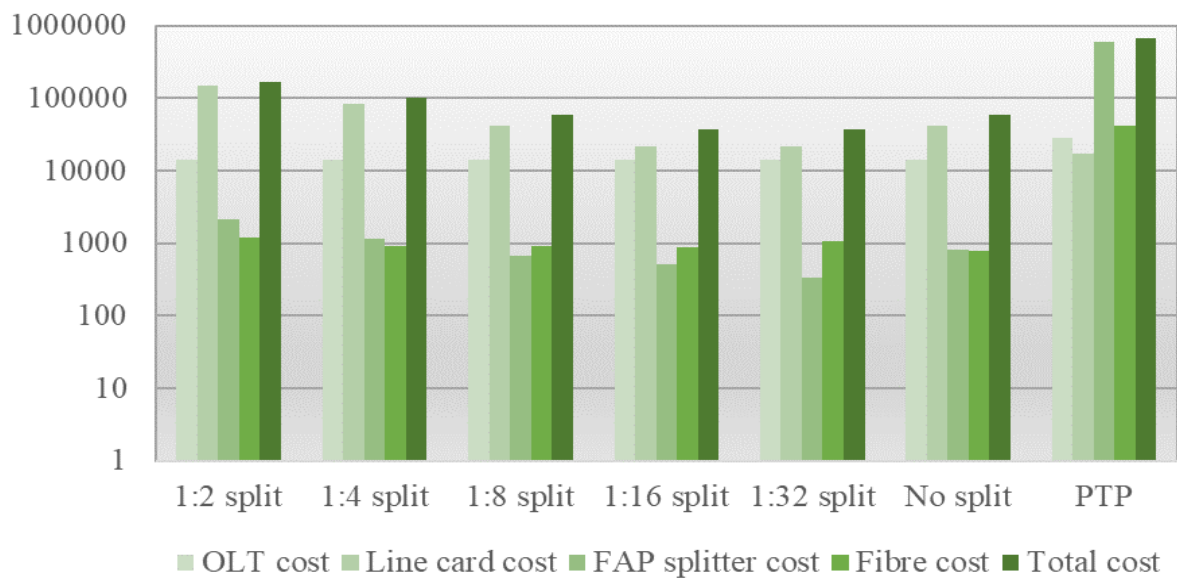
Figure 51: Cost comparisons for 100 m × 100 m, 4-PON SCN- GPON planning

❖ Final 100 m × 100 m network map examples

After the cost comparison studies were done, the optimal results were shown in geographic maps to present the planned SCN-GPON network visually. For simplification and conciseness, we compared only the 1:16 and 1:2 split scenario maps that exhibited the lowest and highest total cost values, respectively, for fixed split scenario GPONs with 4 PON ports per line card. The maximum cost 1:2 split ratio map is shown in **Figure 52,** and the minimum

cost-bearing 1:16 map is shown in **Figure 53.** The geoprocessing tool ArcMap module from the ArcGIS software suite [121] was used to generate the maps.

The maps showed both distinctive differences and similarities in terms of node and link distributions and formations. For example, in both the 1:2 and 1:16 split maps, one CO location was used to place the OLT equipment. However, the 1:2 scenario utilised 10 out of 11 FAP locations to place the optical splitters, while the 1:16 scenario used 4 FAP locations. The apparent reason being that the 1:2 split scenario allowed only two connections per splitter while 1:16 allowed for 16, thus decreasing the number of splitters to be placed in total. Another difference was that the maximum number of splitters placed in each location was 1 for the 1:16 scenario. Whereas it was a maximum of 4 splitters for the 1:2 scenario, hence effectively increasing both link and facility cost values. It should also be noted that both the 1:2 and 1:16 split scenarios aim to backhaul the same number of SCs and RTs/ONUs. It was because they were fixed before the optimisation simulations and were not parts of the framework.
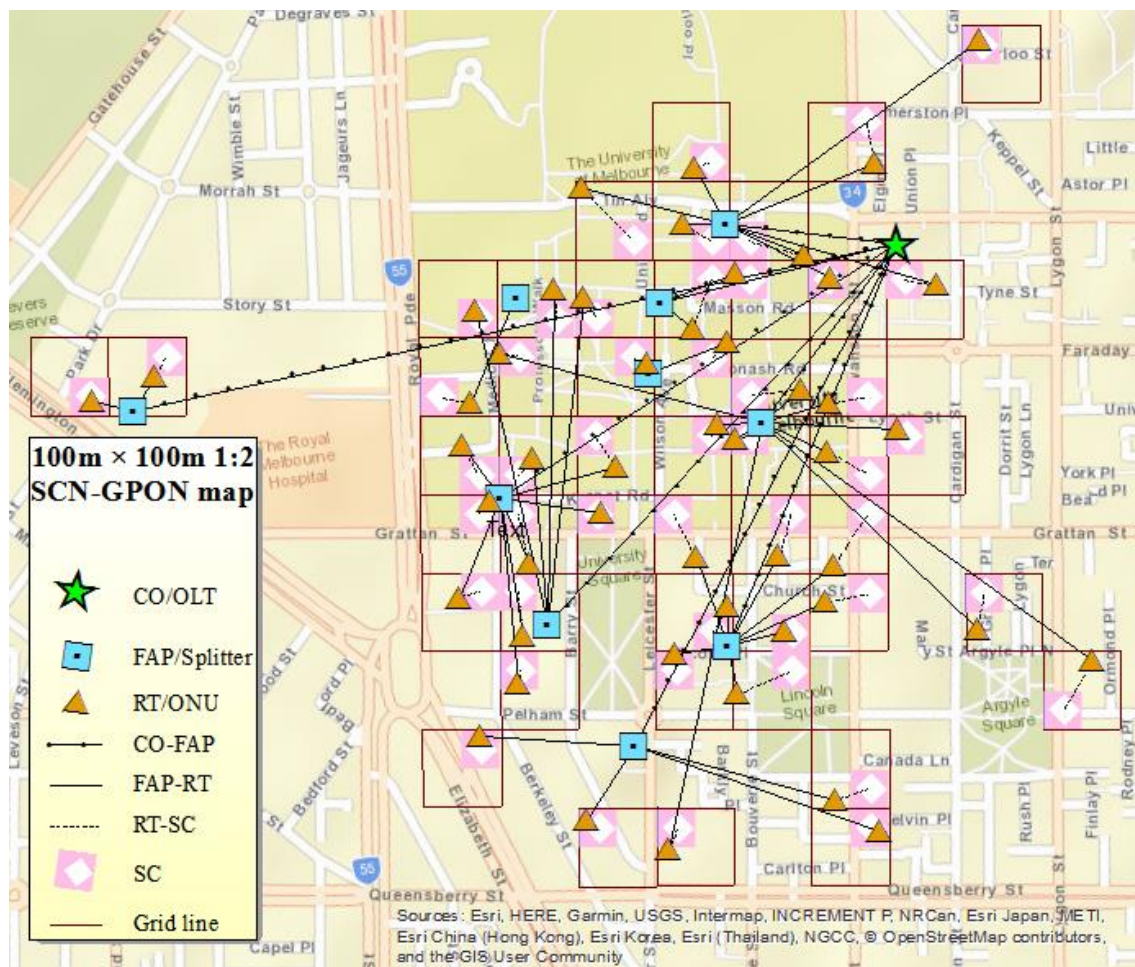
Figure 52: 1:2 GPON-SCN network map (Number of PONs = 4)
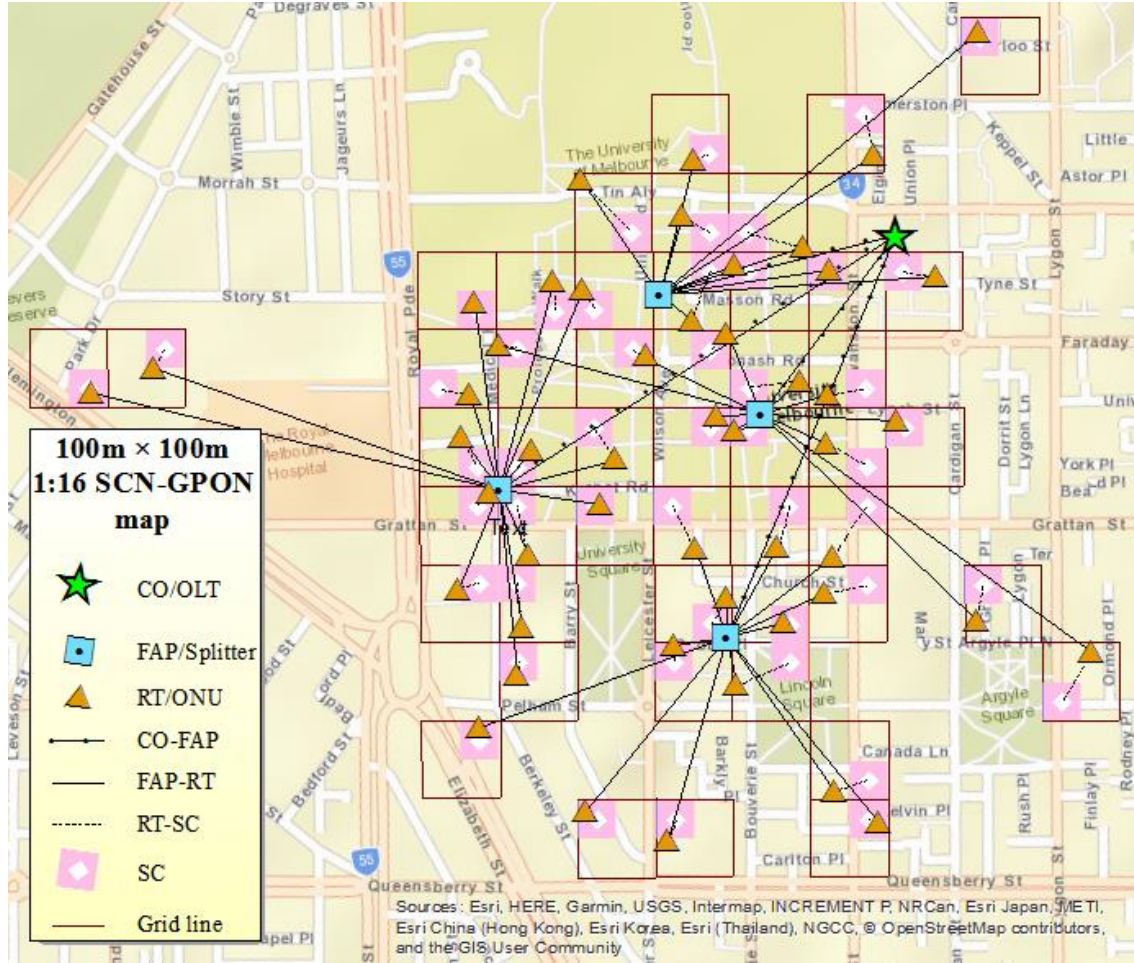
Figure 53: 1:16 GPON-SCN network map (Number of PONs = 4)

4.4.2. 200 m × 200 m SCN-GPON framework

This section discusses the second scenario in our SCN-GPON optimisation case study. Again, it was based on a 900 MHz 4G SCN planning [1] for the 200 m × 200 m cell area. It was then followed by designing an optimised backhaul based on the facility location optimised method [114]. This section includes the following sub-sections-

- 200 m × 200 m cell area SC location selection
- 200 m × 200 m cell area RT location selection
- 200 m × 200 m framework cost comparisons
- Final 200 m × 200 m network map examples

❖ 200 m × 200 m cell area SC location selection

As seen in the work done by case study-1 in **Section 4.4.1**, the SCN planning for the terrain grid with 200 m × 200 m coverage block areas had been pre-performed. The SC location information would then be used as input information for our intended GPON backhaul planning optimisation study. Therefore, the resulting SCN planning can be shown in **Figure 54**, where pink squares signified each potential location block for placing the intended SC for each coverage block. The diamond shape inside the pink square then denoted the cell's centre where the actual SC equipment would be placed. The next session describes the RT mapping part of the GPON framework.
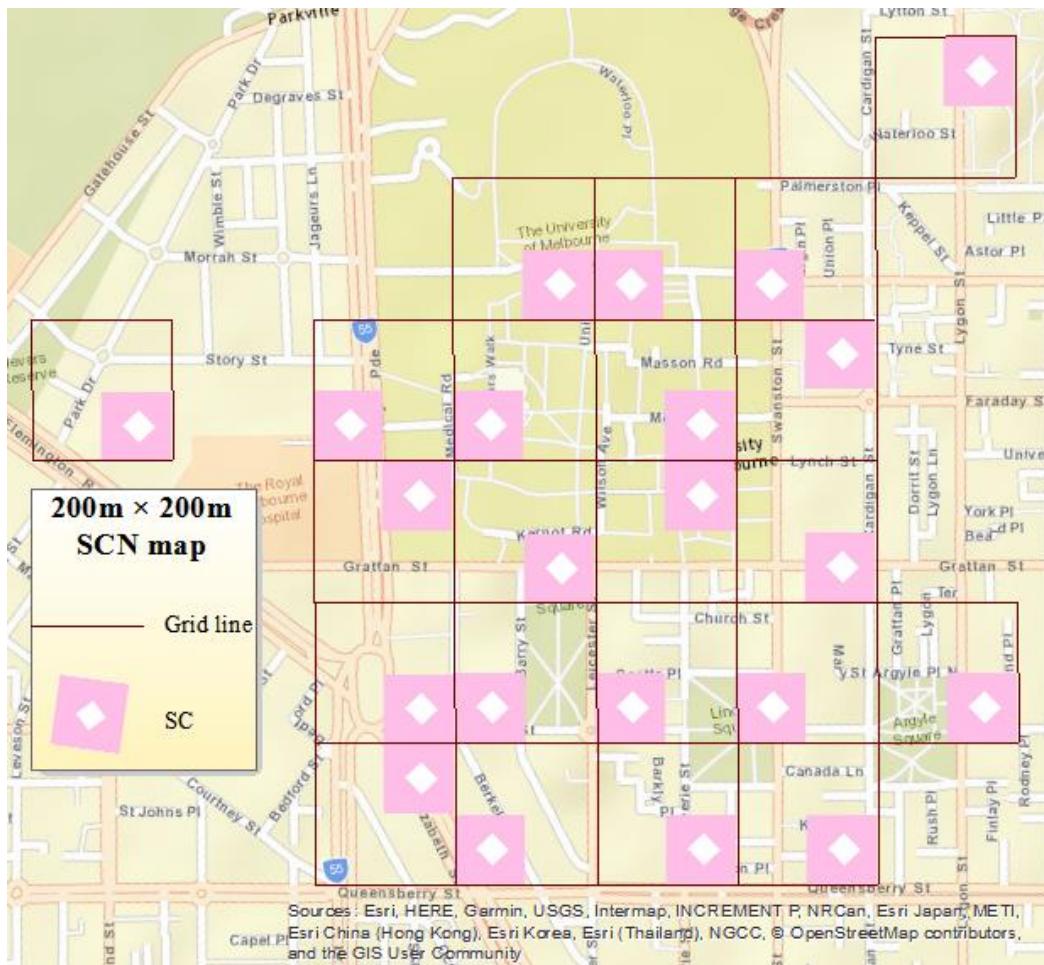
Figure 54: 200 m × 200 m SCN planning over University of Melbourne

❖ 200 m × 200 m cell area RT location selection

In the next step, suitable RT locations were selected to install the ONUs for SCN-GPON connectivity after choosing SC locations. Once again, one RT location was selected for each 200 m × 200 m area coverage block. The RT selection process is divided into two parts-

- Initial RT mapping with 200 m × 200 m SCN
- Final RT selection for 200 m × 200 m SCN

➢ Initial RT mapping with 200 m × 200 m SCN

We again initially enforced the 200 m × 200 m terrain grid SCN map over our intended case study area using the ArcMap tool [121], then aligned it with the existing RT locations. The resultant diagram is then depicted in **Figure 55**, where the multiple RTs existing in 200 m × 200 m scenarios are shown. Then in the next session, the final RT mapping part is discussed.
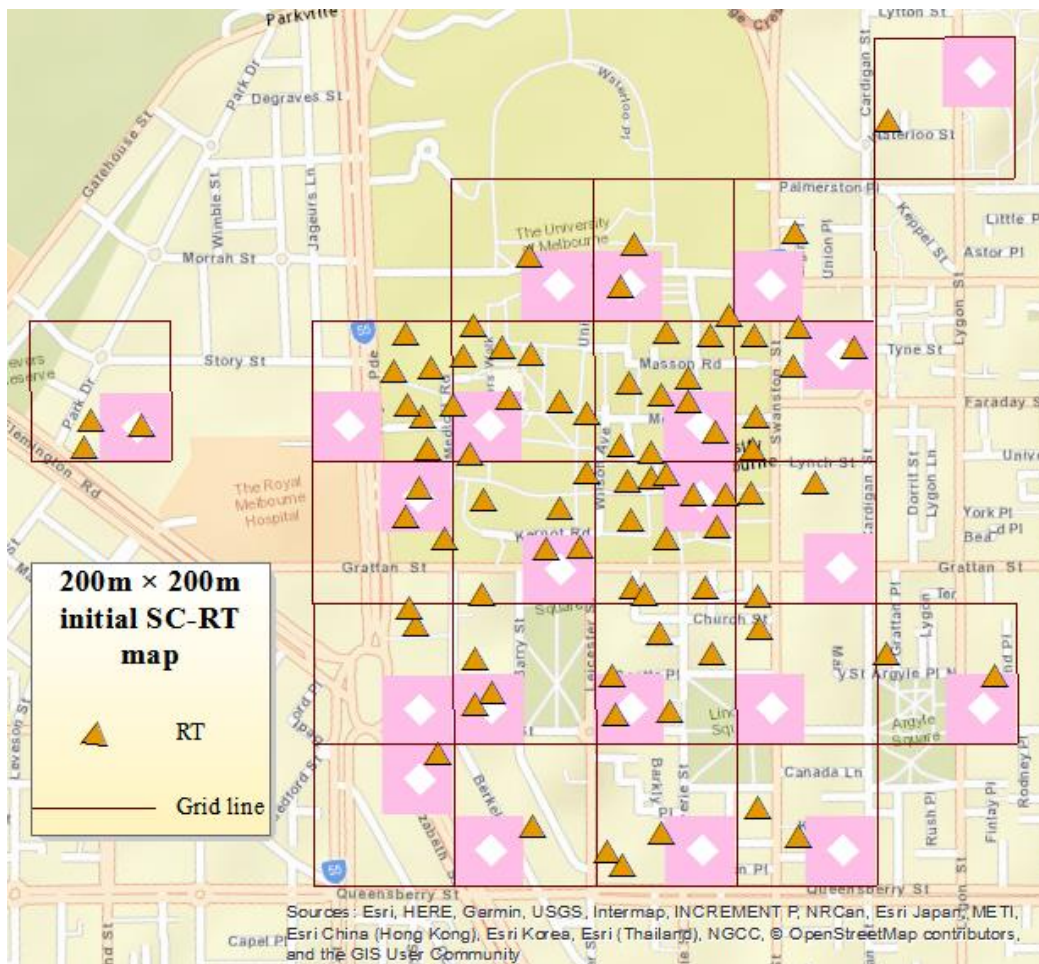
Figure 55: Initial RT locations for 200 m × 200 m SCN map

➢ Final RT selection for 200 m × 200 m SCN

For the second step in the RT selection process, we again selected one RT per SC coverage block, which appeared visually closest to the SC within the block area. The number of RT locations for this 200 m × 200 m SCN was less than that for the 100 m × 100 m SCN terrain grid. Here, the current coverage area was larger, requiring fewer SC locations to connect, with the number of RTs being the same as the SCs. The final RT map is then given below in **Figure 56**. The following section then discusses the 200 m × 200 m cost comparison scenarios.
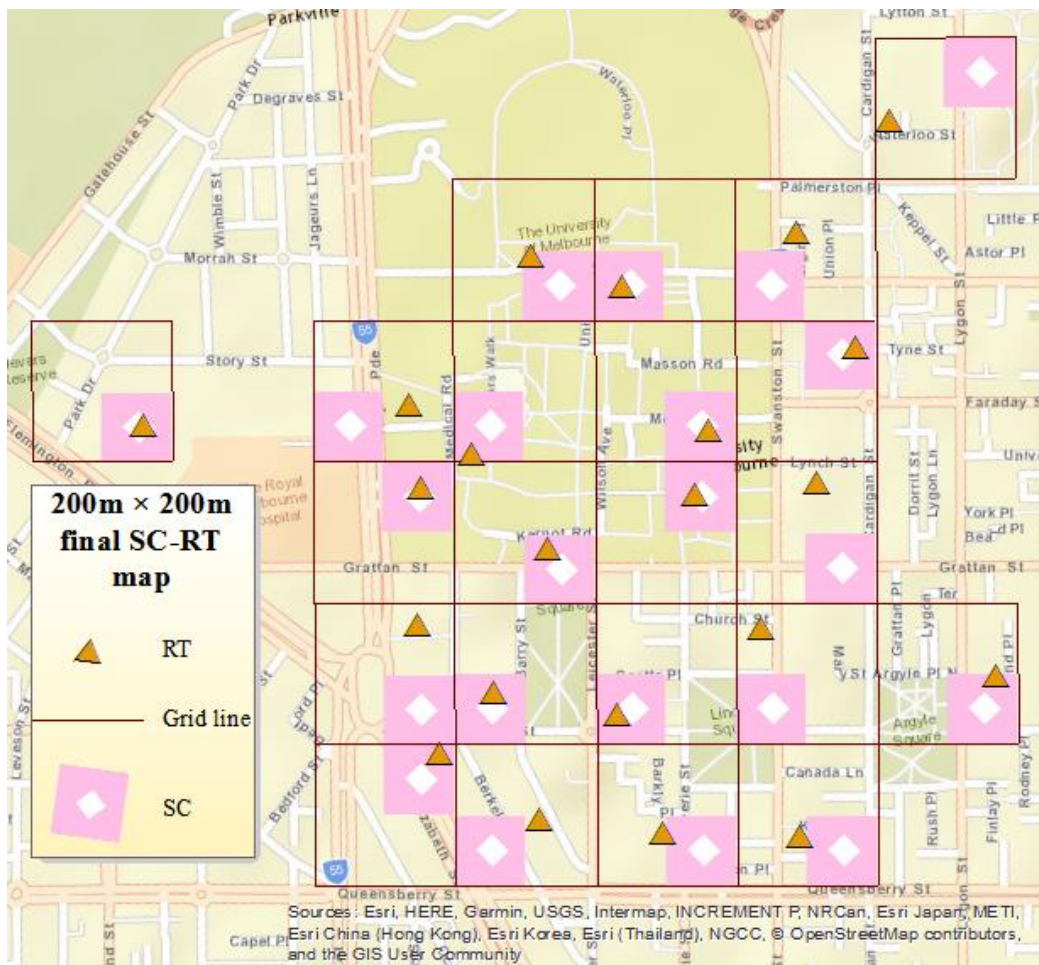
Figure 56: Final RT locations for 200 m × 200 m SCN map

❖ 200 m × 200 m framework cost comparisons

This GPON cost optimisation scenario provides a backhaul planning for a pre-planned 200 m × 200 m SCN. The cost comparison case here includes two sections based on the number of PON ports housed within the OLT line card. The two instances are as follows -

- Number of OLT PON ports 8
- Number of OLT PON ports 4

➢ Number of OLT PON ports = 8

This section shows the cost comparison results for the corresponding GPON backhaul planning for a 200 m × 200 m SCN over the University of Melbourne campus area. This first section discusses the obtained cost values when the OLT line card can hold up to 8 PON ports for connectivity with optical splitters. For this case study, a smaller number of SC and RT/ONUs was backhauled than that of the 100 m × 100 m block size dimensions. It happened since the coverage area size increased from 100 m × 100 m to 200 m × 200 m, allowing fewer SCs to cover the intended case study area. The results are shown in **Figure 57**. As a result, the different network total cost values also decreased, showing somewhat fewer differences for both fixed and non-fixed split cost values in this case study. The OLT equipment cost value stayed the same through different split and PtP network simulation scenarios, while the line card and splitter cost decreased with higher split ratios.

Interestingly, in this case study, the fibre cost appeared not to follow a particular trend of variation related to the split ratio changes. As for some split scenarios, the CO location was different from the others, causing a different fibre route formation to be selected and different cost value to be incurred in such planning. Again, a fixed split ratio provided the most optimal total cost value, which is 1:32 split in this case, compared with the fixed split, non-fixed split and PtP network scenarios.
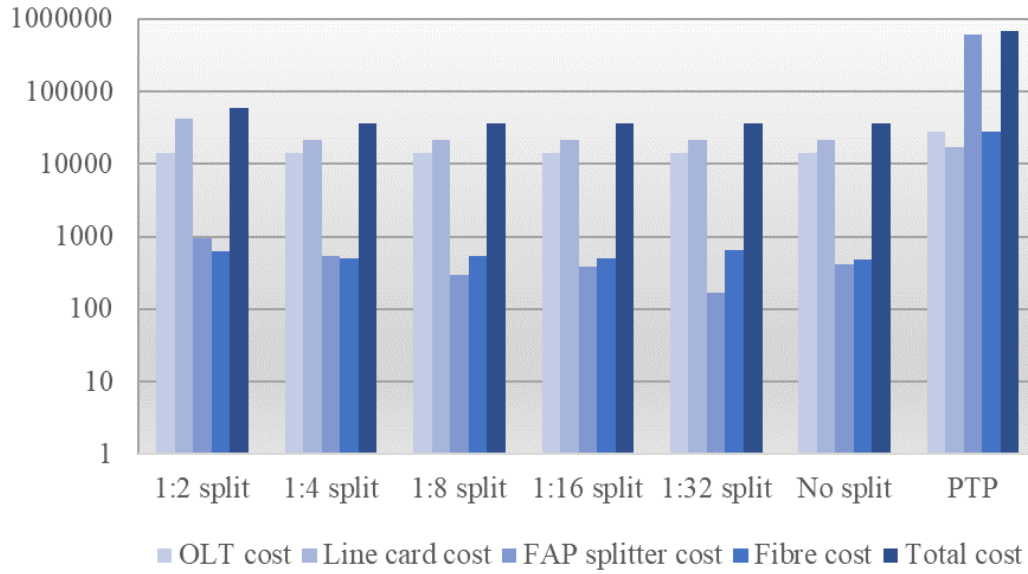
Figure 57: Cost comparisons for 200 m × 200 m, 8-PON SCN- GPON planning

➢ **Number of OLT PON ports = 4**

This second scenario reflects the cost comparison simulation outcomes for a line card type that can allow a maximum of 4 PON ports in the OLT. The results are shown in **Figure 58**. As expected, since PON ports in the line card are decreased from 8 to 4, the total cost increased for some scenarios as the number of split ports became less. The OLT equipment cost remained constant through all fixed and non-fixed scenarios, while again, line card and splitter costs decreased as the split ratio became higher for different GPON types. Once more, fibre cost kept decreasing for the increment of split ratios, except for the 1:32 scenario. For this current case, the reason was the selection of FAP splitter location. Although only one FAP location was chosen for placing optical splitters, the fibre route formation towards that selected FAP location yielded more fibre usages, increasing fibre costs compared to the 1:16 scenario. As a result, the 1:16 scenario turned out to be the most cost-effective solution than no fixed split and PtP scenarios. The cost comparison plot is thereby provided below. The final 200 m × 200 m map examples are then discussed in the next session.

Figure 58: Cost comparisons for 200 m × 200 m, 4-PON SCN- GPON planning

❖ **Final 200 m × 200 m network map examples**

The final backhaul planning arrangements were again mapped using the geoprocessing tool ArcMap [121]. For simplification purposes, we again decided to exhibit the most and least cost valued results as maps, which were the 1:2 and 1:32 GPON maps, for the 8 PON port scenario. After observing the maps in **Figure 59** and **Figure 60**, it was noted that the 1:2 and 1:32 cases both selected the same 1 CO location. In conjunction, the 1:2 GPON selected 7 out of the 11 FAP locations, and the 1:32 scenario utilised only 1 FAP location for optical splitter placement. The maximum number of splitters housed by the 1:2 scenario was two while 1, for the 1:32 case. Therefore, an increased number of splitter usage, resulting in a higher amount of fibre route utilisation, resulted in the 1:2 scenario having the highest cost value among all GPON scenarios. Again, both these least and most expensive GPON backhaul formations aiming towards backhauling the same number of ONUs at the RT, thus providing connectivity with the SCs at the end.

Figure 59: 1:2 GPON-SCN network map (Number of PONs = 8)
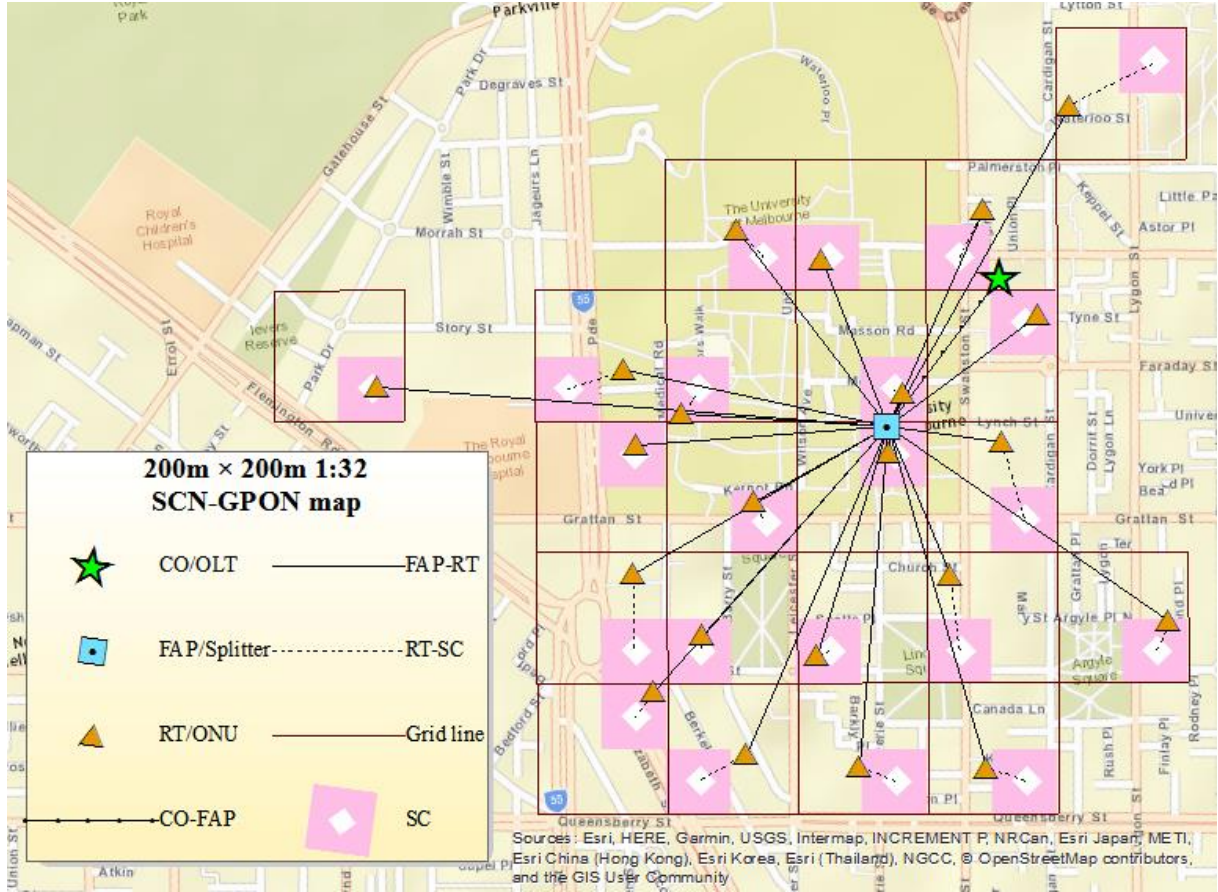
Figure 60: 1:32 GPON-SCN network map (Number of PONs = 8)

4.4.3. 300 m × 300 m SCN-GPON framework

Our last case study scenario in our SCN-GPON optimisation framework formation task, based on a 900 MHz 4G SCN planning [1], for the 300 m × 300 m cell area. Again we first form the SCN planning, then formulate the corresponding optimised backhaul design based on the facility location optimisation method [114]. This section is categorised into the following sub-sections-

- 300 m × 300 m cell area SC location selection
- 300 m × 300 m cell area RT location selection
- 300 m × 300 m framework cost comparisons
- Final 300 m × 300 m network map examples

❖ 300 m × 300 m cell area SC location selection

The SCN selection process was adopted in the other two case studies over a cell area size of 300 m × 300 m for this case study. Once the SCN was planned, the SC location set in each coverage block acted as input to determine the nearest RT locations within the cell block. The resultant SCN map is, therefore, shown in **Figure 61**. Next, we reviewed the RT selection process.
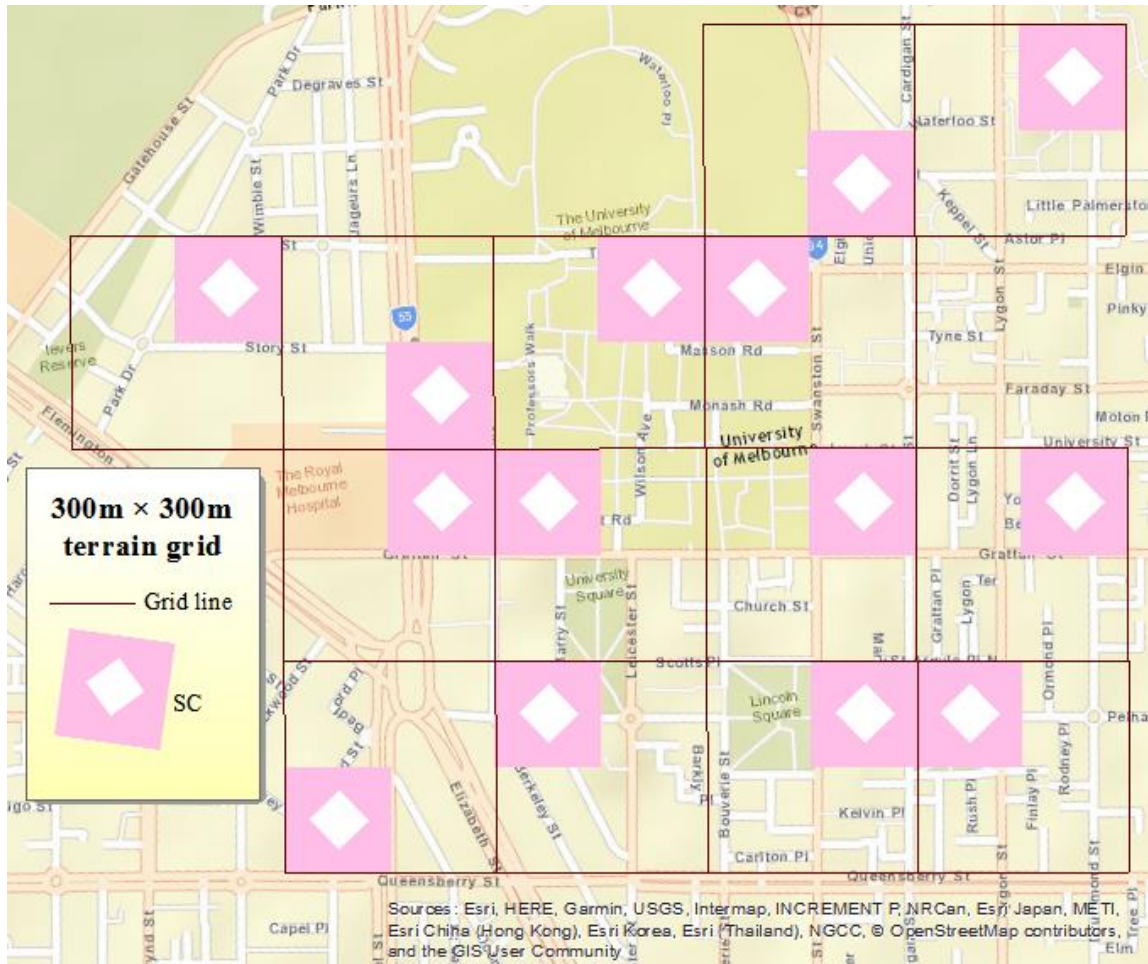
Figure 61: 300 m × 300 m SCN planning over University of Melbourne

❖ 300 m × 300 m cell area RT location selection

As per the adopted case study method, the RT locations were chosen to provide ONU installation to connect with pre-planned SC locations for the 300 m × 300 m terrain grid. This RT selection process is again divided into two parts.

- Initial RT mapping with 300 m × 300 m SCN

- Final RT selection for 300 m × 300 m SCN

➢ **Initial RT mapping with 300 m × 300 m SCN**

We aligned the existing RT locations over our case study area with the 300 m × 300 m terrain grid SCN map. We also illustrated the final RT mapping afterwards, as follows in **Figure 62**.
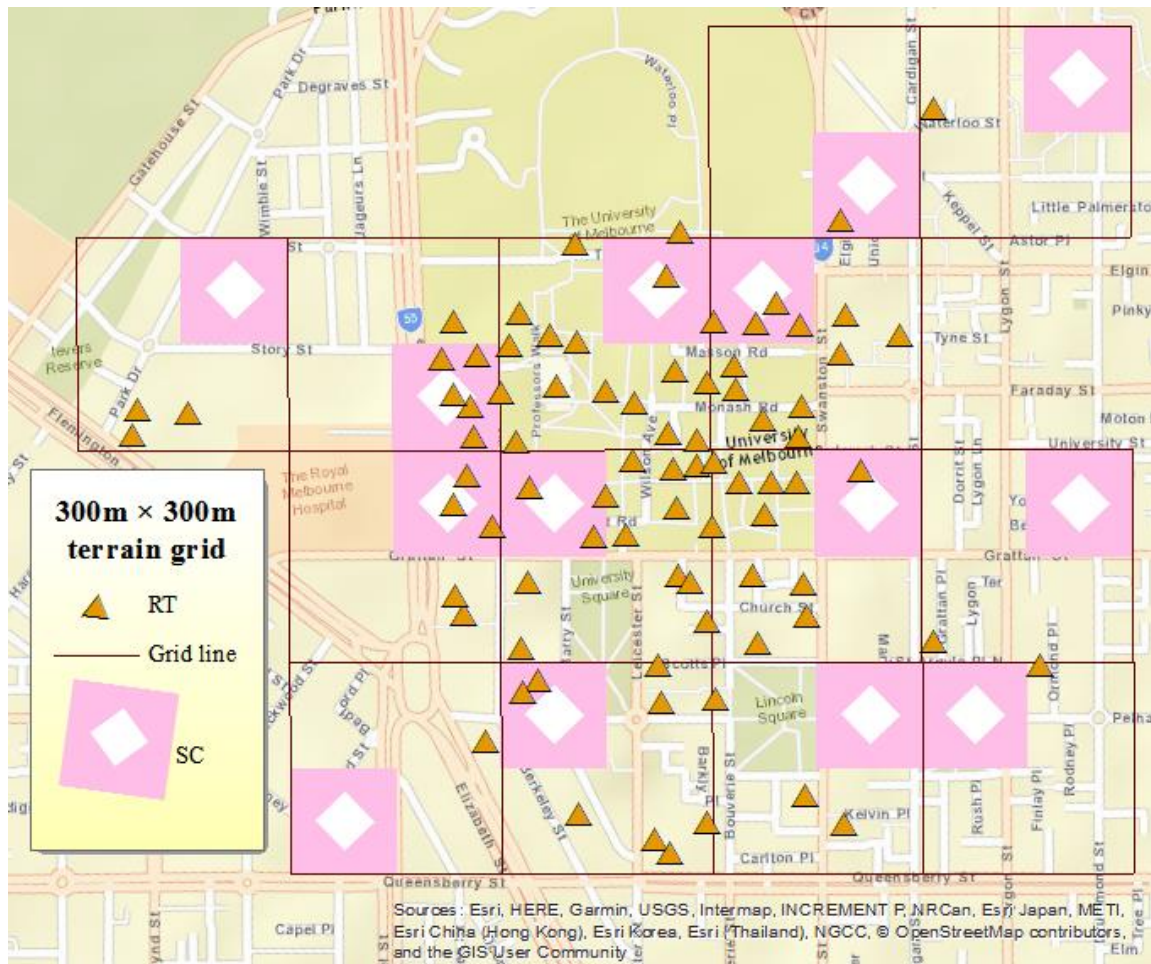
Figure 62: Initial RT locations for 300 m × 300 m SCN map

➢ **Final RT selection for 300 m × 300 m SCN**

For the next step, one RT location from each coverage block was selected based on their closest proximity to the SC within the block. Here, each SC-RT would cover a larger cell area in 300 m × 300 m SCN. Thereby, fewer SCs and RTs were selected than that of the 200 m × 200 m SCN. The final RT map is thereby shown below in **Figure 63**. We then proceed to discuss cost comparison scenarios for the 300 m × 300 m coverage area dimension.
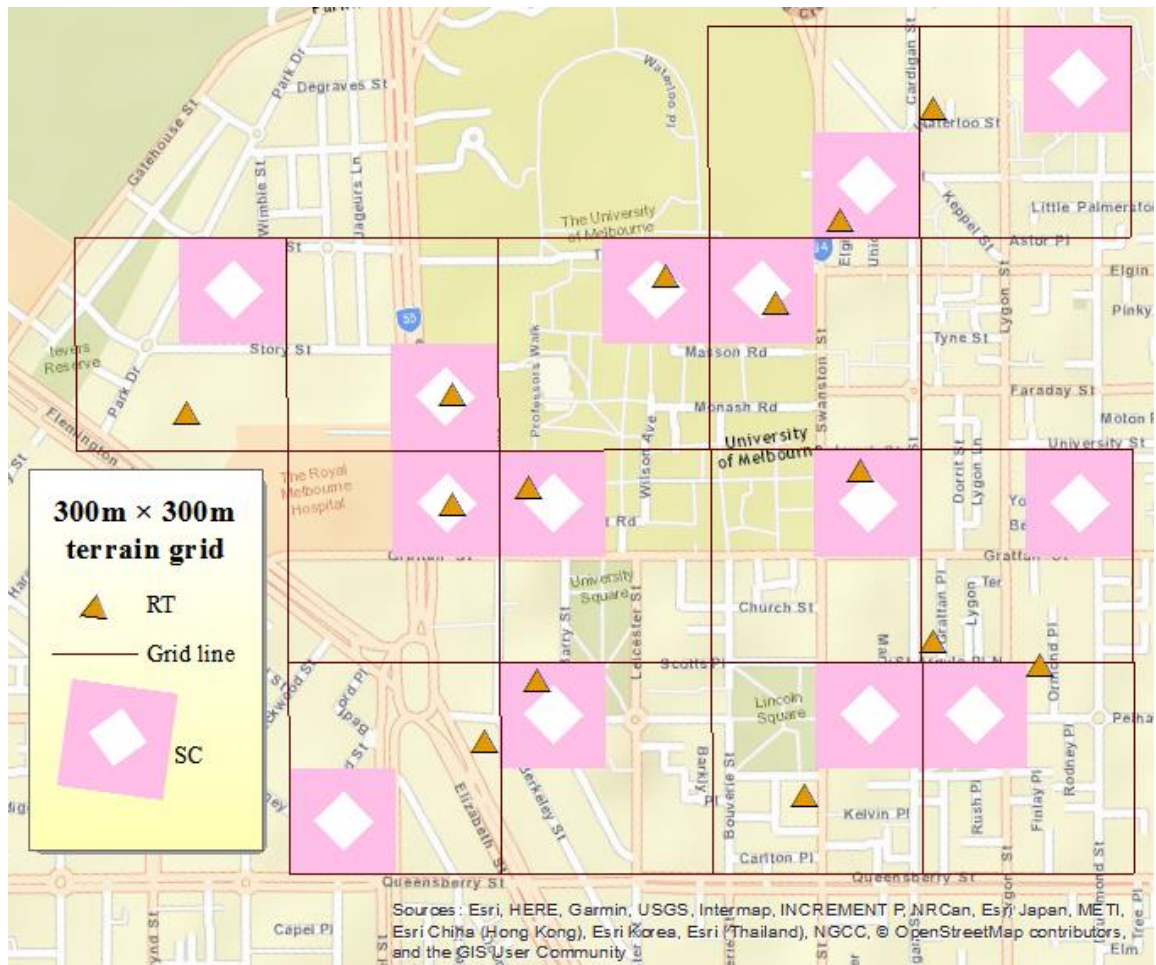
Figure 63: Final RT locations for 300 m × 300 m SCN map

❖ 300 m × 300 m framework cost comparisons

This final GPON cost optimisation scenario in this current chapter aided in depicting a backhaul network layout for a pre-planned 300 m × 300 m SCN. As seen in the previous two case studies of this chapter, the case study included two sections based on the number of PON ports housed within the OLT line card. The two instances are as follows.

- Number of OLT PON ports 8
- Number of OLT PON ports 4

➢ Number of OLT PON ports 8

The cost comparison scenario for GPON backhaul with 300 m × 300 m SCN and 8 PON ports in the OLT is presented in this section. In this case, both OLT equipment and line card costs remained the same for all fixed and non-fixed split scenarios. The splitter costs

decreased with the increase in the split ratio, except for the 1:32 scenario, due to the higher cost for the 1:32 splitter type, though only one type of splitter location and corresponding equipment sets each was considered. The fibre cost decreased with the split ratio becoming higher, except for 1:16 and 1:32 GPONs, as the CO location and fibre routes were different. Ultimately, the 1:8 split provided the most cost-optimal scenario than the other fixed split ratios and the non-fixed split and PtP scenarios. The cost comparison plot for different spit ratios is, therefore, as shown in **Figure 64**. The same comparison study was done for 4 PON ports and described in the following section.
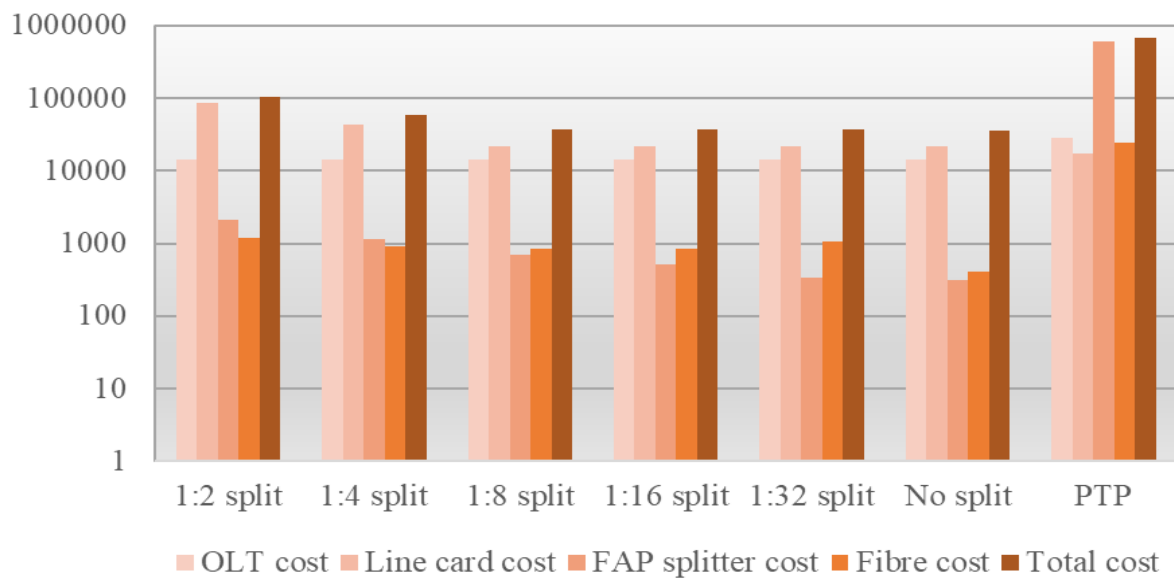
Figure 64: Cost comparisons for 300 m × 300 m, 8-PON SCN- GPON planning

➢ **Number of OLT PON ports = 4**

The 4 PON scenario provided results similar to that of the 8 PON scenario, with a slight increase in total cost values for all fixed and non-fixed split scenarios. The results are shown in **Figure 65** below. For example, OLT equipment and line card costs were constant in all fixed and non-fixed split scenarios. Then the splitter costs lowered with the increment in split ratio, except for the 1:32 scenario. It is because the 1:32 splitter had the highest cost compared to other splitter types, prompting a cost increase, despite only one of the splitter equipment set was used in the framework planning. The fibre cost, which otherwise decreased with split ratios becoming higher, increased for 1:16 and 1:32 networks since the fibre usages for these cases yielded more cost for connection. Finally, we obtained a 1:16 split ratio providing the most cost-optimal network formation, in this case.
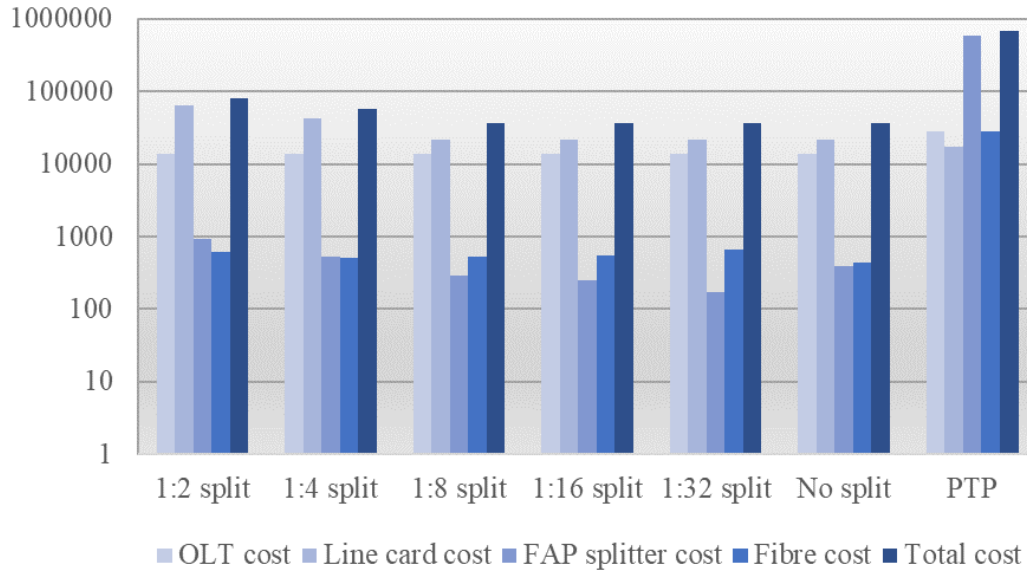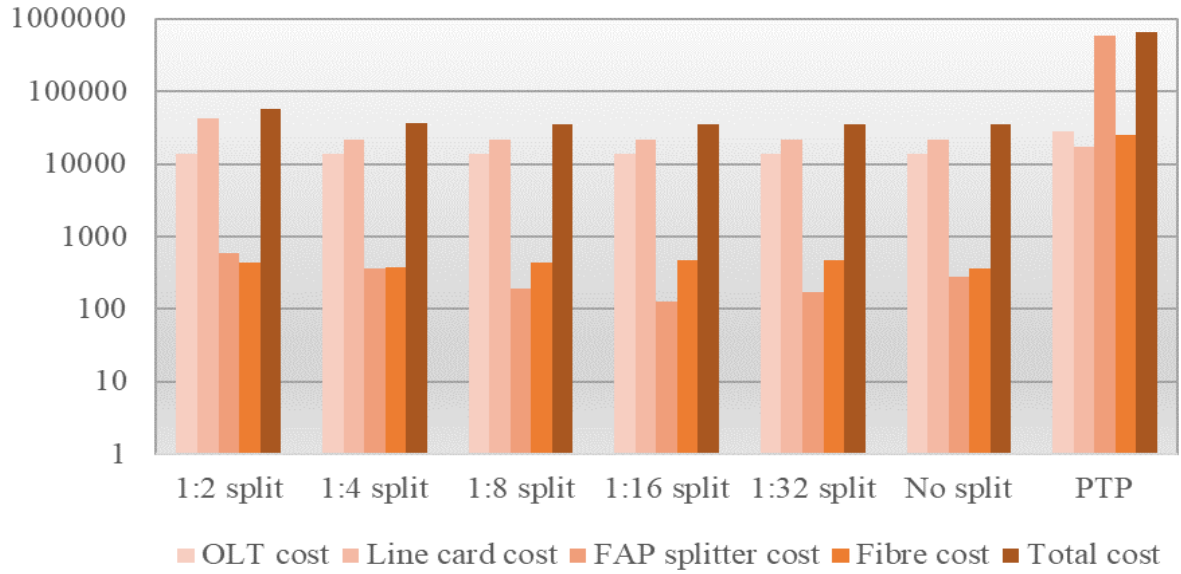
Figure 65: Cost comparisons for 300 m × 300 m, 4-PON SCN- GPON planning

❖ Final 300 m × 300 m network map examples

The final backhaul arrangements comprised various resultant maps and would be evaluated on two of them only for simplification. We will discuss the most and least cost value maps for a maximum of 4 PON ports residing in the OLT line card. The 4 PON port scenarios showed comparatively lower costs than those of 8 PON port cases. In our study, we draw comparisons between the 1:2 and 1:32 GPON map scenarios for 4 PON ports in the OLT, as the most and least cost valued scenarios, respectively, shown in **Figure 66** and **Figure 67**. It can be noted that the 1:2 and 1:32 cases both selected the same 1 CO location. In this instance, the 1:2 GPON selected 5 out of 11 FAP locations, and the 1:32 scenario utilised only 1 FAP location for placing the optical splitter. The maximum number of splitters housed in each selected FAP location for the 1:2 scenario was 2, while the 1:32 scenario used only one splitter for the selected FAP location(s). Both scenarios aimed to backhaul the same number of SCs and RTs/ONUs, where 1:32 GPON offered the least total cost value and thereby was selected as the preferred GPON backhaul architecture. Additionally, the higher amount of link and facility utilisation by the 1:2 GPON let it incur more cost than the 1:32 scenario.
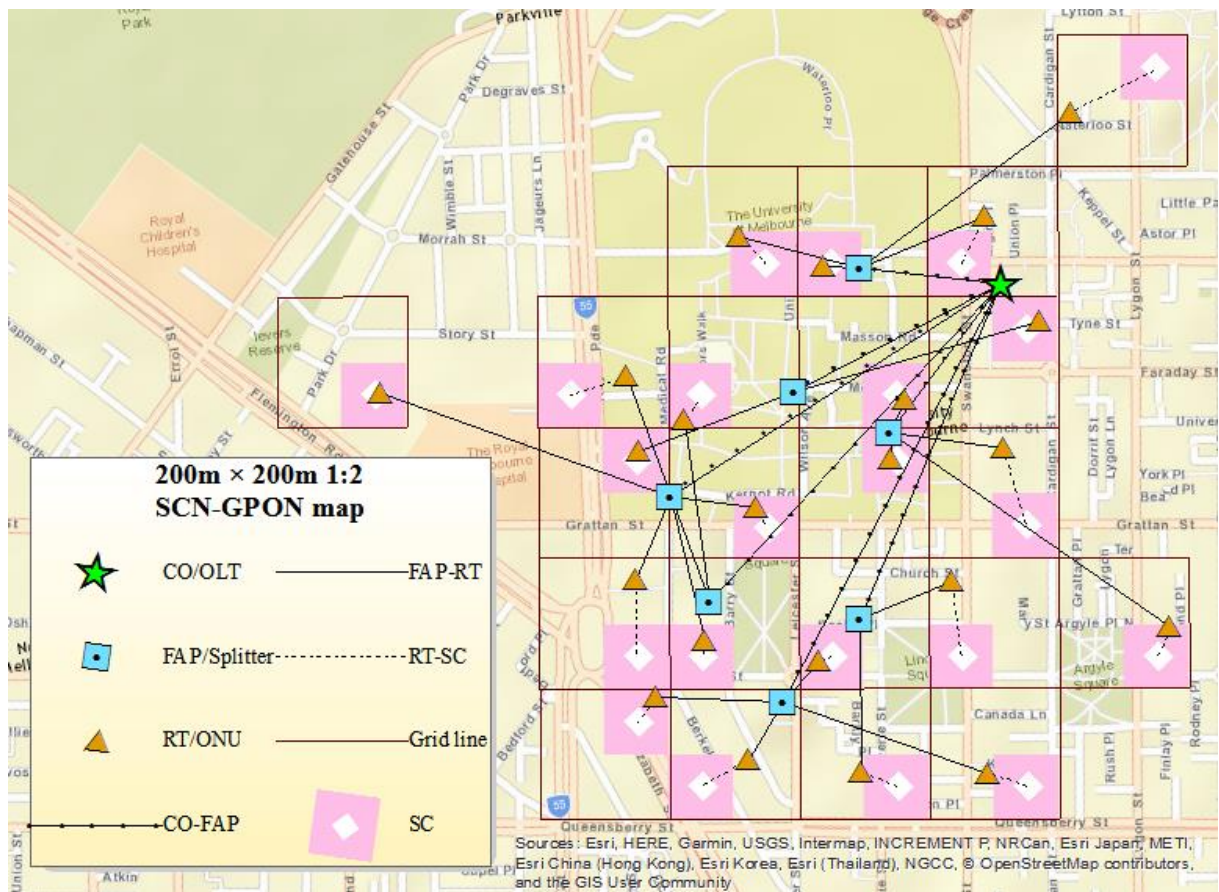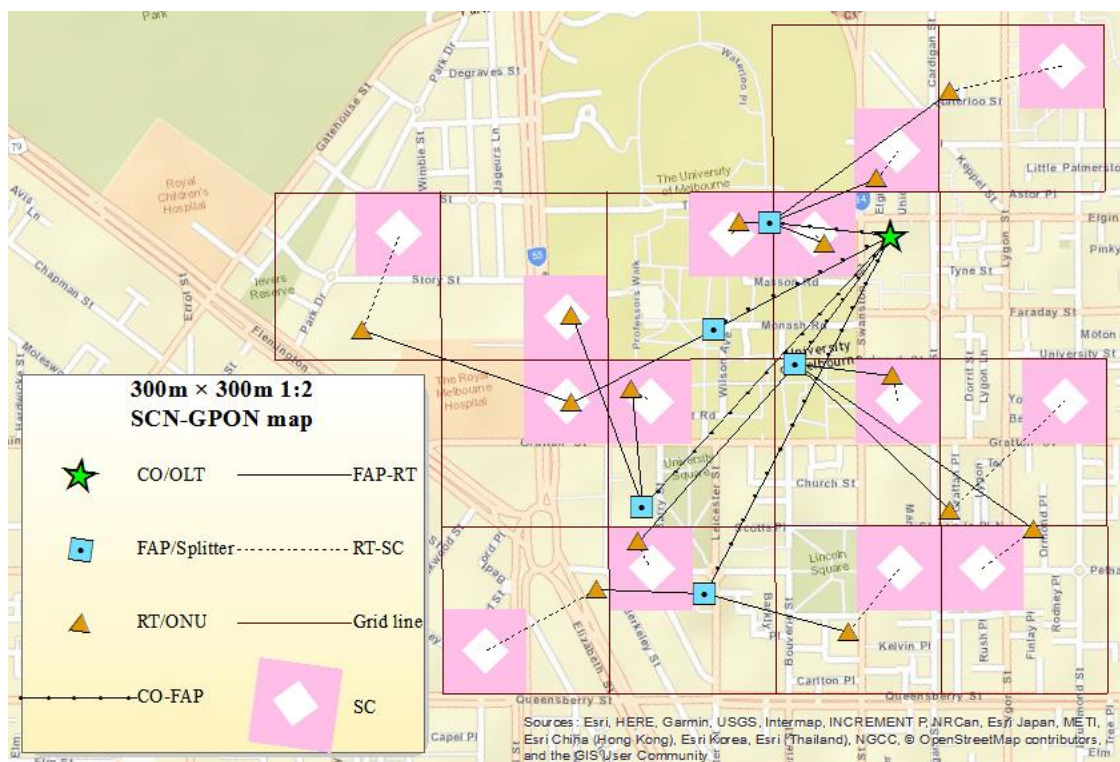
Figure 66: 1:2 GPON-SCN network map (Number of PONs = 4)
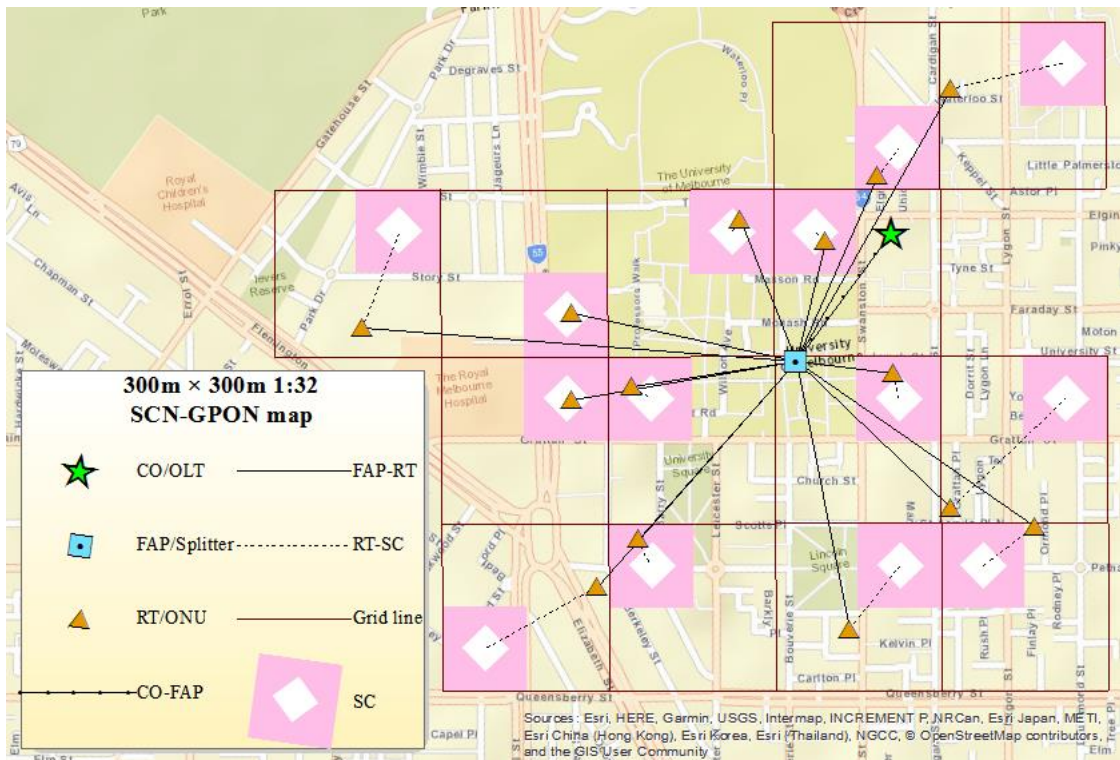
Figure 67: 1:32 GPON-SCN network map (Number of PONs = 4)

4.5. Conclusion

This chapter aimed to expand the previous SCN planning shown in **Chapter3** to show a more generalised network planning method. A planning framework would allow for backhaul connectivity planning for an SCN planning influenced by the surrounding terrain. An optimised backhaul planning framework was formed based on the GPON technology proven for cost and energy minimisation for different pre-planned SCNs with different coverage area sizes. Additionally, the GPON technology planning was varied over different forms of GPON, based on different types of optical splitter and line cards, which are essential components within the GPON technology. The demand for small-cell deployment increases due to the enormous need for growth in data and voice communication traffic over mobile networks. Thereby, the importance of proper backhaul connectivity between end-users and the core network becomes more crucial in terms of the network design aspect.

The backhaul GPON planning included placement provisions for new equipment such as OLT, optical splitters and ONUs, over existing PtP optical network premises. An SCN was first planned by the methodology discussed in **Chapter 3**. For each SC, one optical network RT location was co-located within each SC's nearest vicinity to place the ONUs. Finally, an existing PtP network design was optimised to determine CO and FAP locations for placing OLT and splitter equipment, respectively. Five different optical splitters for two different OLT line cards were studied as different scenarios for the proposed GPON planning. All of these scenarios were tested for three different SCN types based on their coverage area block dimensions. Furthermore, two particular scenarios were considered for cost comparison purposes-optical splitters with different split ratios within one scenario and the corresponding PtP scenario without GPON deployment as backhaul options. Hence data comparison results for a total of seven GPON formations were produced.

Each SCN case study scenario based on different coverage block area values considered two further settings for two different OLT line card types in the CO stage-based on the number of GPON port limitation per card. As per the cost comparison studies, in all cases, the fixed split scenarios provided less total cost values than those of no fixed split and PtP scenarios. Within the different cost components of the total cost value, the OLT equipment value remained constant more or less. Conversely, the line card and splitter values continued to drop with the increase in split ratios for most case study scenarios. Moreover, fibre usage cost kept

decreasing with higher split ratios, except for a few cases. It pertains to the fact that different CO location(s) got selected for different split scenarios, and the corresponding fibre routes extending from selected CO towards the FAP stage were also different in some cases. The cost comparison scenarios also revealed that in most cases involving the different SCN and GPON network types, the 1:16 fixed split scenario was favoured as the most cost-optimal. In other instances, either the 1:8 or the 1:32 ratio GPON networks were most cost-optimal. While there were significant cost differences observed between the PtMP scenarios with splitters and PtP scenario, there were minimal cost differences among all the fixed and non-fixed split scenarios. Thereby plots were displayed on a logarithmic scale for presenting all data with a similar calibration.

The proposed method was to install new equipment such as OLT and optical splitter by connecting them using existing optical fibres and ducts. Henceforth, the equipment cost involved was the CAPEX, and for the fibres, OPEX was considered. Observation of cost components revealed that the number of PON port restrictions for OLT line cards influenced the total cost values obtained through the simulation studies. For example, all the scenarios showed slightly higher if not equal total cost values when the PON port number in the line card was reduced from 8 to 4. The reason is that fewer PON port provisions in a line card yielded additional line card usages, contributing to increment in total cost values for some scenarios. The novelty of this work was that the SCs were pre-selected based on a different framework. This framework considered the significant influences of geographic urban terrain over SC cellular signal propagation and planned the SC locations in positions that offered better signal propagation profiles with fewer path losses. It was different from that of a similar SCN planning method adopted in our previous **Chapter 3**, where SCs were co-located with the nearest RT.

In summary, we designed a novel, generalised and combinatorial optimisation framework to link our previously constructed SCN planning based on the effects of urban geographic characteristics over mobile signal propagations within the SCN area. Also, we proposed this SCN's corresponding backhaul designing and dimensioning process based on the utilisation of existing optical fibre network resources.

This page is left intentionally blank

Chapter 5

Combined Small-cell Network Planning Framework with backhaul dimensioning

5.1. Introduction

This chapter enhances the SCN and backhaul planning process to be combined into one complete framework, regardless of the mobile communication technology to be used. We also aimed to ensure that the framework could offer further expansions in the future if needed. For this combined SCN-GPON framework, the same University of Melbourne campus area was chosen as the case study area, as seen in **Chapter 4**. Again, a terrain grid was envisioned over the area as a form of case study method continuation. This terrain grid formation was utilised to locate a set of potential SC locations, where the set of potential SC locations were placed in equal distance length apart, aligned over the grid's positioning. However, differences persisted within the development of this framework concerning the previous works in this project. Firstly, this current framework eliminated fixed coverage area blocks, as seen in the previous chapters. Hence, the planning framework here was not a combination of two different planning processes as that of **Chapter 4**. It was focused on developing one optimisation framework. The influence of developing such a framework can be attributed to some specific facts. For example, a) the cellular propagation technology is a continually evolving process, introducing new technological advancements in mobile communication. It would require a more uniform, streamlined and generalised optimisation framework, incorporating all parameters and constraints within itself. Then b) the optimisation process was envisioned to be more practical, accurate, methodical, tightened and concise. Next, c) introducing the basis for a more simplified SCN-GPON planning framework that can be easily expanded to various SCN deployment scenarios in the future. Finally, d) ensuring more cost-optimality in terms of lesser equipment utilisations within a more tightened framework.

In our previous two chapters (**Chapters 3** & **4**), we have shown the process of implementing an SCN planning framework based on the influences of the surrounding terrain. We then mapped an appropriate GPON technology backhaul for said SCN to provide complete

connectivity with the core backbone communication network. For SCN planning in 4G cellular technology, we incorporated the influences of surrounding terrain over urban geography and showed how small-cell positioning could be planned based on these influencing factors. A GPON backhaul leveraged existing optical network resources alongside implementing new low-cost passive optical network equipment, reducing the cost of implementation and ensuring appropriate resource utilisation. The idea was first to plan the SCN based on restricted fixed coverage area for each SC placed and then utilise the resources of an existing PtP active optical network to backhaul this pre-planned SCN. Hence, two different network mapping processes were combined to create one final framework, emphasising maintaining the coverage block area dimensions, specifically for mobile communication's 4G technology.

Like Chapter 4, this proposed unified optimisation scenario also utilises the CFLNDP method [113], NP-hard, to find a solution to the network planning problem. Again, this CFLNDP design approach constructs a graph to map the network topology from a given list of existing network node locations and connectivity routes. These nodes would act graph vertices, and positioning of existing links connecting those nodes would represent the edges within the intended optimised network map graph, as mentioned. Each potential link and node from the existing PtP network and potentially chosen SC locations had an assigned cost. These cost values depended on each link and node's capacity and operation within the proposed network design. Again, present research study outcomes of network optimisation scenarios served as a background to this optimisation study. The optimisation process utilised a hierarchical system of network node locations, as seen in **Chapter 4,** which was used to determine the positions for installing GPON network components for our intended network planning. Therefore, in addition to the potential SC locations, other parameters served as input data as well. These were existing RT, FAP and CO locations and existing fibre links connecting them, alongside estimated Euclidean distance from each RT location to each potential SC location.

For this study, signal propagation parameters that counter influences of geographic terrain surrounding the SCs and influence their position selection are not counted as direct parameters. Instead, the signal loss effects due to terrain formation are expressed in terms of maximum coverage distance for each SC location. It would then be mapped manually over the case study area after the potential SC locations are chosen. Another indirect parameter influencing the optimisation study outcome in designing the framework was the RT locations' positions. Previously in **Chapter 4**, the RT locations were chosen from each coverage block,

based on their closest proximity from the pre-selected SC locations. Again, for this case study, each RT location was randomly chosen as restricted to one per square block of the terrain grid formation that pinpointed the potential SC locations. As before, ONUs would thereby be placed in the RT locations, and then they would connect through drop wires with the newly provisioned SC terminal. Here, these SC locations would not be existing within the case study area from before. As for the optical splitters to be placed in optimal FAP locations, fibre incoming to a splitter is split into several fibres in the following network hierarchy stage. Additionally, there can be single or multiple stages of splitters, hence rendering implementation of multiple stages of fibres. For a traditional FTTH-GPON, optical splitters can have 1:2, 1:4, 1:8, 1:16, 1:32 and 1:64 split ratio to connect to 2, 4, 8, 16, 32 and 64 terminal nodes [6].

In summary, we constructed a combined SCN-GPON network design through a discrete CFLNDP method over the locations of existing PtP network nodes and fibre links. This design also utilised a set of SC locations that could potentially provide population and area coverages. This SCN-GPON architecture has already been mentioned in **Chapter 4**, as **Figure 46**.

5.2. Related works

We would look at the following type of optimisation scenarios as theoretical bases for our combined SCN-GPON optimisation framework-

- Design optimisation
- Cost optimisation
- Coverage optimisation

Again, we only review the literature related to our project and have been conducted in recent years.

5.2.1. Design optimisation

Optimising a small-cell-based heterogeneous network that implements PON as backhaul requires proper planning of both the small-cells and the PON. The whole system needs to be positioned and designed so that these two sections complement each other in terms of connectivity, capacity, coverage and cost-efficiency. It can be evident in the following research initiatives-

Small-cell augmentation approach: Iannone *et al.* [37] provided the method of implementing an efficient fibre backhaul for a small-cell network, which utilises existing FTTN residential access network equipment. The authors proposed the deployment of small-cells within the vicinity of existing FTTN RT locations, hence utilising already available electrical and fibre facilities. They also proposed implementing small-cells near the edge of existing macro cell coverage areas, thus enhancing the wireless cellular network's coverage and capacity. They also implemented a heuristic solution to solve the maximum coverage issue for the small-cells and an ILP optimisation method to envision fibre access network design. These two approaches ensured cost-effective deployment involving both small-cells and the PON backhaul network.

The study area included four adjoining wire centres supported by both an FTTN and a wireless network, 705 FTTN RTs and 84 macrocell locations. Each fibre-fed RT was considered a potential location for a low-cost omnidirectional small-cell with 400 m coverage areas. The small-cells were deployed with 250-mW transmitter power, 8-dB antenna gain and about 2-4 m height antennas to ensure appropriate performance in suburban/urban areas. A total of 442 RT-based small-cells are proposed to be placed at distances further than half the nearby macrocell's best-coverage radius. For cost-efficiency, this number was then reduced to 256, using a location-allocation heuristic optimisation method, known as the p-median problem, which still ensured adequate coverage. Using this result as an input parameter, ILP was applied to determine optimal fibre backhaul connectivity by assessing different PON topologies based on existing dark fibre. In this process, splitter locations and fibre routes for the PON were optimised, and derived solutions were compared with a standard gigabit Ethernet PTP deployment method, finally achieving a 56% overall cost reduction [37]. This study [37] centres the small-cell network planning around macrocell coverage and FTTN resource availabilities. It does not necessarily formulate the potential SC location arrangements based on the terrain over the case study area, as what we adopted for our work. Although this study's objective is similar to part of our research work in this chapter, it essentially bears a much different overall outcome than our network planning framework studies.

Backhaul planning approach: Ranaweera et al. developed an optimisation framework for a cost-efficient PON-based backhaul for a small-cell network as an extension of the work done in [37]. They developed an efficient optimisation framework to plan a cost-minimised backhaul for a realistic backhaul network. Their results established that the proposed backhaul

planning technique can reduce cost by over 50% compared to typical point-to-point fibre backhaul deployment cost. This cost reduction was achieved by utilising small-cell's current infrastructure and re-using existing fibre equipment for the proposed PON backhaul deployment. The authors identified fibre, equipment, and labour as major cost contributors for a PON backhaul deployment and proposed reducing PON deployment expenses. The cost reduction approaches included identifying proper optimal positions for splitters, obtaining appropriate fibre routes and deciding only on the specified number of PONs as backhaul for a particular number of small-cells. The authors suggested that this optimisation method can even be applied in planning to small-cell backhaul and optimised tree and branch topologies re-using available dark fibre infrastructure. The proposed PON optimisation framework successfully outputs the optimal dark fibre routes, splitter and OLT locations and the necessary PONs to be used as backhauls. Comparison between PTP and PON architectures as possible backhaul solution was planned, and PON was found to be less expensive since it used less amount of dark fibre than that of PTP. However, additional elements such as fibre, equipment and labour, were needed to be installed for the PON deployments. These were also identified as significant cost contributors and thereby were accordingly optimised to reduce cost. For this, an ILP-based optimisation framework was employed, which used several network parameters, variables and constraints to develop a minimised cost function to deploy the PON successfully as a small-cell backhaul. This cost function would include some specific cost factors. These include- the cost of feeder and distribution fibres, the combined cost of OLT line cards, OLT shared equipment, OLT chassis and Ethernet switch, splitter and enclosure costs, ONU deployment costs, and total labour personnel costs. The optimisation model incorporates several constraints as follows.

- Feeder fibre connectivity remained only between each splitter and one OLT, while COs should only connect with FAPs containing splitters
- Each ONU at RT location connected with only one FAP and FAP connected with each ONU should have at least one splitter
- Connectivity remained between particular CO and particular FAP if only connections were established between them
- The maximum number of ONUs in a PON depend on the split ratio of the corresponding connected splitter, i.e., for 1:m split ratio, only m ONUs can be supported in the PON

- The span of PON decided by maximum transmission length depending on power budget and split ratio, and the combined length of feeder and distribution fibre should not exceed the maximum transmission length

- Installation of splitter with a FAP is determined by the presence of at least one splitter being present with that particular FAP

- Each OLT line card can support up to a fixed number of PONs, where the number of total OLT line cards needed by a specific CO should be equal to or higher than a particular value. This value is the ratio of the total number of PONs connected and the number of PONs supported by each OLT line card, but less than this ratio plus one

- Distinctive bounds on binary and integer variables were used within the framework, while an additional constraint was added later. It ensured that the number of splitters installed at a particular FAP is always less than the maximum allowable number of splitter positions intended for the deployment [6].

This study looks mostly at backhaul optimisation for a small-cell network, considering different cost parameters for such an optimisation approach, synonymous with our work discussed in this chapter. However, the optimisation method in our work was based on the CFLNDP method [114], while this study mentioned above focuses on their own modified ILP formulation approach. They also did not highlight the type of terrain considered a case study area, whereas we explicitly stated that our optimisation focuses on urban area SCN-GPON planning. Additionally, they considered their SCN formulation only by co-locating one SC position with each selected RT location within the optimisation process. On the other hand, our framework would choose the SC locations from a pre-determined set of organised SC location sets, optimised simultaneously alongside the GPON backhaul part.

5.2.2. Coverage Optimisation

Along with the design optimisation method, coverage optimisation is also an intriguing part of ensuring the efficiency of small-cell networks implementing PON backhaul, as evident in the works reviewed below-

Residential access network optimisation: One research approach discussed backhaul implementation using the existing residential FTTN access network and leveraging its equipment. Similar to previously reviewed research initiatives [6, 37-39], potential small-cell

sites are first selected within the surrounding area of existing FTTN remote terminals. Optimisation techniques are then applied to choose the most efficient subset of sites providing maximum coverage, and afterwards, the fibre backhaul architecture is designed. The initial deployment of small-cells is located nearby appropriate and existing residential FTTN RT locations, which allows for utilising of available electrical power and fibre backhaul facilities. Then coverage and capacity were enhanced by placing small-cells only around the edges of the existing macrocell coverage area. Appropriate small-cell sites are finalised from candidate small-cell locations using a heuristic algorithm optimisation approach based on the optimal small-cell covering problem. Finally, an efficient PON architecture is finalised to backhaul these sites based on existing fibre infrastructure and an ILP optimisation method. In this paper, 300 small-cell sites were finalised from the initially selected 613 locations, which provided 95% coverage to the subscribers' total number. It was achieved by considering the small-cell location selection issue as NP-hard p-median problem. The study then applies the GRASP method and the path-relinking heuristic intended for such a p-median problem, where p is the number of finally selected small-cell sites. This result was then applied as input to the backhaul network design problem for these p sites to approximate the optimal choice of dark fibres, splice location and backhaul topology. In this case, PON was selected as the choice for backhauling the selected small-cell sites, as it can share fibres, CO equipment, bandwidth, and node terminals, i.e., small-cells in this case, thus offering cost-efficiency. To ensure optimal and appropriate sharing of these resources by a PON, an ILP based optimisation framework has been proposed in this paper compared to a typical PTP scenario as a benchmark. Similar to the work done in [6], this work also shows that PON backhauling saves over 50% of the cost than if PTP is used as backhaul [38]. In contrast, as mentioned before, we aimed to provide coverage of our backhaul area through the CFLNDP optimisation method and consider a different area coverage approach through a combined SCN-GPON optimisation framework. Our approach was to cover a predefined case study area, where first SC locations are chosen from a pre-selected set of SC locations, and based on that information, the whole formation of SCN-GPON is envisioned.

5.2.3. Cost Optimisation

The implementation of small-cell and PON together already offers the basis of a much cost-efficient network system. Therefore, additional approaches have been proposed through

significant research on developing optimisation frameworks to enhance their cost-efficiency. Examples of this can be seen in the study [39], which deals with cost optimisation aspects of such a network system.

GPON optimisation approach: The research work by Ranaweera et al. proposes a cost-efficient optimisation framework for a GPON backhaul deployment of small-cell networks [39]. As an extension to [6, 37, 38, 85], this framework also shows significant cost-saving of backhaul deployment when this GPON is utilised as backhaul for a small-cell network. This proposed optimisation framework is developed through the ILP method to visualise PON deployments with existing fibre and small-cell backhauling equipment. Here, the optimisation method involves selecting the desired fibre routes, appropriate splitter locations, and the optimal number of PONs for different split ratios. The model is tested for PON deployment for a small section of AT&T's communication network. Again, over 50% of cost reduction was achieved compared to the traditional PTP backhaul. This work is expanded from the concepts of [6, 37, 38, 85]. Hence, their internal setup and parameters are mostly repeated to construct this deployment. This cost optimisation approach has been an essential aspect of our studies as well. Thereby, we decided to utilise this idea in our research project as well. However, the results we obtained were relevant to a somewhat different context than what is projected in this study.

5.3. Joint SCN-GPON planning overview

Similar to our previous approach, we first establish our case study's background, a combined SCN-GPON optimisation framework. The framework aimed to apply to any cellular technology being adopted to determine the SCN architecture type. Then, we discuss the framework implementation in this section. Hence, this section comprises the following-

- Joint SCN-GPON planning methodology
- Joint SCN-GPON planning methodology

5.3.1. Joint SCN-GPON planning methodology

This segment comprises the following sections of the optimisation framework-

- Framework planning backdrop
- Setting up the split ratio and PON port limits

- SCN-GPON cost components
- RT selection process based on terrain grid
- GPON dimensioning process
- SC location selection based on GPON formation

❖ Framework planning backdrop

Considering the availability of information and maintaining coherence and cohesiveness with the previous works, we continue to select The University of Melbourne Parkville campus region as our preferred case study area. As mentioned, the case study area is categorised as an urban cellular propagation region due to its density of the end-user population, as distributed within the block of buildings throughout the study area. In this case, we introduced an optimisation framework for a generic scenario, regardless of the cellular technology adapted into the framework, while still maintaining coherence with the previous works. Thereby, we aimed to include both the SCN and GPON selection process into the same generalised optimisation framework instead of pre-selecting the SC location, then connecting them with an optimised GPON backhaul architecture afterwards. As a result, we did not use a fixed rectangular coverage area for each selected SC location. We instead introduced a rectangular terrain grid over the case study area, just as a part of the framework design process. We envisioned the terrain grid to pinpoint a set of potential SC locations positioned at equal distance from each other. We proposed the rectangular grid positioning over the case study area to pinpoint the Melbourne University campus building locations.

The purpose then shifts from selecting SC locations based on identifying geographical points to location positioning based on favourable proximity from the campus's underlying PtP optical network. However, it does not necessarily discard the geographic terrain influence aspects of the selected SC location, as we can still identify coverage patterns and coverage area positions by geographic aspects of the case study area. When it came to this chapter's terrain grid formulations, they were ultimately formed as the 200 m × 200 m and 300 m × 300 m grids. It was the same approach, as seen in the previous **Chapter 4**, this time to cover all the campus buildings over the case study area. However, as mentioned, the significance of these two terrain grid formulations was only relevant to place potential SC locations in an equidistance manner. As a result, each potential SC location was positioned with a distance from 100 m and 150 m each for the 200 m × 200 m and 300 m × 300 m terrain grids. Thereby, the two case study

approaches considered the equal distance between each potential SC location rather than the terrain grid blocks' dimensions. Final formations of the terrain grid and potential SC locations can be shown in **Figure 68** and **Figure 69,** respectively, for SC locations placed every 100 m and 150 m. The next section elaborates on the optical splitter split ratio and the number of PON ports chosen within the OLT.
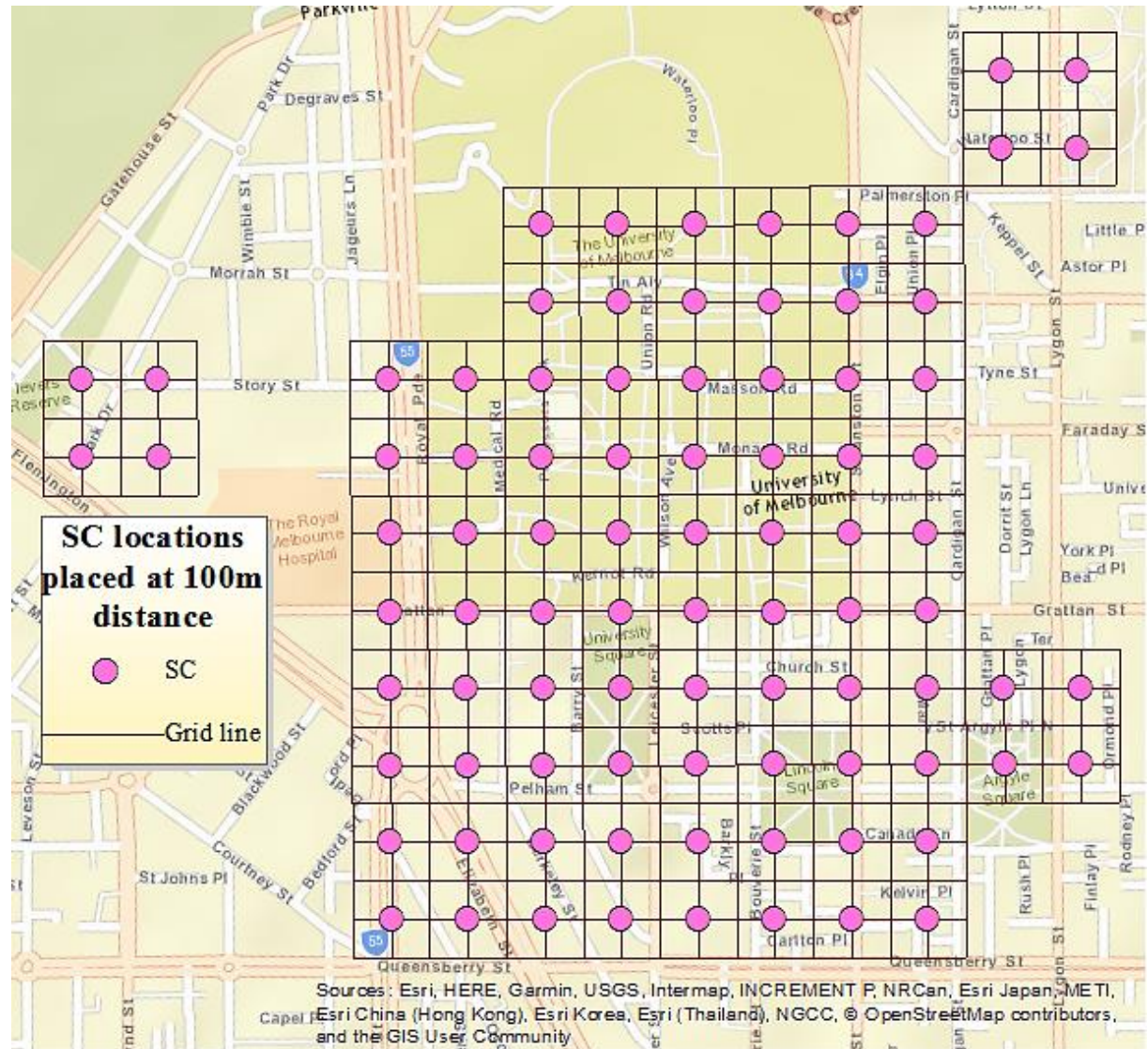
Figure 68: Potential SC locations placed every 100 m distance
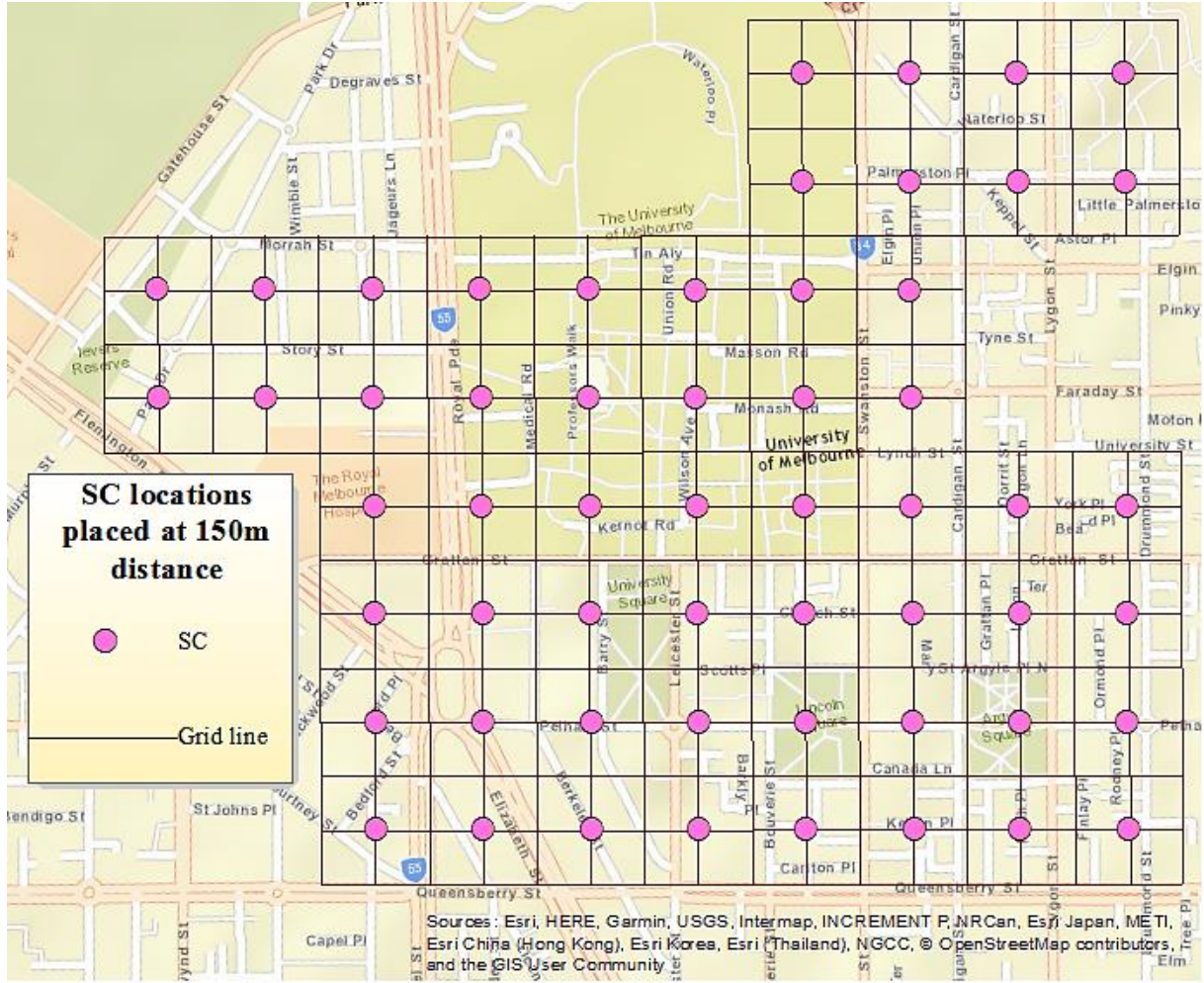
Figure 69: Potential SC locations placed every 150 m distance

❖ Setting up the split ratio and PON port limits

As per the GPON technology, we continued our approach to choosing multiple FAP locations to place the necessary number of splitters and connect to the next stage of nodes, as seen in **Chapter 4**. Again, we fixed the split ratio for each splitter to determine the number of outgoing fibres from the FAP towards multiple RT locations to maintain the GPON connectivity's reliability [6]. For our case studies in this chapter, we utilised five split ratio types-1:2, 1:4, 1:8, 1:16 and 1:32. We also chose a line card based on the fixed number of PON ports it can support [6]. This number varies on the different type of PON technologies existing, as GPON can support up to 16 PONs, XG-PON and TWDM-PON each support 4, and WDM-PON only support 1 PON connection [118]. Again as seen in **Chapter 4,** we considered two PON ports-4 and 8 for our case study [119]. It is a constraint to fix the number of outgoing

fibre connections from the OLT placed in CO location(s) towards the next stage of FAP locations with the optical splitters [6].

❖ SCN-GPON cost components

Following the same approach as in **Chapter 4**, our SCN-GPON combined optimisation framework still followed the three-level connectivity architecture. The first level was the connection from OLT to splitter situated at FAP by level 1 fibre. Then second level connectivity stage included connection from FAP splitter to ONU placed in RT nodes by level 2 fibre. Finally, the level 3 stage comprised the connection from RT to small-cells by level 3 wires, comprising the total link cost. As for the equipment, costs-multiple splitters can be installed in the same node only at the FAP level of the PtP network since the previous OLT level in the hierarchy does not have a splitter. Other aspects of the cost component included the cost of ONU equipment placed at the pre-selected RT locations and the small-cell BTS components placed on selected SC locations. Hence, the equipment cost includes current equipment operational expenses, with purchase and installation costs for adding new equipment. Akin to **Chapter 4**, the sum of splitter and fibre costs were linear functions of the fibre lengths and the number of equipment to be utilised, depending on the level they are both installed together. The RT and SC component numbers were equal since the number of SC placements depended on the number of RT locations selected. The optimisation solution was mainly based on arranging the placed splitters, SC equipment locations and the fibres. This arrangement was planned to serve the connectivity demand, adhering to the network capacity limits, ultimately minimising the overall cost for such a combined SCN-GPON network deployment optimally.

❖ RT selection process based on terrain grid

The RT selection process for the optimisation problem in this chapter slightly varied from **Chapter 4**, though following similar visual observations over the case study area maps. As seen in **Chapter 4**, one RT location from each coverage block was selected if multiple existing RT locations resided in each square block of the terrain grid formulations. Again, the RT selection process was chosen manually, outside the GPON optimisation framework. As mentioned, the process involved choosing one RT location per coverage block and finalise all RT locations in the process. However, this time, the RT location from each square block of the mapped terrain grid over the case study area was not chosen based on being visually closest to

the SC in a coverage block. The intended RT location considered was the most centralised within each coverage block, selected based on visually comparing the existing RT locations within each such block. The idea was to select an RT location within each unit block of the mapped terrain grid that was approximately the most equidistance from the square block edges. It was done to provide a more balanced distribution of the distance between the RT-SC links, as SCs were placed on equal lengths from each other, based on the terrain grid over the case study area. Additionally, as before, another reason for choosing one RT location per square block was to minimise the number of RT locations used in the network planning in a more equalised and organised manner.

As a result, the number of RT locations chosen was different based on the size of the different terrain grid dimensions.

❖ GPON dimensioning process

The following step was to dimension the GPON network that would act as the backhaul for the SC locations selected. For this, the CO and FAP locations were selected based on their most favourable positions from the pre-selected RT locations within the case study area. Hence, the RT locations acted as constant parameters while the CO and FAP locations were the variable values chosen through the optimisation process. As mentioned, the CO locations acted as placeholders for housing OLT equipment of the GPON architecture, while FAP locations were used to install optical splitter equipment. In this scenario, again CFLNDP optimisation method was applied in two different to-and-from directions. First, incoming connection and node arrangements were optimally located towards the fixed set of RT locations and secondly, outgoing connection and nodes were selected from the same RT locations. As before, the RT locations were chosen to place the ONU equipment. This ONU acts as the interface between the optical backhaul and the wireless SCN. This GPON dimensioning process was thereby done to determine the optimal backhaul layout to connect to the SC locations and selected as part of the whole optimisation framework in this chapter.

❖ SC location selection based on GPON formation

The optimisation framework's last step was determining the SC locations based on the selected GPON formation. In this process, the SC locations were selected as the subset of the existing potential SC locations for both type of terrain grids (200 m × 200 m and 300 m × 300

m). These formations are shown in **Figure 67** and **Figure 68**. The SC location selection process was primarily based on each RT-SC pair's distance. It was done to determine SC locations' optimal arrangement based on the pre-selected RT location positions. It would also invoke new link routes between each RT-SC distance pair, where the cost components would include both new link and facility costs, e.g., RT-SC wire connections and SC components. Again, as seen in **Chapter 4**, the RT location selection was not part of the optimisation process. They were pre-selected based on their positions being the most central in each terrain grid square block. In this selection process, the set of RT locations acted as the facility position parameters, while the set of potential SC locations were equivalent to that of the demand nodes. The CFLNDP optimisation method was incorporated as the background to solve this optimisation problem of constructing a combined SCN-GPON framework.

5.3.2. Joint SCN-GPON planning implementation

The previous section in this chapter described the optimization framework development of the combined SCN-GPON architecture. The framework was implemented through proper case studies, and the implementation process will be described and discussed in this section. This framework is a combined optimisation process through cost minimisation that dimensions both the GPON-based backhaul and selecting the best SC locations. The implementation process, therefore, includes the following steps-

- Joint SCN-GPON planning parameters
- Joint SCN-GPON planning variables
- Joint SCN-GPON planning objective function
- Joint SCN-GPON planning constraints

❖ Joint SCN-GPON planning parameters

Similar to **Chapter 4**, the framework is primarily based on the Link, and facility cost components, with additional transport costs involving SC equipment installation labour expenses, were incorporated. The link cost components for the first two fibre levels, namely distribution and feeder fibres, were based on operational costs or OPEX of the links as they utilised existing optical network fibres. For the next level of links, e.g., drop cable was planned as newly laid components, so the cost to be utilised for that was the capital expenditure or CAPEX. Additionally, new GPON components such as OLT, splitter and ONUs and also the

small-cell BTS equipment were being planned to be utilised as a part of our GPON framework. Thereby, the facility cost for them was included within the optimisation framework. For this chapter's framework, the positions of FAPs, COs, RTs within the existing PtP optical network influenced the selection of the SC locations. They also determined the cost of connecting the small cell with the OLT via ONU and splitters. There was a fixed operating cost per unit length of the fibre, and that "fibre-length" was the real distances along with the existing fibre infrastructure for the RT–FAP and FAP–CO fibre pairs. These distances were pre-measured as parameters for the framework. For the newly planned RT-SC routes providing ONU and SC connectivity, direct Euclidean distances were measured from each selected RT location to all the potential SC locations, and these were also used as parameters. Additionally, COs, FAPs, and RTs within a GPON were assigned a unique identifier to determine their sets of location parameters. All these optimisation parameters were then specified as follows.

CO = The set of CO locations where $|CO| = N_c$

FAP = The set of FAPs where $|FAP| = N_f$

RT = The set of RT/ONU locations where $|RT| = N_r$

SC = The set of potential SC locations where $|SC| = N_s$

N_c = Number of total CO locations (Capacity at CO stage)

N_f = Number of total FAP locations (Capacity at FAP stage)

N_r = Number of RT/ONU locations (Capacity at RT stage)

N_s = Number of potential SC locations (Capacity at SC stage)

N_p = Number of PONs per line card

M = Big M integer for conditional operations

e_r = Cost of OLT rack

e_{sh} = Cost of OLT shelf

e_{cc} = Cost of OLT control card

e_{lc} = Cost of OLT line card

e_{fsp} = Cost of an optical splitter

e_{spl} = Cost of fibre splicing

i_{rsfib} = Drop fibre per meter installation CAPEX

i_{scins} = Cost of labour for SC BTS installation

fi_{cf} = Feeder fibre per meter installation OPEX

fi_{fr} = Distribution fibre per meter installation OPEX

R_f = Split ratio

d_{max} = Maximum transmission distance

d_{cf} = Distance of each feeder fibre

d_{fr} = Distance of each distribution fibre

d_{rs} = Distance of each drop fibre

q_{cf} = Feeder fibre per meter OPEX

q_{fr} = Distribution fibre per meter OPEX

q_{rs} = Drop fibre per meter CAPEX

❖ Joint SCN-GPON planning variables

The GPON cost optimisation framework variables were primarily considered for the link, and facility cost components, with an additional variable, included to account for the small transportation cost segment. This variable was the SC location variable that was also involved with the SC facility cost. The variables comprised both integer and binary types, as our

framework was a MILP optimisation problem. This proposed joint SCN- GPON optimised deployment was divided into four stages of determining optimal network node locations and link positions. Here, the first three levels align with the existing PtP network node types- the CO, FAP and RT for the GPON deployment part of the framework. The last stage of determining optimal SC locations was done based on potential new SC locations chosen by the terrain grid alignment process, as discussed earlier. These were considered as the facility equipment installation locations within the optimal network planning process.

Like the GPON planning of **Chapter 4**, CO locations contained OLTs, Ethernet switches, and in-house fibre connecting equipment. The Ethernet switches were connected to OLT, as OLT included the network and PON line cards, and afterwards, the fibre distribution panels. The OLT establishment's total cost was based on the required number of OLT chassis, shared equipment, and line cards, as determined by the number of PONs connected to that OLT. Generally, an OLT chassis can include several line cards, and each line card can hold multiple PONs. Ethernet switches connected the access network to the metro network, and they were the first element within the OLT premises. Then fibre distribution panels were used to attach the outside plant fibre (feeder) to fibre jumpers that entered the CO and terminated on the OLT shelf. Multiple direct links were installed using feeder fibre from selected CO location(s) to select FAP location(s) to establish OLT to splitter connectivity. The GPON planning stage was to select the subset of FAP locations for holding the optical splitters from the set of all FAP locations. The split ratio and the type of installation enclosure determined the cost of a splitter establishment, precisely the number of enclosures and splitters installed at each FAP location. Hence, multiple links from each FAP location towards RT locations were designed using distribution fibre. Afterwards, from RT to all SC locations, a direct new single link from each RT to SC was planned by placing drop fibre. In this chapter, the SCN-GPON framework determined the SC locations based on pre-selected RT locations, and drop fibre costs and SC equipment cost components were included within the framework. Again, the framework had both integer and binary variables, as follows.

I_{cf} = Number of CO-FAP connections (Demand served by CO stage)

I_f = Number of FAP splitters (Demand served by FAP stage)

N_{lc} = Number of line cards at OLT stage at CO location (Demand served by FAP stage)

$$O_c = \begin{cases} 1; \text{ if the } c^{th} \text{ CO is selected to place OLT equipment} \\ 0; \text{ otherwise} \end{cases}$$

$$S_f = \begin{cases} 1; \text{ if the } f^{th} \text{ FAP is selected to place splitter equipment} \\ 0; \text{ otherwise} \end{cases}$$

$$B_s = \begin{cases} 1; \text{ if the } s^{th} \text{ SC is selected to place BTS equipment} \\ 0; \text{ otherwise} \end{cases}$$

$$X_{cf} = \begin{cases} 1; \text{ if the } c^{th} \text{ CO is connected to } f^{th} \text{ FAP splitter} \\ 0; \text{ otherwise} \end{cases}$$

$$X_{fr} = \begin{cases} 1; \text{ if } f^{th} \text{ FAP splitter is connected to any } r^{th} \text{ RT ONU} \\ 0; \text{ otherwise} \end{cases}$$

$$X_{rs} = \begin{cases} 1; \text{ if } r^{th} \text{ RT ONU is connected to any } s^{th} \text{ SC BTS} \\ 0; \text{ otherwise} \end{cases}$$

❖ Joint SCN-GPON planning objective function

Our joint combined SCN-GPON optimisation framework was also similar to that of **Chapter 4**. This joint optimisation framework also followed the CFLNDP optimisation method to determine the SC and PtP node locations and corresponding fibre/wire routes. Again, this was done by minimising the corresponding link and facility cost components, ultimately generating an optimised SCN-GPON network layout plan. So, the objective function comprised of the decision variables for the link and facility cost components. Finding the cost-optimal values to the decision variables could be implemented onto the objective function itself to estimate the total cost needed to finalise the optimal SCN-GPON architecture. The objective function, therefore, can be denoted as follows.

$$
\text{minimise}
\begin{bmatrix}
\left(e_r + e_{sh} + e_{cc}\right) \sum_{c \in CO} O_c + e_{lc} \sum_{c \in CO} N_{lc} O_c \\[2mm]
+ \left(e_{fsp} + e_{spl}\right) \sum_{f \in FAP} S_f + \left(e_{fsp} + e_{spl}\right) \sum_{f \in FAP} \left(I_f - S_f\right) \\[2mm]
+ \left(e_{bs} + e_{spl} + i_{scins}\right) \sum_{s \in SC} B_s \\[2mm]
+ \left(q_{cf} + fi_{cf}\right) \sum_{c \in CO} \sum_{f \in FAP} d_{cf} I_{cf} + \left(q_{fr} + fi_{fr}\right) \sum_{f \in FAP} \sum_{r \in RT} d_{fr} X_{fr} \\[2mm]
+ \left(q_{rs} + i_{rsfib}\right) \sum_{r \in RT} \sum_{s \in SC} d_{rs} X_{rs}
\end{bmatrix}
\tag{32}
$$

As before, the two primary cost components for the link and facility deployment are a combination of several subcomponents. This framework has the extra cost components for the RT-SC link and the SC facility components compared with those mentioned in **Chapter 4**. The sub-divided cost components are denoted as follows.

$\left(e_r + e_{sh} + e_{cc}\right) \sum_{c \in CO} O_c = $ Cost for OLT equipment installation at all selected CO location

$e_{lc} \sum_{c \in CO} N_{lc} O_c = $ Cost for line card installation at all selected CO locations

$\left(e_{fsp} + e_{spl}\right) \sum_{f \in FAP} S_f = $ Cost for the first splitter installation at all selected FAP locations

$\left(e_{fsp} + e_{spl}\right) \sum_{f \in FAP} \left(I_f - S_f\right) = $ Cost for any additional splitter installations after the first, at

all remaining selected FAP locations

$\left(e_{bs} + e_{spl} + i_{scins}\right) \sum_{s \in SC} B_s = $ Cost for the small-cell BTS equipment installation at all selected

SC locations

$\left(fi_{cf} + q_{cf}\right) \sum_{c \in CO} \sum_{f \in FAP} d_{cf} I_{cf} = $ Total cost of all distribution fibre routes between OLT

and splitter

$\left(fi_{fr} + q_{fr}\right) \sum_{f \in FAP} \sum_{r \in RT} d_{fr} X_{fr} = $ Total cost of all feeder fibre routes between splitter and

ONU

$$\left(q_{rs} + i_{rsfib}\right) \sum_{r \in RT} \sum_{s \in SC} d_{rs} X_{rs} = \text{Total cost of all drop fibre routes between ONU and SC}$$

❖ Joint SCN-GPON planning constraints

For the type of cost components, the constraints were primarily related to link and facility cost components, although a small transport cost component was included within one of the facility cost components, e.g., the SC facility cost component. The constraint types were mostly the same as that of **Chapter 4** since the same premises and the same optimisation method was applied. However, some additional constraints were added to the optimisation problem for sufficing to the objective function's added components. The list of the constraint is as follows.

- Feeder fibre capacity conservation
- Feeder fibre conditional connectivity
- Distribution fibre capacity conservation
- Drop fibre capacity conservation
- PON reach limit
- Optical splitter & quantity conditional connectivity
- OLT equipment quantity restriction
- Splitter equipment quantity restriction
- SC equipment quantity restriction
- Line card connectivity restrictions
- Integer variable constraints
- Binary variable constraints

➤ Feeder fibre capacity conservation

$$I_f = \sum_{c \in CO} I_{cf}, \qquad \forall f \in FAP \tag{33}$$

This constraint maintained the demand conservation that each one splitter at the FAPs, connected with only one OLT in the CO. Hence, outgoing demand from CO level, e.g., the number of feeder fibre connections from OLT was equal to the number of splitters, e.g., incoming demand to the FAP level, ensuring that the OLT in CO connected only with the FAPs housing splitters.

$$\sum_{c \in CO} X_{cf} = S_f, \qquad \forall f \in FAP \tag{34}$$

This constraint maintained the connectivity conservation aspect for the CO and FAP node levels. Each FAP location with a splitter connected with only one connection of the OLT line card port for the CO-FAP link(s), where the OLT is placed on a selected CO location.

$$X_{cf} \leq O_c, \qquad \forall c \in CO, \forall f \in FAP \tag{35}$$

This constraint assured that demand was only served at facilities selected through the optimisation framework for CO and FAP node levels. Hence this explicitly implied that each CO location should contain at least one OLT if that CO location had connectivity with an optical splitter at a FAP.

➢ Feeder fibre conditional connectivity

$$X_{cf} \leq I_{cf}, \qquad \forall c \in CO, \forall f \in FAP \tag{36}$$

$$I_{cf} \leq X_{cf} M, \qquad \forall c \in CO, \forall f \in FAP \tag{37}$$

These inequalities signified that demand flow was supplied through only the link chosen by the optimisation framework for the CO-FAP connections. More specifically, they pointed towards the conditional relation. This relation indicated the number of connections between CO and FAP levels of the existing PtP optical network and the possibility of a connection between those selected CO and FAP location(s). The first inequality implied that if the cth CO had no connection towards the fth FAP, that particular CO would not have any OLT placed. It means if I_{cf} was zero, then X_{cf} was also set to zero. The second inequality then denoted that for even at least one outgoing connection existed from the cth CO towards the fth FAP, then the cth CO would house at least one OLT, i.e. if I_{cf} was non-zero, then the value of X_{cf} would be 1. These two inequalities expressed the conditional constraint for a connection probability between the cth CO and f^{th} FAP with the total number of

connections between the cth CO and f^{th} FAP. Hence these inequalities specified towards a non-linear mathematical relationship and had the mathematical form of, $X_{cf} = \min\left(1, I_{cf}\right)$.

➢ Distribution fibre capacity conservation

$$\sum_{f \in FAP} X_{fr} \leq 1, \qquad \forall\, r \in RT \tag{38}$$

This constraint ensured that all demands should be served between the FAP and RT node levels. Hence, each ONU positioned at the RT level for the selected RT locations should connect to a maximum of one splitter at the FAP level.

$$X_{fr} \leq S_f, \qquad \forall\, f \in FAP,\ \forall\, r \in RT \tag{39}$$

This constraint confirmed that only optimally selected facilities would serve the connectivity demand for FAP and RT node levels. Therefore, FAP locations selected throughout the optimisation framework should have at least one optical splitter installed, only if that FAP location had connectivity with an ONU at RT level.

$$\sum_{r \in RT} X_{fr} \leq R_f I_f, \qquad \forall\, f \in FAP \tag{40}$$

This inequality maintained facility capacity limit for the distribution fibre connectivity between FAP and RT levels, based on the split ratio for each FAP level optical splitter in use. At each splitter for the fth FAP, the maximum number of outgoing connections towards r^{th} RT should not exceed the multiplication value of the splitters' total number at the fth FAP and the fixed split ratio. For example, say, a FAP had a 1:8 split ratio, and there were a total of 2 splitters at that FAP to connect to selected RT locations. In this case, a maximum of $8 \times 2 = 16$ connections from that FAP would go outwards to the RTs.

➢ Drop fibre capacity conservation

$$\sum_{r \in RT} X_{rs} = 1, \qquad \forall\, s \in SC \tag{41}$$

The constraint above indicated that only selected locations would serve connectivity demand for RT and SC node levels. Thereby, RT locations selected throughout the optimisation

framework must have at least one ONU installed, only if that RT location had a link with a BTS in a selected SC location.

$$\sum_{r \in RT} \sum_{s \in SC} X_{rs} \leq B_s \tag{42}$$

This constraint ensured that all demands should be served between the RT and SC node levels as well. Hence, each ONU positioned at the RT level for selected RT locations should connect with one BTS maximum at SC level.

➢ PON reach limit

$$X_{cf} d_{cf} + X_{fr} d_{fr} + X_{rs} d_{rs} \leq d_{\max}, \ \forall \ c \in CO, f \in FAP, \ \forall \ r \in RT, \ \forall \ s \in SC \tag{43}$$

This constraint was one of the new additions to the framework in this chapter, which was different from the previous constraints mentioned in **Chapter 4**. The combined length of feeder fibres, distribution fibres, and drop fibres between the SC and OLT levels should stay within the maximum allowed transmission distance of a GPON itself. For example, a 1:64 split individual 10GPON can theoretically reach 50 km of transmission distance [120]. Therefore, the combined length of network links should remain under the km level imposed by the GPON type implemented in the framework.

➢ Optical splitter & quantity conditional connectivity

$$S_f \leq I_f, \quad f \in FAP \tag{44}$$

$$I_f \leq S_f M, \quad f \in FAP \tag{45}$$

These inequalities ensured that demand flow only conducted from the chosen FAP location by the optimisation framework. These constraints show the condition between the number of splitters at the fth FAP and a splitter existing at the fth FAP.

. The first inequality ensured that the optimisation framework did not select the FAP location if no splitter was placed at that FAP location. It means, if I_f was zero, S_f would also become zero.

The second inequality signified that the fth FAP would be a selected location for placing a splitter if there was at least one splitter placed at that f^{th} FAP location. Thereby,

only if I_f had a non-zero value, then S_f would be 1. Again, as it was a set of condition-based constraints, they indicated a non-linear relationship by nature, expressed as, $S_f = \min\left(1, I_f\right).$

➤ OLT equipment quantity restriction

$$\sum_{c \in CO} O_c \le N_c \tag{46}$$

This inequality provided control over the maximum number of facilities, e.g., node locations selected at the CO level over the existing PtP optical network. The total number of selected CO locations, e.g., facilities, housing OLT equipment, should not exceed the total number of CO locations residing in the existing PtP optical network premises.

➤ Splitter equipment quantity restriction

$$\sum_{f \in FAP} S_f \le N_f \tag{47}$$

This inequality fixed the maximum number of node locations selected at the FAP level for the existing PtP optical network. The total number of selected FAP locations containing splitter equipment should not be more than the total number of FAP locations.

➤ SC equipment quantity restriction

$$\sum_{s \in SC} B_s \le N_s \tag{48}$$

This inequality limited the maximum number of SC node locations selected within the existing case study area. The total number of selected SC locations containing BTS equipment should not be more than the total number of potential SC locations.

➤ Line card connectivity restrictions

$$N_{lc} \ge \sum_{c \in CO} \sum_{f \in FAP} \left(\frac{I_{cf}}{N_p} \right) \tag{49}$$

$$N_{lc} \le \left\{ \sum_{c \in CO} \sum_{f \in FAP} \left(\frac{I_{cf}}{N_p} \right) \right\} + 1 \tag{50}$$

This constraint restricted the number of line cards within an OLT at the cth CO based on its number of ports that could support up to a fixed number, N_p PONs. Hence, for every N_p number of PONs, one line card should be placed at the OLT.

The first constraint provided the lower bound for the variable indicating the number of line cards to be placed at OLT, while the second constraint provided the upper bound. The first constraint states that the minimum number of line cards is at least the number of fibre connections between the cth CO and the fth FAP, divided by the number of PONs connected at the OLT. Now, in this case, the division result had not produced any remainder. Then by the second constraint, the maximum number of line cards is one greater than the number of CO-FAP fibre connections divided by the number of PONs connected to the OLT. In this case, however, the division produces a non-zero remainder.

➤ Integer variable constraints

$$I_{cf} \geq 0, \qquad \forall\ c \in CO,\ f \in FAP \tag{51}$$

$$I_f \geq 0, \qquad \forall\ f \in FAP \tag{52}$$

$$N_{lc} \geq 0, \qquad \forall\ c \in CO \tag{53}$$

These constraints restricted the integer variables' values to either zero or any non-zero value to align with the optimisation framework's mixed-integer aspect. In that way, it was ensured that the integer variable values stay within the positive range.

➤ Binary variable constraints

$$O_c \in \{0,1\}, \qquad \forall\ c \in CO \tag{54}$$

$$S_f \in \{0,1\}, \qquad \forall\ f \in FAP \tag{55}$$

$$B_s \in \{0,1\}, \qquad \forall\ s \in SC \tag{56}$$

$$X_{cf} \in \{0,1\}, \qquad \forall\ c \in CO,\ f \in FAP \tag{57}$$

$$X_{fr} \in \{0,1\}, \qquad \forall\ f \in FAP,\ r \in RT \tag{58}$$

$$X_{rs} \in \{0,1\}, \qquad \forall \; r \in RT, \; s \in SC \qquad\qquad (59)$$

The binary variables were used to specify the possibility of the existence of links and facilities. Thereby, all binary variables within the framework would be issued a value of either 0 or 1 to indicate whether a link/facility was present or not, respectively.

The following section implements the objective function, adhering to the variables, parameters and constraints, as discussed above. The outcomes present with appropriate SCN-GPON planning maps, as intended.

5.4. Joint SCN-GPON planning results

This section evaluates the case study results for the proposed combined SCN-GPON optimisation framework. Following the network planning methodology and implementation approaches mentioned in Section 5.3, these results are obtained through defined case studies. There were two case study approaches utilised for implementing the framework to identify the best possible network architecture by studying the obtained outcomes. The optimisation method produced a combined and more generalised framework by including both the SCN and backhaul dimensioning within the same page to maintain efficiency for the whole network design process. The purpose was to establish a simplified optimisation framework that can be used for cost and resource minimisation, regardless of the network technology to be used for SCN planning. The optimisation framework would primarily consider the distances between every two levels of the network nodes to produce a cost minimised network design. Unlike its predecessor framework, as developed in **Chapter 4**, not only locations of the GPON backhaul nodes were optimally selected, but also the SCN locations were determined within the same framework. In future, such selected SC locations could then be studied for their terrain-influenced cellular signal propagation patterns to determine their respective coverage area and direction of signal propagation. In this way, the SC locations were no longer restricted to having a fixed coverage radius of 200 or 300 m. This framework would allow the SC locations to have different coverage areas and signal directions, depending on the influence of surrounding terrain.

For this chapter, the focus was more on optimal location selection of both SCN and GPON architectures, based on cost and resource utilisation. Instead of performing separate location selection methods for choosing the front-end SC node locations and dimensioning

GPON component locations, the framework selected all such nodes within one combined optimisation framework. The SC locations were chosen primarily based on proximity to the existing PtP nodes for the case study area. Simultaneously the PtP node and corresponding fibre route position information are fed to the optimisation framework to select the most suitable subsets of locations to plan our proposed combined SC-GPON network architecture. The initial set of potential SC locations, from which the final SC locations were selected, were determined by the terrain grid approach. Here, the intended case study area, e.g., the University of Melbourne Parkville campus, was first virtually mapped into a terrain grid. Then from each block of the grid, one most centrally located RT location, mainly a campus area building, was selected by visual comparison. Then for each terrain grid block, four potential SC locations were chosen, which comprised the whole set of SC locations, placed equidistant apart from each other. These pre-selected RT node positions and the potential SC locations and existing CO and FAP node positions were utilised to optimise case studies. Next, we performed our optimisation process to determine the final optimal SC, FAP and CO node locations, which could house the SC BTS, splitter and OLT equipment, respectively. Here, the visually selected RT location would contain the ONU device that could bridge the whole design's wired and wireless network components at the SC-RT interface. The ultimate purpose was to select the mobile network node components first, on which further coverage area and signal directivity aspects are discussed in the following chapter.

As similar to **Chapter 4**, the CFLNDP optimisation method was implemented that considered wireless and optical network equipment locations as a set of network nodes and the connectivity provisions going throughout the networks as network links. Ultimately, cost minimization was to be achieved by optimally selecting network nodes and links. Again, five split ratio variants of optical splitters and two types of GPON port connections within the line card were imposed as constraints within the framework. Moreover, the cost components-both collectively and separately in terms of link and equipment components were compared. The network formation presented with the lowest total cost value after comparison was chosen as the most optimal network architecture for the intended combined SCN-GPON framework.

Akin to **Chapter 4**, we ran our optimisation simulation scenarios in AMPL mathematical programming software [122]. We ran the simulations on a desktop computer with 16 GB RAM and Microsoft Windows 7 operating system. Once the optimal network map information was obtained through simulations, we again used the ArcGIS geoprocessing tool

[121] to produce the relevant network maps with the optimally chosen network nodes and links. We then stored the results in a Dropbox [123] cloud service account.

We conducted the following two case study approaches.

- SC locations placed every 100 m
- SC locations placed every 150 m

5.4.1. SC locations placed every 100 m

This section focuses on the first scenario for our combined SCN-GPON optimisation case study, based on the facility location optimised method [114]. This approach utilises potential SC locations arranged by placing them every 100 m in a terrain grid formation. This section contains the following sub-sections-

- RT position selection for SC locations placed every 100 m
- Combined optimisation framework cost comparison scenario
- Optimised network map examples for SC locations placed at 100 m distance

❖ RT mapping for SC locations placed every 100 m

The RT locations within the existing PtP optical network premises were selected to install the ONUs for SCN-GPON connectivity. For resource minimisation, one RT location was selected for each 200 m × 200 m terrain grid block, when potential SC locations were envisioned to be sitting every 100 m. Hence, from all RT locations situated within the current PtP optical network over the University of Melbourne campus, the most central RT location within each terrain grid block was chosen by visual pinpointing. The RT selection process is thereby divided into two parts-

- Initial RT mapping for SC locations placed every 100 m
- Final RT mapping for SC locations placed every 100 m

➢ Initial RT mapping for SC locations placed every 100 m

For the SCN-GPON framework mapping process, the same 200 m × 200 m terrain grid map as in **Chapter 3** was chosen using the ArcMap tool [121] over our intended case study area. The grid map was then accurately aligned with the existing RT locations, resulting in the

following diagram in **Figure 70** below, where multiple RT locations exist in each 200 m × 200 m block of the terrain grid. This diagram is the same as **Figure 55** in **Chapter 4** -
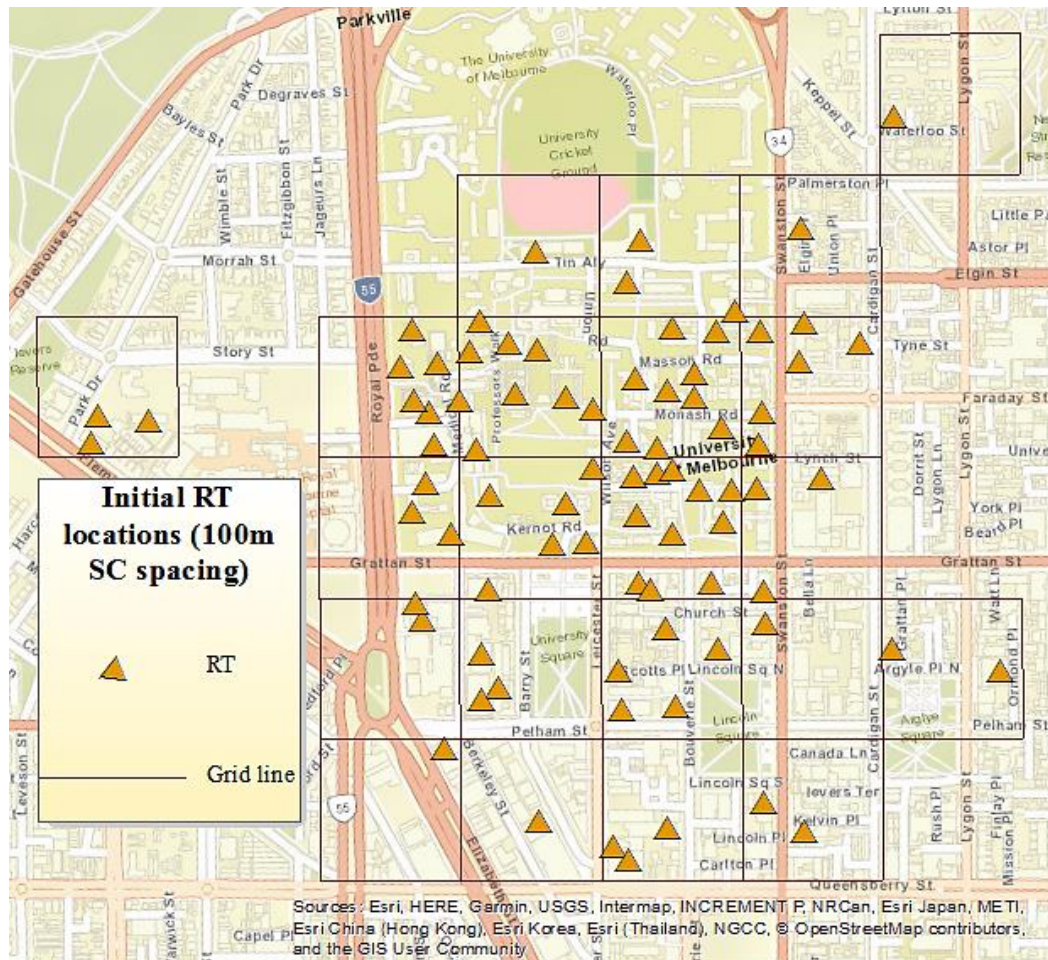
Figure 70: Initial RT locations for SC locations placed every 100 m

➤ **Final RT mapping for SC locations placed every 100 m**

This step selected the most centralised RT location from each block of the 200 m × 200 m terrain grid by visual observation, as shown in **Figure 71** below. These selected RT locations deployed an ONU each, providing the SCN-GPON connectivity. Once the RT locations were fixed, this information was used as a parameter through appropriate constraints to determine the rest of the nodes and links for the optimal combined SCN-GPON architecture. The next section of this chapter then discusses the framework cost comparison scenarios.
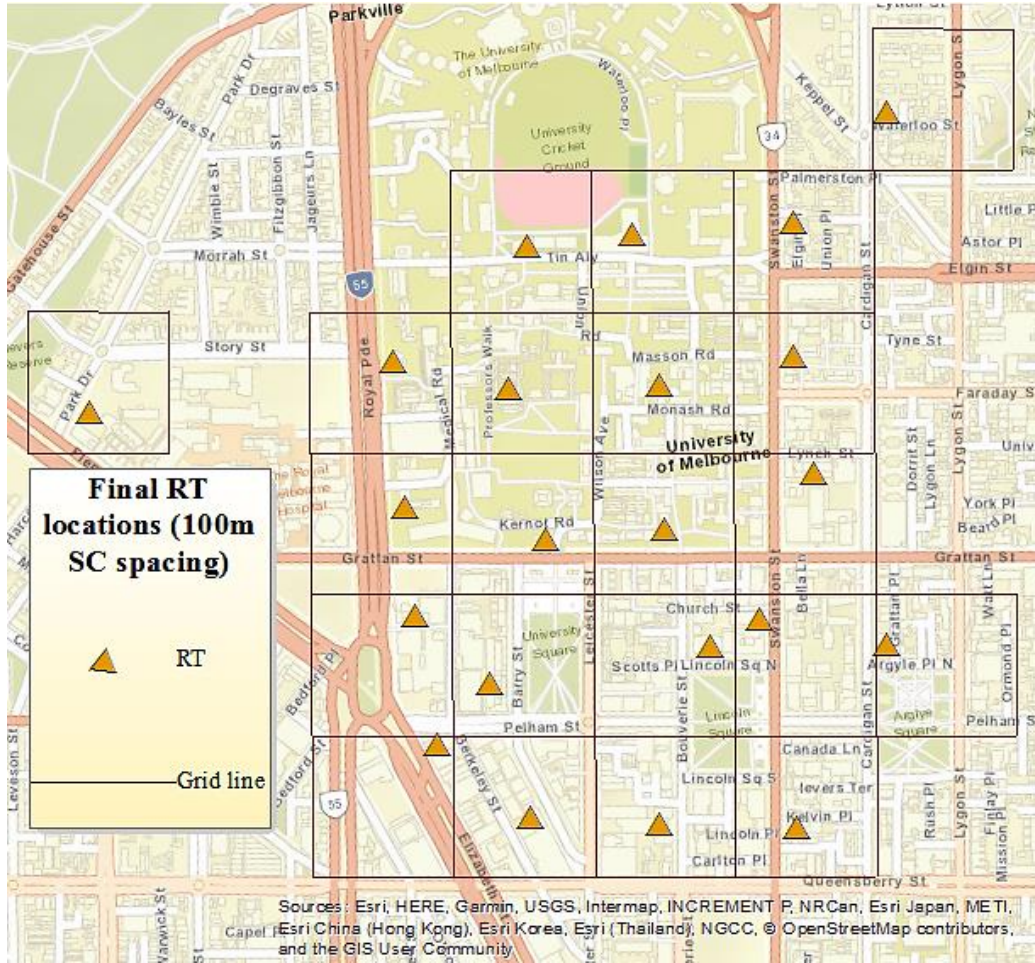
Figure 71: Final RT locations for SC locations placed every 100 m

❖ Cost comparisons for SC locations placed every 100 m

The cost optimisation scenarios aimed at the terrain grid arrangement for SC locations placed every 100 m depended on the number of PON ports in the OLT line card. This line card connection restriction would influence the total cost values for the different GPON planning scenarios. Hence, as similar to **Chapter 4**, we again apply the following two type of PON port capacity restriction in line cards and obtain two sets of cost comparison results-

- Number of OLT PON ports 8
- Number of OLT PON ports 4

➢ Number of OLT PON ports = 8

This section focuses on the cost comparison outcomes obtained for an OLT line card equipment supporting a maximum of eight ports for PON connections when potential SC

locations were placed at 100 m distance each. We only focused on the fixed split scenarios on optical splitter types for this study. It has already been established in **Chapter 4** that the most cost-optimal arrangement would be from one of the fixed split scenarios. Again, minimal differences were observed in terms of the total cost among the different splitter type scenarios. When the individual different cost components were observed, a particular trend in cost values was apparent. It was evident that for all five types of optical split scenarios, the costs for OLT equipment, line card and small-cell BTS equipment stayed the same. However, the splitter equipment costs decreased as the split ratio increased for different network types. With the increase in the split ratio, the number of outgoing connections from each splitter increased, allowing fewer splitter equipment usages per location. As for the fibre usage costs, no linear relation was evident between the fibre cost and the split ratio. As the selected fibre routes from each FAP to RT link was different for each split scenario since based on the split ratio limit, the number of FAP locations utilised got changed. Hence, the amount of utilised existing fibre ducts for FAP-RT feeder fibre varied and eventually influenced the fibre cost. Finally, the case study outcomes showed a 1:16 split ratio GPON planning as the cost-optimal network design for a combined generalised SCN-GPON architecture, with the OLT line card supporting at most 8 PONs. The cost comparison chart is displayed in **Figure 72** below. For the following section, cost comparison scenarios for a 4 PON port OLT line card are discussed.
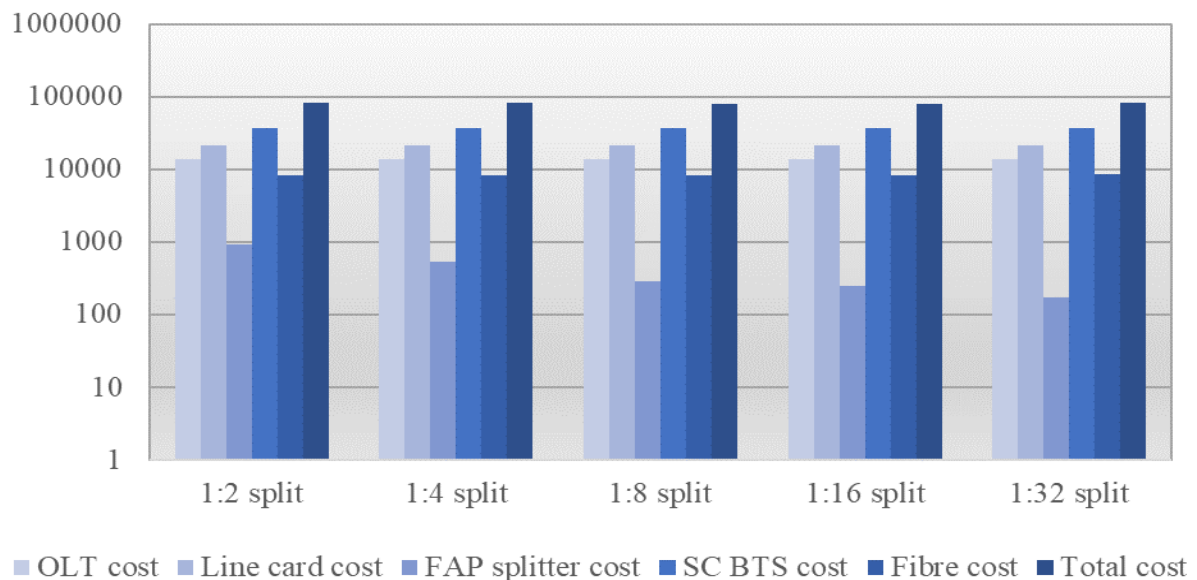
Figure 72: Cost comparisons for 100 m, 8-PON SCN-GPON planning

➢ Number of OLT PON ports = 4

This section focuses on the cost comparison scenarios when the OLT line card can contain a maximum of 4 PON ports. The cost comparison scenarios were highly similar to those obtained for the 8 OLT PON port instance, except for changes observed in the fibre usage costs. It materialised as the maximum number of PON ports in the OLT line card was increased from 4 to 8. Thereby, the fibre routes coming out of the FAP and going towards RT got altered, thus influencing the fibre usage costs. The other individual cost values for OLT, line card, FAP splitter and SC BTS equipment remained unchanged as the optimally selected node locations and fibre routes remained unchanged. The cost comparisons are thereby presented below in **Figure 73** as chart arrangements.
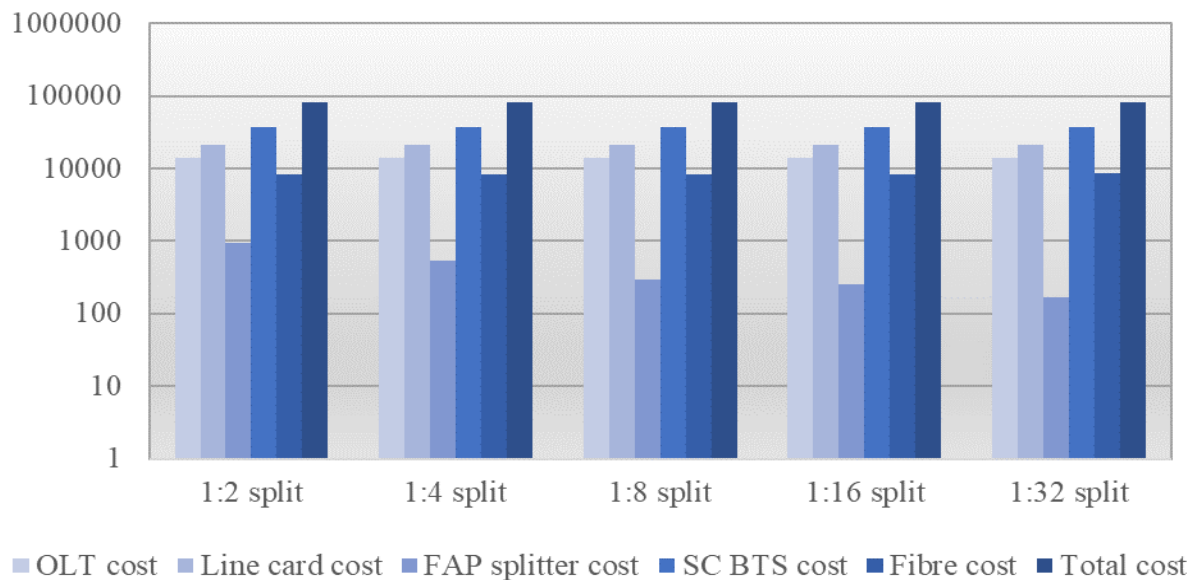
Figure 73: Cost comparisons for 100 m, 4-PON SCN-GPON planning

❖ Network maps for SC locations placed every 100 m

The final SCN-GPON arrangements were represented into maps by the geoprocessing software ArcMap [121], showing the CO, FAP, RT, and SC's optimal locations with the corresponding logical connections. We will discuss the results on the most and least cost-optimal results, which were 1:2 and 1:16 split ratio maps, respectively, in **Figure 74** and **Figure 75**, for the 8 PON port scenario. The maps showed that both 1:2 and 1:16 network scenarios selected the same 1 CO location. Alongside, the 1:2 GPON selected 7 out of 11 FAP locations, and the 1:16 scenario utilised only 2 FAP locations for placing the optical splitters to connect

to the pre-selected RT locations. As splitter usage increased for the 1:2 scenario, the fibre route utilisation increased, ultimately rendering the 1:2 split ratio the highest cost value among all the GPON scenarios investigated. In this study, both the least and the most expensive network scenarios were connected with the same number of ONUs at the pre-selected RT locations. In turn, it provided connectivity to the same number of SCs as the number of RT locations.
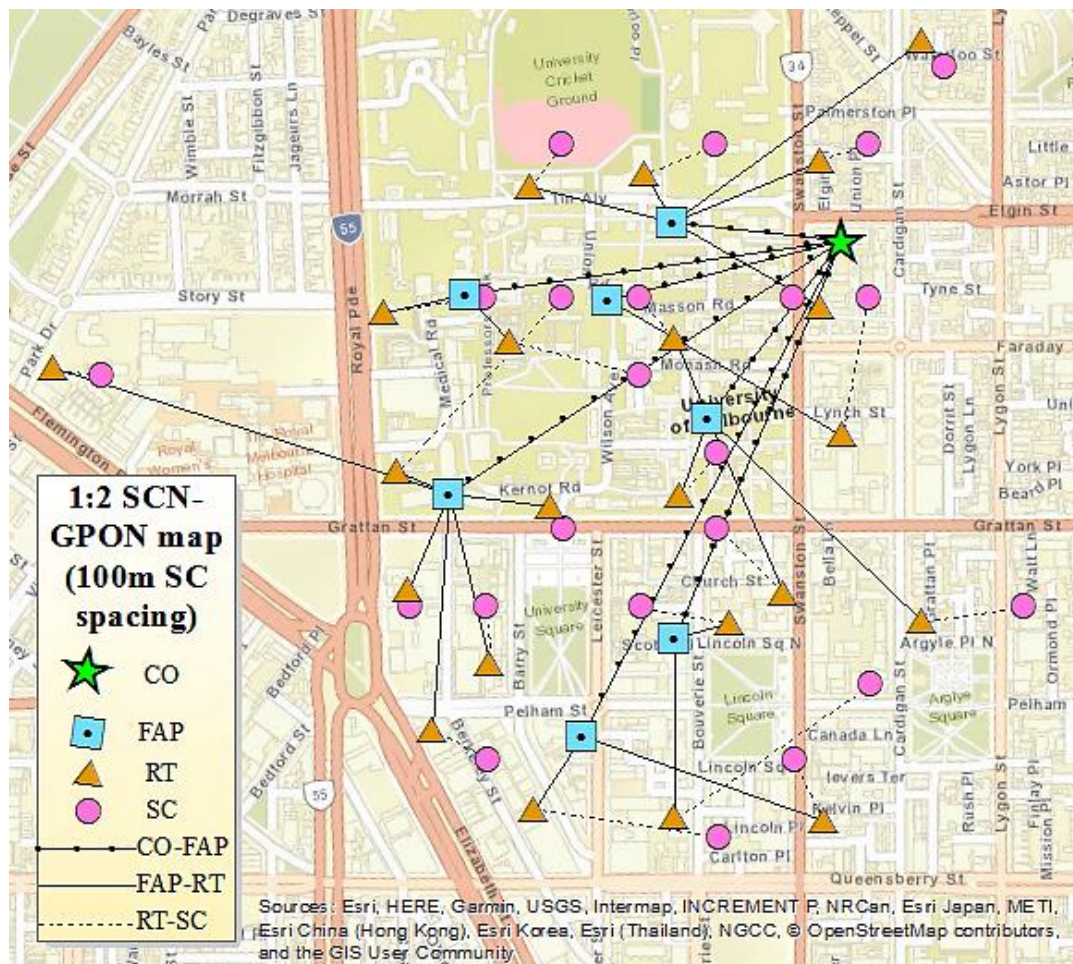
Figure 74: 1:2 combined SCN-GPON network map (Number of PONs = 8)
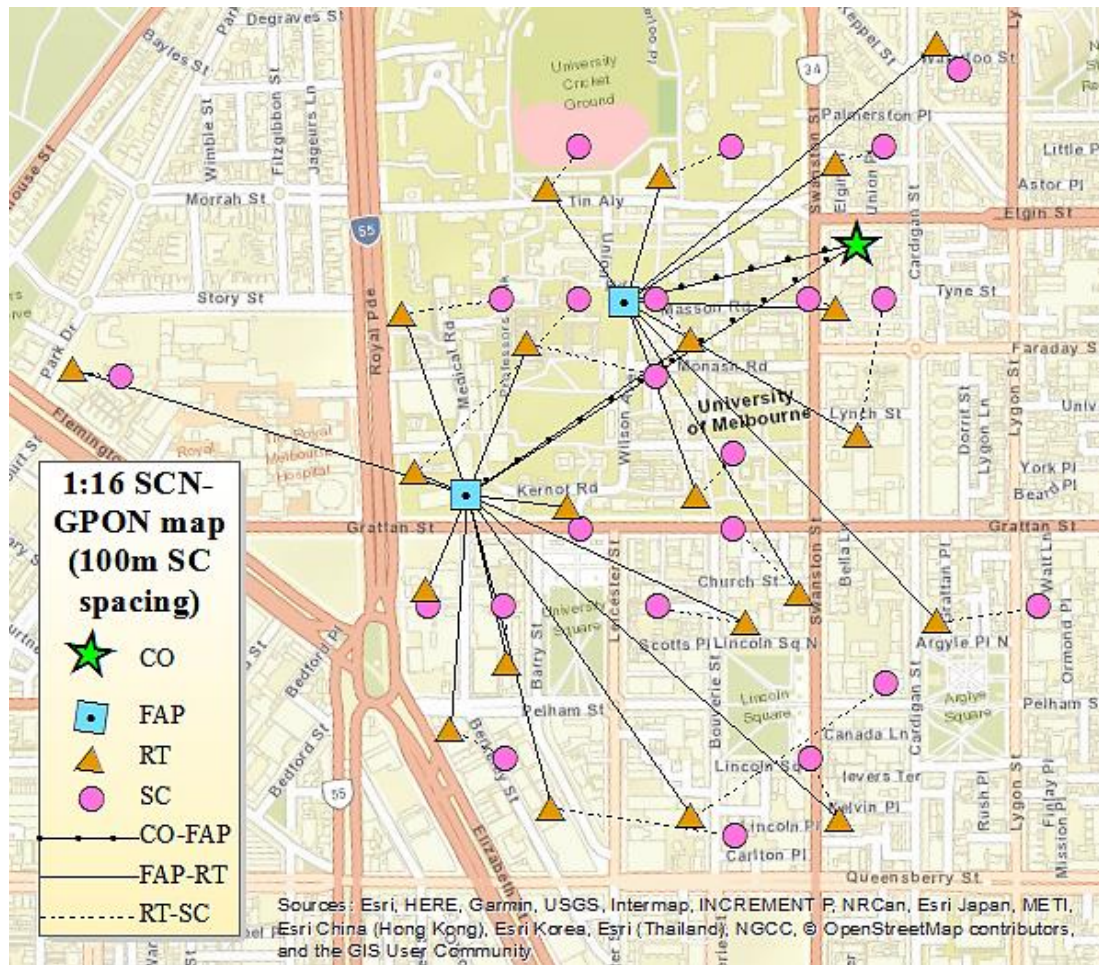
Figure 75: 1:16 combined SCN-GPON network map (Number of PONs = 8)

5.4.2. SC locations placed every 150 m

This section discusses the results based on a terrain grid formation of SC locations placed every 150 m over the case study area. This approach organises potential SC locations placed every 150 m in a terrain grid formation. This section contains the following sub-sections-

- RT position selection for SC locations placed every 150 m
- Combined optimisation framework cost comparison scenario
- Optimised network map examples for SC locations placed at 150 m distance

❖ RT mapping for SC locations placed every 150 m

This section elaborates on the RT location selection process over the 300 m × 300 m terrain grid to utilise the selected RT location information as a parameter for the combined SCN-GPON optimisation framework. As envisioned, these selected RT locations would act as the housing sites for installing the ONU equipment. As previous, one RT per 300 m × 300 m block was visually selected from the set of all RT locations within the existing PtP optical networks. The idea was to put one RT nearby each SC location which was placed 150 m apart from another, within the terrain grid over the case study area. The RT selection process is again divided into two parts-

- Initial RT mapping for SC locations placed every 150 m
- Final RT mapping for SC locations placed every 150 m

➢ Initial RT mapping for SC locations placed every 150 m

The initial RT mapping below in **Figure 76** has virtually the same RT locations and terrain grid formation as that of **Figure 62** since the same RT locations and the same terrain grid formation was utilised.
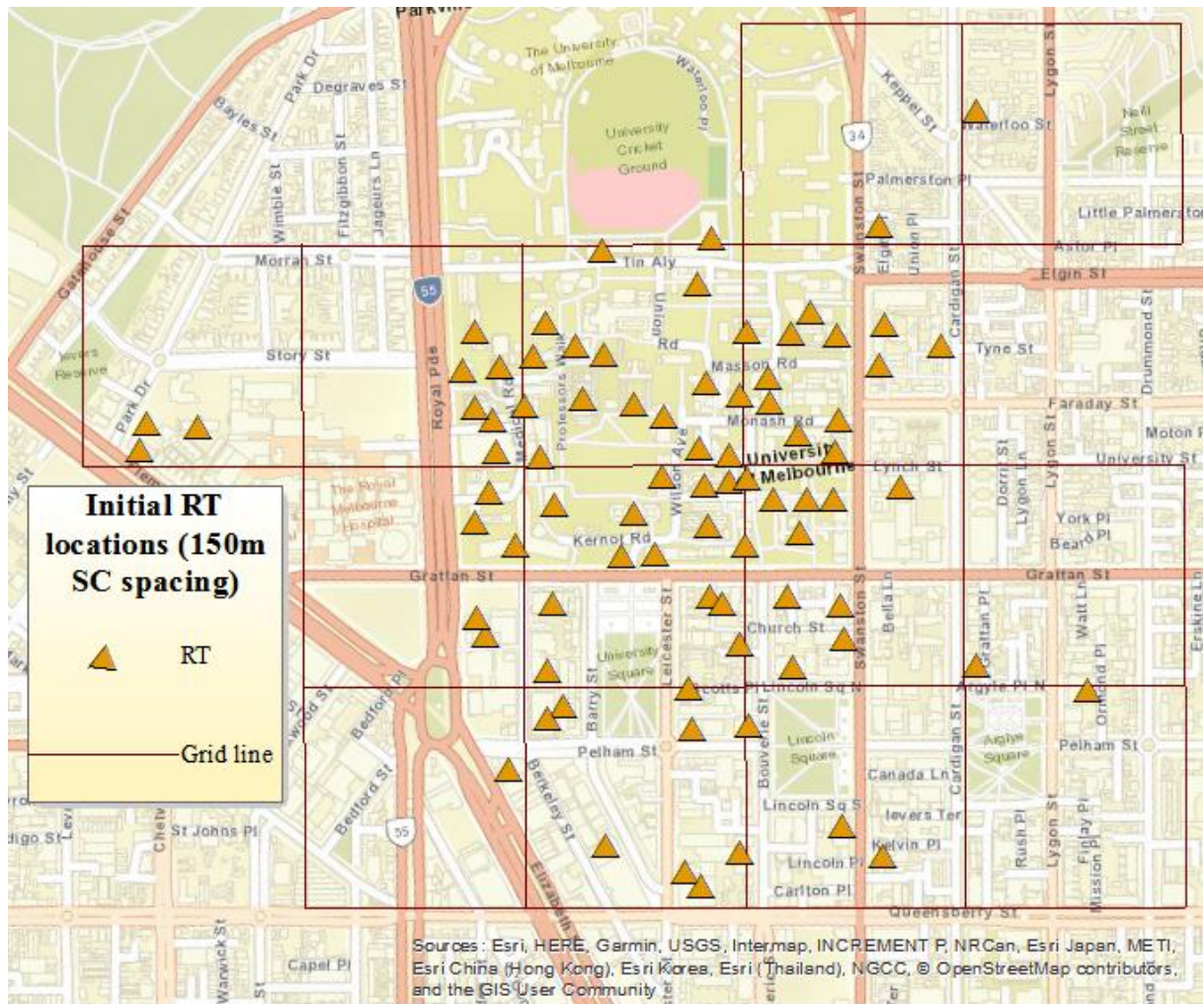
Figure 76: Initial RT locations for SC locations placed every 150 m

➢ Final RT mapping for SC locations placed every 150 m

From the previously constructed map (as shown in **Figure 76**) of all RT locations placed over a terrain grid having 300 m × 300 m sized blocks, we selected our intended subset of RT locations, again based on visual comparisons. Hence, the selected RT location for each 300 m × 300 m terrain grid block was the most centrally located RT, as it appeared visually. The RT locations selected in this process for the 300 m × 300 m terrain grid are shown below in **Figure 77**. The subsequent section then discusses the cost comparison scenarios done in this case study.
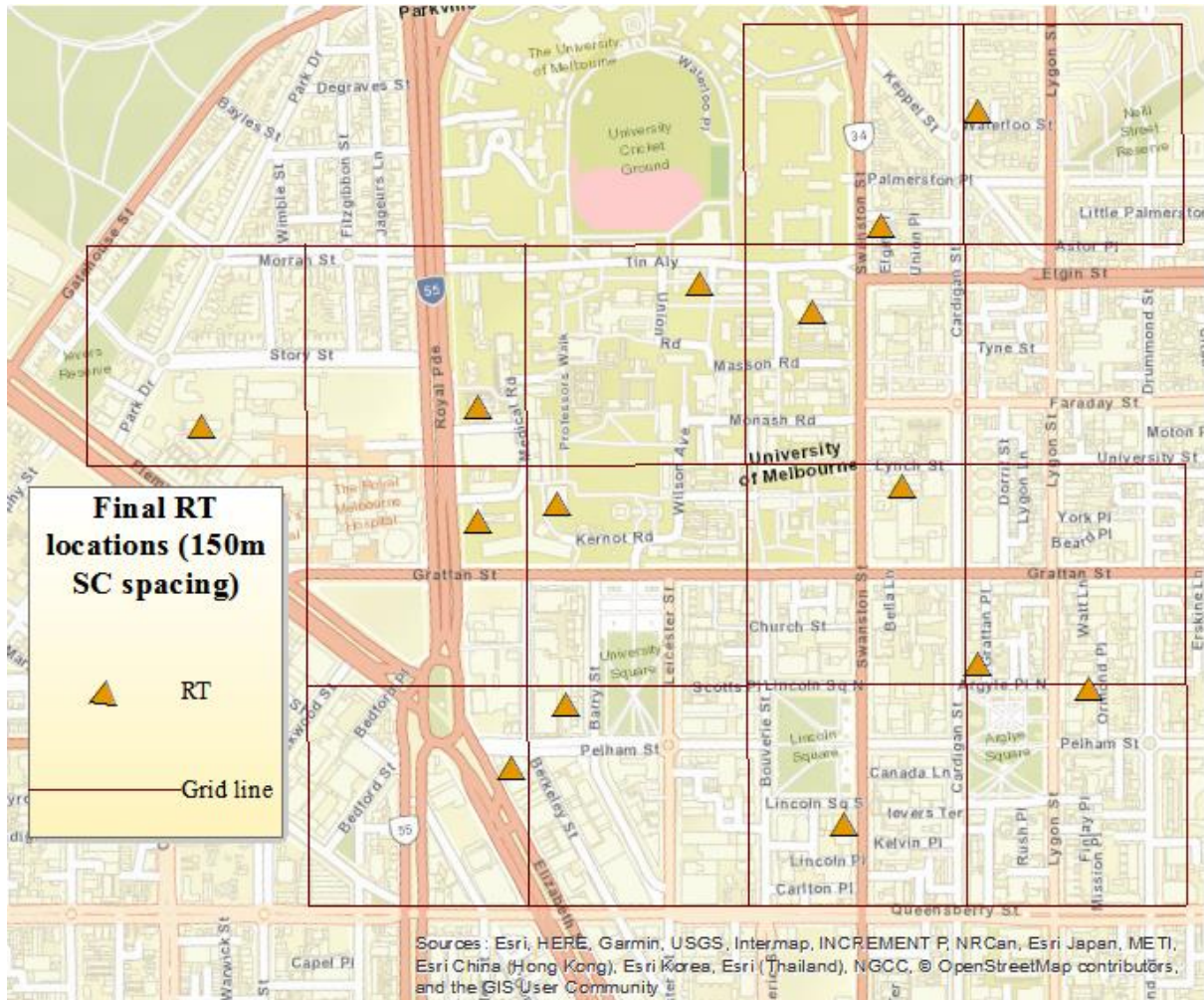
Figure 77: Final RT locations for SC locations placed every 150 m

❖ Cost comparisons for SC locations placed every 150 m

This section discusses cost comparison scenarios for the SCN-GPON optimisation scenarios, where SC locations were placed every 150 m, with a varying number of PON ports in the OLT line card. As previous, cost comparison results were obtained with the following two types of PON port capacity restrictions-

- Number of OLT PON ports 8
- Number of OLT PON ports 4

➢ Number of OLT PON ports = 8

This section elaborates on the cost comparison outcomes obtained for an OLT line card equipment supporting a maximum of 8 ports for PON connections. Again, only fixed optical

split ratios were considered for the splitter types utilised in the framework. It was observed that the cost comparisons presented with very little difference for total network cost related to each split ratio type. Then, for all of the split scenarios, it was apparent that the individual costs for OLT equipment, line card and SC BTS equipment remained constant, while the splitter equipment costs decreased with the increase in split ratio. As before, the number of outgoing connections from each splitter increased with the split ratio's increment, eventually decreasing the number of FAP locations used to house an optical splitter. Again, no linear relation could be established between the fibre cost and the split ratio. The selected fibre routes from each FAP to RT differed for each split scenario based on the split ratio limit. Thereby, the number of FAP locations to be selected will change. Finally, the case study results showed that the 1:8 split ratio GPON formation with the OLT line card supporting 8 PON ports exhibited the least total cost value for a combined generalised SCN-GPON network. The cost comparison chart is provided below in **Figure 78**.
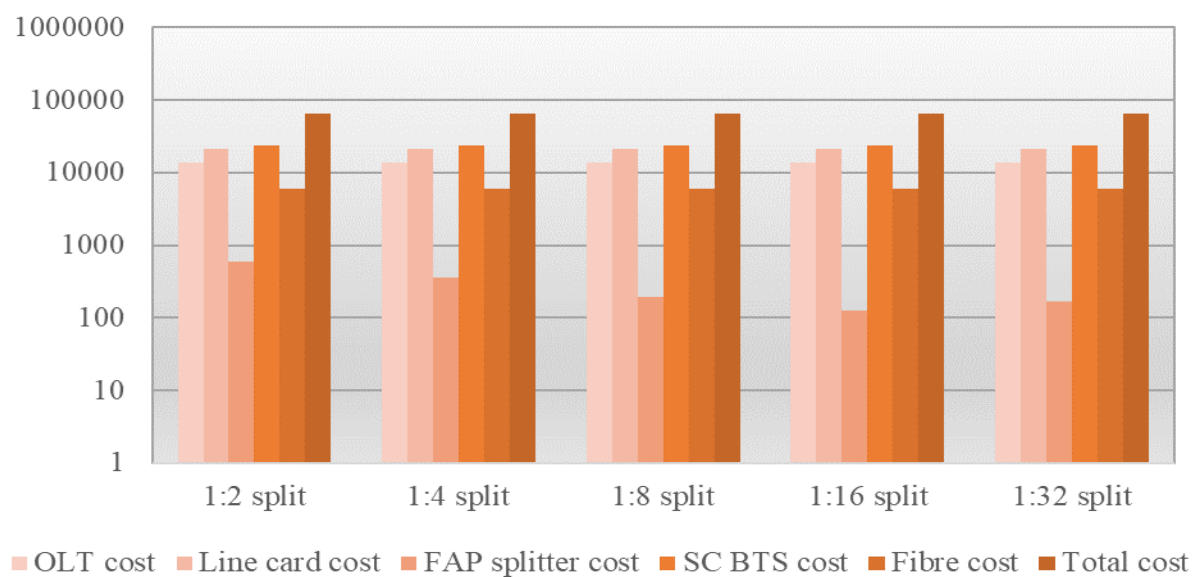
Figure 78: Cost comparisons for 150 m, 8-PON SCN-GPON planning

➢ **Number of OLT PON ports = 4**

The cost comparison scenarios for 4 PON ports presented the same results when the number of PON ports was 8 in the OLT line card. As the potential set of SC locations was set at a higher distance of 150 m apart, a smaller number of potential SC locations existed within the case study area. Additionally, their proximities to the RT locations changed as well, and a smaller number of potential SC locations meant fewer options to select and form the subset of

optimal SC locations within the framework. Here, the SC locations were chosen as optimally distanced from the pre-selected fixed RT locations. Thereby, the framework always resorted to choosing the same SC locations for the same split ratio type, regardless of the line card port limit is 8 or 4. Since the same SC locations were selected for a fixed split ratio type, the fibre routes chosen as links were also considered the same. The cost comparison scenarios are henceforth provided in **Figure 79**.
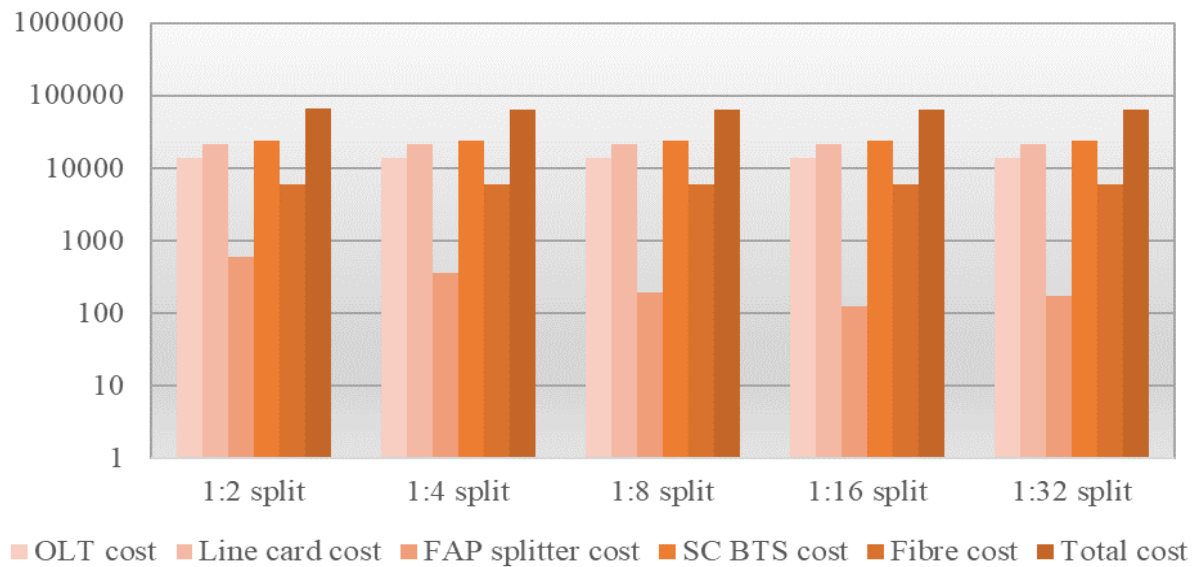
Figure 79: Cost comparisons for 150 m, 4-PON SCN-GPON planning

❖ **Network maps for SC locations placed every 150 m**

This case study's final section was to obtain the optimal network map for the SC locations placed at 150 m distance apart. As previous, the most cost-optimally generated network formation was then compared with the design that yielded the highest total cost in terms of the resources utilised. When observed, the resultant network maps shown in were the same for both 8 and 4 PON ports; therefore, network map examples belonging only to the 8 PON port scenario were discussed. For this case study, the 1:8 network design shown in **Figure 81** had the lowest total cost, while the 1:2 design of **Figure 80** rendered the highest total cost among all the split ratio type network designs investigated. When the designs were observed, both 1:2 and 1:8 scenarios selected the same CO location but different FAP locations. Here, for the optical splitter placement, the 1:2 network chose 7 out of the 11 FAP locations, and the 1:8 scenario selected only 1 FAP location. In this case, multiple splitters were allowed to be

placed in each selected FAP locations. Thereby, the 1:2 scenario had a maximum of 3 splitters chosen for a single FAP location, while the 1:8 scenario used only one splitter for the only selected FAP location within that scenario. Both the scenarios had the same number of RT and SC locations chosen, and as the 1:8 network architecture generated comparatively a less total cost value, it was chosen as the preferred optimal SCN-GPON architecture.

16
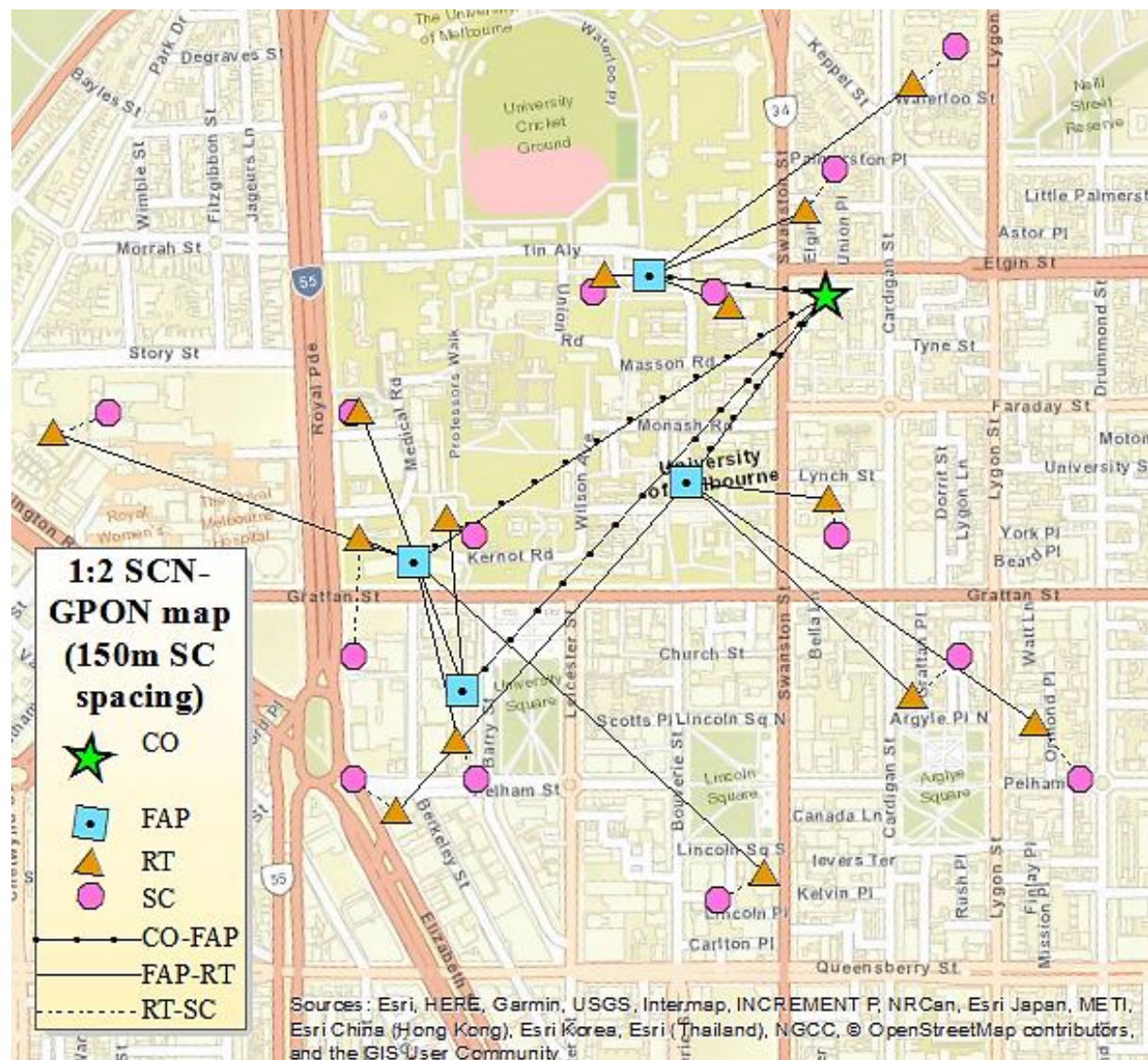
Figure 80: 1:2 combined SCN-GPON network map (Number of PONs = 8)
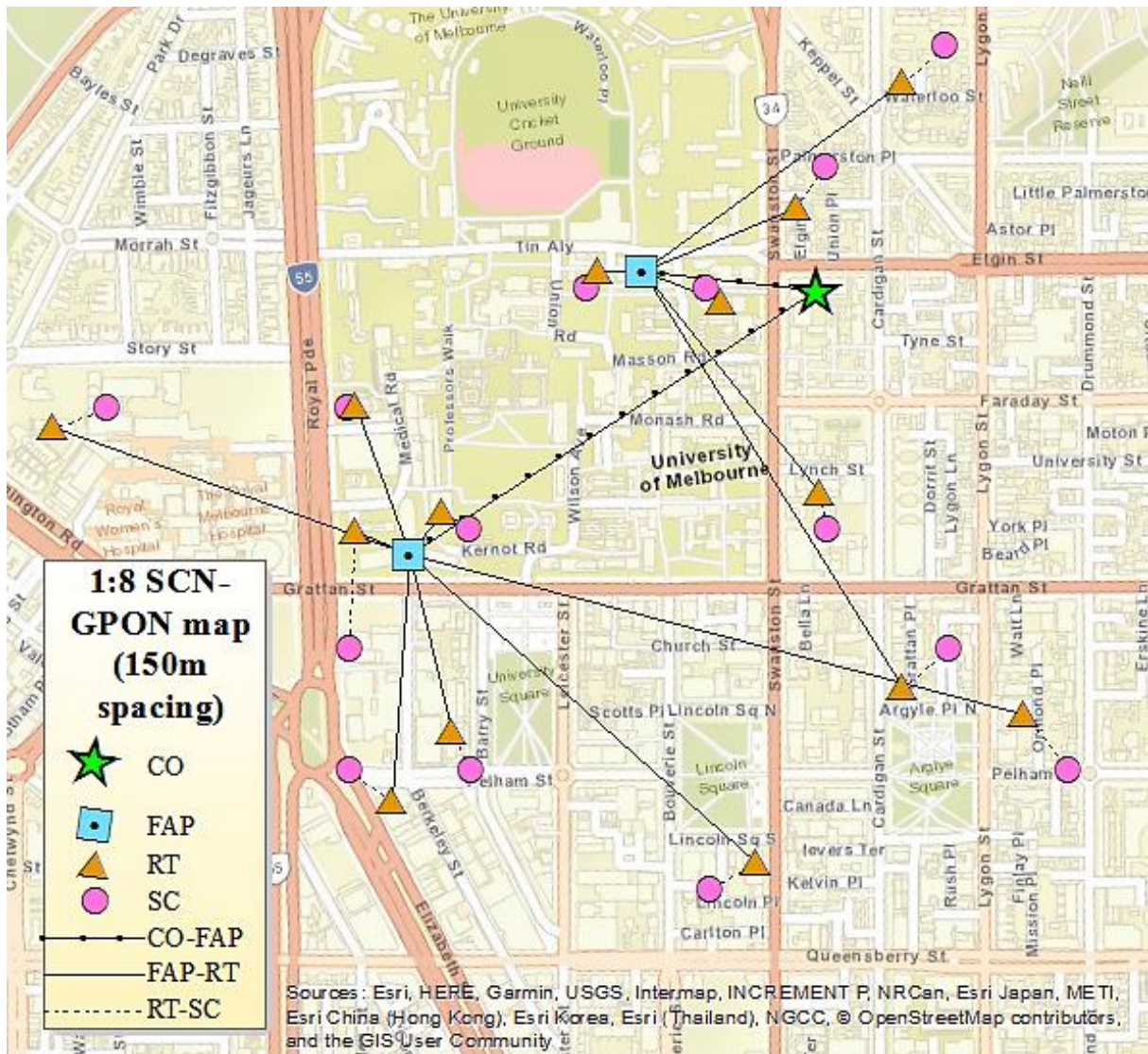
Figure 81: 1:8 combined SCN-GPON network map (Number of PONs = 8)

5.5. Conclusion

This chapter aims to further expand the SCN and backhaul planning process by combining both the SCN and GPON-based backhaul planning within the scope of one single framework. The idea was to offer a more generalised work on optimising such a combined process, regardless of the type of technology used. In this planning process, a set of potential locations were chosen as parameters, from which a subset of SC locations was chosen. These potential SC locations were organised at equal distance from each other, within a terrain grid pattern. The GPON technology was used for backhaul implementation, while the SC location selection was based on its optimal positioning for this proposed backhaul planning. Then both

the processes were simultaneously performed as part of one framework. The GPON technology adopted was tested for the different optical splitters and line cards, and the most optimal formation was selected as the final planned network. Deployment of small-cell networks has been a challenging task all through as it requires an ample amount of planning, testing and implementation methods to apply. Hence, we have already discussed a novel SCN implementation method in **Chapter 3** and a planning process for a backhaul optimisation framework for such an SCN arrangement in **Chapter 4**.

Once again, the GPON backhaul planning process included selecting proper locations for placing GPON equipment such as OLT, optical splitters and ONUs, over existing PtP optical network node locations, e.g., CO, FAP RT locations. The optimisation method was primarily based on CO and FAP locations and a subset of pre-selected RT locations. The RT location was selected by the terrain grid formation containing the potential SC locations, where each of the four potential SC locations was allocated with one RT location each, at an approximate equidistance length. Afterwards, the existing PtP node locations and existing fibre routes were scanned through the optimisation framework to finalise the optimal link and node locations to form the intended backhaul network.

As per **Chapter 4**, again, five different optical splitter ratio categories and two types of PON port restriction in OLT line cards were utilised for planning the GPON backhaul section within the framework. These scenarios were then studied for two different potential SC location arrangements, as these potential locations were considered to be placed at two different equal distances from each other. The cost comparison studies showed that the OLT equipment and line card value remained constant, while the splitter and fibre/wire values varied based on the different case study set-ups. Here, different optical split ratio types and PON port limitations influenced the selection of the FAP locations, and subsequent fibre routes terminated at the SC locations via the RT node level. The studies revealed that either the 1:8 split or the 1:16 split ratio types were the most cost-optimal network arrangements. It was also observed that there were minimal differences among the different split ratio scenarios in terms of total cost values yielded by each network formation obtained through the framework planning process. Proper data plots 0were again generated on a logarithmic scale for displaying the data within a similar standardisation.

We considered both the CAPEX and the OPEX for our proposed optimisation framework, as seen in **Chapter 4**. The primary assumptions, premises, and optimisation methods for the frameworks in **Chapter 4** and 5 are quite similar. Within the framework, it was proposed that new GPON equipment such as OLT, optical splitter, ONU, alongside new BTS components, should be installed at selected locations-respectively at selected CO, FAP, RT and SC positions. These were connected using existing optical fibres and ducts among the existing CO, FAP, and RT locations while using new cables and ducts between the RT and SC node levels. Also, it was observed that for some instances, the number of PON port limitations in the OLT line card had effects on determining the total cost values for different case study scenarios. Then decreasing the maximum number of PON ports from 8 to 4 within a line card affected the fibre routes getting selected within the framework, resulting in slightly higher costs in some instances. The originality of the work can be attributed to proposing a combined optimisation scenario to connect both the SCN and GPON backhaul parts, regardless of the mobile technology standard to be adopted. Thus, the framework is not limited to mobile technology to be utilised. The framework was also expanded from previous works as the coverage area was not fixed to a particular location with a specific fixed coverage area shape for each of the SCs selected and backhauled. Hence, this framework approach can be utilised for any initial SCN planning attempt for any mobile technology to be used. However, following the previous work, envisioning a terrain grid over the case study area for potential SC location arrangement was still maintained. This terrain grid approach was then used to perform the SC location process within the framework, not separately.

In summary, we devised a comprehensive optimisation framework that planned out a more compact optimisation method by incorporating the selection and dimensioning process of both an SCN and its corresponding GPON-based backhaul. This work is a significant expansion to our previous chapter by combining the SCN and GPON planning process within the same framework, irrespective of a particular cellular technology incorporated. This framework can be implemented with any mobile technology and perform future studies on network coverage formation, capacity analysis, and possible signal loss measurements. All these can be done to rectify further the process of determining the network coverage areas for each selected SC location.

This page is left intentionally blank

Chapter 6

5G Small-cell Network planning Framework with Spectrum Refarming Enhancements

6.1. Introduction

The combined SCN-GPON framework proposed in this chapter has enhanced SCN planning with backhaul dimensioning to incorporate both coverage and capacity provisions based on the 5G cellular technology. The framework utilised signal propagation aspects and maximum coverage area restrictions in terms of the 5G network. The aim was to conform to SCN planning coverage on how the population was distributed over the case study area and how the SCN planning would cover such a population when the 5G cellular signal propagation parameters were adopted. Also, the capacity attained by that user population for different data rates in terms of the 5G cellular signal capacity was another aspect for the SCN planning. Hence, only the relevant signal propagation related aspects of the 5G cellular network were considered within our case studies in this chapter, rather than the network's underlying equipment and hardware infrastructure such as the RAN or non-3GPP access network connecting with the 5G core network [124]. Therefore, firstly, SCN locations were chosen based on minimal distance from backhaul nodes, and then, a new design aspect for coverage of population and area was introduced. Here, each SC was able to cover a particular amount of population within a corresponding fixed radius. To do so, first, based on the number of end-users attained by the selected SC location BTS, a frequency was allocated to the cell. Based on that frequency being influenced by surrounding geographic terrain, the cell tower's ability to handle coverage area was studied and determined for signal propagation of each selected small-cell location. This frequency allocation process was performed based on the spectrum refarming method to incorporate the trend of emerging wireless cellular technology, as per the Australian Communications and Media Authority (ACMA) standard in Australia [125]. Hence, we resorted to applying two specific frequencies per the discussion in [125] for the 5G cellular

technology and account for the geographic influences concerning such spectrum refarming propositions.

Furthermore, the framework also selected proper CO, FAP and RT locations to place OLT, optical splitter and ONU equipment. This node selection process was based on proximity to the selected SC locations, alongside the data rate and no. of outgoing connections from each FAP and RT stages, similar to **Chapter 4** and **5**. Again, as per our previous works, the optimisation process within this current chapter utilised a hierarchical system of network node locations as inputs. As an outcome, the framework would determine the positions for installing GPON network components for our intended backhaul planning. Therefore, in addition to the potential SC locations, other parameters that served as input data were existing locations of RT, FAP and CO, and existing fibre links connecting them. For the final part of the framework, population data blocks over the said case study area and their corresponding distances from each SC were also included as input parameters.

As we look back into previous **Chapters 3**, **4** and **5**, the primary aim was to determine the SCN planning framework and then dimension a backhaul layout for the planned SC. For the first work in **Chapter 3**, a framework was proposed for determining a novel small-cell planning method. It was done based on studying the influence of surrounding geographic terrain over the case study area. The framework selected the most effective locations for placing the SC equipment. It also maintained the maximum number of cells per square km area and established proper coverage for each selected SC location. It also showed that the 4G MAPL limit was maintained for signal loss reduction. In terms of the work presented in **Chapter 4**, the concept was to expand the SCN planning further to incorporate designing a GPON-based backhaul network. To utilise better available information, the case study area chosen in **Chapter 4** was different from that of **Chapter 3**; however, the SCN planning process performed was the same. Afterwards, a GPON-based backhaul network was envisioned over the case study area where the SCN was planned through the CFLNDP optimisation method. The optimisation was done to offer cost and energy minimisations by utilising the existing optical network resources and installing new low-cost GPON equipment.

As for **Chapter 5**, the work proposed was focused on building a more generalised framework involving small cell network planning. The idea was to build an optimisation framework, select small cell locations from a set of potential geographic points, placed at equal

distance from each other over a terrain grid formation. The framework was similar to the work presented in **Chapter 4** as it followed this same facility location optimisation problem to pinpoint the network node locations. This work could be linked back to the previous optimisation works as it retains the facility location problem. Additionally, it can also use the calculation method for a signal loss profile to determine the optimised SCN part's coverage pattern as future expansion. However, the difference was that the current framework would optimise both the front end SCN and the GPON backhaul in one single framework, regardless of the mobile technology to be adopted.

6.2. Related works

The following theoretical studies can construct the foundation of our research work performed for this chapter, as discussed below-

- Cost, capacity, and coverage optimisation on SCN backhaul
- 5G small-cell path loss calculation methods

6.2.1. Cost, capacity, and coverage optimisation

One of the primary conditions of the cellular communication network and backhaul planning is to ensure the appropriate serving of coverage and capacity within a particular region while implementing such a network. Thereby, we look at some prior studies relevant to the work we envisioned and implemented to propose a novel heterogeneous framework. This framework was planned based on cost, capacity and coverage optimisation of small-cell and corresponding backhaul optical network.

The study done in [126] proposes cost optimised architectures for a 5G mobile core network, with Network Functions Virtualization (NFV) and Software-Defined Networking (SDN). These factors contribute to optimising 5G networks for cost minimisation, deployment flexibility and network scalability enhancement. In this work, the authors formulate three simulation models for the optimal dimensioning and planning of a 5G mobile core network. It was based on SDN and NFV in terms of network load and data centre resources cost. The suggested models show optimal positioning of 5G cellular network core cloud infrastructure or data centres and the optimal mobile core network divergence between SDN and NFV. The optimisation solutions project the trade-offs between the different data centre deployments,

whether they were centralised or distributed, and the different cost elements, i.e., optimal network load cost or data centre resources cost. They proposed a Pareto optimal multi-objective model that achieves a balance between network and data centre cost, albeit showing an unequal relationship between inputs and outputs. Although this study perpetrates to cost optimisation of core 5G cellular network architecture, which is similar to our aimed study approach in this chapter, there is a difference in persistence. For example, we look at the actual position of the SCN formation for a 5G cellular architecture in terms of their geographic positions and corresponding distances. Such positions should be near the vicinity of an existing optical network, which should serve as the background for our proposed backhaul architecture for the optimal SC locations.

Coverage optimisation: The work [127] by Ranaweera et al. demonstrates that a small-cell backhaul network based on an existing optical fibre infrastructure can be designed in a cost-efficient manner, despite the fibre resources being sporadically placed. This framework also ensures that such a small-cell backhaul architecture's coverage and capacity are met accordingly, as per the network requirements, on a suburban geographic area. In network optimisation, specifically for data and communication networks, it is of utmost importance that the number of users within a network area be served optimally with the available network resources. Thereby, based on the maximal coverage problem [63], appropriate constraints were applied to an optimisation framework to solve the coverage and capacity needs within a small-cell backhaul network planning study [127]. In this study, the researchers first aimed to select potential small-cell locations, where small-cells were considered to be placed on a light pole near a road intersection. The reasons for choosing such a location pertained to the fact that light poles' height would match that of a small-cell antenna, and such a location would have direct access to utility power. The cost components in this study were primarily related to the deployment of fibre routes.

The small-cell was assumed to have direct P2P fibre connectivity with an existing fibre access point. Since the study proposed new fibre deployments, the costs for fibre installations and new fibres were included within the framework's scope. The framework implemented user population coverage within its constraints to ensure that it is less than the intended small-cell radius within a fixed distance. Also, all households having a population value attached were covered by the selected small-cell locations. The provision of meeting the capacity requirement was also included in the framework, using a separate constraint, which depended on the per

small-cell capacity and the per-user average capacity requirement. The study showed that total network deployment cost increased significantly when both coverage and capacity provisions were incorporated within the framework. The deployment cost increased almost two times than that when only coverage requirements were included in the framework. It occurs as more small-cell BTSs were required to meet both the coverage and capacity requirements compared to when only coverage meeting requirement was considered. The study asserted that even additional capacity requirements related to hot-spot coverage could also be met by modifying the framework accordingly. Hence it was evident that such a framework can be implemented in diverse deployment scenarios. There is a significant difference between this work and our envisioned framework. For our work, we would be incorporating the aspect of spectrum refarming and corresponding parameters/constraints into our SCN optimisation section, which has not been within the scope of this work mentioned above.

6.2.2. 5G small-cell path loss calculation methods

Since we are focused on 5G cellular technology, the purpose was to focus on a particular path loss method. It would then be used to calculate the coverage radius limit, based on the corresponding MAPL of 150 dB [128] as the maximum path loss restriction for the 5G cellular technology. Besides, we again decided to address the geographic properties within our optimisation framework development process. Hence, we opted to base our calculation process on a path loss calculation method that explicitly incorporated geographic terrain slope aspects. We considered the path loss models for our radius calculation as the Fujitani model for Mobile Propagation Loss Correction Formula for a Slope Terrain Area [129] and the Ericsson path loss model [130]. The purpose was to combine both these models, account for geographic influence over 5G cellular signal propagation, and then calculate the maximum coverage radius for a selected SC location. It was done so that a selected SC location could offer proper signal propagation to a receiver without further degrading the signal propagation levels than the 5G MAPL level. Below discussed are our preferred 5G path loss calculation models to be utilised in this chapter-

- Ericsson 9999 model
- Fujitani model

❖ Ericsson 9999 model

The Ericsson model [130] has been modified and extended from the Hata path loss model [103], intended for operation within the 150-1500 MHz (1.5 GHz) cellular frequency range. It incorporated some parameters that could be fitted depending on the geographic propagation environment, e.g., urban, suburban and rural areas. As we have seen previously, that Hata model can be applied for microcell scenarios [57], making the Ericsson model fit the small-cell scenario. Hence, the Ericsson model is applicable for both 5G frequency small-cell signal propagation over urban geographic areas, making it more fitting for our case study. The Ericsson 9999 model incorporates the following parameter values for different geographic scenarios-

Table 2: Ericsson 9999 model geographic parameters

	a_0	a_1	a_2	a_3
Urban	36.2	30.2	-12.0	0.1
Suburban	43.20	68.93	-12.0	0.1
Rural	45.95	100.6	-12.0	0.1

The above parameters are then incorporated within the following equation-

$$PL(dB) = a_0 + \left[a_1 \left\{ \log_{10}(d) \right\} \right] + \left[a_2 \left\{ \log_{10}(h_b) \right\} \right] + \left[a_3 \left\{ \log_{10}(h_b) \right\} \left\{ \log_{10}(d) \right\} \right]$$
$$- \left[3.2 \left\{ \log_{10}(11.75 h_m) \right\}^2 \right] + g(f) \tag{60}$$

where,

$$g(f) = 44.49 \log_{10}(f) - 4.78 \left\{ \log_{10}(f) \right\}^2 \tag{61}$$

and,

d = Distance between transmitter and receiver (m)

h_b = Base station antenna height (m)

h_m = User terminal antenna height (m)

f = Frequency (MHz)

❖ Fujitani model

Another model that we incorporated within our case studies was the Fujitani model [129] to further bolster the aspect of geographic terrain in terms of terrain slope effects between the SC transmitter and receiver. This model introduced the path loss difference K_s (dB) element for the elevation angle θ_m (mrad) between the SC transmitter and receiver. Here, a sizable elevation angle towards the measurement point should be on the slope's elevated height point. Hence, the correction value to reduce the urban path loss should also be significant for such a scenario. The Fujitani slope model is as follows.

$$K_s\left(dB\right)=0.0186\theta_m\left(mrad\right)+16.13 \tag{62}$$

The following section introduces our 5G SCN-GPON planning discussion, covering the planning methodology and the corresponding mathematical model.

6.3. 5G SCN-GPON planning overview

This section overviews the spectrum refarming-based SCN-GPON optimisation framework planning process. This planning approach intends to provide a complete generalised framework that offers to consolidate the planning of both a 5G technology-based SCN and its corresponding GPON backhaul. Then to incorporate aspects of allocating appropriate 5G small-cell frequencies based on the coverage and capacity constraints. The methodology of the framework and its implementation is described below-

- Spectrum refarming-based SCN-GPON optimisation framework methodology
- Mathematical model of the spectrum refarming-based SCN-GPON optimisation framework

6.3.1. 5G SCN-GPON planning methodology

This section elaborates on the following components of the combined 5G SCN-GPON framework-

- Optimisation framework area grid formation
- Population distribution over the case study area
- Selection of 5G frequency types
- Coverage area considerations
- Population capacity targets for different data rates
- Assigning appropriate 5G frequency to each SC
- Setting SC bandwidth restriction
- Imposing optical network standard restrictions
- Assigning RT data rate limit by GPON split ratio

❖ Optimisation framework area grid formation

To maintain coherence with our previous works and ensure the availability of the proper data, we decided to continue with the same University of Melbourne Parkville campus area as our intended case study premises. Additionally, this area is an urban cellular propagation region, with the frequent presence of building blocks, and a high population density, hence still relevant for case study approaches discussed within this chapter. Continuing from the previous works, we move to a more particular cellular technology to be used in this chapter, the 5G mobile communications. Alongside this, we incorporate crucial network requirements such as capacity and coverage provisions within the framework to propose a more independent network planning architecture. As before, both the SCN and GPON selection processes were incorporated through the same optimisation framework. However, additional aspects of population coverage within a particular radius of each selected small-cell were included in the process and maintaining the capacity for different cellular frequency and data rates within the 5G technology. We continued using the rectangular terrain grid formation over the case study area as part of the framework design process. It was done again to acquire a set of potential SC locations placed in an equidistance manner, also identifying the building locations of the Melbourne University campus were mapped within this terrain grid. The building locations were important for two purposes-they can contain users most concentrated within a coverage area and act as participating nodes within the P2P campus optical network for planning the GPON backhaul. This framework was significantly different from the previous works regarding selecting both the geographical SC locations and corresponding backhaul nodes and link routes. Here, the SC locations were chosen by two aspects. Firstly, based on their desirable

proximity from the underlying PtP optical network of the case study area. Secondly, they can offer the most cost-optimal SC locations that maintained the coverage area restriction. It was also provisioned that they could maximise the population being covered within their respective cell coverage area.

Additionally, the small-cells chosen could assign appropriate frequencies to themselves, based on the amount of user population covered by each small-cell, for different fixed data rates allowed to per-user within their respective cell area. We used the set of potential SC locations at a 100 m distance from each other for this case study, forming the intended terrain grid, as shown in **Figure 68** of **Chapter 5**. Again, no fixed cell area shape concept over the case study area was applied; however, the maximum distance for each SC to provide coverage over the geographic area was maintained for coverage mapping purposes. Moreover, we introduced a concept called the "population block" within our framework. For this, the intended terrain grid over the case study area has been further divided into $50\,\text{m} \times 50\,\text{m}$ blocks of equal dimensions, as shown in **Figure 82** below. Here, each such area would have a population value attached to approximate the need for mobile data usages for the intended end-user population distribution over the case study area. Details of this approximation process are mentioned in a separate section below.
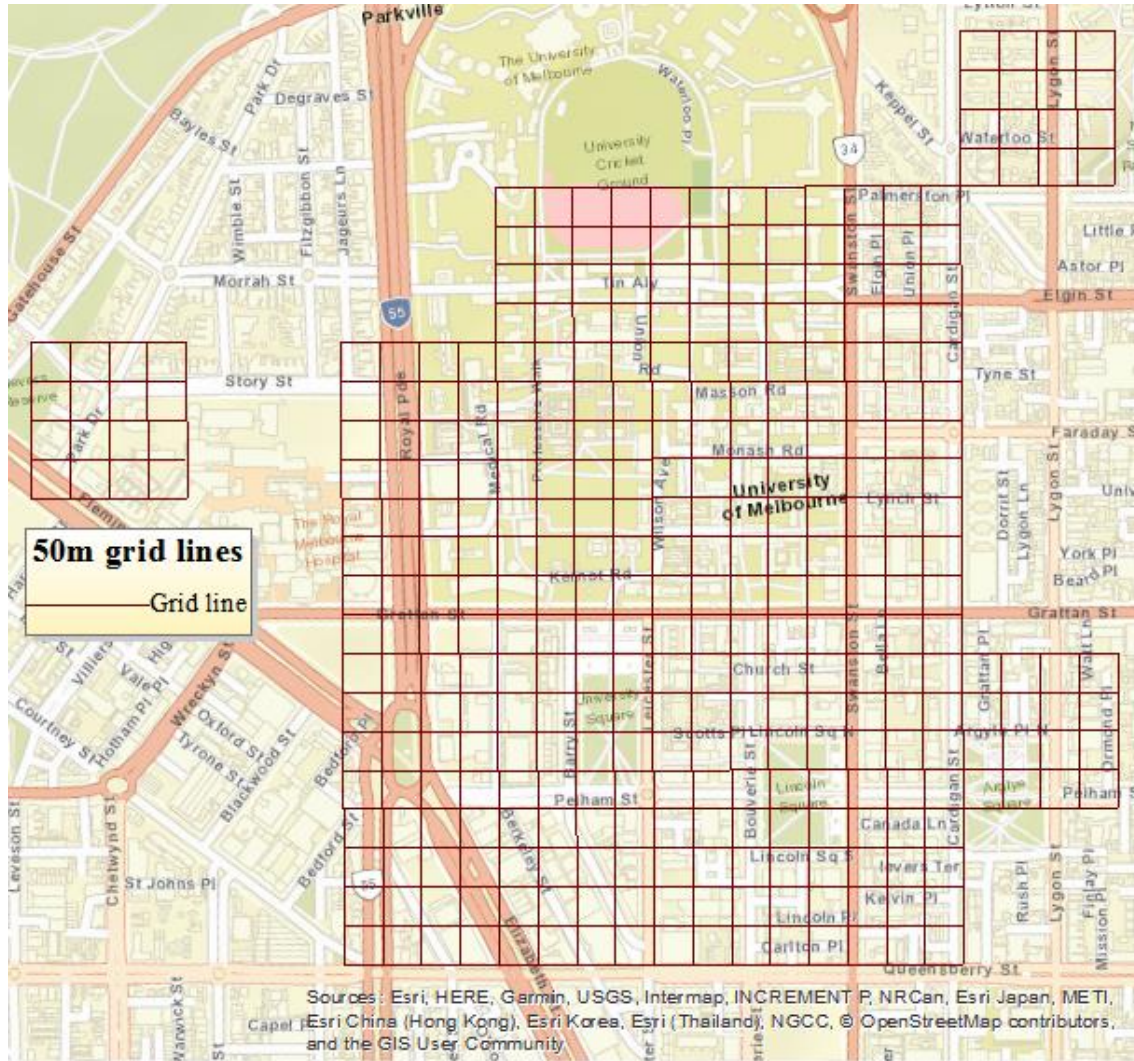
Figure 82: Terrain grid divisions to indicate population area blocks

❖ Population distribution over the case study area

This section focuses on one of the primary design considerations for this chapter: population distribution over the case study area. It included the prospect of coverage optimisation by each small-cell location, based on the population it could cover within a fixed SCN coverage area. To achieve this, first, the terrain grid over the case study region was divided into an equal dimension of 50 m $\times$ 50 m area blocks. These blocks each had a population value associated with them; hence we would term them "population block" in this chapter. Each population value associate with each population block was a fraction of the total estimated population over the case study area, and this association was a random approach. The purpose was to see that for each selected SC location, how many blocks of the user

population could connect to it, e.g., how much population could be covered by each such SC location. It can be aligned with the basic idea of the CFLNDP method [114], which we used as a basis of our proposed optimisation method, where the small-cell locations would be equivalent to the facility locations to be located within the CFLNDP method. The population blocks can then be the demand nodes to which each selected facility in a chosen location connects, based on its maximum capacity. The purpose of this would be to ensure maximum user coverage with the mean of handling their data consumption capacity. A heat map had been superimposed over our original terrain grid formation, previously shown in **Figure 82**, to display the population distribution over the said case study area. It then resulted in the visual representation, as shown in **Figure 83** below.
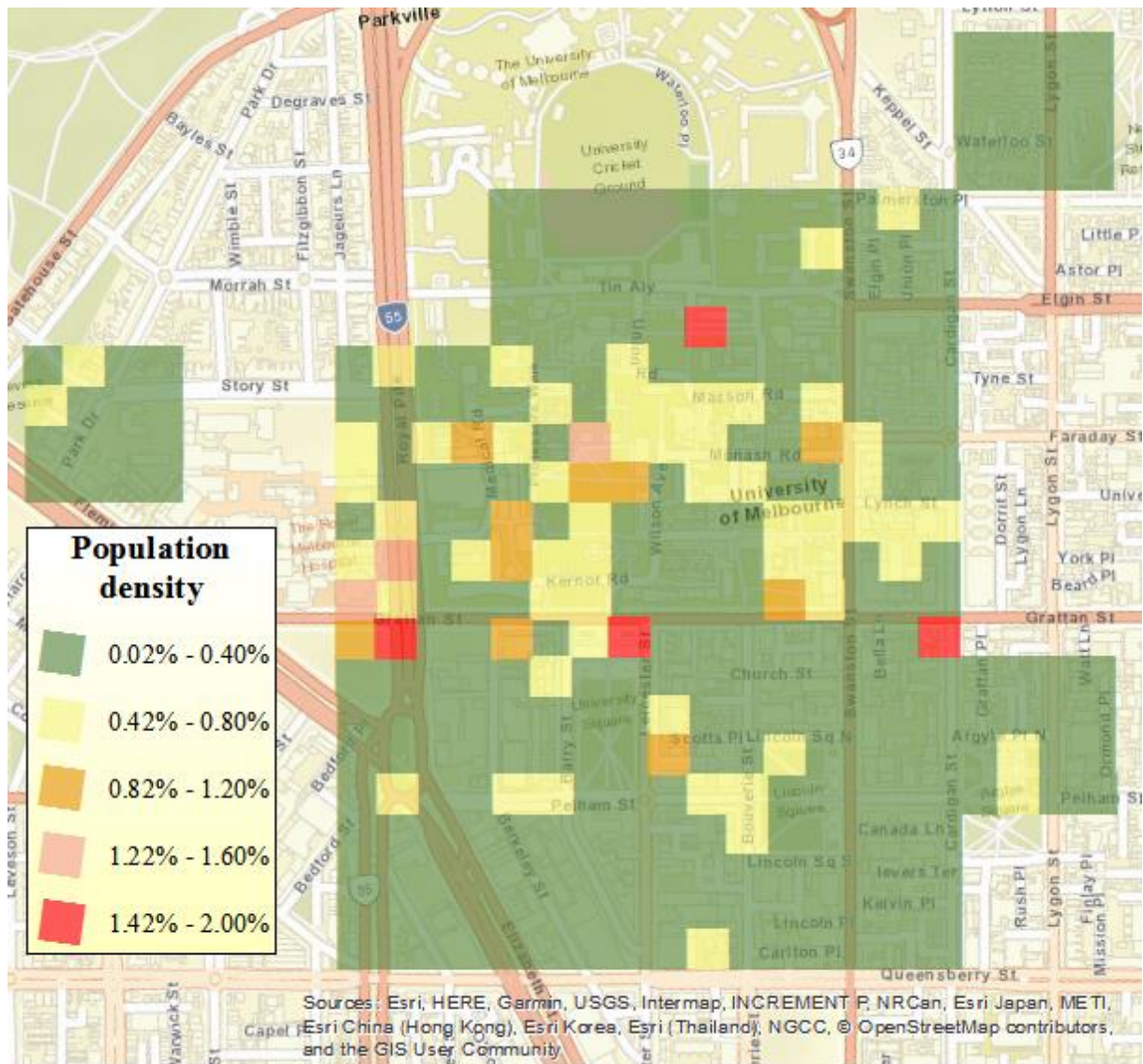
Figure 83: Population distribution over the case study area

❖ Selection of 5G frequency types & data rates

Since we aimed to build our framework based on 5G technology, we decided to choose the frequency rates based on Australian needs. Hence, as per the ACMA standard in Australia [125], the current focus of 5G technology implementation for cellular communications is on utilizing 1.5 and 3.6 GHz radio frequency spectrum bands. The typical usages of 1.5 GHz and 3.6 GHz bands are utilised in satellite [124] and military services [130]. These frequencies are also considered good candidates for frequency refarming purposes [125]; hence we have chosen them as our preferred frequency types to be implemented within our framework. We also considered per-user data rates of 1, 2, 5, 10 and 15 Mbps for mapping our capacity needs for this framework within an urban cellular propagation scenario, e.g., university campus. Different data rates were chosen to approximate different data usage scenario for the same population distribution. In future, higher data rates can be utilised as parameters to investigate different capacity demand scenarios further.

❖ Coverage area considerations

To determine the amount of coverage attainment ability for each selected SC location, we want to implement a coverage area restriction for our framework. The idea was to determine how much maximum path loss a selected SC location can tolerate before the propagated SC signal degrades down to an unacceptable receiving level. We previously incorporated the influence of geographic terrain over SC signal propagation in our work of **Chapter 3**. It was done by calculating the amount of path loss due to the terrain slope between the SC antenna's transmission point towards a receiving point, e.g., user equipment. For that work, we incorporated a modified Hata model version [57] to determine the path loss from the SC location towards the edge of a fixed coverage area for 4G cellular technology. For this chapter, we aimed at SCN planning for 5G technology, without the restrictions of a fixed coverage area shape. However, we would incorporate the maximum propagation area restriction for an SC to be calculated based on an appropriate 5G signal loss formula. Hence, we would incorporate the above Ericsson [130] and Fujitani [129] models together to calculate the signal loss for selected 5G carrier frequencies, integrating terrain slope influences as well, for our intended SCN planning aspects. For this SCN planning, we would determine the maximum coverage distance a selected SC can allow through reverse calculation from the MAPL value for 5G technology

[128], using the combination of the above formulae. Hence, we would aggregate the above models into the following equation, by combining the following equations-

$$PL(dB) = a_0 + \left[a_1 \left\{ \log_{10}(d) \right\} \right] + \left[a_2 \left\{ \log_{10}(h_b) \right\} \right] + \left[a_3 \left\{ \log_{10}(h_b) \right\} \left\{ \log_{10}(d) \right\} \right]$$
$$- \left[3.2 \left\{ \log_{10}(11.75 h_m) \right\}^2 \right] + g(f) \tag{63}$$

and,

$$K_s(dB) = 0.0186\theta_m(mrad) - 16.13 \tag{64}$$

We then generated the following form of the equation of total path loss and calculated the maximum coverage distance to be incorporated into our SCN planning-

$$PL_{total}(dB) = PL(dB) - K_s(dB)$$
$$\therefore PL_{total}(dB) = a_0 + \left[a_1 \left\{ \log_{10}(d) \right\} \right] + \left[a_2 \left\{ \log_{10}(h_b) \right\} \right] + \left[a_3 \left\{ \log_{10}(h_b) \right\} \left\{ \log_{10}(d) \right\} \right]$$
$$- \left[3.2 \left\{ \log_{10}(11.75 h_m) \right\}^2 \right] + g(f) - 0.0186\theta_m(mrad) - 16.13$$

(65)

❖ Population capacity targets for different data rates

We aimed to see how much total capacity for each selected SC location could be attained for specific data rates when it attempts to cover a certain fraction of the said population. Thereby, based on the total attained capacity by each selected SC, an appropriate frequency type would be assigned by the framework. It pertained to direct implementation of the MCLP optimisation method [63], in light of network coverage target, similar to that performed in the work of Ranaweera *et al.* [127]. In this context, a population capacity attainment meant that a selected small-cell could connect to a particular population block(s) situated within a coverage area radius from the said small-cell.

❖ Assigning appropriate 5G frequency to each SC

Because we aimed at envisioning an optimisation scenario for the 5G cellular technology, we needed to set constraints for our framework regarding the physical aspects of 5G itself, e.g., set a particular frequency associated with each selected 5G SC BTS, to serve the coverage and capacity requirements of the framework better. Hence, based on the maximum

data capacity and the maximum coverage distance attained by a selected SC, a particular frequency, either 1.5 or 3.6 GHz, would be assigned to selected SC BTS. For example, a selected SC location may connect with a fixed number of people, using a fixed data rate and cover this population until a fixed geographic distance. If all these conform to a particular SC frequency, that frequency would be assigned to that SC location to install an SC BTS at that selected location. It could lead to a trade-off scenario, as sometimes, the distance covered by an SC to connect with a fixed number of population may not follow the parameters for one particular frequency. Hence, unless all the constraints are met, the framework would continue to search for suitable FAP, RT and SC locations to cover 100% of the case study area population.

❖ Setting SC bandwidth restriction

The maximum bandwidth capacity of each SC BTS was set at two different capacity limits for the 1.5 and 3.6 GHz frequencies to conform with the physical limitations of small-cell SC BTS standards. This process was based on the targeted 5G LTE spectral efficiency per MHz signal. The estimated 5G spectral efficiency is 10bps/Hz in a frequency channel [131], and possible 5G channel bandwidth can be up to 400 MHz [132]. So, based on these two quantities, we calculated two different maximum capacities of the SC BTS, for the 1.5 and 3.6 GHz frequencies, at 900 Mbps and 1250 Mbps, respectively. Each SC's total capacity would be the per-user data rate multiplied by the no. of users connecting with the SC. Once an SC reaches the maximum allowable capacity limit for a particular frequency and particular data rate, it would stop connecting with any more users. Instead, the framework would select other suitable SC locations to connect with the remaining user population, eventually covering 100% of the users within a specific area for a fixed frequency and corresponding data rate.

❖ Imposing optical network standard restrictions

As per our previous works, we continued placing multiple optical splitters in each selected FAP location to connect to the next stage of nodes, the RTs. It was done in the same context as before, e.g., to create more available locations to place the splitters, thus optimising existing node locations to have more potential positions to place GPON equipment. Again, we applied one fixed split ratio restriction while determining FAP locations to place optical splitters within each optimisation result scenario. As seen in **Chapter 4**, a fixed split ratio

option would offer better cost optimisation than that of the variable split ratio for each different selected splitter locations. As we know, the split ratio limits the number of outgoing fibres from the FAP towards multiple RT locations in the next stage to maintain the reliability of the GPON connectivity [6]. Hence, for this chapter, we employed three types of split ratios-1:2, 1:4 and 1:8, and different data rate per-user scenarios, which ultimately increased the number of different case study situations. We again selected a line card for our case study, based on the fixed number of PON ports it can support [6], e.g. we considered two number of PON ports-4 and 8 [119]. Again, it was imposed to limit the number of outgoing fibre connections from the OLT placed in CO location(s) towards the next stage of FAP locations with the optical splitters [6]. It would allow maintaining the data bandwidth provisions per line card connection from OLT.

❖ Assigning RT data rate limit by GPON split ratio

As we continued with the 10GPON system [6] as our underlying technology for the intended backhaul planning for the SCN network, we maintained the GPON parameter approximations similar to **Chapters 4** and **5**. Following that, another constraint applied to the framework optimisation process was to limit the maximum data one RT can handle. It was corresponding to the total data bandwidth covered by all the SCs connected under each RT. This restriction for maximum RT data handling limit depended on the chosen split ratio and maximum data capacity for the GPON system within our framework. For example, within our 10GPON system, the maximum data rate would be 10Gbps [62]. Hence, for example, a 1:4 split ratio was applied for the optical splitter placement. It meant that each optical splitter set at the FAP location before the RT level in an optical network hierarchy would have four outgoing fibre connections. As a result, each selected RT would allow for a maximum of 10 Gbps/4 = 2.5 Gbps of data rate for the remaining network nodes, setting a restriction on data rate handling for such nodes.

6.3.2. 5G SCN-GPON planning implementation

Like the combined SCN-GPON architecture development process, this chapter also aimed to develop another combined optimisation framework, however adopting the parameters of a particular cellular technology type and expanded constraints. This section thereby would describe the mathematical model applied to develop the said optimisation framework. This

framework has been aimed to address more real-life aspects of a combined 5G SCN-GPON planning. Thereby, the framework integrates both coverage and capacity attainment along with achieving cost minimisation. The implementation process thereby includes the following stages-

- 5G SCN-GPON planning parameters
- 5G SCN-GPON planning variables
- 5G SCN-GPON planning objective function
- 5G SCN-GPON planning constraints

❖ 5G SCN-GPON planning parameters

Following the same approach as **Chapters 4** and **5**, the GPON optimisation part of the framework comprises Link and facility cost components, as parameters, for the first three network nodes, e.g., CO, FAP and RT node levels. The link cost components were considered for the distribution and feeder fibres and were based on OPEX of the utilised existing optical network fibres. Since GPON components such as OLTs, optical splitters and ONUs would still be laid out as new components, their costs were counted towards the facility costs seen in each corresponding node levels. Ultimately, cost parameters associated with the node levels mentioned above influenced the following segment of 5G SCN and the subsequent frequency refarming optimisation. As before, we applied the same cost parameters as previous chapters for the link and facility cost calculation purposes to maintain continuity of information applied within our research. Moreover, the set of CO, FAP, and RT node levels was given identifier indices to organise them within the relevant locations accurately.

Additionally, per previous **Chapters 4** and **5**, the 5G SCN optimisation part of our framework would involve cost components for an existing PtP optical network. The link cost components were considered only for the drop fibre section to be installed. Thereby, the CAPEX of the drop fibre equipment would suffice. Again, new components such as BTS equipment installed at SC locations would have their costs counted towards the facility cost seen in each corresponding node level. Ultimately, cost parameters associated with that SC BTS installation had influenced the 5G SCN planning section of the optimisation framework premises and the subsequent frequency refarming optimisation. As before, link and facility cost parameters were recorded for calculation purposes, alongside a minor transportation cost

segment (the SC equipment cost segment) to maintain continuity of information applied within our research. Additionally, the set of SC and terrain block (TB) node levels were given identifier indices and organised within a set of locations. All associated optimisation parameters for our SCN-GPON optimisation framework would be given as below.

CO = The set of CO locations where $|CO| = N_c$

FAP = The set of FAPs where $|FAP| = N_f$

RT = The set of RT/ONU locations where $|RT| = N_r$

SC = The set of potential SC locations where $|SC| = N_s$

TB = The set of potential RT locations where $|TB| = N_t$

N_c = Number of total CO locations (Capacity at CO stage)

N_f = Number of total FAP locations (Capacity at FAP stage)

N_r = Number of RT/ONU locations (Capacity at RT stage)

N_s = Number of potential SC locations (Capacity at SC stage)

N_t = Number of population TB locations (Demand at TB stage)

N_p = Number of PONs per line card

M = Big M integer for conditional operations

e_{15} = Cost of 1.5 GHz frequency SC BTS equipment

e_{36} = Cost of 3.6 GHz frequency SC BTS equipment

e_r = Cost of OLT rack

e_{sh} = Cost of OLT shelf

e_{cc} = Cost of OLT control card

e_{lc} = Cost of OLT line card

e_{fsp} = Cost of an optical splitter

e_{spl} = Cost of fibre splicing

e_{onu} = Cost of ONU equipment

i_{rsfib} = Drop fibre per meter installation CAPEX

i_{scins} = Cost of labour for SC BTS installation

fi_{cf} = Feeder fibre per meter installation OPEX

fi_{fr} = Distribution fibre per meter installation OPEX

R_f = Split ratio

d_{max} = Maximum transmission distance

d_{cf} = Distance of each feeder fibre

d_{fr} = Distance of each distribution fibre

d_{rs} = Distance of each drop fibre

q_{cf} = Feeder fibre per meter OPEX

q_{fr} = Distribution fibre per meter OPEX

q_{rs} = Drop fibre per meter CAPEX

❖ 5G SCN-GPON planning Variables

This framework would discuss the corresponding decision variables as we are considering both the GPON and SCN sections. Again, we focused primarily on the link and facility cost components, with a minor transportation cost segment discussed in the framework's SCN segment. As we were still resolving a MILP optimisation problem, the

variables tended to be both integer and binary types, aligned with the existing PtP network node variants. It corresponded to the facility location selection part of our intended optimisation problem. Therefore, similar to the previous chapters, node locations within the existing PtP premises had been leveraged to dimension the GPON backhaul. These locations would be chosen as facilities to contain the necessary equipment that would allow the formation of the GPON. Hence, again selected CO locations would house OLTs, ethernet switches, and in-house fibre connecting equipment to form the OLT section of the proposed GPON. It would provide connectivity to the next level of GPON nodes, using multiple direct links established through feeder fibres. As before, FAP level nodes were selected to contain optical splitters based on fixed split ratio provisions connected with the selected OLT nodes. Finally, the selected FAP locations were connected with designated RT locations, housed the ONU equipment, and signified the GPON network's boundary perimeter. The FAP-RT level connectivity was acquired through the usage of distribution fibre to establish multiple links. The detailed connectivity process has been already described in **Chapters 4** and **5**, hence not re-discussed here. We also focus on the variables applied within the 5G SCN optimisation part of our framework. Again, we focused primarily on the link and facility cost components, with a smaller transportation cost segment discussed in the framework's SCN segment. As before, for our MILP implementation, both integer and binary variable types were considered. Here, the RT-SC level connectivity was implemented using drop fibre and multiple links, similar to the higher-level hierarchy of the GPON part discussed before. Following the same methodology described in **Chapters 4** and **5**, the RT-SC wired connectivity between newly established ONU and BTS equipment, respectively, was achieved. Also, we include aspects of the SC-TB connectivity, which translated to the wireless connectivity between the SC BTS and suitable terrain area blocks containing the user population. Thereby, as before, the following integer and binary variables were considered within the GPON optimisation part-

I_{cf} = Number of CO-FAP connections (Demand served by CO stage)

I_{fr} = Number of FAP-RT connections (Demand served by FAP stage)

I_f = Number of FAP splitters (Demand served by FAP stage)

I_r = Number of RT ONUs (Demand served by RT stage)

N_{lc} = Number of line cards at OLT stage at CO location (Demand served by FAP stage)

$$O_c = \begin{cases} 1; \text{ if the } c^{th} \text{ CO is selected to place OLT equipment} \\ 0; \text{ otherwise} \end{cases}$$

$$S_f = \begin{cases} 1; \text{ if the } f^{th} \text{ FAP is selected to place splitter equipment} \\ 0; \text{ otherwise} \end{cases}$$

$$P_r = \begin{cases} 1; \text{ if the } r^{th} \text{ RT is selected to place ONU equipment} \\ 0; \text{ otherwise} \end{cases}$$

$$X_{cf} = \begin{cases} 1; \text{ if the } c^{th} \text{ CO is connected to } f^{th} \text{ FAP splitter} \\ 0; \text{ otherwise} \end{cases}$$

$$X_{fr} = \begin{cases} 1; \text{ if } f^{th} \text{ FAP splitter is connected to any } r^{th} \text{ RT ONU} \\ 0; \text{ otherwise} \end{cases}$$

$$X_{rs} = \begin{cases} 1; \text{ if } r^{th} \text{ RT ONU is connected to any } s^{th} \text{ SC BTS} \\ 0; \text{ otherwise} \end{cases}$$

$$B_{15} = \begin{cases} 1; \text{ if the } s^{th} \text{ SC is selected to place 1.5 GHz BTS equipment} \\ 0; \text{ otherwise} \end{cases}$$

$$B_{36} = \begin{cases} 1; \text{ if the } s^{th} \text{ SC is selected to place 3.6 GHz BTS equipment} \\ 0; \text{ otherwise} \end{cases}$$

❖ 5G SCN-GPON planning objective function

Our research project aimed to plan and dimension different cost-effective and optimal SCN and corresponding backhaul network architectures. Thereby, the combined SCN-GPON optimisation framework's objective in this chapter was similar to that of **Chapters 4** and **5**. It meant adapting to the CFLNDP optimisation method to select SC and PtP node locations, e.g., CO, FAP and RT locations, and the intermediate fibre/wire routes connecting the selecting locations. It would be achieved by minimising the corresponding link and facility cost components, adhering to the additional capacity and coverage limits seen in such a network architecture. Hence, this chapter's objective function included the decision variables for the

link and facility cost components so that the cost-optimal values to the decision variables were determined. It would adhere to the said objective function's implementation while calculating the planned 5G SCN-GPON network architecture's total cost. The objective function is as follows.

$$
\text{minimise}
\begin{bmatrix}
\left(e_r + e_{sh} + e_{cc}\right) \sum_{c \in CO} O_c + e_{lc} \sum_{c \in CO} N_{lc} O_c \\[2mm]
+ \left(e_{fsp} + e_{spl}\right) \sum_{f \in FAP} S_f + \left(e_{fsp} + e_{spl}\right) \sum_{f \in FAP} \left(I_f - S_f\right) \\[2mm]
+ \left(e_{onu} + e_{spl}\right) \sum_{r \in RT} P_r + \left(e_{onu} + e_{spl}\right) \sum_{r \in RT} \left(I_r - P_r\right) \\[2mm]
+ \left(e_{15} + e_{spl} + i_{scins}\right) \sum_{s \in SC} B_{15} + \left(e_{36} + e_{spl} + i_{scins}\right) \sum_{s \in SC} B_{36} \\[2mm]
+ \left(q_{cf} + fi_{cf}\right) \sum_{c \in CO} \sum_{f \in FAP} d_{cf} I_{cf} + \left(q_{fr} + fi_{fr}\right) \sum_{f \in FAP} \sum_{r \in RT} d_{fr} X_{fr} \\[2mm]
+ \left(q_{rs} + i_{rsfib}\right) \sum_{r \in RT} \sum_{s \in SC} d_{rs} X_{rs}
\end{bmatrix}
\tag{66}
$$

Here, link and facility deployment costs were the two primary cost components considered. The basic setting of the objective function was similar to that of **Chapters 4** and **5**, with additional cost components in the framework, compared with the cost components of these chapters. These were the RT-related cost components to establish ONU equipment at selected RT locations and cost components for establishing SC equipment corresponding to different frequency types. The total objective function was divided into different sub-components, as seen below-

$\left(e_r + e_{sh} + e_{cc}\right) \sum_{c \in CO} O_c =$ Cost for OLT equipment installation at all selected CO location

$e_{lc} \sum_{c \in CO} N_{lc} O_c =$ Cost for line card installation at all selected CO locations

$\left(e_{fsp} + e_{spl}\right) \sum_{f \in FAP} S_f =$ Cost for the first splitter installation at all selected FAP locations

$\left(e_{fsp} + e_{spl}\right) \sum_{f \in FAP} \left(I_f - S_f\right) =$ Cost for any additional splitter installations after the first, at all remaining selected FAP locations

$$\left(e_{onu} + e_{spl}\right) \sum_{r \in RT} P_r = \text{Cost for the first ONU installation at all selected RT locations}$$

$$\left(e_{onu} + e_{spl}\right) \sum_{r \in RT} \left(I_r - P_r\right) = \text{Cost for any additional ONU installations after the first, at all}$$

remaining selected RT locations

$$\left(e_{15} + e_{spl} + i_{scins}\right) \sum_{s \in SC} B_{15} = \text{Cost for the 1.5 GHz frequency SC BTS equipment}$$

installation at all selected SC locations

$$\left(e_{36} + e_{spl} + i_{scins}\right) \sum_{s \in SC} B_{36} = \text{Cost for the 3.6 GHz frequency SC BTS equipment}$$

installation at all selected SC locations

$$\left(fi_{cf} + q_{cf}\right) \sum_{c \in CO} \sum_{f \in FAP} d_{cf} I_{cf} = \text{Total cost of all distribution fibre routes between OLT}$$

and splitter

$$\left(fi_{fr} + q_{fr}\right) \sum_{f \in FAP} \sum_{r \in RT} d_{fr} X_{fr} = \text{Total cost of all feeder fibre routes between splitter and}$$

ONU

$$\left(q_{rs} + i_{rsfib}\right) \sum_{r \in RT} \sum_{s \in SC} d_{rs} X_{rs} = \text{Total cost of all drop fibre routes between ONU and SC}$$

❖ 5G SCN-GPON planning constraints

Since we incorporated two different optimisation aspects within our work, the framework elements utilised GPON and 5G SCN optimisation framework constraints. Considering the similar setting of this current framework, in comparison to our previous works, only link and facility cost components were primarily selected to be included within the GPON part of the optimisation process. However, there had been one constraint that bore significance more as a combined GPON-SCN constraint, but for simplification, that constraint has been considered within the GPON part of the framework discussion. Additionally, we discuss the optimisation constraints within the 5G SCN part. We still incorporated the link and facility cost components alongside the transport cost component of the SC facility. However, this

component was slightly expanded than the previous chapter since it involved counting cost for establishing SC installation for different frequency types. Therefore, altogether, the following constraint types were considered as below.

- Feeder fibre capacity conservation
- Feeder fibre conditional connectivity
- Distribution fibre capacity conservation
- Distribution fibre conditional connectivity
- Split ratio constraint
- PON reach limit
- Number of OLT equipment restriction
- Number of splitter equipment restriction
- Number of ONU equipment restriction
- Optical splitter location & quantity condition
- ONU location & quantity condition
- Line card connectivity restrictions
- Drop fibre capacity conservation
- Covered population bandwidth consumption restriction
- RT capacity calculation for all connected SCs
- SC-population terrain block connectivity restriction
- Population restriction for each terrain block
- SC coverage distance restriction
- Identifying maximum transmission distance
- 1.5 GHz frequency transmission distance condition
- 3.6 GHz frequency transmission distance condition
- Number of SC equipment restriction
- RT capacity restriction
- Number of terrain block restriction
- 1.5 GHz frequency bandwidth conditions
- 1.5 GHz bandwidth and transmission distance conditions
- 3.6 GHz frequency transmission distance conditions
- 3.6 GHz bandwidth and transmission distance conditions
- Integer variable constraints

- Binary variable constraints

➢ Feeder fibre capacity conservation

$$I_f = \sum_{c \in CO} I_{cf}, \qquad \forall f \in FAP \tag{67}$$

This constraint retained the demand maintenance between the number of splitters and CO-FAP feeder fibre links. It ensured that one optical splitter at the FAPs would connect with only one OLT in the CO. Hence, total outgoing demand from OLT at CO level, which was the number of total outgoing feeder fibre connections, was the same as the total incoming demand to the FAP level, e.g., the total number of splitters. It ultimately safeguarded that the OLT in CO would only connect with a FAP containing splitters.

$$\sum_{c \in CO} X_{cf} = S_f, \qquad \forall f \in FAP \tag{68}$$

This constraint maintained that proper connectivity is maintained between the CO and FAP node levels. In this case, each FAP location housing an optical splitter would be connected with only one connection of the OLT line card port for each CO-FAP link. Here, the OLT would be installed on a selected CO location.

$$X_{cf} \leq O_c, \qquad \forall c \in CO, \ \forall f \in FAP \tag{69}$$

This constraint confirmed that only the facilities selected through the optimisation framework from a set of potential node locations would serve connectivity demand for CO and FAP levels of the existing PtP network. As mentioned before, CO and FAP nodes of a PtP optical network that acted as the basis for our intended GPON backhaul optimisation would respectively house OLT and optical splitter equipment. Hence, this constraint ultimately ensured that each CO location should contain at least one OLT if that CO location had connectivity with an optical splitter at a FAP.

➢ Feeder fibre conditional connectivity

$$X_{cf} \leq I_{cf}, \qquad \forall c \in CO, \ \forall f \in FAP \tag{70}$$

$$I_{cf} \leq X_{cf} M, \qquad \forall c \in CO, \ \forall f \in FAP \tag{71}$$

These inequalities indicated that demand flow between CO and FAP node levels was delivered through only a network link selected for the CO-FAP connectivity by the optimisation framework. The constraints mainly adhere to the condition corresponding to the relationship between the number of CO-FAP connections and the possibility of a connection between those selected CO and FAP location(s) that form such CO-FAP links. The first inequality signified that the cth CO would not have any OLT placed in it if that c^{th} CO had no connection towards the fth FAP, i.e. if the number of CO-FAP links l_{cf} were zero, then the possibility of CO-FAP link X_{cf} would also be zero. The second inequality then indicated that for at least one outgoing connection went out from the cth CO towards the fth FAP; the cth CO would contain at least one OLT. It implied that when I_{cf} had a non-zero value, the X_{cf} variable would have a value of 1. Hence, these two inequalities conveyed the conditional limit for a connection existing between the cth CO and f^{th} FAP, depending on the total number of connections existing between the cth CO and f^{th} FAP. Hence these constraints yielded towards a non-linear mathematical relationship, as expressed as, $X_{cf} = \min\left(1, I_{cf}\right)$.

➢ **Distribution fibre capacity conservation**

$$I_r = \sum_{f \in FAP} I_{fr}, \qquad \forall \ r \in RT \tag{72}$$

Similar to the constraint signifying CO-FAP demand maintenance between the number of splitters and the number of CO-FAP feeder fibre links, this constraint ensures the demand conservation for the FAP-RT connectivity. It confirmed that one ONU at the RT node levels would link with only one optical splitter at the FAP level. Hence, total outgoing demand from splitter at the FAP level, e.g., the number of total outgoing distribution fibre connections, would equal the total incoming demand going into the RT level or the total number of ONUs. It would assure that the splitter at a FAP would only connect with an RT that would house an ONU.

$$\sum_{f \in FAP} X_{fr} = P_r, \qquad \forall \ r \in RT \tag{73}$$

This constraint ensured that all incoming and outgoing demands should be conserved between the FAP and RT node levels. The constraint would signify that each ONU positioned at the RT level in each selected RT location must connect to only one splitter at the FAP level for each FAP-RT distribution fibre link.

$$X_{fr} \le S_f, \qquad \forall f \in FAP, \ \forall r \in RT \tag{74}$$

This constraint ensured that the optimally selected facilities would only maintain connectivity demand for FAP and RT node levels within the optimisation framework. Hence, if a selected FAP location had connectivity with an ONU at RT level, then that selected FAP should have at least one optical splitter installed within itself.

➢ Distribution fibre conditional connectivity

$$X_{fr} \le I_{fr}, \qquad \forall \ \forall f \in FAP, \ \forall r \in RT \tag{75}$$

$$I_{fr} \le X_{fr}M, \qquad \forall \ \forall f \in FAP, \ \forall r \in RT \tag{76}$$

These constraints implied that on the fact that demand flow between FAP and RT level nodes was only supplied through optimally selected FAP-RT links for by the optimisation framework. The constraints mainly expressed the condition conforming to the relationship between the number of FAP-RT connections and the possibility of a connection between such chosen FAP and RT location(s), forming such FAP-RT links. The first constraint denoted that a selected f^{th} FAP would not contain an optical splitter if that f^{th} FAP had no connection towards a selected r^{th} RT location. So, when the number of FAP-RT links or I_{fr} were zero, the possibility of FAP-RT link X_{fr} would be zero. The second constraint then designated that if at least one outgoing connection went out from the fth FAP towards the rth RT, then that selected f^{th} FAP would certainly install at least one optical splitter, e.g. if I_{fr} the value were a non-zero quantity, then X_{fr} would have a value of 1. Thus, these two inequalities expressed the conditional restrain for a connection prevailing between the fth FAP and the rth RT, subject to the total number of connections between the fth FAP and the rth RT. Hence these

constraints would conform to the non-linear mathematical relationship, as expressed as,
$X_{fr} = \min(1, I_{fr})$.

➤ Split ratio constraint

$$\sum_{r \in RT} X_{fr} \leq R_f I_f, \qquad \forall f \in FAP \tag{77}$$

This above inequality upheld the facility capacity restriction for the distribution fibre connectivity between the FAP and RT levels, established on the split ratio for each FAP level optical splitter in use. At each splitter for the fth FAP, the maximum number of outgoing connections towards the rth RT would be under the multiplication value of the splitter's total number at the fth FAP and the fixed split ratio. For example, say a FAP had a 1:16 split ratio, and two splitters were placed at that FAP to connect to selected RTs. Then, in this case, a maximum of $16 \times 2 = 32$ connections from that FAP would go outwards to the RTs.

➤ PON reach limit

$$X_{cf}d_{cf} + X_{fr}d_{fr} + X_{rs}d_{rs} \leq d_{\max}, \; \forall \, c \in CO, \, f \in FAP, \; \forall \, r \in RT, \; \forall \, s \in SC \tag{78}$$

This constraint had been the same as denoted in the previous **Chapter 5** to define the restriction assure that the GPON link length reach was met. Hence, the combined length of feeder fibres, distribution fibres, and drop fibres between the last SC and the OLT within our proposed network architecture should remain within the maximum allowed transmission distance of a GPON. For example, a 1:64 split individual 10GPON can reach up to 50 km of transmission distance, while a typical PON reach could be 20km in practice. Therefore, the combined length of network links should remain under the distance level imposed by the GPON type provisioned within the framework.

➤ Number of OLT equipment restriction

$$\sum_{c \in CO} O_c \leq N_c \tag{79}$$

This constraint would restrict the maximum number of OLT facilities, e.g., node locations, to be chosen at CO level over the existing PtP optical network. The total number of

selected CO locations containing OLT equipment would be less or equal to the total number of CO locations within the PtP optical network premises chosen for our case study.

➢ Number of splitter equipment restriction

$$\sum_{f \in FAP} S_f \leq N_f \qquad (80)$$

This constraint restricted the maximum number of FAP node locations at the existing PtP optical network to be selected for installing optical splitters. This total number of selected FAP locations would exceed the total number of FAP locations.

➢ Number of ONU equipment restriction

$$\sum_{r \in RT} P_r \leq N_r \qquad (81)$$

This constraint imposed the highest number of RT node locations restriction over the existing PTP optical network in our case study area. Hence the total number of SC locations to install BTS equipment should not be more than the total number of potential SC locations.

➢ Optical splitter location & quantity condition

$$S_f \leq I_f, \quad f \in FAP \qquad (82)$$

$$I_f \leq S_f M, \quad f \in FAP \qquad (83)$$

These constraints above certified that data demand from the chosen FAP locations by the optimisation framework is appropriately sustained. Hence, the constraints conform to the conditional relation between the number of splitters at the fth FAP and the possibility of a splitter existing at a selected FAP location. The first inequality stated that the optimisation framework could not choose a FAP location if no splitter were installed at that selected FAP location. Hence, for I_f with a value of zero, then S_f would also adhere to the value of zero.

The second inequality thereby suggested that the selected f^{th} FAP would be eligible of enlisting a splitter if that location was chosen to be a suitable location by the framework to place an optical splitter. Henceforth, only if I_f had a non-zero value, the variable S_f would have a value of 1, indicating the possibility of having that location selected as a suitable splitter

location. Again, the constraints would denote the following non-linear relationship by nature, expressed as, $S_f = \min(1, I_f)$.

➢ ONU location & quantity condition

$$P_r \leq I_r, \quad r \in RT \tag{84}$$

$$I_r \leq P_r M, \quad r \in RT \tag{85}$$

These conditional constraints above ensured that the selected RT locations' data flow with the optimisation framework is appropriately maintained. The constraints show the conditional relationship between the number of ONUs placed at the rth RT and an ONU being placed at that selected RT location. The first inequality specified that if no splitter were installed at the selected r^{th} RT location, then that node could not be chosen by the optimisation framework for placing an ONU. Hence, mathematically, with a value of zero, the value P_r would also be zero.

The second inequality then completed the aforementioned conditional relation. It denoted that the selected r^{th} RT would eventually be picked as a suitable location by the optimisation framework to place an ONU if that location indeed contains an ONU in the first place. Mathematically it meant that only if I_r had a non-zero value, then P_r the value would be 1. Thus, the constraints would denote the non-linear relationship $P_r = \min(1, I_r)$.

➢ Line card connectivity restrictions

$$N_{lc} \geq \sum_{c \in CO} \sum_{f \in FAP} \left(\frac{I_{cf}}{N_p} \right) \tag{86}$$

$$N_{lc} \leq \left\{ \sum_{c \in CO} \sum_{f \in FAP} \left(\frac{I_{cf}}{N_p} \right) \right\} + 1 \tag{87}$$

This constraint limited the number of line cards placed within an OLT at the cth CO, depending on its number of ports allowing the connectivity option of a fixed number of N_p

PONs. Hence, for each N_p number of PONs, one additional line card should be installed at the OLT.

The first constraint gave the minimum limit for the number of line cards to be put at OLT, while the second constraint would provide the maximum limit. In that case, the number of line cards needed at the OLT would be the number of connections from the cth CO towards the fth FAP, divided by the number of PONs connected to the OLT. In this instance, that division result would not incur a remainder. Additionally, the second constraint then indicated that the maximum number of line cards at the OLT could be one greater than the number of CO-FAP fibre connections divided by the number of PONs. It is because the result was not divisible and yielded a non-zero remainder.

➢ Drop fibre capacity conservations

$$\sum_{r \in RT} X_{rs} = B_{15} + B_{36}, \qquad \forall\, s \in SC \tag{88}$$

This constraint indicated that only selected locations would supply connectivity demand for RT and SC node levels. Thereby, RT locations selected throughout the optimisation framework must have at least one ONU installed, only if that RT location had a link with a BTS in a selected SC location. Since we have two different types of SC locations to include within the optimisation works, the total number of RT-SC link possibilities would be equal to the total number of selected SC locations of both types.

$$\sum_{r \in RT} \sum_{s \in SC} X_{rs} \leq P_r \tag{89}$$

This constraint ensured that all connectivity demands between the RT and SC node levels should be met appropriately, adhering to the number of RT location possibilities at selected RT locations. Thus, each ONU put at the RT level for selected RT node positions should connect with a maximum of one BTS at SC level for each RT-SC link.

➢ Covered population bandwidth consumption restriction

$$bw_{pusr} \sum_{t \in TB} X_{st} tb_{pop} = SC_{cnsbw}, \qquad \forall\, s \in SC \tag{90}$$

The bandwidth consumed by each selected SC would be calculated on each SC-population terrain block connectivity link, based on the population in a connected terrain block multiplied by per-user bandwidth.

$$SC_{cnsbw} \leq bw_{36max}, \qquad \forall\ s \in SC \tag{91}$$

The total bandwidth consumed by each selected SC would not exceed the maximum bandwidth allocated for the higher of the two frequency types to be implemented within the framework.

➢ RT capacity calculation for all connected SCs

$$RT_{cap} \leq MX_{rs}, \qquad \forall\ r \in RT,\ \forall\ s \in SC \tag{92}$$

$$RT_{cap} \leq SC_{cnsbw}, \qquad \forall\ r \in RT,\ \forall\ s \in SC \tag{93}$$

$$RT_{cap} \geq SC_{cnsbw} - \left\{ M\left(1 - X_{rs}\right) \right\}, \qquad \forall\ r \in RT,\ \forall\ s \in SC \tag{94}$$

The constraints above signify the calculation of total bandwidth consumption of an RT, as determined by the bandwidth consumptions of all its connecting SC BTS. The calculation is the sum of all products of the total RT-SC links from each RT ONU, multiplied by bandwidth consumption for each SC location connected with that RT ONU. It is a nonlinear calculation converted to be linear to suit our MILP programming approach of optimisation. It highlights the nonlinear expression of the product of a binary and a continuous variable, influenced by the nonlinear expression $RT_{cap} = min\left\{ 1, \left(SC_{cnsbw} X_{rs} \right) \right\}$. If the X_{rs} value is zero, then RT_{cap} will be zero as per the first inequality, meaning if the rth RT had no connection towards the sth SC. Thereby, it would not contribute towards adding to the bandwidth consumption by that connected RT ONU. In contrast, if the X_{rs} value is 1, the second inequality ensured that the RT_{cap} value would have some non-zero value. It would denote that when an SC has a BTS placed in its location, it would add to the total bandwidth consumed by its connecting r^{th} RT ONU.

➤ SC-population terrain block connectivity restriction

$$\sum_{s \in SC} X_{st} = T_b, \qquad \forall\ t \in TB \qquad\qquad (95)$$

The above constraint signified a special relationship that enabled the coverage of population and a suitable SC location. The constraint ensured that each selected optimised SC location would cover a particular population, hence covering the total population over the case study area. Thereby, SC locations selected by the optimisation framework must have at least one SC BTS housed, only if that SC location would attempt to connect to and thus cover a population block.

$$X_{st} \leq B_{15} + B_{36}, \qquad \forall\ s \in SC,\ \forall\ t \in TB \qquad\qquad (96)$$

All connectivity demands between the RT and SC node levels should be met appropriately, adhering to the number of RT location possibilities at selected RT locations. Thus, each ONU put at the RT level for selected RT node positions should connect with a maximum of one BTS at SC level for each RT-SC link.

➤ Population restriction for each terrain block

$$\sum_{t \in TB} T_b tb_{pop} \geq pop_{req}\, pop_{tot} \qquad\qquad (97)$$

$$\sum_{t \in TB} T_b tb_{pop} \leq pop_{tot} \qquad\qquad (98)$$

All the terrain blocks' total population should suffice to at least the required population percentage and the maximum population value over the case study area.

➤ SC coverage distance restriction

$$\sum_{s \in SC} X_{st} d_{st} = tx_{dist15}, \qquad \forall\ s \in SC,\ \forall\ t \in TB \qquad\qquad (99)$$

$$tx_{dist15} \leq maxTx_{dist15}, \qquad \forall\ s \in SC,\ \forall\ t \in TB \qquad\qquad (100)$$

Maximum coverage distance or transmission distance for an SC was set as equal to or less than that corresponding to the larger of the two transmission distance values. It was associated with our intended two SC frequency values chosen to perform spectrum refarming.

➢ Identifying maximum transmission distance

$$max_{st} \geq tx_{dist}, \qquad \forall\ s \in SC,\ \forall\ t \in TB \tag{101}$$

$$RT_{cap} \leq tx_{dist} + M\left(max_{stflg}\right), \qquad \forall\ s \in SC,\ \forall\ t \in TB \tag{102}$$

$$\left(1 - max_{stflg}\right) \geq 1, \qquad \forall\ s \in SC,\ \forall\ t \in TB \tag{103}$$

It was necessary to identify the maximum transmission distance from each selected SC BTS using the above constraints. The maximum transmission distance was later applied to perform frequency refarming optimisation. The first inequality denoted that maximum transmission distance would be higher among all elements in the transmission distance set. The second inequality signified the conditional situation that if there is one SC-terrain block connectivity that exists, max_{st} would get some non-zero value. Here, the last inequality implied that there should be only one maximum transmission distance value among all transmission distance values. As these signified a non-linear conditional relationship, we again performed linearisation of the constraint using a big M variable as seen before.

➢ 1.5 GHz frequency transmission distance condition

$$minTx_{dist15} \leq max_{st} + \left\{M\left(1 - 15dlLim_{flg}\right)\right\}, \qquad \forall\ s \in SC,\ \forall\ t \in TB \tag{104}$$

$$minTx_{dist15} \geq max_{st} - \left\{M\left(15dlLim_{flg}\right)\right\}, \qquad \forall\ s \in SC,\ \forall\ t \in TB \tag{105}$$

$$max_{st} \leq maxTx_{dist15} + \left\{M\left(1 - 15duLim_{flg}\right)\right\}, \qquad \forall\ s \in SC,\ \forall\ t \in TB \tag{106}$$

$$max_{st} \geq maxTx_{dist15} - \left\{M\left(15duLim_{flg}\right)\right\}, \qquad \forall\ s \in SC,\ \forall\ t \in TB \tag{107}$$

$$0 \leq 15dlLim_{flg} + 15duLim_{flg} - \left\{2\left(15dist_{flg}\right)\right\} \leq 1, \qquad \forall\ s \in SC \tag{108}$$

For assigning the 1.5 GHz frequency appropriately to elected SC BTS, the maximum transmission distance max_{st} of each SC with the 1.5 GHz frequency should be satisfying the distance limit to cover a specific population. Hence the above constraints were implemented based on the IF-ELSE condition to check if the SC distances would fall within the range of the 1.5 GHz frequency requirement of coverage area limits. The first two inequalities compared

the maximum transmission distance in any direction for each SC with a lower bound $minTx_{dist15}$ of the transmission distance and set a flag variable $15dlLim_{flg}$ to 1 or 0, respectively. It would indicate whether the maximum transmission distance of SC was higher than the minimum coverage area. The following two inequalities then performed a similar comparison for an upper bound of transmission distance and set the flag variable $15duLim_{flg}$ 1 or 0. It would respectively indicate if the transmission distance fell under the upper bound or not. The following remaining inequality then checked the two flag variable values, and if both were 1, a third logical variable $15dist_{flg}$ was set to 1. It would then check if the maximum transmission distance fell under the range of the 1.5 GHz coverage area upper and lower bound restrictions. As IF-ELSE conditioning is nonlinear, they have been converted to linearity using the big-M method and restructuring the inequalities as above.

➢ 3.6 GHz frequency transmission distance condition

$$maxTx_{dist36} \geq max_{st} + 1 - \left\{ M \left(1 - 36dist_{flg} \right) \right\}, \qquad \forall\ s \in SC,\ \forall\ t \in TB \qquad (109)$$

$$max_{st} \geq maxTx_{dist36} + 1 - \left\{ M \left(36dist_{flg} \right) \right\}, \qquad \forall\ s \in SC,\ \forall\ t \in TB \qquad (110)$$

As similar to the previous constraint related to the 1.5 GHz frequency requirement of coverage area limits, the above constraints were implemented based on a relevant IF-ELSE condition. This condition would check if the maximum SC distance max_{st} for each SC would similarly fall within the transmission distance range bounds of the 3.6 GHz frequency. However, the comparison was made based only on the transmission distance's upper bound for the 3.6 Hz frequency. Here, the lower bound would already have been checked under the 1.5 GHz constraints, as 1.5 GHz frequency would allow for a higher transmission distance than the upper bound of the 3.6 GHz frequency distance. Following the big-M linearised conditional checking, the inequalities above compared the maximum transmission distance variable with the transmission area upper bound of the 3.6 GHz frequency. Then, again a flag variable $36dist_{flg}$ was set to 1 or 0, based on the IF-ELSE comparison, to respectively indicate if the transmission distance fell within the 3.6 GHz upper bound or not. However, again as it was a non-linear operation, linearization was applied.

➢ Number of SC equipment restriction

$$\sum_{s \in SC} B_{15} + B_{36} \leq N_s \tag{111}$$

The total number of selected SC locations containing BTS equipment should not be more than the total number of potential SC locations. Here, both SC location types utilised in the optimisation process were considered in this constraint.

➢ RT capacity restriction

$$\sum_{s \in SC} RT_{cap} \leq \frac{PON_{cap}}{R_f}, \qquad \forall\ r \in RT \tag{112}$$

The maximum bandwidth capacity of an RT ONU, based on its connectivity with multiple SC locations, would render a total bandwidth consumption. The above constraint ensures that this bandwidth value should not exceed the maximum GPON capacity divided by the split ratio in use for the GPON.

➢ Number of terrain block restriction

$$\sum_{t \in TB} T_b \leq N_t \tag{113}$$

The total number of terrain blocks containing population connecting with an SC location for population coverage purposes should not be more than the total number of terrain block within the dataset.

➢ 1.5 GHz frequency bandwidth conditions

$$bw15_{max} \geq SC_{cnsbw} + 1 - \left\{ M\left(1 - 15bw_{flg}\right) \right\}, \qquad \forall\ s \in SC \tag{114}$$

$$SC_{cnsbw} \geq bw15_{max} + 1 - \left\{ M\left(15bw_{flg}\right) \right\}, \qquad \forall\ s \in SC \tag{115}$$

The above constraints performed a conditional comparison of bandwidth consumption by each SC location, with the maximum allowable bandwidth limit for the 1.5 GHz frequency. The linearised inequalities above set the flag variable $15bw_{flg}$ to either 1 or 0. It depended on whether or not each SC consumed bandwidth stayed within the 1.5 GHz bandwidth limit.

➢ 1.5 GHz bandwidth and transmission distance conditions

$$BS_{15} \geq 15bw_{flg} + 15dist_{flg} - 1, \qquad \forall\ s \in SC \tag{116}$$

$$BS_{15} \leq 15bw_{flg}, \qquad \forall\ s \in SC \tag{117}$$

$$BS_{15} \leq 15dist_{flg}, \qquad \forall\ s \in SC \tag{118}$$

We wanted to correctly associate each selected SC location with the appropriate frequency type, based on each selected location's ability to satisfy transmission distance and bandwidth consumption restrictions successfully. Hence, a logical AND operation was performed, as above. We would compare both the flag variables $15bw_{flg}$ and $15dist_{flg}$ respectively signifying the bandwidth and distance statuses. If both bore values of 1, the corresponding location variable BS_{15} would be set to 1, indicating that the selected location would have the 1.5 GHz frequency as the carrier signal for its intended BTS equipment.

➢ 3.6 GHz frequency transmission distance conditions

$$bw36_{min} \leq SC_{cnsbw} + \left\{ M \left(1 - 36blLim_{flg} \right) \right\}, \qquad \forall\ s \in SC \tag{119}$$

$$bw36_{min} \geq SC_{cnsbw} - \left\{ M \left(36blLim_{flg} \right) \right\}, \qquad \forall\ s \in SC \tag{120}$$

$$SC_{cnsbw} \leq bw36_{max} + \left\{ M \left(1 - 36buLim_{flg} \right) \right\}, \qquad \forall\ s \in SC \tag{121}$$

$$SC_{cnsbw} \geq bw36_{max} - \left\{ M \left(36buLim_{flg} \right) \right\}, \qquad \forall\ s \in SC \tag{122}$$

$$0 \leq 36blLim_{flg} + 36buLim_{flg} - \left\{ 2 \left(36bw_{flg} \right) \right\} \leq 1, \qquad \forall\ s \in SC \tag{123}$$

The above inequalities linearised an IF-ELSE condition. They would check if a selected SC location covered some population for the corresponding bandwidth consumption to stay within the upper and lower bounds of the 3.6 GHz frequency bandwidth range. The first two inequalities compared the SC's consumed bandwidth for each selected location with a corresponding lower bound $bw36_{min}$ for the 3.6 GHz frequency, then set a flag variable $36blLim_{flg}$ to 1 or 0, respectively. This approach was adopted when SC's total consumed

bandwidth was higher than that minimum bandwidth consumption. The following two inequalities would also complete the similar operation, albeit for an upper bound of consumed bandwidth, and set a flag variable $36buLim_{flg}$ to either 1 or 0. These 1 and 0 values would then be respectively denoting whether consumed SC bandwidth satisfied the upper bound restriction of consumed bandwidth or not. Upon checking if the above two flag variable values were 1, a third logical variable $36bw_{flg}$ was set to 1, indicating that the selected s_{th} SC location will successfully meet the bandwidth range constraint. If the flag variables both were not 1, the bandwidth indicating variable $36bw_{flg}$ would be 0.

➢ 3.6 GHz bandwidth and transmission distance conditions

$$BS_{36} \geq 36bw_{flg} + 36dist_{flg} - 1, \qquad \forall \ s \in SC \tag{124}$$

$$BS_{36} \leq 36bw_{flg}, \qquad \forall \ s \in SC \tag{125}$$

$$BS_{36} \leq 36dist_{flg}, \qquad \forall \ s \in SC \tag{126}$$

Again, the flag variables $36bw_{flg}$ and $36dist_{flg}$ respectively signifying the bandwidth and distance conditions for the 3.6 GHz frequency were compared. So, when both variables carried the value of 1, the location variable BS_{36} corresponding to the 3.6 GHz carrier frequency would be set to 1 for its corresponding SC location to operate with a 3.6 GHz frequency.

➢ Integer variables constraints

$$I_{cf} \geq 0, \qquad \forall \ c \in CO, f \in FAP \tag{127}$$

$$I_{fr} \geq 0, \qquad \forall f \in FAP, \ r \in RT \tag{128}$$

$$I_f \geq 0, \qquad \forall f \in FAP \tag{129}$$

$$Ir \geq 0, \qquad \forall \ r \in RT \tag{130}$$

$$N_{lc} \geq 0, \qquad \forall \ c \in CO \tag{131}$$

The constraints above regulated the values of the integer variables to either zero or any non-zero value to maintain the mixed-integer aspect of the optimisation framework. The restrictions also ensured that the integer variables be positive.

➢ Binary variable constraints

$$O_c \in \{0,1\}, \qquad \forall\ c \in CO \tag{132}$$

$$S_f \in \{0,1\}, \qquad \forall\ f \in FAP \tag{133}$$

$$P_r \in \{0,1\}, \qquad \forall\ r \in RT \tag{134}$$

$$B_{15} \in \{0,1\}, \qquad \forall\ s \in SC \tag{135}$$

$$B_{36} \in \{0,1\}, \qquad \forall\ s \in SC \tag{136}$$

$$X_{cf} \in \{0,1\}, \qquad \forall\ c \in CO,\ f \in FAP \tag{137}$$

$$X_{fr} \in \{0,1\}, \qquad \forall\ f \in FAP,\ r \in RT \tag{138}$$

$$X_{rs} \in \{0,1\}, \qquad \forall\ r \in RT,\ s \in SC \tag{139}$$

The binary variables were used to specify the possibility of the existence of links and facilities. Hence, all binary variables within the framework would be issued a value of either 0 or 1 to indicate whether a link/facility was present or not, respectively. Here, only binary variable constraints were covered, as the integer variables all belonged to the GPON optimisation segment.

Now that all the variables, parameters and constraints to the objective function have been identified above, we present the 5G cellular technology-based SCN-GPON network maps and comparative studies on establishing the most optimal results in the following section.

6.4. 5G SCN-GPON planning results

This section centres on our simulation results for our spectrum refarming based case study scenarios, which comprises the last part of our research. Following the network planning methodology and implementation approaches mentioned in Section 6.3, these results are obtained through designated case studies. The case studies in this section aimed to extend

beyond the scope of geographic location optimisation to form a combined SCN-GPON network. This optimisation process included parameters about the signal transmission capabilities of the small-cells. Hence, we included frequency refarming to assign appropriate frequencies within the SC part of our network, based on coverage area and user capacity handling provisions for each SC location. Following the current and upcoming global cellular communications trends, we focused on the 5G mobile communication technology parameters for the spectrum refarming aspect within our optimisation framework discussed in this chapter. Also, we maintained 10GPON as our preferred technology to support our GPON backhaul optimisation part of the framework. As before, existing PtP optical network node locations were chosen to house our proposed GPON-based optical backhaul, as connected hierarchically with fibre/cable communication links. Additionally, a set of potential small-cell locations were pre-selected based on their positioning over a terrain grid architecture, as envisioned over our case study area of the University of Melbourne campus.

Following the previous chapters, the SCN planning adhered to the signal propagation over urban geographic terrain, incorporating the maximum coverage area provision to signal transmission characteristics over an urban geographic area. Moreover, each SC's ability to handle a certain amount of data transmission capacity within a particular coverage area limit was also included in the framework optimisation process. Therefore, appropriate SC locations were then chosen over the case study area combining all these above characteristics. Afterwards, the framework shifted to a GPON-based backhaul dimension, which acted as the interface between the core network and mobile technology users over the case study area. The GPON backhaul planning based on the optimisation part studied in this chapter has followed the same aspects as in **Chapters 4** and **5** of this thesis. The cost minimisation approaches considered both the CAPEX and the OPEX to determine the optimal GPON formation offering minimal cost utilisation. Thereby, in this section, we would observe the additional effects of SCN optimisation within our proposed SCN-GPON framework in this chapter.

The optimisation results indicated that the data rate on which the SC BTS would transfer cellular signal played a crucial role in determining the capacity to be handled by each SC. The aim was to observe the overall network architecture formed through the optimisation process for different data rate levels. The network maps produced through the framework's implementation would be expected to bear a different architecture for different data rates. For simplification, the data rate levels considered in our case study would be lower amounts, and

in future, could be expanded to higher data rates to include more result scenarios. As coverage and capacity were the added addition to our framework formation process, we based the case studies on different data rates for different transmission frequency types. Here, each frequency had its coverage area and data transmission capacity characteristics.

We primarily used the AMPL mathematical programming software [122] to run our desired discrete optimisation simulation scenarios. We then obtain corresponding outcomes that gave us the location and link connectivity positions to help construct the optimal network plans for different 5G data transmission rates. Since this involved an extensive computation process, we resorted to using a virtual machine at the NECTAR cloud [133] to run our simulations. The virtual cloud machine we used comprised four instances of 32 GB RAM instances and totalled 128 GB of RAM, with a Linux Ubuntu operating system [134], with a 500 GB hard drive. Approximate time to obtain Once the appropriate network locations and corresponding links were identified, we used the ArcGIS geoprocessing tool to visually map out the results. Finally, all the results were stored in a secured folder at a Dropbox [123] cloud service account.

Here, we observe and discuss our framework implementation results using case study scenarios based on different data rate settings.

- 2 Mbps data rate
- 5 Mbps data rate
- 10 Mbps data rate
- 15 Mbps data rate

Additionally, we performed a cost comparison scenario for the same GPON backhaul network based on the same split ratio but different data rates to see how cost values change with the change in data rates. It was discussed at the end of this section after the data rate scenario result sub-sections were presented.

6.4.1. 2 Mbps data rate

We started our optimisation results with the 1 Mbps data rate for our combined SCN-GPON optimisation framework. The 2 Mbps data rate is an upgrade from the 1 Mbps, and theoretically, it could produce a different set of optimisation results. However, it was evident that the optimisation results for both 1 and 2 Mbps were mostly similar upon the comparison.

The small difference observed at the SCN part was that the SCs chosen in the 2 Mbps scenario were slightly different from the 1 Mbps results. Therefore, we decided to start presenting our results from the 2 Mbps scenario to maintain the chapter's conciseness. We thereby confer to the following sub-sections related to our results-

- 2 Mbps framework cost comparison scenario
  2 Mbps Optimised network map examples

❖ 2 Mbps framework cost comparison scenario

The 2 Mbps scenario would render different SCN-GPON cost comparison scenarios through optimisation, in particular, due to the expected change at the SCN side of the SCN-GPON network maps generated. With the data rate increment, the SCN-GPON planning would require more SC locations to be selected to cover the increment in data capacity attained by each selected SC location, corresponding to higher data rates. Again, we had the following scenarios at play-

- Maximum 8 OLT PON ports for 2 Mbps scenario
- Maximum 4 OLT PON ports for 2 Mbps scenario

➢ Maximum 8 OLT PON ports for 2 Mbps scenario

This section focuses on the scenario where PON port restriction at OLT line card was set to a maximum of 8 PON ports. Again, 1:2, 1:4 and 1:8 split ratios were considered, with small differences observed among their corresponding total cost levels. However, compared with the previous 1 Mbps scenarios, total cost levels increased for all these three network types since more SC locations were chosen to cover the increased data capacity levels. When observed, the case study results showed that the cost components for the OLT equipment, line card and BTS equipment stayed the same for all network types within this current scenario of case studies. The variation in costs for some components did not adhere to a linear increment or decrement for the different network types for the other cost components. For example, ONU and optical fibre costs vary in a non-linear pattern as the number of split ports increased. It has happened most likely due to the selections of different CO-FAP routes for different split ratio were chosen, e.g., the 1:8 split ratio network formation opted for a different CO location to be used for placing the OLT equipment than that of the 1:2 and 1:4 split ratio types.

Conversely, splitter costs went down as the split ratio for the GPON type splitters changed due to fewer FAP locations being used to place the splitters as the number of split ports increased. The most cost minimal results were offered by the 1:4 split ratio network, while the 1:8 scenario had the maximum total cost. A cost comparison representation is thereby given below in **Figure 84** for this case study.
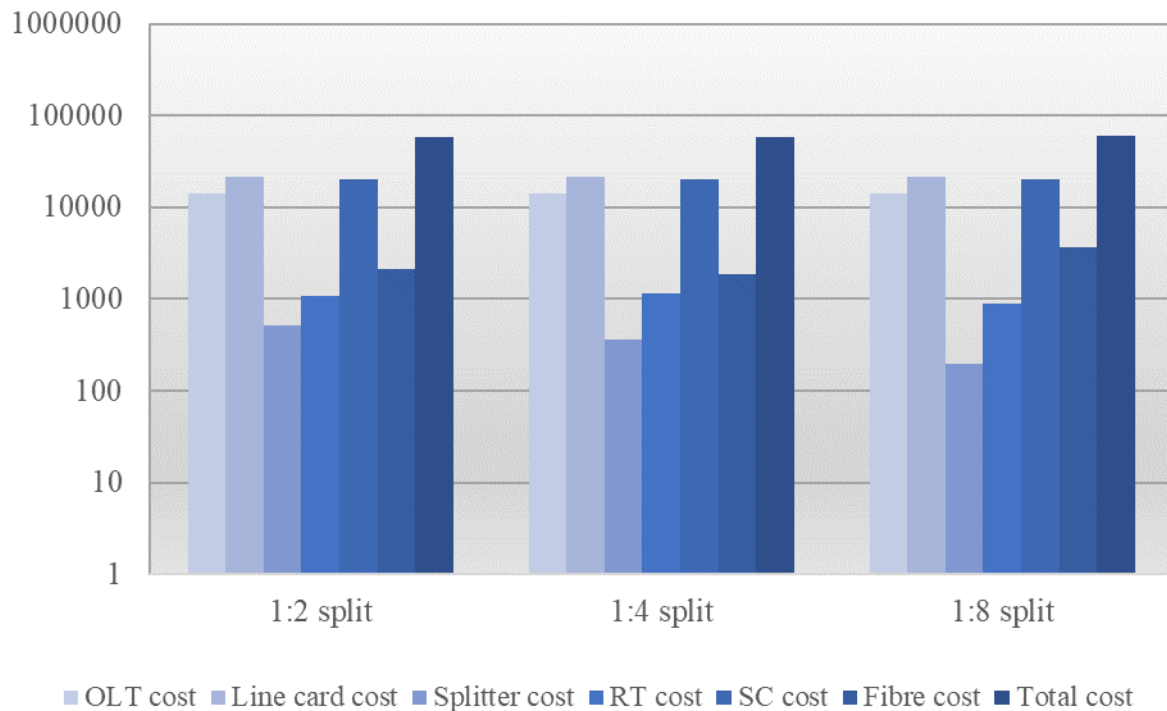
Figure 84: Cost comparisons for 2 Mbps, 8-PON SCN-GPON planning

➢ **Maximum 4 OLT PON ports for 2 Mbps scenario**

This section describes the results of optimisation case studies when the number of maximum PON ports in an OLT line card is reduced to 4 from the previous maximum of 8 ports. The results revealed a significant difference between the highest and lowest cost results, as the number of PON ports outgoing from the CO node level becomes restricted than before. More SC locations than that of 1 Mbps results were selected to cater to additional higher-speed data flow capacity through the planned network. Result observations revealed that OLT and line card costs remained constant for all the network types, while FAP level splitter cost decreased with increment in the number of split ports towards the FAP-RT links. Although the ONU cost at the RT level increased, with the number of split ports, the SC level's BTS equipment cost and the optical fibre cost decreased. The most and least cost-optimal solutions

were 1:8 and 1:2 split ratio networks, respectively, so the 1:8 network was chosen as the desired network topology. This selection was based on cost minimisation, with 1 CO location for OLT placement, 1 line card, 2 FAP locations for the splitters, 12 RT for ONU units and 12 SC locations for the BTS units. The cost comparison scenarios for this instance is given below in **Figure 85**.
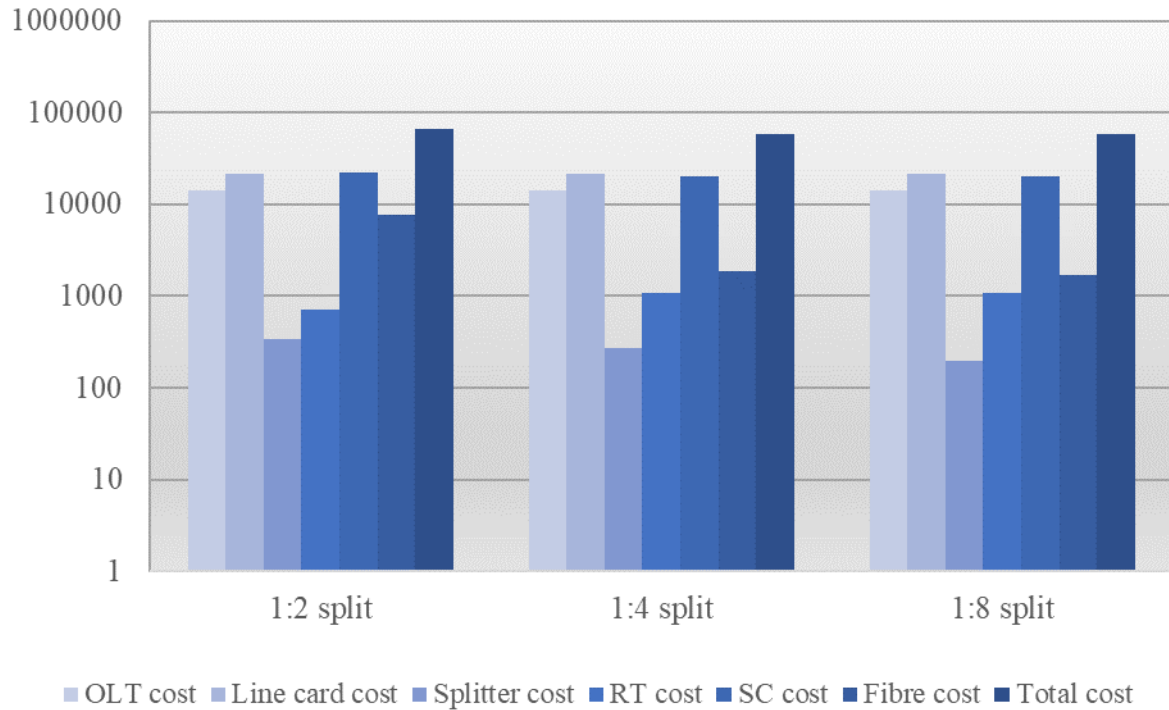
Figure 85: Cost comparisons for 2 Mbps, 4-PON SCN-GPON planning

❖ 2 Mbps Optimised network map examples

Following the chapter's case study methodology, the network maps were rendered for both the 8 and 4 PON port restriction limits at OLT line card units. For a maximum of 8 PON ports, we selected 1:4 network map with the least total cost rendered, while the 1:8 map had the highest cost. However, for the 4 PON port scenario, the highest total cost was rendered for the 1:2 network type, while the lowest total cost was seen for 1:8 network scenario. It was also apparent that the 4 PON port scenarios bore lower costs than the 8 PON port scenario. Hence, we chose the 4 PON port scenario's highest and lowest network maps as examples in this section. The network formations and selected nodes within the different scenarios were significantly different for the different network types, leading to different cost values. It can be

due to multiple reasons, e.g., change of PON port limitations from 8 to 4 and increment of data rates from 1 to 2 Mbps. Additionally, the total cost levels became higher than that of network optimisation results for the 1 Mbps data rate, as theoretically, the total capacity to be handled increased proportionally with the increase in data rates. Therefore, the results highlighted that the change significantly influences our intended network scenarios' total cost in the capacity handled to cover 100% area and user population.

While the planned networks' capacity directly influenced the total cost-optimality, the coverage aspects were not deemed straightforward constraints to affect the optimisation process's costs. The basis for this phenomena would be that constant values bounded both the coverage parameter aspects of our intended network planning. These parameters include the maximum area coverage by each SC and total user population coverage by all the SC locations. In this instance, the maximum cell coverage area was constrained within the limits of the two proposed SC frequency types, and the selected SC locations also achieved 100% total population coverage. All the SC locations were allocated with the 1.5 GHz carrier frequency, as the locations appropriately conformed to both the capacity and coverage restrictions of the 5G 1.5 GHz frequency. For both 8 and 4 port scenarios, we deemed that the 1:2 and 1:8 network scenarios offered the highest and lowest cost scenarios, respectively, for all different scenarios of 2 Mbps network formations. Henceforth, the 1:2 and 1:8 network scenarios are rendered as maps in Figure 86 and Figure 87.
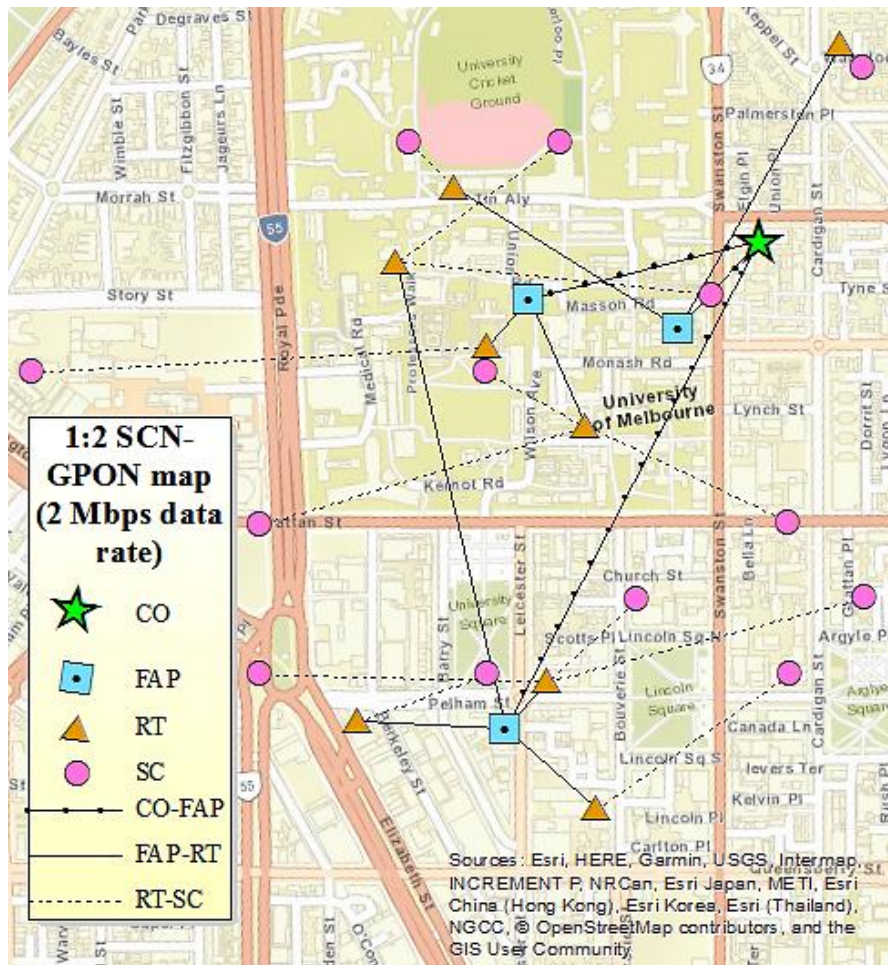
Figure 86: 2 Mbps, 1:2 split, 4-PON, SCN-GPON network map
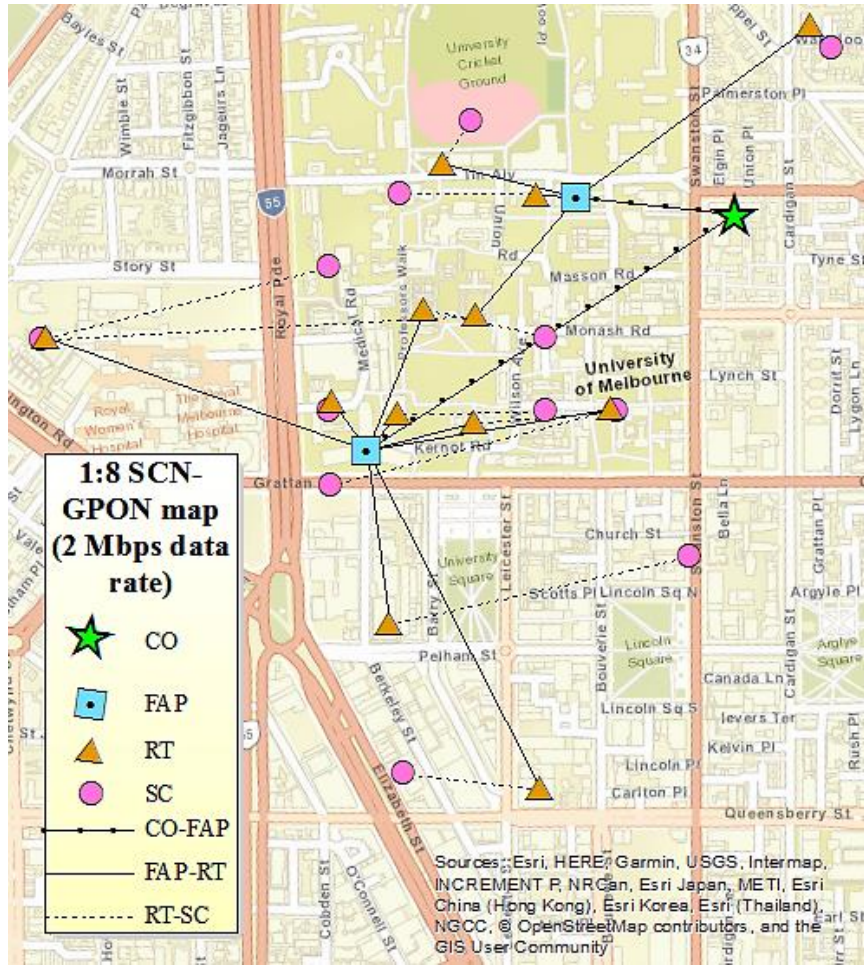
Figure 87: 2 Mbps, 1:8 split, 4-PON, SCN-GPON network map

6.4.2. 5 Mbps data rate

The next case study was based on the higher 5 Mbps data rate and produced a network map involving a higher number of optimised network nodes than the previous studies of lower data rates. A higher node utilisation estimate was considered a higher data rate would yield higher capacity attainment by the optimal network topology. This arrangement would also be maintaining ample coverage of SC wireless signals before signal level degrades beyond the 5G network MAPL [128]. Again, the following sub-sections suffice from the case study results-

- 5 Mbps framework cost comparison scenario
- 5 Mbps Optimised network map examples

❖ 5 Mbps framework cost comparison scenario

The cost comparison scenarios would produce a different result graph than the previous two data rate scenarios. As mentioned in the previous section, the increased node utilisation would see a rise in cost for the 5 Mbps data rate. Hence, by our preferred OLT PON port limitation aspects, we considered the following two cases for our research-

- Maximum 8 OLT PON ports for 5 Mbps scenario
- Maximum 4 OLT PON ports for 5 Mbps scenario

➢ Maximum 8 OLT PON ports for 5 Mbps scenario

This section is based on the case study scenario when the maximum number of PON ports allowed within the OLT line card was set as 8. The studies still utilised 1:2, 1:4 and 1:8 split scenarios for the GPON section of our planned network. The total cost for the 5 Mbps data rate appears to have increased significantly than those of the previous 1 and 2 Mbps data rates. It also showed a noteworthy difference in total cost between the highest and lowest cost network types. Observation of the 5 Mbps results revealed that their corresponding cost values stayed the same for all three network types for the OLT equipment, line card and BTS equipment. However, the other cost components did not show any linear variations with the change of the network types. For example, the change of costs for the splitter, ONU, BTS and fibre appeared as highest for the 1:2 split network and lowest for the 1:8 network, among the three network types.

Significant differences were observed in selecting the proper nodes and link routes in different network node hierarchy levels. It occurred for the different split ratios of the optical splitters, causing differences in the said cost components. For example, different FAP and RT locations were chosen for different split ratios, though the CO and SC location choices stayed the same. Here, the splitter costs went down as the split ratio for the GPON type splitters increased. It happened as more split ports going out meant a smaller number of FAP locations were needed to be utilised for placing optical splitters there. The highest total cost observed was for the 1:2 split ratio network, while the 1:8 ratio network gave the lowest total cost. In the end, 1 CO location, 5 FAP locations and 28 RT and SC locations were chosen to layout this desired and optimal 1:8 SCN-GPON map. A cost comparison representation is thereby given below for this case study in **Figure 88**.
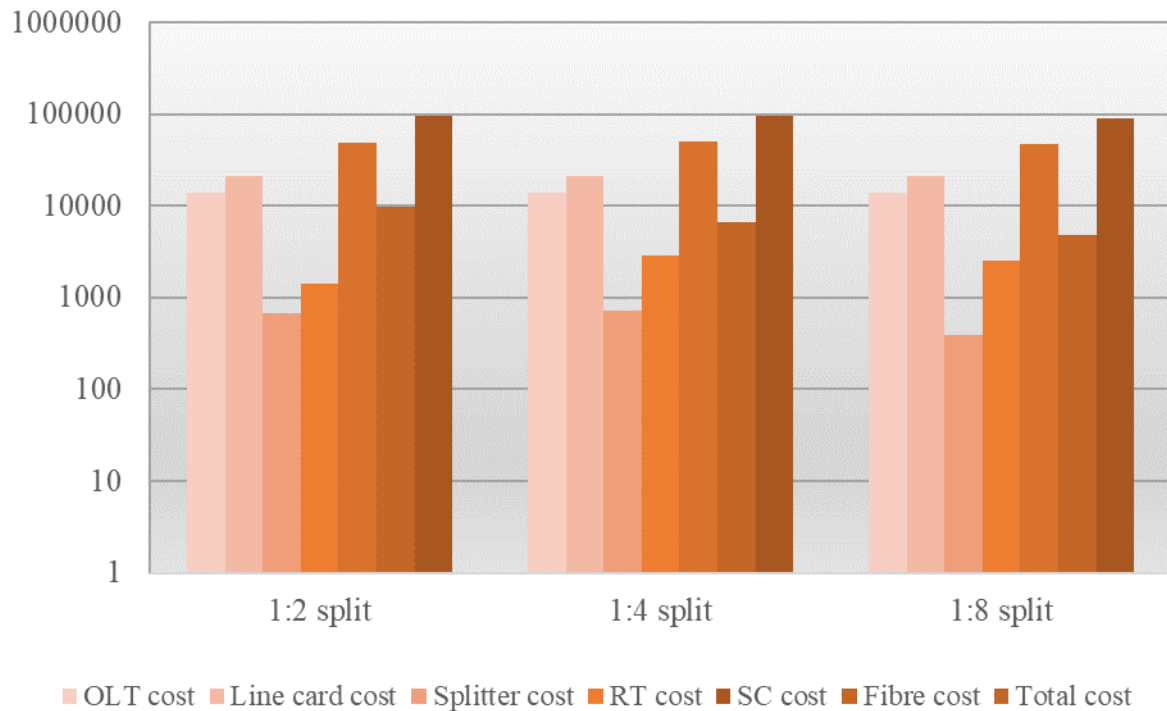
Figure 88: Cost comparisons for 5 Mbps, 8-PON SCN-GPON planning

➤ Maximum 4 OLT PON ports for 5 Mbps scenario

When the maximum number of PON ports was reduced to 4 from 8, a distinguishable difference in the optimal network plan based on cost variations was observed. Here, the total cost for all 1:2, 1:4 and 1:8 split type network plans had a significant increment in total and some of the cost components compared with the 8 PON port instance. Additionally, the 1:2 scenario used a different CO location for the OLT placement than those of the 1:4 and 1:8 split scenarios and all of the 8 PON port network plans for different split scenarios. It ultimately led to a different CO-FAP route that should be outgoing from the OLT to be placed at the selected CO location. Also, since the number of maximum PON ports was then 4, a smaller number of connections outgoing from the CO was allowed, also forcing to change the optimisation process chosen by the study. Here, the smallest and largest total costs were exhibited by the 1:8 and 1:4 split ratio networks, respectively. It was seen that while OLT and SC BTS cost component remained unchanged for both said network types, all other cost components, e.g., splitter, ONU, fibre and line card, were increased for the 1:4 network significantly.

For the multiple line cards, optical splitters and ONU units were designated to be put in their corresponding locations. This network approach originated from the selected CO

285

location and went through some of the selected FAP locations and some RT locations. Since the number of split ports per 1:4 splitter is less than the 1:8 splitters, more than one equipment unit was needed to be provisioned in a single selected location. As a result, cost component values became significantly higher for the 1:4 split network. In the desired result of the 1:8 split ratio network plan, there were 1 CO location, 4 FAP locations, 29 RT and 29 SC locations selected. A cost comparison has been presented in **Figure 89**, for different split ratio networks, for 4 PON port limitation.
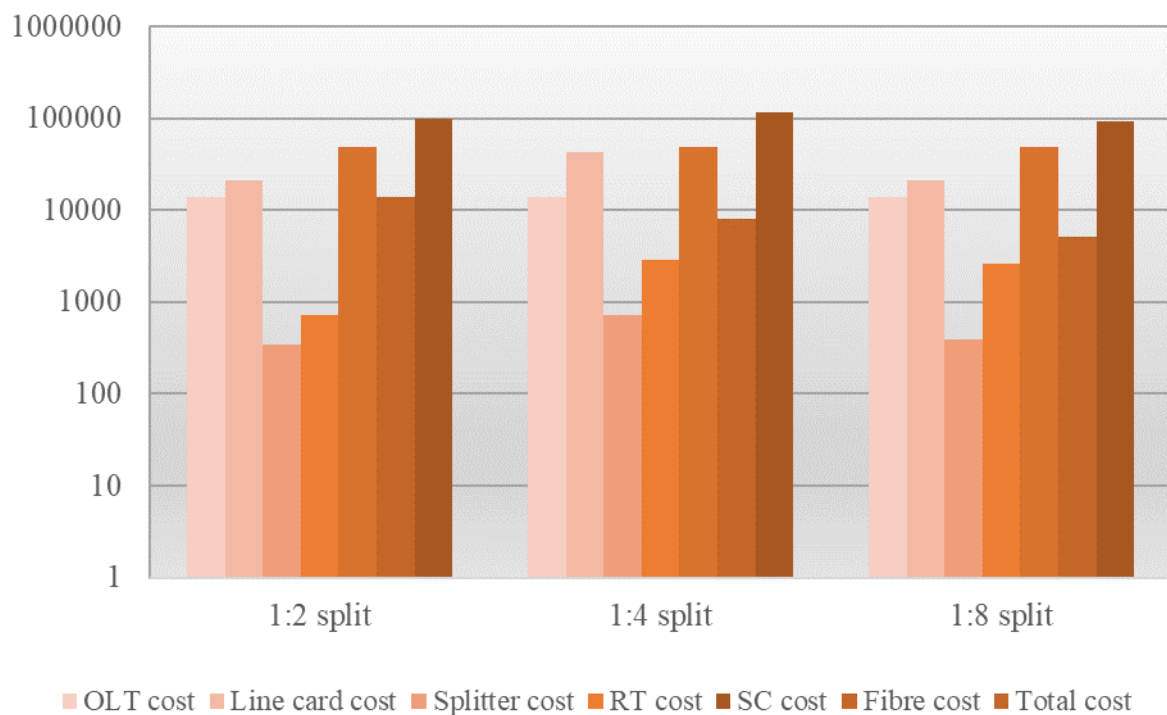
Figure 89: Cost comparisons for 5 Mbps, 4-PON SCN-GPON planning

The case studies were performed on 5 Mbps for a maximum of 8 and 4 PON port scenarios to provide a more visual comparison of optimisation results. We aimed to display the two instances of most and least expensive scenarios for the 8 PON port limitation scenario to utilise the time and space constraints of this thesis. Hence, in this section, we are focused on discussing the geographic map representations for the 1:2 and 1:8 split ratio networks to restrict 8 PON ports. However, it was noted that although the most expensive network scenario cost was higher in the 4 PON port instance. Additionally, the lowest cost scenario showed less cost for the least expensive network scenario within the 8 PON port illustration. It was noted that the total cost amounts were increased in general for all instances, with the increment of the data

rate to 5 Mbps. As the higher data rate per-user of the network rendered capacity addressing the requirement to increase, more node locations and additional link routes were selected. It was done for complete connectivity among such selected nodes within the dataset of the different existing network node and link locations. Such an optimal result ensured that 100% of the total user population over the case study area was also covered. The framework also maintained cell area restrictions to ensure signal propagation intensity levels were maintained within the 5G MAPL limit. It was also observed that only 1.5 GHz carrier frequency was assigned to all selected SC locations. Therefore, the geographic map representations of our previously mentioned 1:2 and 1:8 networks for the 8 PON port scenario are presented as follows, respectively, in **Figure 90** and **Figure 91**.
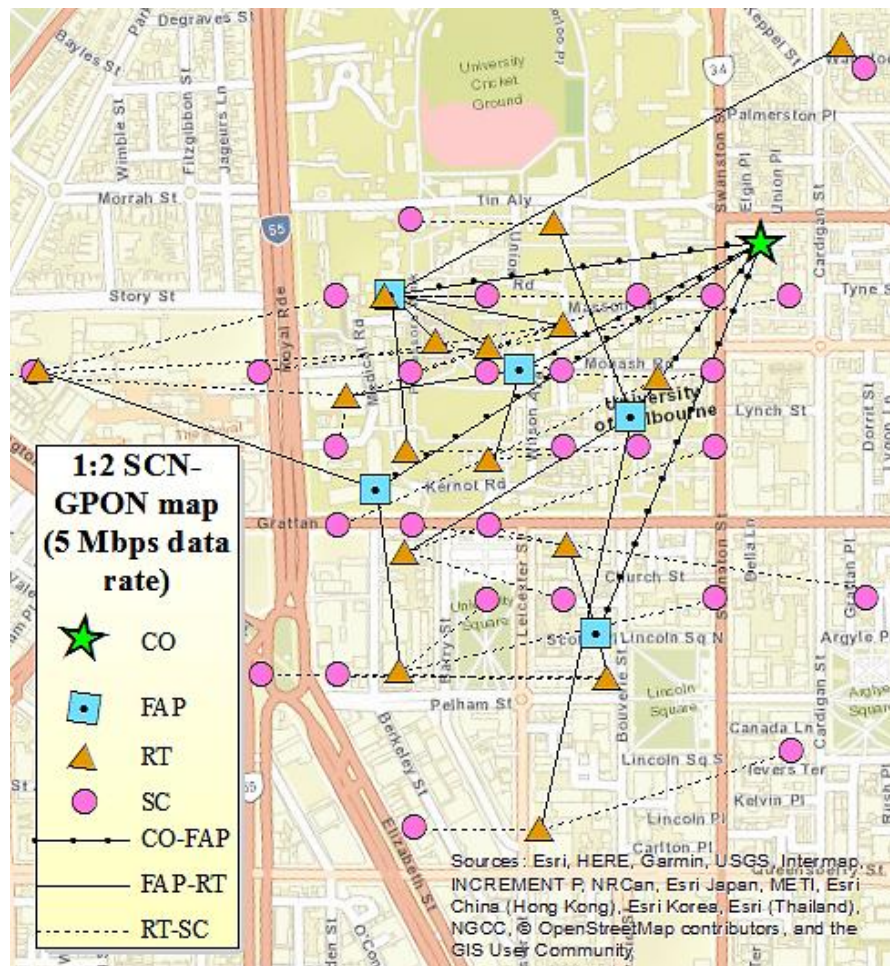
Figure 90: 5 Mbps, 1:2 split, 8-PON, SCN-GPON network map
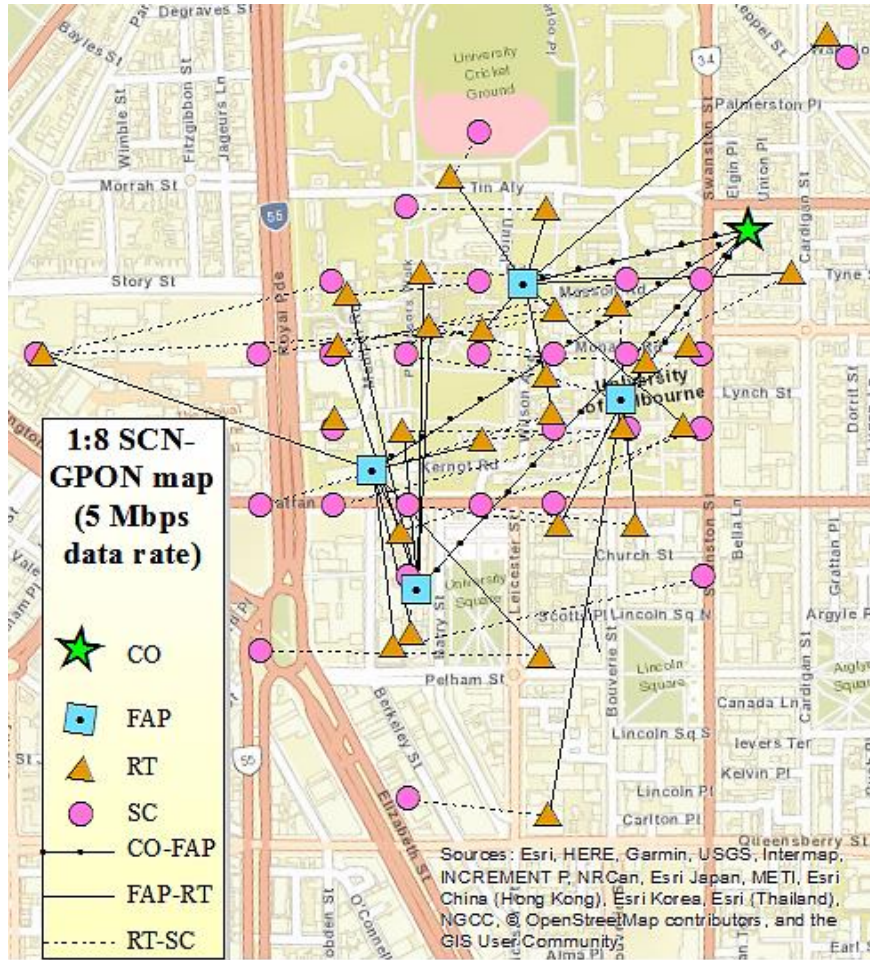
Figure 91: 5 Mbps, 1:8 split, 8-PON, SCN-GPON network map

6.4.3. 10 Mbps data rate

This section discusses another SCN-GPON planning scenario based on a higher 10 Mbps per-user data rate aspect. We mapped this study as well over the same population distribution within the same case study area. Again, both CFLNDP [114] and maximal coverage [63] optimisation techniques were employed to render our intended optimal SCN-GPON plan. The following segments were the two approaches resulting from this 10 Mbps data rate study.

- 10 Mbps framework cost comparison scenario
- 10 Mbps Optimised network map examples

❖ 10 Mbps framework cost comparison scenario

We continued to analyse our ensuing cost optimisation study results, based on the different types of split ratios, e.g., 1:2, 1:4 and 1:8. for the two PON port restriction scenarios GPON segment of our optimised network to be planned. Hence, the following scenarios were discussed with appropriate examples-

- Maximum 8 OLT PON ports for 10 Mbps scenario
- Maximum 4 OLT PON ports for 10 Mbps scenario

➢ Maximum 8 OLT PON ports for 10 Mbps scenario

We again observed higher total cost rendering for each of the 1:2, 1:4 and 1:8 split ratios to form an optimised SCN-GPON design for each such data rate applied as case study parameters. While observing the total cost amounts rendered for each of the split ratio scenarios, both the total and individual costs within significantly increased to counter the utilisation of the higher capacity and coverage amounts. It ultimately saw an extended deployment of the network elements such as the different hierarchy node locations and existing routes over the case study area, hence subsequent increment of the corresponding costs. The observations over 8 PON ports scenario showed that the total cost for the 1:8 split ratio scenario was the least expensive, e.g., it rendered the most cost-optimal SCN-GPON plan. Conversely, the 1:2 network plan was the most expensive and, therefore, the least desired result. It was observed that the 1:8 network utilised 1 CO location, 5 FAP locations, 44 RT locations and 57 SC locations within the resultant network plan. Here, multiple equipment units were placed in different selected node locations to perform the best utilisation of nodes and link routes. The cost comparison scenarios for all such three network types are presented below in **Figure 92**.
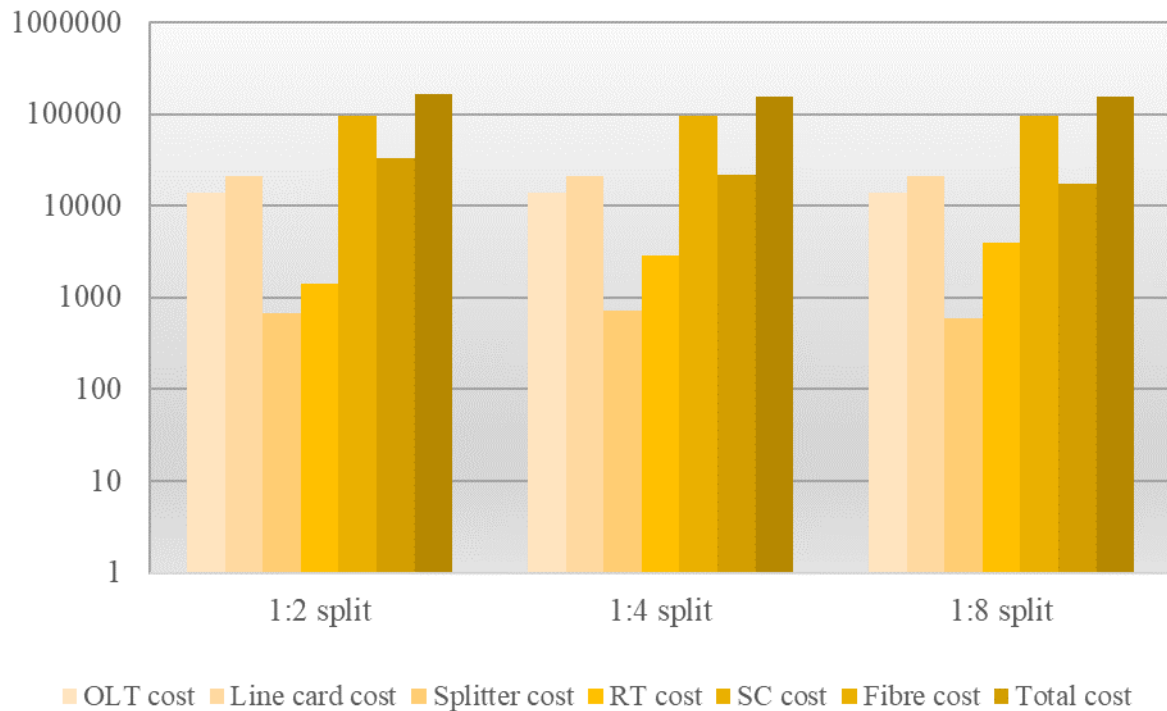
Figure 92: Cost comparisons for 10 Mbps, 8-PON SCN-GPON planning

➢ **Maximum 4 OLT PON ports for 10 Mbps scenario**

This section looks at the case study of SCN-GPON network planning performed of OLT PON port restriction lowered to 4 ports for the 10 Mbps scenario. As expected, with a smaller number of PON ports, the selection of CO-FAP routes for placing distribution fibre changed than the previous 8 PON ports scenario. Also, total costs and some individual equipment cost components for the 1:2, 1:4 and 1:8 scenarios increased as the node and link usage in the network planning changed. In this case study, the 1:2 network delivered the highest total cost while the 1:8 split type network plan rendered the least total cost, making this 1:8 network the desired optimal network formation to deploy. As we also observed the individual cost components for all network types, we found that while the OLT cost component and the number of line cards stayed the same.

Conversely, other components such as the splitter cost, ONU cost, BTS cost and fibre cost changed for the different network types. Again, multiple equipment units were placed on a single selected location for the different node type locations chosen through the optimisation process. Then although the 1:2 network rendered a much lower ONU cost than the optimal 1:8 network, the fibre cost for the selected 1:8 network was much less in comparison with the 1:2

network. Multiple FAP-RT routes were chosen from the selected FAP locations, minimising the need for placing fibres over a larger area within the case study region. Mainly, the 1:8 network chose 1 CO, 4 FAP, 32 RT and 57 SC locations within the SCN-GPON network plan formed. The cost comparisons for the different network types are thereby provided below in **Figure 93**.
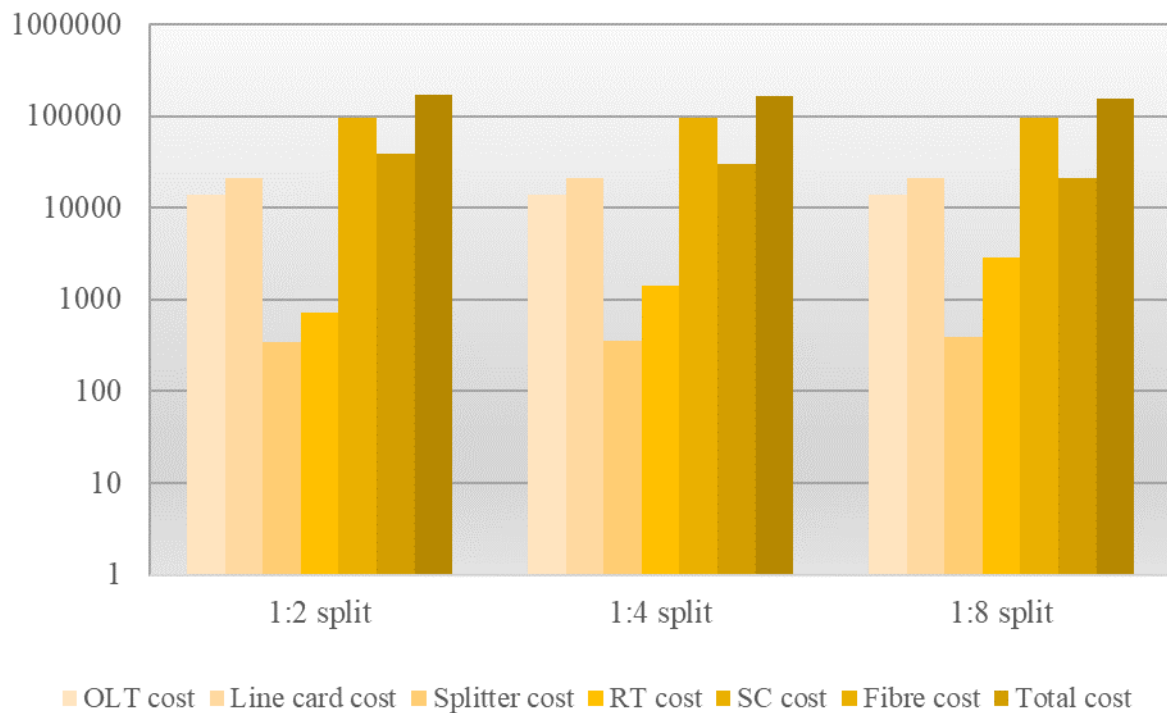
Figure 93: Cost comparisons for 10 Mbps, 4-PON SCN-GPON planning

❖ 10 Mbps Optimised network map examples

For the 10 Mbps data rate, the case studies were performed before, over the two PON port limitation types of 8 and 4 ports per line card. Again, only two network type map examples would be presented in this section. We chose the comparatively lower cost 8 PON port scenarios of 1:2 and 1:8 network types. Again, a higher data rate increased user data consumption for the same population over the case study area. It caused the need for addressing higher capacity by the network, hence resulting in a higher number of potential SC locations to be selected.

Interestingly, this 10 Mbps data rate study selected both the 1.5 and 3.6 GHz SC carrier frequencies for the first time, sufficing to distribute the selected SC locations' capacity needs.

The optimally chosen network plan also covered 100% of the population, conforming to the cell coverage area limitations for the SC carrier frequency assigned to the optimally selected SC locations. It also maintained the proper wireless signal strength levels. The geographic maps of the 1:2 and 1:8 networks are presented in **Figure 94** and **Figure 95**.
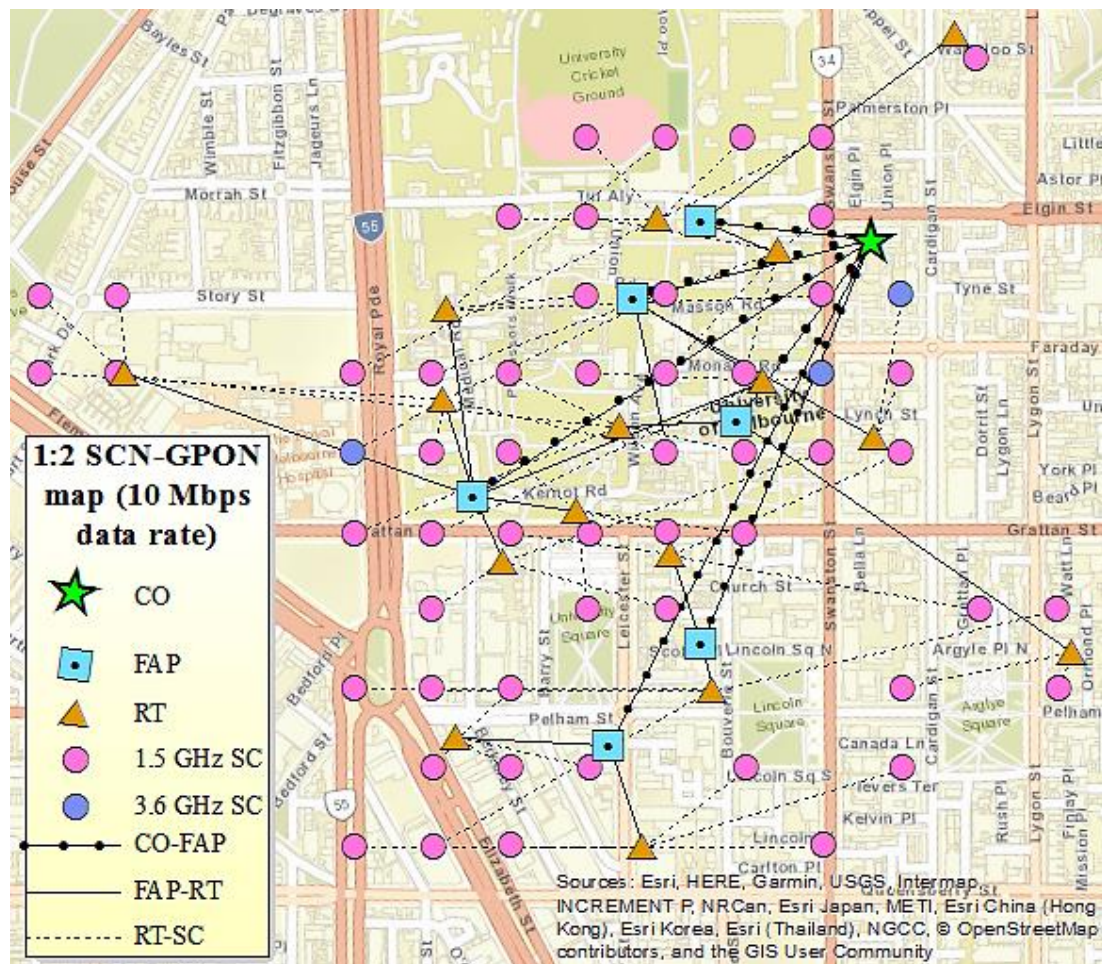
Figure 94: 10 Mbps, 1:2 split, 8-PON, SCN-GPON network map
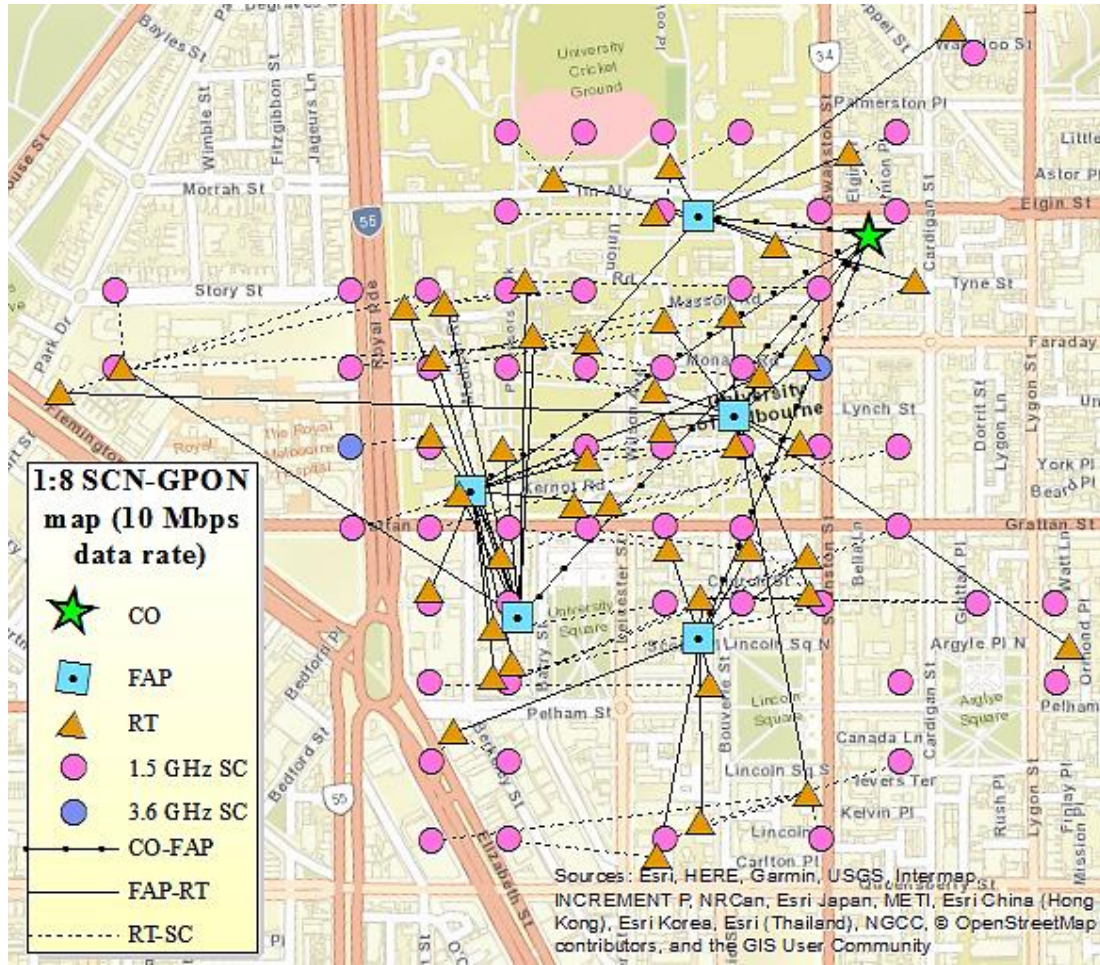
Figure 95: 10 Mbps, 1:8 split, 8-PON, SCN-GPON network map

6.4.4. 15 Mbps data rate

In this section, we discuss the last instance of our case studies performed within the scope of this last segment of our research works within the project. For this last case study scenario, we applied a 15 Mbps per-user data rate to cover our desired user population over the chosen case study area. We utilised both the CFLNDP [114] and maximal coverage [63] optimisation techniques. The two sub-sections within this part are written as follows.

- 15 Mbps framework cost comparison scenario
- 15 Mbps Optimised network map examples

❖ 15 Mbps framework cost comparison scenario

We adhered to the same premises of multiple split ratios and PON port limits, e.g., 1:2, 1:4 and, 1:8 ratios with 8 and 4 PON port restrictions, respectively, to perform our intended case studies. Hence, the following two instances were discussed in this section-

- Maximum 8 OLT PON ports for 15 Mbps scenario
- Maximum 4 OLT PON ports for 15 Mbps scenario

➢ Maximum 8 OLT PON ports for 15 Mbps scenario

As observed before, for this 8 PON port restriction scenario, total cost rendering for each of the 1:2, 1:4 and 1:8 split ratios were higher. This phenomenon was observed after comparison to all the lower data rate cases previously studied to form an optimised SCN-GPON network. As expected, both the total and individual cost segments increased to adhere to the higher capacity and coverage due to the incrementing data rate. As a result, more node locations and link routes were eventually utilised to construct the network architectures for the different network types. The case study observations over this 8 PON port restriction showed that the 1:8 split ratio scenario showed the least expensive, e.g., most cost-optimal SCN-GPON network formation, while 1:2 network rendering presented with the most expensive total cost. This 1:8 network would employ 1 CO location, 5 FAP locations, 50 RT locations and 83 SC locations. The cost comparison scenarios for these three network types are provided below in **Figure 96**.
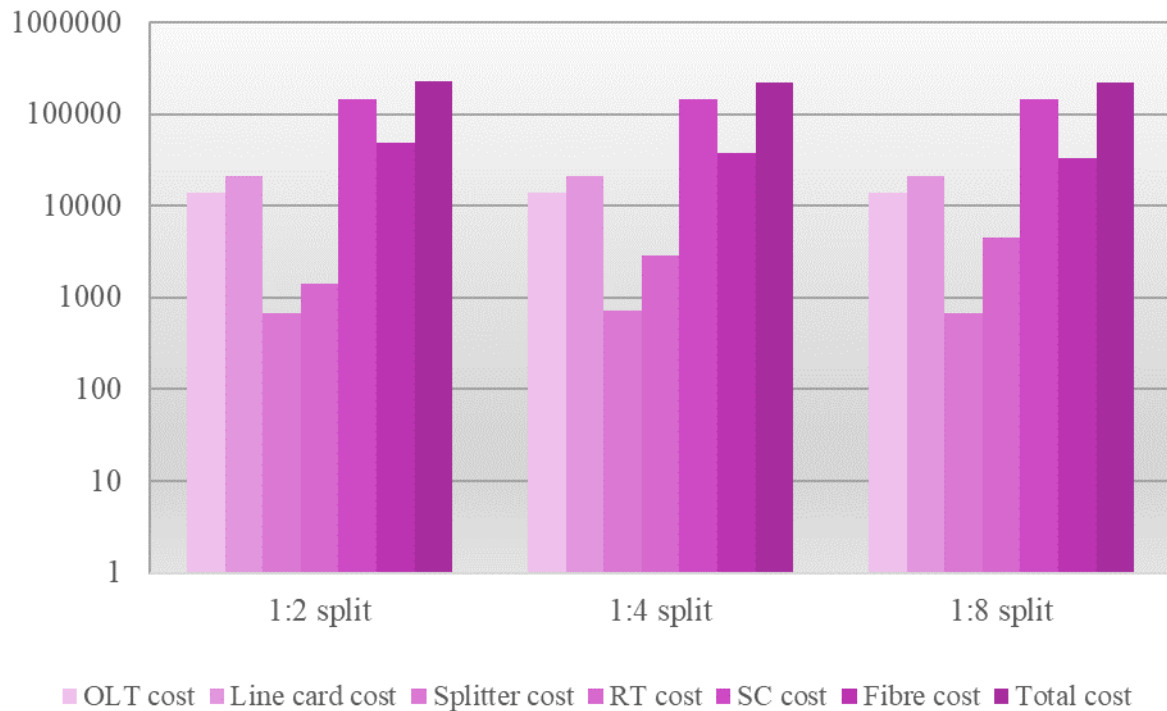
Figure 96: Cost comparisons for 15 Mbps, 8-PON SCN-GPON planning

➢ **Maximum 4 OLT PON ports for 15 Mbps scenario**

This segment describes the last study scenario, when the number of PON ports was reduced to 4 from 8, resulting in a significant change in both the total cost and individual equipment type cost components. For example, the total and individual cost amounts for the 1:2, 1:4 and 1:8 split type network plans increased notably compared with the 8 PON port limitation instance. Restricting the maximum number of PON ports to 4 from 8 changed the utilisations of the node and link routes, resulting in such cost variations. Here, the highest and lowest total costs were provided by the 1:2 and 1:8 network types, respectively. Except for the OLT cost component, all other cost components related to the splitter, ONU, fibre, and line card increased significantly for the 1:2 network. In the optimal formation of the 1:8 split ratio network plan, there were 1 CO location, 3 FAP locations, 24 RT and 82 SC locations selected. Also, in this case, multiple pieces of equipment were placed in the same optimally selected node location on various occasions. A cost comparison scenario is provided in **Figure 97** for this case study instance of 4 PON port restriction.

■ OLT cost ■ Line card cost ■ Splitter cost ■ RT cost ■ SC cost ■ Fibre cost ■ Total cost
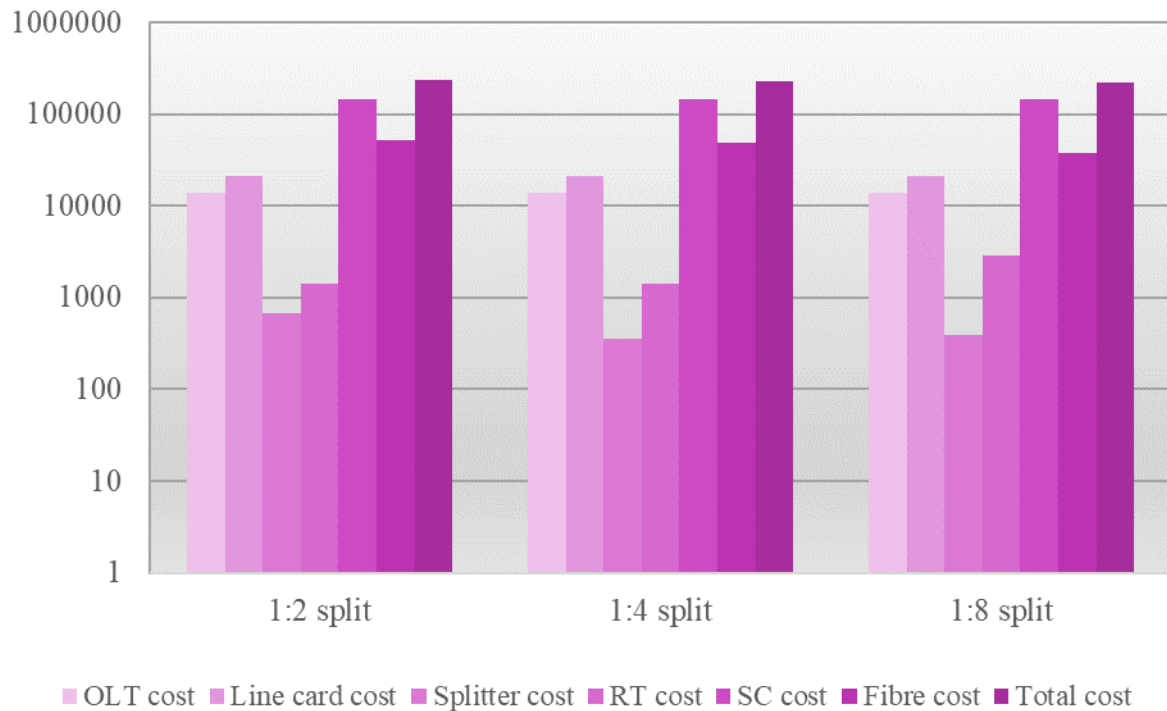
Figure 97: Cost comparisons for 15 Mbps, 4-PON SCN-GPON planning

❖ 15 Mbps Optimised network map examples

In this instance of discussing visual representations of some of our resultant SCN-GPON maps for the 15 Mbps data rate, the case studies were performed following the previously applied simulation process with changed appropriate parameters. It was achieved for the two PON port restriction types of 8 and 4 ports in each line card. Again, we are resorting to only two network map examples to be provided in this section. We selected the comparatively lower cost 8 PON port scenarios of 1:2 and 1:8 network types as our geographic map examples. The node and link route utilisations were much higher for both the 15 Mbps case study scenarios than those of the previous 1, 2, 5 and 10 Mbps data rate scenarios. Due to the increment of user data consumption due to the higher per-user data rate, a higher capacity was addressed by our resultant network plans for the same population over the case study area. As a result, many potential SC locations were selected within the 15 Mbps data rate network plans. As seen in the 10 Mbps data rate studies before, the 15 Mbps network planning scenario also selected both the 1.5 and 3.6 GHz SC carrier frequencies. It was done to maintain the necessity of attending higher capacity needs by the selected SC locations. Again, the optimally selected network covered 100% of the population over the case study area. It also corresponded

to the cell coverage area restrictions for the SC carrier frequencies assigned to the optimally selected SC locations while affirming the proper wireless signal strength levels. The corresponding geographic maps of the 1:2 and 1:8 networks are presented in Figure 98 and Figure 99.
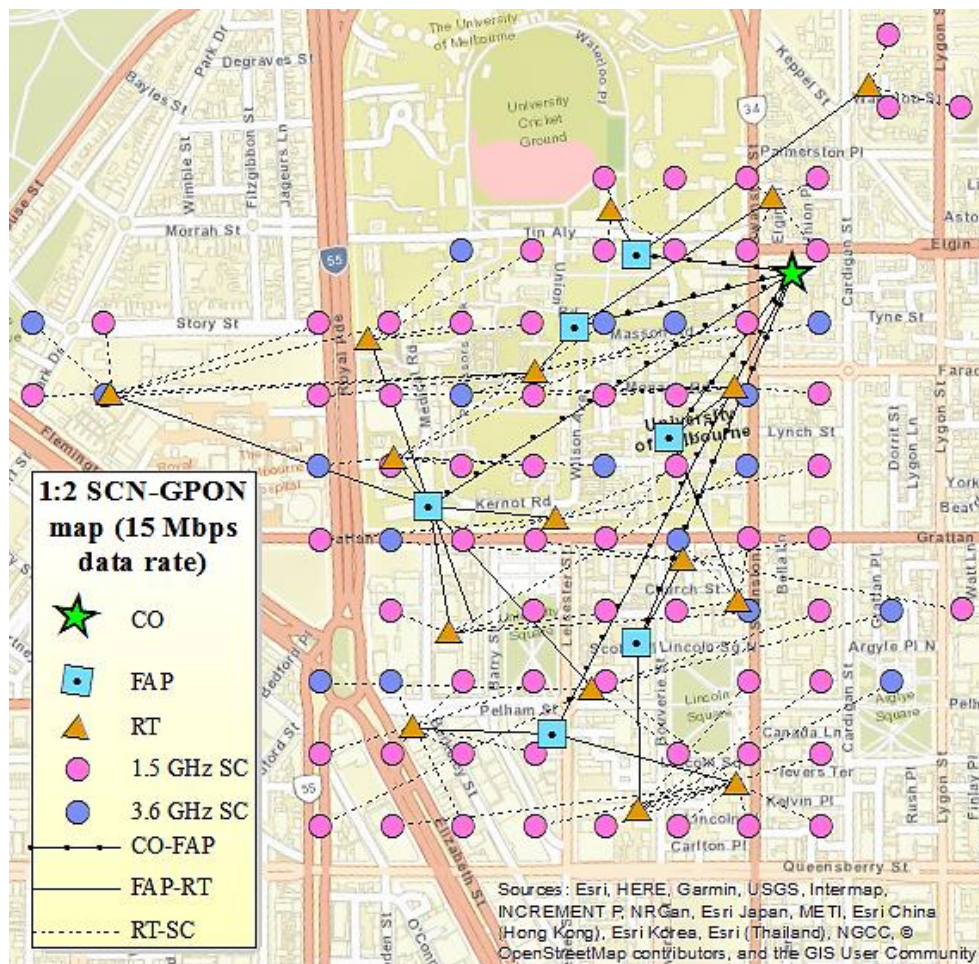
Figure 98: 15 Mbps, 1:2 split, 8-PON, SCN-GPON network map
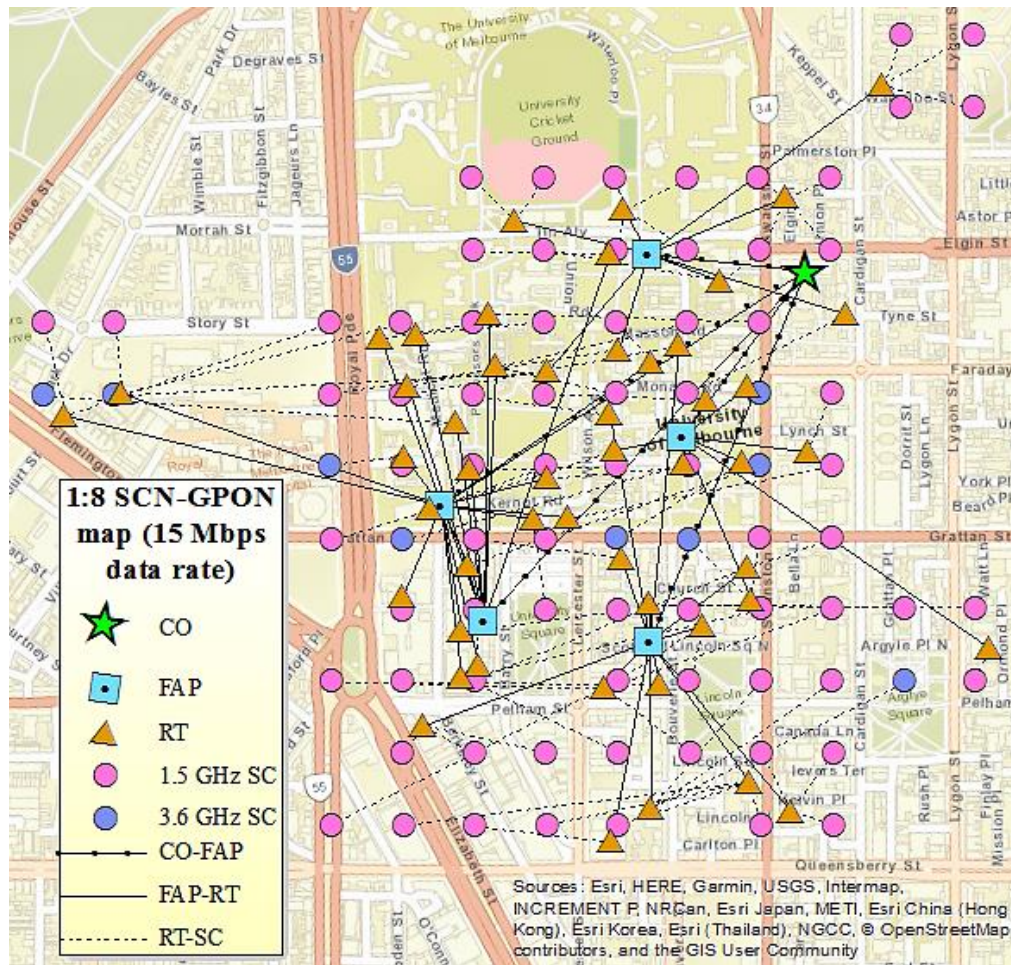
Figure 99: 15 Mbps, 1:8 split, 8-PON, SCN-GPON network map

6.4.5. 1:8 split, 8-port data rate cost comparison

This section discusses the trend of change with the total cost for a fixed network type, in our case, the 1:8 GPON scenario and 8 PON ports at the OLT unit line card. As observed in **Figure 100** below, it is seen that for the same GPON type with the same corresponding parameter(s), the total cost of network deployment increases with the increase of data rates. It can be attributed to the fact that as the data rate increased, the no. of node and link utilisations within the planned network would increase. It would lead to the procurement of more hardware resources to implement the network, and as a result, the total cost would increase as well. **Figure 100** below shows a 4-fold increase in the network's total implementation cost, given the y-axis with units in dollars. It has been evident when different total cost values have been compared from lowest to highest data rates within our case studies.
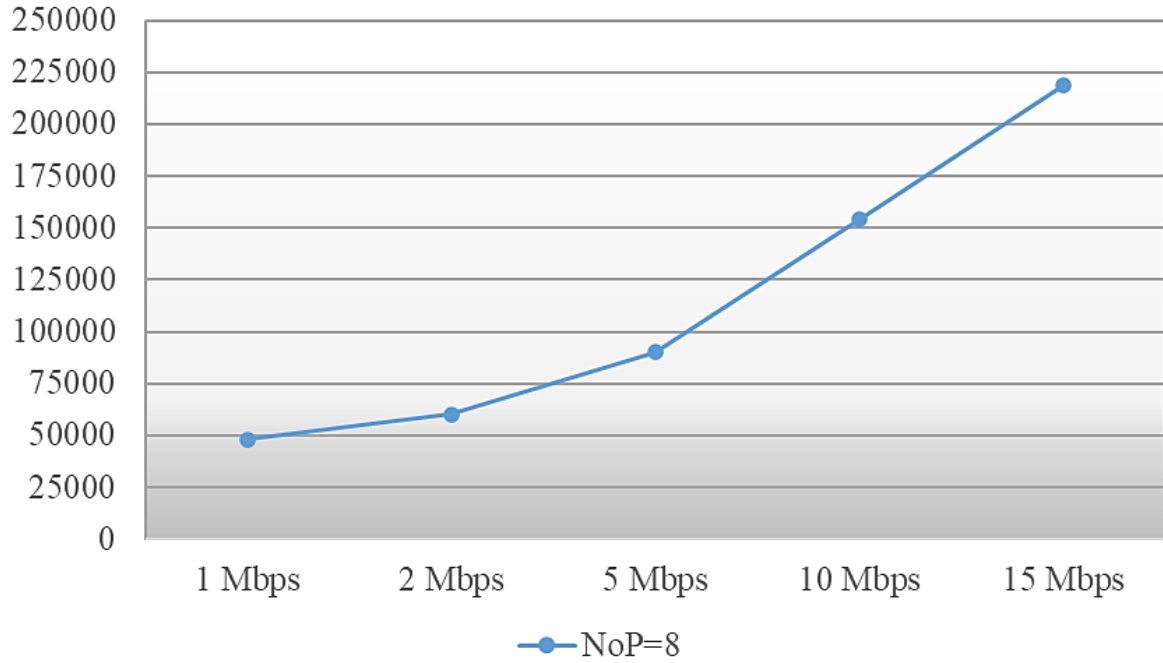
Figure 100: Cost comparisons for various data rates, 8-PON, 1:8 SCN-GPON

6.5. Conclusion

As a further extension of our case studies so far, in this chapter, we sought to incorporate the aspect of cellular spectrum refarming. It was achieved in terms of the 5G cellular network within the premises of our SCN-GPON planning and dimensioning process. Optimising the design of a small-cell mobile communication network, in conjunction with a proper backhaul network, for current and emerging technology trends has been an essential research topic in recent years. This topic has primarily focused on our research work to be studied from different aspects, as observed throughout this thesis's different chapters. For example, a novel 4G SCN implementation method was described in **Chapter 3**. Then a planning process of a backhaul optimisation framework to provide connectivity to the SCN design of the third chapter has been explored in **Chapter 4**. Afterwards, a combined SCN-GPON generalised framework has been proposed in **Chapter 5**. Hence, by our previous case studies, we continued to explore the idea of planning a combined SCN-GPON network, including constraints based on the network node and route distances and the network capacity at different node levels of both the SCN and GPON parts.

As seen before, the combined SCN-GPON framework continued to employ different types of optical splitter ratios and line card capacities as constraints for the GPON optimisation segment. The optimisation process would also be determining the choice of a carrier frequency(s) for the SCN part based on typical coverage and capacity limits of such carrier frequency(s). We carried on exploring the optimal selection process of SC locations from a set of pre-defined equidistant-spaced potential geographic location points over our case study area, as organised within a terrain grid formation. We adopt the GPON technology the same as the previous chapters for the backhaul implementation, leveraging an existing PtP optical network architecture's equipment and resources. However, the SC locations this time were chosen on two aspects. The first aspect was how optimally they were positioned concerning the selected node and route locations for the planned GPON backhaul. Secondly, each selected SC location can cover the potential user population, adhering to a particular carrier frequency coverage distance and capacity limit associated with each such selected SC location. In this chapter, there were three optical split ratio types, two OLT PON port limitation types, five data rate types for the GPON optimisation part. Then two carrier frequency choices were employed within the SCN planning section. These parameters were then combined to render a complete and combined SCN-GPON network plan, covering both wireless and wired data transmission mechanism aspects.

For our GPON backhaul optimisation part, optimal existing PtP node locations and link routes were chosen to place proposed GPON equipment and cables, respectively. For instance, existing PtP locations such as the CO, FAP and RT locations were optimally selected to place the necessary corresponding GPON nodes, e.g., CO, FAP and RT locations. Also, existing PtP link routes were chosen to place the proposed GPON fibres optimally, as per the optimisation framework. We essentially continued most of the same approach of optimisation, as seen in **Chapters 4** and **5**. It was done by considering cost minimisation approaches involving both CAPEX and the OPEX to determine the optimal GPON design providing the minimal costs in implementing. We still applied multiple splitter types and OLT PON port restrictions at the line card as parameters to our GPON optimisation segment in this chapter. However, we explored only three types of optical split ratios for the splitters but maintained the two type of PON port restrictions as before.

Furthermore, we incorporated a new form of constraint, which restricted the ONU level data consumption ability, based on the split ratio applied over each case study type. It was done

by dividing the total data consumption capability of our proposed GPON backhaul, 10Gbps, by different split ratios, e.g., 1:2, 1:4 and 1:8. Then, we set the division's result as the intended maximum data handling capacity of each ONU.

From the cost comparison scenarios, it was evident that the primary elements determining cost differences were SC and fibres' costs. In most cases, the 1:8 split type came out as the optimal choice for the GPON part of the framework, based on its utilization of splitter ports. Unlike previous chapters, only one type of SC location inter-distance was considered. However, significant new parametric approaches were included in the studies, such as different data rates adopted by each selected SCs and the provision of choosing different wireless carrier frequencies for each SC. Based on their covered user population within a particular distance, the optimally chosen SC locations would cover 100% of the user population over the case study area for different fixed data rates. The 100% population coverage over the total case study area was provisioned since the SCN-GPON network planning should mitigate wireless network blackspots' effect by providing total user coverage over the total network area. Concerning the previous chapters, we continued incorporating the terrain grid approach of organizing the potential SC locations and then proposed a GPON backhaul implementation. The novelty of this chapter's research work was that instead of fixing the coverage areas for each selected SC location, the framework looked at an SC's capabilities of covering a geographic area. It also depended on the SC's associated parameters, namely, SC frequency type, corresponding particular maximum cell coverage distance, and data consumption within that maximum cell area and frequency.

In short, a complete SCN-GPON framework was formed that ultimately generated the most optimal network architecture, covering the whole case study area and the total population over it. For simplification, we based our case studies on the 5G technology and related characteristics only, e.g., signal level restriction, data rate and carrier frequency characteristics. Hence, additional aspects of a 5G cellular access network such as the hardware architecture were neither considered nor considered within our work scope to maintain conciseness. We also retained some essential optimisation characteristics from the previous chapters, such as the terrain grid formation, leveraging existing PtP resources for our GPON planning, then OLT and split ratio restrictions. However, significant additions were incorporated within the SCN-GPON framework, for instance, the user population coverage and different data rate handling of SCs, in conjunction with choosing a proper carrier frequency for each selected SC.

This page is left intentionally blank

Chapter 7

Concluding Remarks

7.1. Summary of project contributions

With the continuous demand for data growth, especially over cellular networks, it has become essential that additional network support should be provided alongside traditional modes of cellular network data transmissions. Hence, small-cells have been established as an optimal approach of adhering to the quintessential demand of data usage in present days to provide additional capacity attainment, coverage enhancement, and traffic offloading. Therefore, to satisfy appropriate cellular network capacity and coverage requirements, this research project has proposed various approaches to envision a comprehensive cost-minimised SCN planning framework alongside a GPON-based backhaul network.

Chapter 1 of the thesis has contained the introduction segment, providing an overview of the research project itself. It introduced the small-cell network, its advantages, and challenges in terms of implementation. The backhaul network then was outlined, with different approaches of existing backhaul methods being discussed and challenges faced during a backhaul implementation highlighted. This chapter also included the research project's motivation and objective, alongside this thesis's original contributions.

Chapter 2 has evaluated the related literature on the small-cell network and optical backhaul dimensioning and planning through different categories of case studies. The literature review has been divided into segments. These are-small-cell network optimisation methods, small-cell backhaul optimisation scenarios, small-cell network planning approaches with backhaul dimensioning, and small-cell spectrum refarming analyses. We first studied the research works performed on small-cell planning and optimisation in small-cell network design, cell capacity attainment, coverage satisfaction methods and energy optimisation techniques. Secondly, we reviewed distinct small-cell backhaul optimisation approaches based on design and cost components. We analysed combined SCN and GPON-based backhaul planning techniques, envisioned in cost, design and coverage optimisation aspects. Lastly, we

discussed the aspect of spectrum refarming in general based on established research works, which is then included as a constraining aspect over our proposed SCN planning approach.

Chapter 3 focused on two case study approaches to establish a generalised simple SCN planning framework. They considered the influences of surrounding urban area geographical terrain for two different carrier frequencies belonging to the 4G cellular technology. This chapter's case study area was a rectangular geographic land, divided into square-shaped coverage blocks of equal dimensions, with each block being a cell coverage area containing one SC location. This chapter's case studies ultimately resulted in planning a novel SCN framework incorporating such a network's corresponding characteristics. These included terrain influence, cell coverage area, antenna height, appropriate signal coverage. The SCN planning framework incorporated the 4G carrier frequencies of 1800 & 900 MHz, with square coverage block areas of 100 m, 200 m and 300 m sides. To conform to SCN planning constraints, we also considered an adequate antenna height of 9 m and signal losses under MAPL value of 165.5 dB. The case studies revealed that the distance between a transmitting SC BTS and a receiving UE transmitter and their surrounding geographic elevation and terrain slope significantly swayed mobile signal propagation characteristics, either individually or collectively. For example, the case studies showed a smaller distance between the selected cell location and a receiving point induced less path loss, while a higher distance increased the loss level. A lower terrain slope value (positive or negative) between an SC and a receiver is attributed to less signal loss for a particular direction, while a higher slope value for the same context would induce higher signal attenuation. By considering all these factors, the most optimal SC location within each coverage block was chosen to place an SC BTS unit while maintaining the MAPL limit for 4G technology. It opened up a new research prospect as in previous works, mostly higher elevation locations were selected as suitable SC locations. Such studies sometimes overlooked the role of terrain slope influences and geographic elevation values over cellular signals propagating from such SC locations [109]. One shortcoming for this chapter was the lack of automated datasets on geographic information, as the author manually extracted data. Hence the level of accuracy of obtained data could have been better.

Chapter 4 focused on forming an optimised backhaul connectivity planning for the SCN architecture, based on geographical terrain effects, as mentioned in **Chapter 3**. The backhaul network planning was based on the GPON technology for cost and energy minimisation, with different GPON parameters, for different pre-planned SCN with different

coverage area sizes. The backhaul GPON planning would optimally select geographic locations that could theoretically house new network equipment such as OLT, optical splitters and ONUs, corresponding to this proposed GPON backhaul. Within the GPON planning, five optical splitters with two different OLT line cards were tested for three different SCN types based on their coverage area dimensions. Additionally, two unique scenarios, namely optical splitters with different split ratios and the corresponding PtP scenario without GPON deployment as backhaul options, were studied to justify our optimal choices of the different planned GPON architectures. The fixed split ratio splitter formations provided less total cost values for the cost comparison studies than those of no fixed split and PtP scenarios. We considered the CAPEX for the newly proposed GPON equipment costs. For calculating the GPON framework cost of fibres, just OPEX was considered since existing fibre and corresponding equipment was being leveraged for the proposed GPON backhaul planning. For this work, the novel approach adopted was that instead of co-locating SC locations with the nearest RT, the SCs were pre-selected by a different framework. This SCN planning framework ensured that the planned SC locations could offer better signal propagation profiles with fewer path losses, as influenced by surrounding geographic terrain characteristics. One limitation to this chapter's work could be attributed to the fact that the 4G SCN planning was performed separately with the optical backhaul dimensioning, and the planning and dimensioning case studies could be consolidated as one single framework to render a more generalised optimisation framework in this process.

Chapter 5 emphasised combining both the SCN and GPON-based backhaul planning within one cost-optimised framework, regardless of the type of cellular technology used. In this optimisation process, a set of potential SC was envisioned at equal distance from each other, within a terrain grid pattern, from which optimal SC locations were chosen. Then the GPON technology was again used for backhaul implementation, and their proximity chose the optimal positioning of the SC locations compared to the backhaul planning. Both these SCN and GPON planning processes were collectively implemented within the same framework. The GPON backhaul planning case studies in this chapter have incorporated different optical splitters and line cards as constraints to build the corresponding network optimisation frameworks. The GPON backhaul planning process optimally selected the locations for installing GPON equipment such as OLT, optical splitters and ONUs, over corresponding PtP optical network node locations. Here, the existing PtP node locations and fibre routes were

leveraged within the cost-minimising optimisation framework to select the optimal link and node locations to form the intended backhaul network. We incorporated both the CAPEX and the OPEX within this optimisation approach, as similar to **Chapter 4**. One novelty aspect of this work was to propose a combined optimisation scenario to connect both the SCN and GPON backhaul while not being limited to the mobile technology used.

Additionally, the SC BTS locations' coverage area did not have a fixed value or shape, making the framework more genialised to have any SCN implementation possible. However, potential BTS location arrangement within a terrain grid was still included within the framework to continue the previous work. Conversely, this very approach of excluding specific parameters related to the wireless segment off this network plan could be seen as an unexplored issue that needed some discussion.

Finally, **chapter 6** proposed incorporating the method of spectrum refarming within an envisioned SCN-GPON planning and dimensioning process for the 5G cellular technology. For this framework, we included constraints based on the network node and route distances, network capacity at different node levels of both the SCN and GPON parts, and 5G frequency parameters, e.g., cell area and cell capacity limits. We continued with SC locations' optimal selection process from a set of pre-defined equidistant-spaced geographic location points organised in a terrain grid over our case study area. In conjunction with our works in previous chapters, we continued leveraging the equipment and resources of an existing PtP optical network architecture to plan and dimension our GPON-based backhaul network. In this chapter, the SC locations were chosen based on their optimal positioning to the planned GPON backhaul. For an appropriate carrier frequency coverage distance and capacity limit, each optimally selected SC location's ability to attain the required network data capacity for a particular user population was considered. We conformed to optimisation for the backhaul optimisation part very similar to **chapters 4** and **5**. Here, we considered cost minimisation approaches involving both CAPEX and OPEX to optimise network resources. Like the previous chapters, GPON was chosen as the preferred backhaul technology, while SCN part planning was based on potential SC locations organised within a terrain grid. The novelty of this chapter's research work was that the optimisation was to optimally plan a wireless SCN and wired GPON backhaul together with necessary constraints depicting real-life modern and innovative characteristics of such networks. Due to resource restrictions, a smaller dataset was

used in the simulations to obtain results. Therefore, it can be seen as a limitation to our studies performed in this chapter.

7.2. Further investigation

As part of this project's research prospect's growth further, possible new investigative methods can be incorporated in the future to accomplish more significant outcomes. Since the small-cell optimisation process is a much diverse and emerging technology trend, it offers many research prospects. There are numerous prospects to enhance the current works being done on such an optimisation study. In this section, we discuss possible future directions for our intended research works in this thesis. These can be discussed as follows.

- Suburban & rural network planning
- Larger case study areas & sample sizes
- Additional geographical terrain constraints
- Extensive spectrum refarming optimisation

7.2.1. Suburban & rural network planning

The effect of suburban [135] and rural [136] terrain types over small-cell network planning and backhaul dimensioning can be considered for a future research direction on SCN planning. They can be enhanced approaches over our research that studied the influence of urban geographic terrain characteristics over SCN planning. Our research work observes that geographic characteristics over signal propagations can be significant to plan wireless small-cell networks. Moreover, the effect of geographic characteristics over wireless signal propagations has been studied broadly over the years to improve such signal propagation of cellular networks. Thereby, the influences of suburban and rural terrain types over wireless signals [103] can be extensively incorporated within the study of an actual small-cell network planning and dimensioning. The effect of suburban and rural geographic terrain can cause a significant impact over small-cell signal propagation [102]. Hence, they should be studied extensively in the future. Also, there were terrain grid formations over intended case study areas, corresponding to suburban and rural areas' cell area limits. Moreover, we should also account for the influences on signal propagations due to foliage, water bodies, the atmosphere over the case study areas.

As an expansion to the proposed framework in **Chapter 3**, we would need to consider additional physical geographic element influences over cellular signal propagation. Such elements can include vegetation [137], water body [138], atmospheric effects [139] in terms of small-cell propagation scenarios. We should also consider the effects of population density on the fixed area provision for a terrain grid pattern over the intended case study area. It means that for each terrain grid block, the amount of population assumed to be covered by cellular signal should be counted following the geographic element influences mentioned above. It is noteworthy that small-cell network planning over suburban & rural areas may not be related to capacity enhancement, as population density in suburban and rural areas is typically lower than in urban areas. Henceforth, small-cell's installation over such areas should be based more on relevant aspects such as maintaining LoS coverage to counter the effects of vegetative obstructions, water body interferences, and atmospheric influences. Thereby, the corresponding future research direction should be much relevant as such parameters significantly influence small-cell propagations. Such cell planning should be envisioned so that the influencing parameters mentioned above are encountered to position small-cells optimally over an intended case study area.

7.2.2. Larger case study areas & sample sizes

Small-cell network planning and backhaul dimensioning have been researched widely around the globe for sometimes. Past research showed that robust, generalised small-cell network planning could be implemented over bigger geographic regions, considering the influence of macrocell existence on small-cell's signal propagations [140]. Small-cell planning frameworks can also be planned over much larger urban geographic areas to attain coverage needs, such as countering black spots [141] within macrocell networks. Additionally, such frameworks can avoid unwanted effects on signal propagation due to macrocell positioning [140] over a case study area. Since small-cells are part of the heterogeneous network, it is crucial to consider the effects of macrocell over such small-cells while planning the framework for small-cell positioning.

Additionally, the geographic information such as the elevation of potential SC location and slope parameter values from potential SC locations towards the edge of fixed coverage areas should be extracted from reliable information sources. It should be done to calculate signal propagation losses and determine the correct positioning of small-cells to provide signal

propagations with minimal power losses, typically over larger geographic areas, which can have different terrain types. Also, various backhaul options [142], besides the proposed GPON scenario, can also be explored for such case study areas, subjected to availability around the SCN planning region(s).

Chapter 4 expanded the previous geographic terrain-influenced SCN planning work performed in Chapter 3 to allow for a cost-effective and energy-efficient backhaul network dimensioning. This backhaul planning optimisation framework was devised using the GPON technology that has been proven for cost and energy efficiency of deployment for different pre-planned SCNs with different coverage area sizes. The GPON-based backhaul planning incorporated different GPON optical splitters and line cards, which are essential components within the GPON technology, while leveraging existing PtP optical network elements within the case study area. We also continued to follow the same SCN planning approach, as in **Chapter 3**, to maintain coordination within our research work. This work showed flexibility since both the SCN and GPON planning were done separately and, therefore, can be adjusted according to the needs of a case study area with larger proportions. Also, as they were separate frameworks, various other types of backhaul options could be included in case of non-availability or difficulty associated with deploying the GPON framework. So, by utilising the same optimisation techniques stated in **Chapter 3**, an SCN would be planned over a larger case study area and connected with an optimal backhaul architecture. In some cases, the availability of a PtP optical network within the vicinity of an SCN planning area cannot be guaranteed. As a result, alternative backhaul solutions such as microwave and copper wires [140] can be utilised for such cases in future research directions.

7.2.3. Additional geographical terrain constraints

The need for a composed optimisation framework, incorporating both the small-cell and backhaul network [37], has been the subject of various research works over the years. Hence, it would be an exciting research direction to base such a combined framework on a particular parameter, such as the geographic terrain properties, to SC signal propagations. The effect of geographic terrain can significantly affect the signal propagation of SCs [57]. Thereby it has already been proven as a significant factor for determining appropriate SC locations over a particular case study area [1]. The aim would be to incorporate such geographic characteristics within the premises of a combined optimisation framework to derive an

optimisation approach that is more comprehensive and expansive. It may change the outcomes of typical SCN-backhaul optimisation methods, as geographic characteristics can affect the SC coverage areas and signal directions, hence changing the requirements for positioning the SCs more optimally.

Chapter 5 proposed a new combined SCN and backhaul planning process for one single framework. It was a generalised framework that can be expanded, modified, or incorporated for planning any SCN-GPON based framework, regardless of the cellular technology being used. A set of potential geographic locations was considered to be arranged at equidistance length from each other on a terrain grid pattern (as in **Chapters 3** and **4**) was selected. This data was then used as the input parameters to select a subset of appropriate SC locations optimally. Additionally, the GPON technology for the backhaul implementation was utilised, using the existing PtP resources within an optical network deployed over our case study area.

Furthermore, the SC location selection was based on its optimal positioning from the proposed backhaul network links and nodes, as indicated by the SC location set information. This research work can be further enhanced to suit particular cellular network technology types, e.g., 3G, 4G or 5G if needed. In that case, to maintain better coordination to our previous chapter works, we can incorporate more geographic parameters, e.g., the elevation of SC locations, slope factors for a specific direction and distance conforming to the propagation direction and cell radius, respectively, for the cellular technology in use for the proposed planning. If such parameters are incorporated within the optimisation framework itself, the need for utilizing a separate SCN framework will not suffice. Hence in future, research can be taken on how to implement such parameters within the combined single SCN-backhaul framework successfully.

7.2.4. Advanced spectrum refarming optimisation

For extending our research scope, more choices regarding spectrum refarming can be incorporated while considering other factors such as geographic influence, atmospheric effects, vegetation, and water body impacts over signal propagations. The purpose would be to incorporate these features and employ relevant radio resource optimisation techniques [143] within the scope of our optimisation method for planning the SCN-backhaul network. Furthermore, the characteristics of different geographic area types, larger case study areas, and

incorporating terrain characteristics can be included in the framework. As seen, spectrum refarming [54] has been a prevalent trend in terms of predicting the pattern of current and future technology of wireless cellular propagations [125]. Thereby, it would be an interesting perspective to see how spectrum refarming can get affected by the surrounding terrain aspects for the different frequencies applied. Hence, based on such aspects, proper SCN planning can be constructed for practical implementations.

In **Chapter 6,** the aspect of cellular spectrum refarming in terms of the 5G cellular network was incorporated to expand our SCN-GPON planning and dimensioning process. Continuing from the works shown in **Chapter 5**, we incorporated constraints within our optimisation framework. These constraints were based on the network node and route distances, network capacity at different node levels of both the SCN and GPON parts. The SCN-GPON framework included different optical splitter ratios and line card capacities as constraints for the GPON optimisation segment. The framework also included choosing a carrier frequency(s) for the SCN part based on typical coverage and capacity limits of such carrier frequency(s). Again, the optimal SC locations were obtained from a set of pre-defined equidistant-spaced potential geographic location points organised within a terrain grid formation over our case study area. To enhance this current state of the SCN-GPON framework, we can incorporate more wireless frequencies following the spectrum refarming for the 5G approach. Additionally, the spectrum refarming can be implemented within possible 3G and 4G cellular networks in situations where 5G implementation is yet to exist or may not be needed. Thereby, numerous variations of such spectrum refarming implementations can be researched as combined into different contexts.

7.3. Conclusion

With the rapid expansion of data communication, it is of utmost importance that the bandwidth, capacity, and coverage of wireless networks should be designed, enhanced, and optimised accordingly. Henceforth, the formation of heterogeneous wireless networks involving both macro and small-cells is provisioned as a practical choice. More specifically, implementing small-cells should be carefully researched due to the practical complexities associated with the deployment of such small-cell networks within the heterogeneous network setting. Developing such a network requires precise positioning for the proposed small-cells,

concerning several influencing factors that can sway designing a planning framework for small-cells. Therefore, our studies aimed to achieve proper small-cell location selection, considering the effects of geographical terrain and dimensioning a proper backhaul architecture to that Small-cell network. Within the scope of our research project, a geographical terrain-oriented cell planning is described within this report. Then a separate backhaul network planning was linked with the SCN rendering. Next, a combined SCN-GPON generalised network plan was proposed. Finally, spectrum refarming for 5G networks was included in the SCN-GPON optimisation framework. In conclusion to this thesis, it can be cited that the report provided novel research works performed through extensive case studies, which can be expanded to include further research ideas.

This page is left intentionally blank

Appendices

Appendix A: Optimisation cost table

Cost parameters	Cost value (normalised)
e_{15} = Cost of 1.5 GHz frequency SC BTS equipment	-0.10
e_{36} = Cost of 3.6 GHz frequency SC BTS equipment	0.00
e_r = Cost of OLT rack	0.14
e_{sh} = Cost of OLT shelf	0.98
e_{cc} = Cost of OLT control card	0.56
e_{lc} = Cost of OLT line card	4.05
e_{fsp} = Cost of an optical splitter	-0.40 (1:2 splitter)
	-0.40 (1:4 splitter)
	-0.40 (1:8 splitter)
	-0.39 (1:16 splitter)
	-0.38 (1:32 splitter)
e_{spl} = Cost of fibre splicing	-0.41
e_{onu} = Cost of ONU equipment	-0.40
i_{rsfib} = Drop fibre per meter installation CAPEX	-0.41
i_{scins} = Cost of labour for SC BTS installation	-0.38
fi_{cf} = Feeder fibre per meter installation OPEX	-0.42
fi_{fr} = Distribution fibre per meter installation OPEX	-0.42
q_{cf} = Feeder fibre per meter OPEX	-0.42
q_{fr} = Distribution fibre per meter OPEX	-0.42
q_{rs} = Drop fibre per meter CAPEX	-0.42

This page is left intentionally blank

References

[1]   I. Akhter, C. Ranaweera, C. Lim, A. Nirmalathas, and E. Wong, "Small-cell network site planning: A framework based on terrain effects and urban geography characteristics," in *Optical Fibre Technology, 2014 OptoElectronics and Communication Conference and Australian Conference on*, 2014, pp. 422-424.

[2]   H.-L. Fu, P. Lin, and Y.-B. Lin, "Reducing Signaling Overhead for Femtocell/Macrocell Networks," *IEEE Transactions on Mobile Computing,* vol. 12, p. 1587, 2013.

[3]   J. Hoydis, M. Kobayashi, and M. Debbah, "Green small-cell networks," *Vehicular Technology Magazine, IEEE,* vol. 6, pp. 37-43, 2011.

[4]   P. Dhawan, A. Mukhopadhyay, and C. Urrutia-Valdés, "Macro and Small Cell/Wi-Fi Networks: An Analysis of Deployment Options as the Solution for the Mobile Data Explosion," *Bell Labs Technical Journal,* vol. 18, pp. 59-79, 2013.

[5]   (2020, Cisco Annual Internet Report (2018–2023). 6. Available: https://www.cisco.com/c/en/us/solutions/collateral/executive-perspectives/annual-internet-report/white-paper-c11-741490.pdf

[6]   C. Ranaweera, M. G. C. Resende, K. Reichmann, P. Iannone, P. Henry, B.-J. Kim*, et al.*, "Design of Cost-Optimal Passive Optical Networks for Small Cell Backhaul Using Installed Fibers [Invited]," *Journal of Optical Communications and Networking,* vol. 5, pp. 230-239, 2013.

[7]   H. Claussen, L. T. Ho, and L. G. Samuel, "An overview of the femtocell concept," *Bell Labs Technical Journal,* vol. 13, pp. 221-245, 2008.

[8]   (2013, February 6). Cisco Visual Networking Index: Global Mobile Data Traffic Forecast Update, 2012–2017. Available: http://www.cisco.com/en/US/solutions/collateral/ns341/ns525/ns537/ns705/ns827/white_paper_c11-520862.pdf

[9]   B. Han, P. Hui, V. A. Kumar, M. V. Marathe, J. Shao, and A. Srinivasan, "Mobile Data Offloading through Opportunistic Communications and Social Participation," *IEEE Transactions On Mobile Computing,* vol. 11, pp. 821-834, 2012.

[10]   Alcatel-Lucent, "Metro cells: A cost-effective option for meeting growing capacity demands," USA, Strategic White Paper2011.

[11]   "Nokia siemens networks small cells executive summary: Liquid radio," Espoo, Finland2012.

[12]   S. C. F. Resources. (2013, February). Small Cell Market Status.

[13]   J. Research, "Mobile Data Offload & Onload Wi-Fi, Small Cell & Carrier-Grade Strategies 2013-2017," 2013.

[14]   B. Gopal and P. Kuppusamy, "A comparative study on 4G and 5G technology for wireless applications."

[15]   M. Esfandiari, "Reliability evaluation of SBC's "fiber to the node" network," in *Optical Fiber Communication Conference, National Fiber Optic Engineers Conference*, 2006.

[16]   J. G. Andrews, H. Claussen, M. Dohler, S. Rangan, and M. C. Reed, "Femtocells: Past, Present, and Future," *Andrews, J.G.; Claussen, H.; Dohler, M.; Rangan, S.; Reed, M.C.,* vol. 30, pp. 497-508, 2012.

[17]   J. Hoydis and M. Debbah, "Green, cost-effective, flexible, small cell networks," *IEEE Communications Society MMTC,* vol. 5, pp. 23-26, 2010.

[18]   S. Liu, J. Wu, C. H. Koh, and V. K. N. Lau, "A 25 Gb/s(/km2) urban wireless network beyond IMT-advanced," *Communications Magazine, IEEE* vol. 49, pp. 122-129, 2011.

[19]   Y.-H. Chen, H.-L. Chao, S.-H. Wu, and C.-H. Gan, "Resource allocation with CoMP transmission in ultra dense cloud-based LTE small cell networks," in *Personal, Indoor, and Mobile Radio Communications (PIMRC), 2017 IEEE 28th Annual International Symposium on*, 2017, pp. 1-5.

[20]   T. Zahir, K. Arshad, A. Nakata, and K. Moessner, "Interference Management in Femtocells," *IEEE Communications Surveys & Tutorials,* vol. 15, pp. 293 -311, 2013.

[21]   Y. J. Sang, H. G. Hwang, and K. S. Kim, "A self-organized femtocell for IEEE 802.16 e system," in *Global Telecommunications Conference, 2009. GLOBECOM 2009. IEEE*, 2009, pp. 1-5.

[22]   S. Prasad and R. Baruah, "Femtocell mass deployment: Indian perspective," in *Anti-counterfeiting, Security, and Identification in Communication, 2009. ASID 2009. 3rd International Conference on*, 2009, pp. 34-37.

[23]   C.-K. Han, H.-K. Choi, and I.-H. Kim, "Building femtocell more secure with improved proxy signature," in *Global Telecommunications Conference, 2009. GLOBECOM 2009. IEEE*, 2009, pp. 1-6.

[24]   T. Chiba and H. Yokota, "Efficient route optimization methods for femtocell-based all IP networks," in *Wireless and Mobile Computing, Networking and Communications, 2009. WIMOB 2009. IEEE International Conference on*, 2009, pp. 221-226.

[25]   S. Huan, K. Linling, and L. Jianhua, "Interference avoidance in OFDMA-based femtocell network," in *Information, Computing and Telecommunication, 2009. YC-ICT'09. IEEE Youth Conference On*, 2009, pp. 126-129.

[26]   P.-P. N. C. S. W. Group. (2008). *IEEE Standard for a Precision Clock Synchronization Protocol for Networked Measurement and Control Systems*. Available: http://standards.ieee.org/reading/ieee/interp/1588-2008.html

[27]   T. Wada, N. Saitou, T. Hara, and M. Okada, "Frame synchronization among base stations for tdd systems," in *Communications, Control and Signal Processing (ISCCSP), 2010 4th International Symposium on*, 2010, pp. 1-4.

[28]   J. Yoon, J. Lee, and H. S. Lee, "Multi-hop based network synchronization scheme for femtocell systems," in *Personal, Indoor and Mobile Radio Communications, 2009 IEEE 20th International Symposium on*, 2009, pp. 1-5.

[29]   S. Chia, M. Gasparroni, and P. Brick, "The next challenge for cellular networks: backhaul," *Microwave Magazine, IEEE,* vol. 10, pp. 54-66, 2009.

[30]   O. Tipmongkolsilp, S. Zaghloul, and A. Jukan, "The Evolution of Cellular Backhaul Technologies: Current Issues and Future Trends," *Communications Surveys & Tutorials, IEEE,* vol. 13, pp. 97-113, 2011.

[31]   A. H. Jafari, D. López-Pérez, H. Song, H. Claussen, L. Ho, and J. Zhang, "Small cell backhaul: challenges and prospective solutions," *EURASIP Journal on Wireless Communications and Networking,* vol. 2015, p. 206, 2015.

[32]   N. Alliance, "Guidelines for LTE backhaul traffic estimation," *White paper, July,* 2011.

[33]   A. Lucent, "Leveraging VDSL2 for mobile backhaul: meeting the long-term challenges in the mobile broadband era," Strategic white paper2011.

[34]   W. Coomans, R. B. Moraes, K. Hooghe, A. Duque, J. Galaro, M. Timmers*, et al.*, "XG-FAST: Towards 10 Gb/s copper access," in *Globecom Workshops (GC Wkshps), 2014*, 2014, pp. 630-635.

[35]   J. Robson. (2012, Small Cell Backhaul Requirements. Available: http://www.ngmn.org/uploads/media/NGMN_Whitepaper_Small_Cell_Backhaul_Requirements.pdf

[36]   J. Robson, "Small cell deployment strategies and best practice backhauls," *Cambridge Broadband Networks Limited,* 2012.

[37]   P. P. Iannone, K. C. Reichmann, C. Ranaweera, and M. G. C. Resende, "A small cell augmentation to a wireless network leveraging fiber-to-the-node access infrastructure for backhaul and power," in *Optical Fiber Communication Conference and Exposition and the National Fiber Optic Engineers Conference (OFC/NFOEC)*, Anaheim, CA, 2013, pp. 1-3.

[38]   C. Ranaweera, M. G. C. Resende, K. Reichmann, P. Iannone, P. Henry, B.-J. Kim*, et al.*, "Design and optimization of fiber optic small-cell backhaul based on an existing fiber-to-the-node residential access network," *Communications Magazine, IEEE,* vol. 51, pp. 62-69, 2013.

[39]   C. S. Ranaweera, P. P. Iannone, K. N. Oikonomou, K. C. Reichmann, and R. K. Sinha, "Cost Optimization of Fiber Deployment for Small Cell Backhaul," in *Optical Fiber Communication Conference and Exposition and the National Fiber Optic Engineers Conference (OFC/NFOEC), 2013*, Anaheim, CA, 2013, pp. 1-3.

[40]   S. Ou, K. Yang, and H.-H. Chen, "Integrated Dynamic Bandwidth Allocation in Converged Passive Optical Networks and IEEE 802.16 Networks," *Systems Journal, IEEE,* vol. 4, pp. 467-476, 2010.

[41]   C. Lin, *Broadband optical access networks and fiber-to-the-home: systems technologies and deployment strategies*: Wiley. com, 2006.

[42]   N. Ansari and J. Zhang, "PON Architectures," in *Media Access Control and Resource Allocation*, ed: Springer New York, 2013, pp. 11-22.

[43]   A. Agata and Y. Horiuchi, "PON network designing algorithm for suboptimal deployment of optical fiber cables," in *Asia Communications and Photonics*, 2009, pp. 76330L-76330L-6.

[44]   J. Robson. (2011, Guidelines for LTE backhaul traffic estimation. [White paper].

[45] J. Robson and L. Hiley, "Easy small cell backhaul: an analysis of small cell backhaul requirements and comparison of solution," *Cambridge Broadband Networks Limited,* 2012.

[46] D. Bojic, E. Sasaki, N. Cvijetic, T. Wang, J. Kuno, J. Lessmann*, et al.*, "Advanced wireless and optical technologies for small-cell mobile backhaul with dynamic software-defined management," *IEEE Communications Magazine,* vol. 51, pp. 86-93, 2013.

[47] Z. Bharucha, E. Calvanese, J. Chen, X. Chu, A. Feki, A. De Domenico*, et al.*, "Small Cell Deployments: Recent Advances and Research Challenges," *arXiv preprint arXiv:1211.0575,* 2012.

[48] D. Bladsjö, M. Hogan, and S. Ruffini, "Synchronization aspects in LTE small cells," *IEEE Communications Magazine,* vol. 51, pp. 70-77, 2013.

[49] R. Schwartz and M. Rice, "Rethinking small cell backhaul: a business case analysis of cost-effective small cell backhaul network solutions," in *Wireless*, 2012, p. 20.

[50] G. Lampard and T. Vu-Dinh, "The effect of terrain on radio propagation in urban microcells," *Vehicular Technology, IEEE Transactions on,* vol. 42, pp. 314-317, 1993.

[51] W. C. Lee and D. J. Lee, "Microcell prediction in dense urban area," *Vehicular Technology, IEEE Transactions on,* vol. 47, pp. 246-253, 1998.

[52] L. M. Correia, D. Zeller, O. Blume, D. Ferling, Y. Jading, I. Gódor*, et al.*, "Challenges and enabling technologies for energy aware mobile radio networks," *Communications Magazine, IEEE,* vol. 48, pp. 66-72, 2010.

[53] M. Hughes and V. M. Jovanovic, "Small Cells - Effective Capacity Relief Option for Heterogeneous Networks," in *Vehicular Technology Conference (VTC Fall), 2012 IEEE*, Quebec City, QC, 2012.

[54] S. Han, Y.-C. Liang, and B.-H. Soong, "Spectrum refarming: A new paradigm of spectrum sharing for cellular networks," *Communications, IEEE Transactions on,* vol. 63, pp. 1895-1906, 2015.

[55] V. Sivaraman, C. Russell, I. B. Collings, and A. Radford, "Architecting a national optical fiber open-access network: The Australian Challenge," *Network, IEEE,* vol. 26, pp. 4-10, 2012.

[56] "3rd Generation Partnership Project; Technical Specification Group GSM/EDGE Radio Access Network; Radio network planning aspects (Release 11)," in *3GPP TR 43.030 V11.0.0 (2012-09)*, ed, 2012.

[57] M. A. Nisirat, M. Ismail, L. Nissirat, S. AlKhawaldeh, and A. Tahbuob, "Micro cell path loss estimation by means of terrain slope for the 900 and 1800 MHz," in *Computer and Communication Engineering, 2012 International Conference on*, 2012, pp. 670-674.

[58] D. Har, H. Xia, and H. L. Bertoni, "Path-loss prediction model for microcells," *Vehicular Technology, IEEE Transactions on,* vol. 48, pp. 1453-1462, 1999.

[59] P. E. Mogensen, P. Eggers, C. Jensen, and J. B. Andersen, "Urban area radio propagation measurements at 955 and 1845 MHz for small and micro cells," in *Global Telecommunications Conference, 1991.'Countdown to the New Millennium. Featuring a Mini-Theme on: Personal Communications Services*, 1991, pp. 1297-1302.

[60] P. Harley, "Short distance attenuation measurements at 900 MHz and 1.8 GHz using low antenna heights for microcells," *Selected Areas in Communications, IEEE Journal on,* vol. 7, pp. 5-11, 1989.

[61] H. Holma and A. Toskala, *WCDMA for UMTS: HSPA Evolution and LTE*: LibreDigital, 2010.

[62] L. Chen, S. Dahlfort, and D. Hood, "Evolution of PON: 10G-PON and WDM-PON," in *Asia Communications and Photonics Conference and Exhibition*, 2010, pp. 709-711.

[63] R. Church and C. ReVelle, "The maximal covering location problem," in *Papers of the Regional Science Association*, 1974, pp. 101-118.

[64] "3GPP TR 32.835 v1.3.0. 3rd Generation Partnership Project; Technical Specification Group Services and System Aspects; Telecommunication management; Study of Heterogeneous Networks Managemen (Release 12)," 2013.

[65] W. Ni and I. B. Collings, "A New Adaptive Small-Cell Architecture," *Selected Areas in Communications, IEEE Journal on,* vol. 31, pp. 829-839, 2013.

[66] P. Mogensen, K. Pajukoski, E. Tiirola, E. Lahetkangas, J. Vihriala, S. Vesterinen*, et al.*, "5G small cell optimized radio design," in *Globecom Workshops (GC Wkshps), 2013 IEEE*, 2013, pp. 111-116.

[67] G. W. Costa, A. F. Cattoni, I. Z. Kovacs, and P. E. Mogensen, "A fully distributed method for dynamic spectrum sharing in femtocells," in *Wireless communications and networking conference workshops (WCNCW), 2012 IEEE*, 2012, pp. 87-92.

[68] Y. H. Tam, R. Benkoczi, H. S. Hassanein, and S. G. Akl, "Optimal Cell Size in Multi-hop Cellular Networks," in *Global Telecommunications Conference, 2008, IEEE*, New Orleans, LO, 2008, pp. 1-5.

[69] A. Asghar, H. Farooq, and A. Imran, "Concurrent Optimization of Coverage, Capacity and Load Balance in HetNets through Soft and Hard Cell Association Parameters," *IEEE Transactions on Vehicular Technology,* 2018.

[70] W. Guo and T. O'Farrell, "Capacity-Energy-Cost Tradeoff in Small Cell Networks," in *Vehicular Technology Conference (VTC Spring), 2012 IEEE 75th*, Yokohama, Japan, 2012.

[71] A. Lozano, A. M. Tulino, and S. Verdu, "Optimum power allocation for parallel Gaussian channels with arbitrary input distributions," *Information Theory, IEEE Transactions on,* vol. 52, pp. 3033-3051, 2006.

[72] P. Mogensen, W. Na, I. Z. Kovacs, F. Frederiksen, A. Pokhariyal, K. I. Pedersen*, et al.*, "LTE Capacity Compared to the Shannon Bound," in *Vehicular Technology Conference, 2007*, Dublin, Ireland, 2007.

[73] J. Kim and D. Cho, "A joint power and subchannel allocation scheme maximizing system capacity in dense femtocell downlink systems," in *Personal, Indoor and Mobile Radio Communications, 2009 IEEE 20th International Symposium on*, Tokyo, Japan, 2009, pp. 1381-1385.

[74] G. Fusco, N. H. Azimi, and H. Gupta, "Capacity optimization of femtocell networks," in *Sensor, Mesh and Ad Hoc Communications and Networks (SECON), 2013 10th Annual IEEE Communications Society Conference on*, 2013, pp. 460-468.

[75] D. Karvounas, P. Vlacheas, A. Georgakopoulos, V. Stavroulaki, and P. Demestichas, "Enriching self-organizing networks use cases with opportunistic features: a coverage and capacity optimization paradigm," *International Journal of Network Management,* vol. 23, pp. 272-286, 2013.

[76] H.-F. Geerdes, *UMTS radio network planning: mastering cell coupling for capacity optimization*: Vieweg+ Teubner, 2008.

[77] I. Ashraf, H. Claussen, and L. T. Ho, "Distributed radio coverage optimization in enterprise femtocell networks," in *Communications (ICC), 2010 IEEE International Conference on*, 2010, pp. 1-6.

[78] R. Poli, W. W. B. Langdon, N. F. McPhee, and J. R. Koza, *A field guide to genetic programming*: Lulu. com, 2008.

[79] L. T. Ho, I. Ashraf, and H. Claussen, "Evolving femtocell coverage optimization algorithms using genetic programming," in *Personal, Indoor and Mobile Radio Communications, 2009 IEEE 20th International Symposium on*, 2009, pp. 2132-2136.

[80] E. Hemberg, L. Ho, M. O'Neill, and H. Claussen, "A symbolic regression approach to manage femtocell coverage using grammatical genetic programming," in *Proceedings of the 13th annual conference companion on Genetic and evolutionary computation*, 2011, pp. 639-646.

[81] L. Mohjazi, M. Al-Qutayri, H. Barada, and K. Poon, "Femtocell coverage optimization using genetic algorithm," in *Telecom World (ITU WT), 2011 Technical Symposium at ITU*, 2011, pp. 159-164.

[82] R. I. Mckay, N. X. Hoai, P. A. Whigham, Y. Shan, and M. O'Neill, "Grammar-based genetic programming: a survey," *Genetic Programming and Evolvable Machines,* vol. 11, pp. 365-396, 2010.

[83] P. A. Alexander, "Domain knowledge: Evolving themes and emerging concerns," *Educational Psychologist,* vol. 27, pp. 33-51, 1992.

[84] Y. Chen, Z. Guo, X. Yang, Y. Hu, and Q. Zhu, "Optimization of Coverage in 5G Self-Organizing Small Cell Networks," *Mobile Networks and Applications,* pp. 1-11, 2017.

[85] P. Iannone, K. Reichmann, M. Resende, C. Ranaweera, R. Sinha, and K. Oikonomou, "Design and optimization of fiber-optic small-cell backhaul based on existing fiber," in *Optical Communication (ECOC 2013), 39th European Conference and Exhibition on*, 2013, pp. 1-3.

[86] B. Badic, T. O'Farrrell, P. Loskot, and J. He, "Energy Efficient Radio Access Architectures for Green Radio: Large versus Small Cell Size Deployment," in *Vehicular Technology Conference Fall (VTC 2009-Fall), 2009 IEEE 70th*, Anchorage, AK, 2009, pp. 1-5.

[87] G. He, S. Zhang, Y. Chen, and S. Xu, "Architecture design and performance evaluation for future green small cell wireless networks," in *Communications Workshops (ICC), 2013 IEEE International Conference on*, 2013, pp. 1178-1182.

[88] T. Pamuklu and C. Ersoy, "Optimization of Renewable Green Base Station Deployment," in *Green Computing and Communications (GreenCom), 2013 IEEE and Internet of Things (iThings/CPSCom), IEEE International Conference on and IEEE Cyber, Physical and Social Computing*, 2013, pp. 59-63.

[89] A. Gupta and R. K. Jha, "Power optimization using optimal small cell arrangements in different deployment scenarios," *International Journal of Communication Systems,* vol. 30, p. e3279, 2017.

[90] I. Ashraf, F. Boccardi, and L. Ho, "Sleep mode techniques for small cell deployments," *Communications Magazine, IEEE,* vol. 49, pp. 72-79, 2011.

[91] H. Holma and A. Toskala, *Lte for umts: evolution to lte-advanced*: John Wiley & Sons, 2011.

[92] L. M. del Apio, E. Mino, L. Cucala, O. Moreno, I. Berberana, and E. Torrecilla, "Energy Efficiency and Performance in mobile networks deployments with femtocells," in *Personal Indoor and Mobile Radio Communications (PIMRC), 2011 IEEE 22nd International Symposium on*, 2011, pp. 107-111.

[93] W. Xiong, C. Wu, L. Wu, X. Guo, Y. Chen, and M. Xie, "Partitioning Algorithm for PON Network Design," in *Applied Informatics and Communication*, ed: Springer, 2011, pp. 1-8.

[94] A. Mitcsenkov, P. Bakos, G. Paksy, and T. Cinkler, "Technology-independent topology design heuristics for point-to-multipoint optical access networks," in *ONDM*, 2013, pp. 298-303.

[95] W. Xiong, C. Wu, L. Wu, X. Guo, Y. Chen, and M. Xie, "Ant colony optimization for PON network design," in *Communication Software and Networks (ICCSN), 2011 IEEE 3rd International Conference on*, 2011, pp. 380-383.

[96] J. W. Chinneck, "Practical optimization: a gentle introduction," *Systems and Computer Engineering), Carleton University, Ottawa. http://www. sce. carleton. ca/faculty/chinneck/po. html,* 2006.

[97] T. G. Orphanoudakis, C. Matrakidis, C. Politi, and A. Stavdas, "Passive Optical Network design optimization for wireless backhauling," in *Transparent Optical Networks (ICTON), 2011 13th International Conference on*, 2011, pp. 1-4.

[98] P. Lafata, "ADVANCED ALGORITHM FOR OPTIMIZING THE DEPLOYMENT COST OF PASSIVE OPTICAL NETWORKS," *Advances in Electrical & Electronic Engineering,* vol. 11, 2013.

[99] (2015, Spectrum Refarming: Benefits, challenges, and solutions. Available: http://www.viavisolutions.com/sites/default/files/technical-library-items/spectrum-refarming-wp-maa-nse-ae_0.pdf

[100] K. Schwab, *The fourth industrial revolution*: Crown Business, 2017.

[101] J. D. Parsons and P. J. D. Parsons, *The mobile radio propagation channel* vol. 2: John Wiley New York, 2000.

[102] A. Kamar, S. J. Nawaz, M. Patwary, M. Abdel-Maguid, and S.-U.-R. Qureshi, "Optimized algorithm for cellular network planning based on terrain and demand analysis," in *Computer Technology and Development, 2010 2nd International Conference on*, 2010, pp. 359-364.

[103] T. S. Rappaport, *Wireless communications: principles and practice* vol. 2: prentice hall PTR New Jersey, 1996.

[104] Google. *Google Earth.* Available: http://earth.google.com/

[105] Y. A. Alqudah, "On the performance of Cost 231 Walfisch Ikegami model in deployed 3.5 GHz network," in *2013 The International Conference on Technological Advances in Electrical, Electronics and Computer Engineering (TAEECE)*, 2013, pp. 524-527.

[106] E. Dahlman, S. Parkvall, and J. Skold, *4G: LTE/LTE-advanced for mobile broadband*: Academic Press, 2013.

[107] Z. Li, C. Zhu, and C. Gold, *Digital terrain modeling: principles and methodology*: CRC press, 2010.

[108] *GPS Visualizer: Assign elevation data to coordinates* [Online software tool]. Available: http://www.gpsvisualizer.com/elevation

[109] J. D. Parsons and P. J. D. Parsons, *The mobile radio propagation channel*: J. Wiley, 2000.

[110] (08/11/2017). *Slope Calculation from Contour Lines in a Topographic Map.* Available: http://geokov.com/education/slope-gradient-topographic.aspx

[111] Z. Li, Q. Zhu, and C. Gold, "Digital terrain modeling: principles and methodology," ed: CRC Press, 2005.

[112] A. R. P. a. N. S. A. (ARPANSA), "About mobile phones," 2012.

[113] C. Liu, L. Zhang, M. Zhu, J. Wang, L. Cheng, and G.-K. Chang, "A novel multi-service small-cell cloud radio access network for mobile backhaul and computing based on radio-over-fiber technologies," *Journal of Lightwave Technology,* vol. 31, pp. 2869-2875, 2013.

[114] S. Melkote and M. S. Daskin, "Capacitated facility location/network design problems," *European journal of operational research,* vol. 129, pp. 481-495, 2001.

[115] I. Cale, A. Salihovic, and M. Ivekovic, "Gigabit passive optical network-GPON," in *2007 29th International Conference on Information Technology Interfaces*, 2007, pp. 679-684.

[116] T. U. o. Melbourne, "University of Melbourne Optical network diagram," I. Akhter, Ed., ed, 2014.

[117] R. L. Church, "Location modelling and GIS," *Geographical information systems,* vol. 1, pp. 293-303, 1999.

[118] R. Sánchez Fuentes, "Planning, optimization and operation of access and Ethernet optical networks for the provisioning of high-speed symmetrical services," 2016.

[119] M. Technologies. GPON Communications-High Speed Fibre Networks. Available: http://www.madisontech.com.au/pdfs/Madison-GPON_Brochure_Spreads.pdf

[120] D. Nesset, K. Farrow, and P. Wright, "Bidirectional, Raman extended GPON with 50 km reach and 1: 64 split using wavelength stabilised pumps," in *European Conference and Exposition on Optical Communications*, 2011, p. Th. 12. C. 1.

[121] E. ESRI, "ArcMap 10.2," *Redlands, USA,* 2014.

[122] A. O. Inc. *AMPL | Streamlined Modeling For Real Optimization*. Available: https://ampl.com/

[123] D. Inc., "Organize all your team's content, tune out distractions, and get everyone coordinated with the world's first smart workspace.."

[124] 3GPP, "3GPP TR 21.915 V15.0.0 (2019-09)," 2019.

[125] T. A. C. a. M. A. (ACMA). (2016). *Future use of the 1.5 GHz and 3.6 GHz bands*. Available: https://www.acma.gov.au/theACMA/~/media/A91252334B314FC5AA10E056B7BA9B78.ashx

[126] A. Basta, A. Blenk, K. Hoffmann, H. J. Morper, M. Hoffmann, and W. Kellerer, "Towards a cost optimal design for a 5G mobile core network based on SDN and NFV," *IEEE Transactions on Network and Service Management,* vol. 14, pp. 1061-1075, 2017.

[127] C. Ranaweera, C. Lim, A. Nirmalathas, C. Jayasundara, and E. Wong, "Cost-optimal placement and backhauling of small-cell networks," *Journal of Lightwave Technology,* vol. 33, pp. 3850-3857, 2015.

[128] G. R. MacCartney, J. Zhang, S. Nie, and T. S. Rappaport, "Path loss models for 5G millimeter wave propagation channels in urban microcells," in *Globecom*, 2013, pp. 3948-3953.

[129] T. Fujitani, S. Tomisato, and M. Hata, "Experimental study of mobile propagation loss correction formula for a slope terrain area," in *2010 IEEE 72nd Vehicular Technology Conference-Fall*, 2010, pp. 1-5.

[130] J. Milanovic, S. Rimac-Drlje, and K. Bejuk, "Comparison of propagation models accuracy for WiMAX on 3.5 GHz," in *2007 14th IEEE International Conference on Electronics, Circuits and Systems*, 2007, pp. 111-114.

[131] F. Hu, *Opportunities in 5G networks: A research and development perspective*: CRC press, 2016.

[132] R. S. P. G. (RSPG). (2016, STRATEGIC ROADMAP TOWARDS 5G FOR EUROPE. Available: http://rspg-spectrum.eu/wp-content/uploads/2013/05/RPSG16-032-Opinion_5G.pdf

[133] N. e. C. T. a. R. p. (Nectar). *Nectar Cloud*. Available: https://nectar.org.au/research-cloud/

[134] Canonical, "The leading operating system for PCs, IoT devices, servers and the cloud | Ubuntu."

[135] V. Erceg, A. Rustako, and R. Roman, "Diffraction around corners and its effects on the microcell coverage area in urban and suburban environments at 900 MHz, 2 GHz, and 4 GHz," *IEEE Transactions on Vehicular Technology,* vol. 43, pp. 762-766, 1994.

[136] E. K. Tameh and A. R. Nix, "The use of measurement data to analyse the performance of rooftop diffraction and foliage loss algorithms in a 3-D integrated urban/rural propagation model," in *VTC'98. 48th IEEE Vehicular Technology Conference. Pathway to Global Wireless Revolution (Cat. No. 98CH36151)*, 1998, pp. 303-307.

[137] P. S. Chang, S. P. Thiagarajah, and J. Sheela-Francisca, "Effects of single vegetation obstruction on 5G mobile services in 28GHz," in *2017 IEEE Asia Pacific Microwave Conference (APMC)*, 2017, pp. 1119-1122.

[138] D. J. Lee and W. C. Lee, "Water enhancement for macro and microcell models," in *Vehicular Technology Conference Fall 2000. IEEE VTS Fall VTC2000. 52nd Vehicular Technology Conference (Cat. No. 00CH37152)*, 2000, pp. 818-821.

[139] C. Hanchinal and K. Muralidhara, "A Survey on the Atmospheric Effects on Radio Path Loss in Cellular Mobile Communication System," 2016.

[140] C. S. Chen, F. Baccelli, and R. Laurent, "Joint optimization of radio resources in small and macro cell networks," 2011.

[141] S. S. Jaffry, S. F. Hasan, and X. Gui, "Mobile cells assisting future cellular communication," *IEEE Potentials,* vol. 37, pp. 16-20, 2018.

[142] F. Farias, M. Fiorani, S. Tombaz, M. Mahloo, L. Wosinska, J. C. Costa*, et al.*, "Cost-and energy-efficient backhaul options for heterogeneous mobile network deployments," *Photonic Network Communications,* vol. 32, pp. 422-437, 2016.

[143] D. Budić, K. Skračić, and I. Bodrušić, "Optimizing Mobile Radio Access Network Spectrum Refarming Using Community Detection Algorithms," in *2019 42nd International Convention on Information and Communication Technology, Electronics and Microelectronics (MIPRO)*, 2019, pp. 475-479.

This page is left intentionally blank